

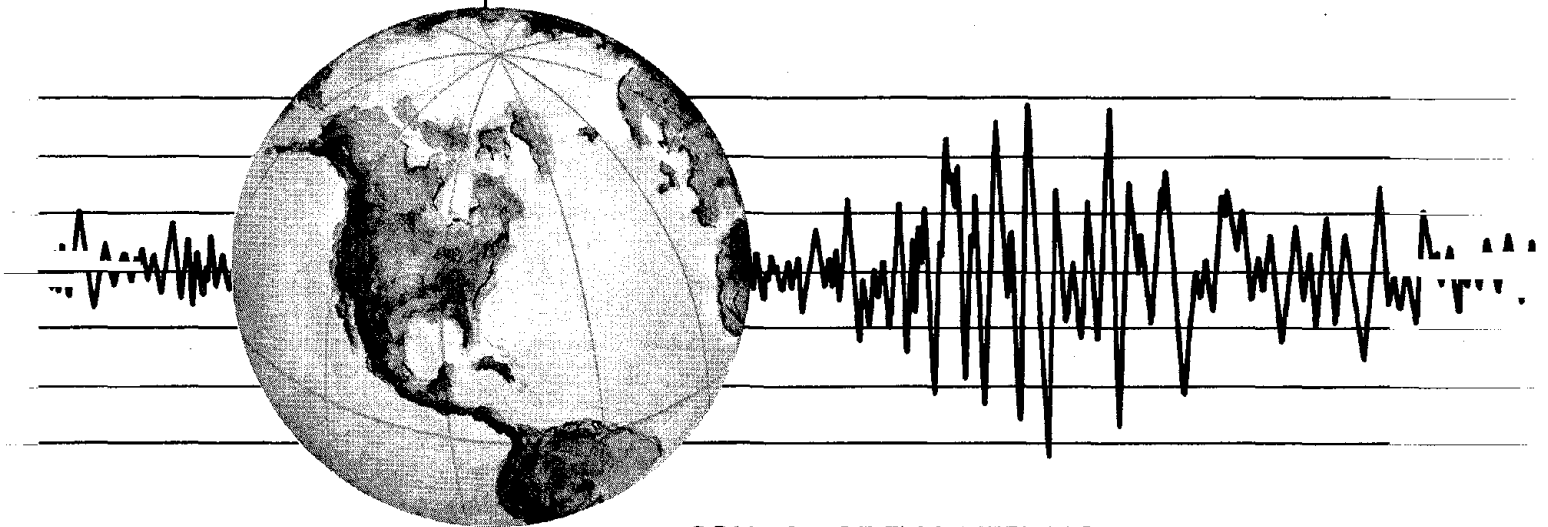
REPORT NO.
UCB/EERC-82/12
AUGUST 1982

EARTHQUAKE ENGINEERING RESEARCH CENTER

by

A. E. AKTAN
V. V. BERTERO
M. PIAZZA

Report to National Science Foundation



COLLEGE OF ENGINEERING

UNIVERSITY OF CALIFORNIA · Berkeley, California

REPRODUCED BY
NATIONAL TECHNICAL
INFORMATION SERVICE
U.S. DEPARTMENT OF COMMERCE
SPRINGFIELD, VA. 22161

For sale by the National Technical Information Service, U.S. Department of Commerce, Springfield, Virginia 22161.

See back of report for up to date listing of EERC reports.

DISCLAIMER

Any opinions, findings, and conclusions or recommendations expressed in this publication are those of the authors and do not necessarily reflect the views of the National Science Foundation or the Earthquake Engineering Research Center, University of California, Berkeley

PREDICTION OF THE SEISMIC RESPONSES OF R/C
FRAME-COUPLED WALL STRUCTURES

by

A. E. Aktan
Associate Research Engineer
Department of Civil Engineering
University of California, Berkeley

V. V. Bertero
Professor of Civil Engineering
University of California, Berkeley

M. Piazza
Research Assistant
University of California, Berkeley

Report to Sponsor:
National Science Foundation

Report No. UCB/EERC-82/12
Earthquake Engineering Research Center
College of Engineering
University of California
Berkeley, California

August 1982

ABSTRACT

This is the second EERC report summarizing the progress of continuing research on "The Seismic Resistant Design of R/C Coupled Structural Walls" at the University of California, Berkeley. The first progress report of this research program, UCB/EERC-81/07, contained the background information, objectives, and scope of the complete program. The present report documents the analytical investigations carried out within the integrated analytical and experimental research program, incorporating a number of observations and conclusions of the experimental phase of the research program as required to modify, assess, or contradict the analytical results.

The analytical efforts to simulate the seismic responses of a 15-story, R/C frame-wall/coupled wall building structure, in conjunction with important observations of the experimental studies on a 1/3-scale, 4-1/2-story subassemblage model of the lower floors of one coupled wall systems of this building, were used to: (1) Assess the state of the art in the analytical seismic response simulation of R/C frame-wall/coupled wall structural systems, and (2) Assess the state of the practice (code) in guiding the designer to achieve an optimum seismic design of these systems.

The conclusions reached after these assessments were: (1) The state of the art in analytical modeling of R/C for the seismic response prediction of frame-wall structural systems is inadequate to predict force and distortion responses, their maxima and distributions within the structure, within reasonable bounds of confidence. It was primarily the uncertainties in defining the basic input quantities for the analyses (strength, stiffness, and energy dissipation characteristics of R/C components of the structure, mainly wall components) which led to this conclusion. (2) The state of the practice was not observed to lead to a design in accordance with the performance criteria expected from the design. The shear strength of the coupled wall system of the structure was assessed to be inadequate at the

collapse limit state of the structure. This was because of substantial flexural overstrength of the coupled wall systems, resulting in the attraction of shear forces far in excess of the design level at the collapse limit state, and because of substantial redistributions of shear from the wall under tension to the wall under compression in the coupled walls, which overloaded the walls under compression in shear.

A third progress report on this research project is being prepared to document the experimental investigations carried out on the 1/3-scale, 4-1/2-story subassemblage test specimen.

ACKNOWLEDGEMENTS

The studies reported herein on the seismic response analysis and seismic resistant design of R/C frame-coupled wall structural systems were conducted as part of an extensive research program on "Seismic Behavior of Structural Components" supported by the National Science Foundation under Grants No. CEE 81-07217 and No. PFR 79-08984. Two subprojects, No. O-22002 and No. O-22082, have been devoted to studies of R/C frame-wall structural systems. Any opinions, discussions, findings, conclusions, and recommendations are those of the authors and do not necessarily reflect the views of the National Science Foundation.

Numerical analysis involved in this study was conducted by M. Piazza as a partial requirement for obtaining his Master of Science degree. Acknowledgement is also due to a large number of other graduate students, as well as technical staff, for their contributions to the analytical and experimental phases of this research project, and to S. Gardner for editing the report and R. Steele for preparing the illustrations.

TABLE OF CONTENTS

	<u>Page</u>
ABSTRACT	iii
ACKNOWLEDGEMENTS	v
TABLE OF CONTENTS	vii
LIST OF TABLES	xi
LIST OF FIGURES	xiii
1. INTRODUCTION	1
1.1 General	1
1.2 Objectives	2
1.3 Scope	3
1.4 Review of Past Work	3
2. THE BUILDING	9
2.1 General	9
2.2 Design of the Building	9
2.3 Evaluation of the Member Cross Sectional Properties	14
3. THE ANALYTICAL MODEL	19
3.1 General	19
3.2 Selection of the Computer Code	20
3.3 Generation of the Analytical Models	21
3.3.1 Interactions	21
3.3.1.1 Planar vs. 3-D Response	21
3.3.1.2 Idealizations Regarding the Interactions in Planar Response	23
3.3.1.3 Interactions between the Structural and Nonstructural Components	24
3.3.2 Deformation Characteristics of the Soil and the Foundation	24
3.3.3 Modeling the Mass Characteristics	25

	<u>Page</u>
3.3.4 Damping Characteristics	26
3.3.5 Topological Characteristics of the Elements	26
3.3.6 Connections and Joints	27
3.3.7 Nonlinear Response	28
3.3.7.1 Geometric Nonlinearities	28
3.3.7.2 Material Nonlinearities	28
3.3.7.3 Effects of Strain Rate	33
3.3.8 Numerical Aspects of the Model	34
4. LINEAR DYNAMIC ANALYSES OF THE BUILDING	37
4.1 General	37
4.2 Linear Dynamic Characteristics of the Structure	37
4.3 Results of Analyses	38
5. INELASTIC TIME-HISTORY ANALYSES OF THE BUILDING	41
5.1 General, Objectives and Scope	41
5.2 Ground Motions	42
5.3 Results of Analysis	44
5.3.1 General	44
5.3.2 Displacements-Distortions	45
5.3.2.1 Time-Histories of Lateral Displacements	45
5.3.2.2 Effective Periods	47
5.3.2.3 Displacement Profiles and Drifts	48
5.3.2.4 Distribution of Plastic Hinging during Response	51
5.3.3 Force Responses	53
5.3.3.1 General	53
5.3.3.2 Shear Force Time-Histories	54
5.3.3.3 Distribution of Seismic Shears throughout the Structure	55
5.3.3.4 Axial Force Responses of the Walls	59
5.3.3.5 Flexural Responses of the Walls	62

	<u>Page</u>
5.3.4 Responses of Coupling Girders	65
6. EVALUATION OF STRUCTURAL RESPONSE	69
6.1 General	69
6.2 Relations between the Demand vs. Supply Relations	69
6.3 Definition of Supplies	70
6.3.1 Service Level Demands	71
6.3.2 Ultimate Limit State Demands	72
6.3.3 Capacity Reduction Factors for Computed Ultimate State Demands	73
6.3.4 Code Assumptions Regarding Computation of Reinforcement	74
6.3.5 The Effect of Redistributions on the Actual Supplies of a Structure	77
6.4 Evaluation of Axial-Flexural Supply vs. Demand Relations	79
6.4.1 Axial-Flexural Supply vs. Demand at the Base of the Walls	79
6.4.2 Axial-Flexural and Shear Supply vs. Demand Relations for the Coupling Girders	83
6.4.3 Shear Strength Supply vs. Demand for the Walls	87
6.4.3.1 General	87
6.4.3.2 Shear Strength Demands Required by Different Provisions	89
6.4.3.3 Establishing the Actual Shear Demands and Shear Capacity of the Walls	92
6.4.4 Deformation Supply vs. Demand Relations	95
6.4.4.1 General	95
6.4.4.2 Experimental Force-Deformation Relations	95
6.4.4.3 Service Level Drifts	96
6.4.4.4 Damage Level Drifts and Rotations	97
6.4.4.5 Collapse Limit State Deformations	99
7. SUMMARY, CONCLUSIONS AND RECOMMENDATIONS	103
7.1 Summary	103

	<u>Page</u>
7.2 Conclusions	104
7.3 Recommendations	108
REFERENCES	111
TABLES	117
FIGURES	129

LIST OF TABLES

<u>Table</u>	<u>Page</u>
2.1 Bilinear Moment-Curvature Relationships: Values of Effective Linear Elastic Flexural Stiffness and Yield Moment for the Wall Section Corresponding to Different Axial Force Levels	119
2.2 Bilinear Moment-Curvature Relationships: Values of Effective Linear Elastic Flexural Stiffness and Yield Moment for the Column Section at Different Axial Force Levels	119
4.1 Magnitude and Distribution of the Earthquake Loading for the Prototype Coupled Wall System (including Torsion)	120
4.2 Linear Demands for One Set of Coupled Walls and One Typical Frame at the Base of the Prototype . .	121
5.1 Periods of the Two Models in Seconds	122
5.2 Maximum Values of Displacements and Drifts Obtained from the Time-History Analyses	123
5.3 The Maximum Shear Forces, Axial Forces and Moments at the Bases of the Walls of the Coupled Wall System .	124
5.4 Maximum Moments Attained by the Coupling Girders . . .	125
5.5 Maximum Shears Attained by the Coupling Girders . . .	126
6.1 Comparison of Factored Code and Analysis Maximum Demands at the Base of Coupled Walls	127
6.2 Coupling Girder Supplies and Demands	128

LIST OF FIGURES

<u>Figure</u>		<u>Page</u>
1.1	Structural Layout of the 15-Story R/C Frame-Coupled Wall Building	131
2.1	Contribution of Beam Stiffness to the Stiffness of Coupled Walls	131
2.2	Wall Cross Section Designed by UBC-73 Provisions .	132
2.3	Coupling Girders Designed by UBC-73 Provisions . .	132
2.4	Frame Columns Designed by UBC-73	132
2.5	Frame Beams Designed by UBC-73	132
2.6	Overturning Moment Resistances at Factored Earthquake Design Load and Collapse State	133
2.7	Assumed Material Stress-Strain Characteristics in Generating Moment-Curvature Responses of the Beams and the Wall Cross Sections	133
2.8(a)	Moment-Curvature Relations for the Wall Cross Section for Different Levels of Axial Force, N . . .	134
2.8(b)	Pre-Yield Moment-Curvature Relations for the Wall Cross Section for Different Levels of Axial Force, N	134
2.8(c)	The Effect of Concrete Tensile Strength on the Section Moment-Curvature Responses	135
2.9	Axial Force-Bending Moment Interaction Diagram for the Wall Section Designed by UBC-73 Provisions	135
2.10 (a, b)	Moment-Curvature Responses in both Bending Directions, Beams Type I and II	136
2.10(c)	Moment-Curvature Responses in both Bending Directions, Beam Type III	137

<u>Figure</u>		<u>Page</u>
2.11	Moment-Curvature Relations for the Frame Beam . .	137
2.12	Moment-Curvature Relations for the Column Section at Different Axial Force Levels	138
2.13	Axial Force-Bending Moment Interaction Diagram for the Frame Column	138
3.1	Coupled Wall-Frame Topological Model	139
3.2	Isolated Coupled Wall Topological Model	139
3.3	Properties of the Beam-Column Elements	140
3.4	Properties of the Beam Elements	140
4.1	Static Displacements, Mode Shapes and Periods . .	141
4.2	Linear Acceleration Spectra for Pacoima and El Centro Records and for 5% Damping Coefficient .	141
4.3	Total Story Shears from Static UBC-73 "E" Load Analysis, of One-Half the Symmetric Building . .	142
4.4	Total Story Shears from Modal Spectral Analysis Corresponding to El Centro: Walls Considered Acting alone and with Frames	142
4.5	Story Shears for Walls Considered Acting alone and with Frames Resulting from Spectral Analysis Corresponding to Pacoima Record	143
4.6	Frame Story Shear Demands by Code and Linear Dynamic Analysis for One Typical Frame of the Prototype .	143
5.1	The Accelerograms Used in the Analyses	144
5.2	Time-History of Lateral Displacements of the Coupled Wall and the Coupled Wall-Frame Models Subjected to the El Centro Ground Motion and with $\xi=5\%$	145
5.3	Time-History of Lateral Displacements of the Coupled Wall and the Coupled Wall-Frame Models Subjected to the Pacoima Ground Motion and with $\xi=5\%$	146
5.4	Displacement Profiles of the Coupled Wall-Frame during El Centro Response for $\xi=5\%$	147

<u>Figure</u>		<u>Page</u>
5.5	Displacement Profiles of the Coupled Wall-Frame during the Pacoima Response for $\xi=5\%$. . .	147
5.6	Comparison of the Envelopes of Maximum Lateral Floor Displacements	148
5.7	Envelopes of Maximum Interstory (δ_r) and Tangential Interstory Drift ($\Delta\delta_r$) for the Coupled Wall-Frame Model Subjected to the Pacoima Ground Motion	148
5.8	Profiles of Interstory Drift (δ_r) and Tangential Interstory Drift ($\Delta\delta_r$) at 3.1 and 3.2 Sec. of the Pacoima Response: Coupled Wall-Frame Model	149
5.9	The Distribution of Plastic Hinges on the Coupled Wall During the Response of the Coupled Wall-Frame Model: El Centro Ground Motion . . .	150
5.10	The Distribution of Plastic Hinges on the Coupled Wall during the Response of the Coupled Wall-Frame Model: Pacoima Ground Motion . . .	151
5.11	The Plastic Hinge Patterns of the Coupled Wall-Frame Model at 2.98 and 3.00 Sec. of Response to the Pacoima Dam Record	152
5.12	Time-Histories of Wall Shear Forces, El Centro Response of the Coupled Wall Model	153
5.13	Time-Histories of Wall Shear Forces, El Centro Response of the Coupled Wall-Frame Model	154
5.14	Time-Histories of Wall Shear Forces, Pacoima Response of the Coupled Wall Model	155
5.15	Time-Histories of Wall Shear Forces, Pacoima Response of the Coupled Wall-Frame Model	156
5.16	The Distribution of Seismic Shears along the Height of the Coupled Wall, for the Coupled Wall Model Subjected to the El Centro Ground Motion . .	157

<u>Figure</u>	<u>Page</u>	
5.17	The Distribution of Coupled Wall Seismic Shears along the Height of the Coupled Wall, for the Coupled Wall-Frame Model Subjected to the El Centro Ground Motion	157
5.18	The Distribution of Seismic Shears along the Height of the Coupled Wall, for the Coupled Wall Model Subjected to the Pacoima Ground Motion	158
5.19	The Distribution of Seismic Shears along the Height of the Coupled Wall for the Coupled Wall-Frame Model Subjected to the Pacoima Ground Motion	158
5.20	Envelopes of Maximum Shear Response, Coupled Wall Model	159
5.21	Envelopes of Maximum Shear Response, Coupled Wall-Frame Model	159
5.22	Time-Histories of Wall Axial Forces, El Centro Responses of the Coupled Wall Model	160
5.23	Time-Histories of Wall Axial Forces, El Centro Responses of the Coupled Wall-Frame Model	161
5.24	Time-Histories of Wall Axial Forces, Pacoima Responses of the Coupled Wall Model	162
5.25	Time-Histories of Wall Axial Forces, Pacoima Responses of the Coupled Wall-Frame Model	163
5.26	Envelopes of Wall Axial Forces, El Centro Analyses	164
5.27	Envelopes of Wall Axial Forces, Pacoima Analyses	164
5.28	Time-Histories of Wall Bending Moments, El Centro Responses of the Coupled Wall Model	165

<u>Figure</u>		<u>Page</u>
5.29	Time-Histories of Wall Bending Moments, El Centro Responses of the Coupled Wall-Frame Model	166
5.30	Time-Histories of Wall Bending Moments, Pacoima Responses of the Coupled Wall Model	167
5.31	Time-Histories of Wall Bending Moments, Pacoima Responses of the Coupled Wall Model	168
5.32	Bending Moment Envelopes of One Wall Pier Obtained during the Time-History Analyses . . .	169
5.33	Moment-Axial Force Relations at the Bases of the Individual Walls, El Centro Responses of the Coupled Wall-Frame Model	170
5.34	Moment-Axial Force Relations at the Bases of the Individual Walls, Pacoima Responses of the Coupled Wall-Frame Model	171
5.35	Moment-Plastic Rotation Relationships for the Fourth Floor Beam, El Centro Responses of the Coupled Wall Model	172
5.36	Moment-Plastic Rotation Relationships for the Fourth Floor Beam, El Centro Responses of the Coupled Wall-Frame Model	173
5.37	Moment-Plastic Rotation Relationships for the Fourth Floor Beam, Pacoima Responses of the Coupled Wall-Frame Model	174
5.38	Envelopes of Maximum Plastic Rotation Attained for the Coupling Girders along the Elevation of the Structure	175
5.39	The Maximum Cumulative Rotation Index (CRI) Attained for the Coupling Girders along the Elevation of the Structure (at either end) . . .	176
5.40	Maximum Positive and Negative Bending Moment Demands from the Coupling Girders, Coupled Wall-Frame Model	177

<u>Figure</u>		<u>Page</u>
5.41	Distribution of Maximum Coupling Girder Shear Forces and Stresses, for the Coupled Wall-Frame Model	177
6.1	Axial-Flexural Supplies and Demands at the Base of One Wall Section	178
6.2	Envelopes of Bending Moment Attained along the Elevation of One Wall	178
6.3	Envelopes of Axial Force in Walls, Coupled Wall-Frame Response	179
6.4	Moment-Rotation Relations of the Coupling Girder Type III at Girder-Wall Interface	179
6.5	Seismic Story Shear Demands for Axial-Flexural and Shear Design of Coupled Wall Based on Different Code Provisions	180
6.6	Shear Strength Supplies and Demands for One Wall	181
6.7	First Floor Lateral Force-Displacement Experimental Response Envelopes for the Two Walls of the Coupled Wall Specimen	182

I. INTRODUCTION

1.1 General

Coupled shear walls are frequently used in the structural systems of tall R/C buildings. If properly located and distributed within the layout of a building structure, and, proper proportioning and detailing of their components and of their connection with the other components of the structural system are attained, coupled walls can provide the building with desirable response characteristics for all limit states, when subjected to lateral loads induced by wind and/or earthquake ground motions [15].

Coupled wall structural systems have been in use against wind loading for decades and a significant number of studies have been carried out regarding their linear behavior. Information on the inelastic behavior of these structural systems under severe loading conditions, however, is limited. The current building code seismic provisions [54] specify simple loading patterns based on a fictitious service load level, and do not consider the actual effects that can be induced by severe earthquake ground motions.

For example, the axial forces originating in the wall components from overturning effects may exceed significantly the gravity forces [4] resulting in the occurrence of net tension or high compression (above balanced conditions) at the base. The difference in the axial forces may lead to significant differences in the flexural and shear stiffnesses and strengths of the coupled walls. Consequently, the shear force distribution in the coupled walls would be considerably different from the distributions obtained through linear analysis with code forces. Another pattern of response particular to these structural systems is the generally higher distortion and energy dissipation demands from the coupling beams of these

structures, compared to frame beams [36].

As a consequence of the considerably different performances of coupled wall structures observed during inspection of damages that occurred during the earthquakes of 1964 Alaska, 1967 Caracas, 1971 San Fernando, and 1972 Managua, a review of the state of the art and of the practice was conducted at Berkeley in 1973. This review indicated an urgent need for a better understanding of the response characteristics of these systems at all the limit states, particularly at those related to damageability and ultimate levels, in order to develop better conceptual methods of designing these systems. Therefore, integrated analytical and experimental research on the seismic response of these systems was initiated at the University of California, Berkeley, in 1971 [11] and these efforts had accelerated by 1979. This report constitutes a part of the analytical studies regarding the seismic response of R/C coupled wall-frame systems for tall buildings.

1.2 Objectives

The main purpose of the study reported herein is to analytically generate a number of linear and nonlinear time-history responses of a 15-story coupled wall-frame building system illustrated in Fig. 1.1 [4] which was designed according to 1973 UBC provisions, with the following specific objectives:

(1) To assess the state of the art in the analytical modeling of R/C wall/coupled wall-frame systems for the purposes of inelastic time-history analyses,

(2) To carry out a qualitative and quantitative assessment of the responses of the structure, within the limitations of the analytical model, to:

(i) Generate data for a quantitative supply vs. demand investigation for the selected structure and thus assess the code design provisions (state of the practice) for this kind of

structural system, making use of the results of the experimental study that is being conducted parallel to the analytical studies, in addition to the analytically generated demands.

(ii) Investigate the problem of coupled wall-frame interaction and the soundness of the code provisions regarding the design of the so-called "dual" wall-frame structural system.

(iii) Generate data for the design of the experimental work involving quasi-static testing of a 1/3-scale, 4-1/2 story sub-assembly of one coupled wall system of the selected building.

1.3 Scope

The study reported herein began with a review of past work on this subject. A brief description of the structural system and the design of the building is followed by a detailed investigation of the state of the art in the analytical modeling of R/C frame-wall structural systems.

General purpose linear and nonlinear structural analysis computer codes, prepared at U.C. Berkeley [39, 55], were used to carry out the linear and nonlinear analyses in this study. The linear dynamic analyses were modal spectral analyses utilizing the first three modes of the analytical models that were constructed. The nonlinear analyses were step-by-step time-history analyses of the analytical models that were constructed, subjected to the 1940 El Centro and 1971 Pacoima Dam (derived version) base motions.

The results of the time-history analyses are presented and discussed in detail, and then used to assess the design of the structure, together with the major findings of the experimental investigations.

1.4 Review of Past Work

A detailed review of past work regarding the response of R/C wall/coupled wall-frame systems is given by Aktan and Bertero [4]. Recent analytical work regarding time-history responses of R/C

coupled wall-frame structures in particular, includes studies by Takayanagi and Schnobrich [48], Takayanagi, Derecho, and Corley [49], Saatcioglu, Derecho, and Corely [42], and Becker and Mueller [9].

Takayanagi and Schnobrich [48] at the University of Illinois generated an analytical model for coupled walls. The walls and beams were represented by line elements. Beams were assumed to form concentrated plastic hinges at the ends, with a number of preselected hysteresis models. Inelasticity was, therefore, incorporated at the member level. The stiffness of the wall elements, on the other hand, were obtained by synthesis of strain distributions along a number of cross sections over which numerical integration was performed. The distribution of inelasticity was, therefore, implemented for the wall elements. Nonlinearities in the shear and axial responses of the wall sections, as well as axial-flexural and flexural-shear interactions, were also incorporated through a number of assumptions on this phenomena at the cross section level.

Static and dynamic analyses of a number of previously tested wall specimens led to an assessment of the analytical mode. Subsequent case studies provided conclusions regarding the effects of hysteretic decay of the coupling beams on structural response: assumed hysteretic pinching and strength decay for these beams increased lateral wall displacements by 20 percent and reduced wall shears by 20 percent but did not affect the maximum wall moments.

Investigations on coupled wall response were carried out at the PCA Laboratories by Saatcioglu, et al. [42] and Takayangai, et al. [49]. In these studies, a general purpose computer code, DRAIN-2D, developed at the University of California, Berkeley [39], was used. A single component beam element model in DRAIN-2D was modified by these investigators to analytically simulate different modes of wall response, observed during experiments on isolated wall tests.

Saatcioglu et al. [42] modified the DRAIN-2D beam element to incorporate the effect of axial force on the flexural yield level. Although a beam-column element exists in the original version of DRAIN-2D [39], the hysteresis associated with this element is not of the degrading stiffness type. The analytical wall element generated at PCA was thus capable of dissipating energy through a set of hysteresis rules with stiffness degradation. The effects of axial force on the pre-yield stiffness, however, were not incorporated.

Saatcioglu et al. [42] investigated the effects of axial force on the

flexural yield level of the wall elements by analyzing twice a 20-story coupled wall-frame structure. In both cases the wall elements were modeled by the degrading stiffness beam element. In one analysis, the effect of axial force on the flexural yield level was neglected. In the second analysis, this effect was incorporated. The bending moments and shear forces in the wall that was under compression were substantially increased (as much as 50 percent) during dynamic response. The wall undergoing tension, on the other hand, was observed to exhibit moment and shear demands which were reduced relative to the case where the effect of axial force on flexural yield was neglected. In these analyses, the frames of the building were not included in the analytical model.

The reasoning behind implementing the effect of axial force on flexural yield of the degrading stiffness beam element in DRAIN-2D, instead of using the existing beam-column element in the element library of this program, was not explicit, as the beam-column element already incorporates the effect of axial force on the flexural yield level. An inadequacy of the beam-column element may have been considered to be the elastic-plastic hysteretic response of this element which did not incorporate stiffness degradation.

Takayanagi et al. [49] at PCA modified the beam element in the DRAIN-2D code further, this time by incorporating an inelastic "shear" spring at each end, in addition to the inelastic flexural springs. The objective was to incorporate the phenomenon of "shear yield" that was defined as a result of the observed behavior during the tests of isolated walls [32] which were under low levels of axial stress and with low flexural capacity. The applied force-shear distortion relations indicated a shear yield-like behavior which accompanied the flexural yield of the test specimens, i.e., the shear distortions were observed to increase under constant load, upon the flexural yielding of the wall at shear force levels well

below the predicted shear capacity of the section [32].

In one-dimensional finite element models, the magnitude of shear that may develop in an element depends on the gradient of the moment along this element, and may significantly exceed the value of shear that may be existing at the time of initial flexural yielding at one end of the element. The main objective of study, reported in Ref. 49, was to study the response of frame-wall structures when the maximum level of shear force that could develop in the wall was predetermined by an assigned "yield" shear. For the shear springs, hysteresis incorporating a pinching effect was postulated.

A 20-story coupled wall-frame structure was selected to investigate the effects of "shear yielding," modeled as explained above. This structure was analytically modeled as consisting of 10 stories, with a fundamental period of 2.2 seconds, equal to the computed period of the actual 20-story structure. Analyses of this analytical model with the EW component of the 1940 El Centro record indicated that the incorporation of shear yielding decreased maximum base shear of the wall by only 8 percent, as compared to when no shear yielding was incorporated. Other response quantities were negligibly affected by the incorporation of shear yield.

The selected structure, its idealized analytical model, and/or the ground motion may not have been very suitable to investigate the critical consequences of the "shear yield" phenomenon. In fact, the analytical representation of the shear yield mechanism by additional hinges at the ends of a one-dimensional element has a conceptual shortcoming, as the actual deformation mechanism is through a "sliding" mode rather than a rotational mode. Since the experimentally observed sliding deformation pattern of the wall cannot be represented by a one-dimensional line model with plastic hinges at each end, the response quantities obtained through this model, especially when wall-frame interaction is significant, should be critically assessed [5].

A study of the seismic resistant design of prefabricated panel

construction [9] may also be considered relevant to the response of R/C coupled walls. In this study the authors modeled horizontal steel connectors between precast concrete panels as the coupling girders of a coupled shear wall. Two dimensionless topology indexes were devised, representing the overall geometry of the system and the ratio of the coupling stiffness to the wall stiffnesses. A parametric investigation, varying these indexes as well as other parameters regarding connector yield strengths, hysteresis and ground motions, led to a number of conclusions on the optimum design of these systems. DRAIN-2D [39] was used in these analyses. The walls were assumed to remain linear, while the connectors were modeled by the degrading stiffness R/C beam element.

The main conclusion on the selection of connector stiffness was that this stiffness should be selected "at the threshold of the insensitive range," i.e., when any further increase in this stiffness does not result in a proportional increase in the overall system stiffness. A number of conclusions regarding the optimum coupling strength for maximum hysteretic damping were reached. The optimum coupling strength was observed to be a function of the stiffness characteristics of the system. As the walls were assumed to remain linear, and no frame contribution (and thus frame-wall interaction) was incorporated, the consequences of the proposed optimum coupling strength on the inelastic deformation capacity of actual wall-frame structures were overlooked in this study.

An assessment of the previous efforts on the analytical stimulation of R/C coupled wall response indicates that existing analytical models for wall elements are all based on one-dimensional idealizations. A wall element that appears to be more complex than those already discussed has been developed in Japan [51]. This element was incorporated in the inelastic analyses of frame-wall structures carried out by Chávez [16]. The model is termed the parabolic model. The flexural and shear deformations are

considered to be independent of each other. The shear force-shear distortion relations are directly prescribed for these members. A tri-linear primary curve and an "origin oriented hysteresis" is used for these relations. Similarly, a tri-linear primary curve and degrading stiffness hysteresis are used for the moment-rotation relations of the plastic hinges at the ends of the member. Conceptually, the response of this analytical model is observed to coincide with the shear-yield phenomenon which was later incorporated by Takayanagi et al. at PCA [49].

2. THE BUILDING

2.1 General

A 15-story office building with 12 ft story height and 180 ft total height was selected as the subject of this study (Fig. 1.1). Detailed information about the design of this building is given elsewhere [4], while brief information is provided in this section for completeness.

2.2 Design of the Building

The building was designed twice, once by the provisions of the 1973 UBC and once by the 1979 UBC [54]. The 1973 UBC design version was selected as the subject of this study.

The typical floor system was proportioned with respect to the serviceability requirements of 1973 UBC as a 6 in. two-way slab system with 24 x 15 in. beams in both directions. The specified materials were 4000 psi normal weight concrete and grade 60 reinforcing steel. Preliminary proportioning of the wall and frame columns for gravity and lateral forces resulted in column dimensions of 30 x 30 in.. The wall thicknesses of 12 in. were selected, based on the minimum thickness requirements of 1973 UBC, for stability.

The frame columns were provided with 2 percent reinforcement and the frame beams were provided with 0.6 percent top and bottom reinforcement. In designing the frames, demands arising from 25 percent of the design lateral loading (1973 UBC) for the building, or, demands arising from the analysis of the building incorporating the interaction between the walls and the frames, or, minimum reinforcement requirements as prescribed by the code, were considered. The wall edge members were detailed with 3.56 percent of main longitudinal reinforcement and 1.8 percent volumetric ratio of spiral

reinforcement as required by the gravity loading and a code prescribed, factored earthquake base shear of 5.4 percent of the building weight [4].

The coupling girders of the coupled wall systems were proportioned by relating these girder dimensions to the overall stiffness of the coupled wall system [18]. It was observed that girder dimensions of 24 x 48 in. resulted in an overall coupled wall stiffness which is "at the threshold of the insensitive range" [9], i.e., any further increase in the girder dimensions did not result in a proportional increase in the overall stiffness. This is illustrated in Fig. 2.1, where the coupled wall stiffness, k_{CW} , is expressed as a percentage of the stiffness of a hypothetical solid wall, k_{SW} , which does not have the openings of the coupled wall.

The coupling girders were detailed in three groups, as indicated in Fig. 1.1, based on the demands of these girders obtained through linear analysis and with the code prescribed loading.

The detailing of the frame columns, frame beams, wall panels and edge members, and the coupling girders, are shown in Figs. 2.2-2.5. These reinforcement details were arrived at after considering a number of possible alternatives [4]. It is observed in these figures that #12 bars are used in some of the coupling girders. A #12 bar is not manufactured. As the main objective in the design of the building was to construct a 1/3-scale model after the prototype, the #12 bars used in the design of the prototype building led to the use of #4 bars in the model.

The proportioning and reinforcement detailing of the components of the coupled wall-frame system, as shown in Figs. 2.2-2.5, constitute a design that satisfies 1973 UBC. It is not necessarily a "good" design. Before a design is concluded, the ultimate (damageability and collapse) limit state behavior should be assessed. This is not an explicit requirement of UBC. In the special case of coupled wall structures, the axial forces of the wall in the ultimate limit

state are significantly different than the "design" axial forces computed from linear analysis with the code prescribed loading. This difference is considered to be of great importance in the actual response characteristic of the coupled wall system. The computations according to code procedure and at the collapse state are shown in Fig. 2.6.

For the case of the symmetric coupled wall, the axial forces at the base of the walls due to the lateral force at the collapse state are:

$$N_p = \sum_{i=1}^n (m_{pi}^l + m_{pi}^r) / \ell \quad (1)$$

where " m_{pi}^l " and " m_{pi}^r " are the plastic moments at the left and right ends of beam "i" at the collapse state and " ℓ " is the length.

Suppose $m_p^l = m_p^r = m_p$ for all beams. Similarly, assume that for all beams $m_e^l = m_e^r = m_e$, which are the code factored design demands.

Then it follows from Fig. 2.6, that based on these assumptions, any overstrength in the flexural capacity of the beams (i.e., m_p/m_e), result in an increase in the base axial forces such that $(N_p/N_e) = (m_p/m_e)$. Since the base axial forces contribute a substantial portion of the system overturning strength, the increase in the system overturning capacity would also be substantial.

Another factor which significantly contributes to the lateral force capacity is the flexural capacity at the base of the wall under compression. The increase in the axial compression at the base would be instrumental in an increase in this wall's flexural capacity until the balanced condition is reached. Consequently, the overturning moment capacity of system would increase further. If the shear capacity of the wall system or the resistance of the soil and foundation system do not possess adequate levels of overstrength to compensate for the overstrength in overturning moment

capacity, the system may be subjected to shear failure or foundation failure before adequate flexural yielding. Any possible mechanisms of overstrength in the overturning moment capacity of the system should, therefore, be accounted for in the shear design of the walls and the design of the foundation. If the girder flexural capacities are observed to lead to excessive levels of axial forces in the walls, the design should be reviewed. Increases in the axial compression levels at the base of a wall approaching and exceeding the balanced conditions, in addition to increasing the possibility of shear failure or foundation failure, also limit the inelastic rotation capacity. Increases in axial tension levels on the walls jeopardize the shear strength of the walls.

The code provisions or design and construction procedures which were observed to either inadvertently or deliberately contribute to significant increases in the flexural strengths of coupling girders and walls, leading to undesirable levels of wall axial forces and an overstrength in the system overturning resistance as discussed above, may be briefly listed as follows:

(1) When stiff girders are selected, the use of linear elastic analysis in design results in increased demands for flexural capacity, the consequences of which are undesirable.

(2) The code requirement of the wall system to resist the total lateral forces of the building lead to increased flexural demands from walls and their coupling girders.

(3) The code requirement that edge members be designed to carry all the vertical stresses of the wall, resulting from gravity effects and lateral forces, leads to increased wall flexural capacity.

(4) The increases in the capacities of the materials above the nominal specified values, due to: (i) the tendency to produce a concrete strength higher than specified; (ii) further increases in concrete strength due to confinement; (iii) the generally higher yield reinforcement as supplied, which is particularly the

case for Grade 60 material; (iv) the earlier and large increase in strength of the reinforcement due to high rate of strain hardening. The actual strength was observed to commonly reach twice the specified nominal yield strength for the material. This phenomenon is not incorporated in present code flexural design; (v) other inadequacies in the computational procedures which underestimate or completely neglect mechanisms of flexural overstrength, such as the extent of the contributions of slab concrete and steel to the flexural capacity of the girders, or the actual extent of redistributions in the structure which may lead to unanticipated levels of deformation hardening.

Although the state of the practice may not enable the incorporation of all the above mechanisms of flexural overstrength in design, the more explicit mechanisms of overstrength, (i) through (iv), should be considered in conjunction with the desirable ultimate limit state response of the structural system. In order to attain an acceptable (optimum) design, the effects of coupling girder stiffness and strength on all the limit states of response should be assessed. This assessment, as discussed above, is particularly critical for the ultimate (damageability and collapse) state response.

Another aspect to assess is the design of the accompanying frame system. The frame beams and columns, upon analysis, were observed to require only minimum reinforcement. The requirement for the presence of these frames by UBC, and the effects of these frames during different limit states of response, requires investigations. It was one of the specific objectives of this study to assess the effects of these frames on response.

The design process may be considered complete only after the additional considerations and assessments discussed in this section are carried out and the designer is satisfied with the outcome, even if the code provisions do not include these additional considerations and assessments of ultimate limit state response.

2.3 Evaluation of the Member Cross Sectional Properties

The moment-curvature relationships for the typical cross sections of the walls, all three types of coupling girders, frame columns and frame beams, shown in Figs. 2.2-2.5, were generated using the computer code RCCOLA [26]. The moment-curvature relations were obtained to define the element force-deformation (or moment-rotation) characteristics which are required for inelastic analysis.

The stress-strain relations that were specified for the reinforcing steel, confined concrete, and unconfined concrete, to generate the moment curvature responses of the typical member cross sections, are shown in Fig. 2.7. The same confined concrete characteristics were assumed to be valid for all elements. Because the volumetric ratio of confining reinforcement varied considerably (between 0.8% and 1.8% for the least confined beam and the wall edge member, respectively), the use of a unique stress-strain relationship is a questionable idealization. The slope of the tail portion of the confined concrete stress-strain diagram should, in fact, change. The change, however, is not significant after transverse reinforcement percentages of 1 percent [35]. Furthermore, the effects of such a change on the moment-curvature relations of a section are not as significant as the effects of a number of other idealizations that were required in obtaining the moment-curvature responses. The assumptions regarding the steel stress-strain relations, the Bernoulli hypothesis, and the value of the spalling strain for unconfined concrete [3] are among the more important variables.

In generating the moment-curvature relation, for the wall cross section shown in Fig. 2.3, the assumption regarding the type of concrete model used for the concrete zone at the interface of the panel and the core of the edge member may be consequential in the ultimate curvature. If this zone is modeled as unconfined concrete, spalling of this material may occur earlier than crushing of the confined

core of edge member. In the actual case, this zone has some degree of confinement; i.e., the concrete in this zone would not exhibit unconfined concrete characteristics. On the other hand, the presence of very high shear stress, in conjunction with compression, would result in an especially adverse stress field for this zone, and may result in a splitting-crushing of concrete in this zone earlier than the attainment of the capacity of the edge member. In fact, this was the observed failure mode in many of the isolated wall specimens with realistic levels of axial force and shear [4].

In this investigation, to the wall panel was assigned the confined concrete stress-strain characteristics shown in Fig. 2.7. The moment-curvature responses of the wall section for a number of different axial force levels are shown in Fig. 2.8 (a, b, and c). An axial force-bending moment interaction diagram, shown in Fig. 2.9, is constructed from such moment-curvature responses, for different strain limiting criteria. Also, the yield moment and linear elastic effective yield flexural stiffness corresponding to different axial force levels are tabulated in Table 2.1. The point on the moment-curvature response corresponding to an effective yield was picked up to obtain the quantities tabulated under Table 2.1. It is observed that there are significant differences in the effective flexural stiffnesses at yield. As the axial force level changes from approximately the balanced load level to 10 percent of the tensile capacity of the section (Fig. 2.8a), i.e., from ~8750 kips to ~1500 kips, the effective flexural stiffness changes 2.4 times from $78 \times 10^9 \text{ kip-in}^2$ to $32 \times 10^9 \text{ kip-in}^2$. The change in the initial flexural stiffness is significantly more, as observed from Fig. 2.8(b). It should be noted that these moment-curvature responses were generated neglecting the tensile strength of concrete. The "effective" flexural stiffnesses were obtained as the slope of the secant to the "effective" yield point, as indicated in Fig. 2.8(a). The changes in the initial flexural stiffness of the wall cross section when the

tensile strength of concrete is incorporated (as $0.1 f'_c$, and until first cracking) can be observed in Fig. 2.8(c) for a number of different axial load levels. Although the initial uncracked flexural stiffnesses are altered due to this parameter, the "effective" cracked flexural stiffness is not observed to be affected significantly.

As the existing element models in DRAIN-2D recognize only a unique value of flexural stiffness for the element regardless of the axial force level, the stiffness corresponding to the gravity load level (2270 kips, Fig. 2.9), 71.6×10^9 kip-in² was selected to represent the wall elements. The local modeling problems regarding the structural members will be discussed in later sections.

The moment-curvature responses generated for the coupling girders are shown in Fig. 2.10. Zero axial load was assumed in generating these responses. Consequently, the analytical models defined for these beams did not incorporate the effects of any axial force on either stiffness or yield level. In general, fluctuating axial force magnitudes of 10 percent of the axial force capacity in tension or compression may result in considerable differences in both the flexural stiffness and the yield level. The main problem in analytical modeling, however, is to incorporate the effects of changing axial force in beam flexural response in a realistic manner. As the analytical model did not incorporate such effects, the level of axial force was considered zero in the moment-curvature generation.

Another consequential assumption regards the effect of slab on beam responses. The contribution of only 42 in. of slab, which is one-quarter of the clear span of the girder, was considered in generating the moment-curvature responses. The contribution of the slab steel, however, was completely neglected. In general, the slab steel (which consisted of two layers of square mesh, #5 bars 10 in. O.C.) would influence the moment capacity (as defined in Fig. 2.10) considerably. An assumption on effective slab width

is required to incorporate the effect of slab steel. The total width of slab associated with each girder is 20 ft (Fig. 1.1). The area of slab steel directly contributing to the positive moment capacity of the beam, for this case, would be 15.5 sq. in.. As the amount of negative moment reinforcement in girder type III (Fig. 2.3) is 10.6 sq. in., the significance of slab steel is obvious. The problem is to determine the effective width of the slab. If all the steel in the 42 in. flange (as defined by 1973 UBC), is totally effective, then the negative moment capacity of the type III girder should increase by approximately 30 percent. Neglecting the slab steel is, therefore, a very consequential assumption. Recent experimental investigations which are still in progress at the University of California, Berkeley [20], indicate that the contributions of slab concrete and slab steel to the flexural stiffness and capacity of the beam depend on the previous loading history and existing level of deformation. At the ultimate limit state response, under extreme deformation levels, all the slab steel in the complete width of the slab were observed to fully contribute to the flexural strength and deformation hardening of the beam-column-slab system.

The moment-curvature responses for the frame beam are shown in Fig. 2.11. Some of the moment-curvature responses and the interaction diagram for the typical frame column are shown in Fig. 2.12 and 2.13, respectively. The variation of the flexural stiffness and yield strength with the axial force level is tabulated in Table 2.2. Local modeling of the girders and beam for nonlinear analysis was carried out by synthesizing the cross sectional responses obtained for the typical members, as has been discussed above. Further discussion on local modeling is included in subsequent sections of this report.

3. THE ANALYTICAL MODEL

3.1 General

The analytical modeling of reinforced concrete structures is not an exact science. Although the common steps in analytical modeling for the purposes of "design" analysis are quite established by building codes (UBC), there is considerable uncertainty in the analytical modeling of reinforced concrete structures for the purposes of response prediction. The main objective in conducting analysis in the preliminary design process is to lead to an optimum (serviceable, safe, and economical) design. As long as this is achieved, the accuracy in the results of such analysis (distribution of force and distortion along the structure) may not be considered important. Analytical modeling of reinforced concrete with the objectives of investigating the reliability of a given design, however, requires a precise estimation of the demands regarding the main response parameters. Therefore, many of the idealizations which are considered appropriate in design analysis should be reconsidered in the case of response prediction for reliability studies, and the sensitivity of response to these idealizations should be investigated.

The literature regarding time-history analysis of reinforced concrete frame-wall structures is sparse, some of which is reviewed in Section 1.4, and the analysts generally concentrate and give details on the results of analysis rather than on the implications of the idealizations carried out in the analytical modeling. In this report, emphasis will be placed upon assessing the limitations of the analytical model of the structure as this is generated. This will be done in conjunction with discussing possible alternatives to each idealization as the model is generated and, in this manner, carrying out an assessment of the state of the art regarding analytical modeling of R/C for time-history response prediction [5].

3.2 Selection of the Computer Code

Several general purpose computer codes are available for the inelastic analysis of reinforced concrete [21, 27, 40, 44]. These computer codes incorporate a number of finite elements, different in topology, and/or in the way nonlinearity is taken into account. It is possible, therefore, that more than one analytical model of a structure may be generated and analyzed by the same computer code. In each case, it is just that particular model and not the structure that is being analyzed.

In addition to the element library, another consideration of importance in selecting a computer code is the numerical aspects of the analytical model which are implemented into the computer code. Different computer codes may employ different solution techniques in solving nonlinear equations of motion. Whether the element states are checked and corrected during a certain integration time step or not may have a considerable effect on results, as well as on the solution time and cost. This, and other aspects of the numerical schemes that a computer code utilizes, which will be discussed subsequently, should be considered in selecting the appropriate code.

Existing codes were surveyed and DRAIN-2D [39] was selected as the basic tool for the analyses. This selection necessitated certain limitations in the analytical models that could be generated, as compared to use of more sophisticated models in conjunction with codes such as ANSR II [29]. This selection necessitated certain limitations in the analytical models that could be generated. Other recent codes, such as ANSR II [29], are capable of analyzing more complex and sophisticated analytical models; however, the credibility of an analytically generated structural response was questionable given the uncertain effects of the existing force and distortion state of the structure, characteristics of the ground acceleration, soil and foundation characteristics, and response characteristics of reinforced concrete elements and systems. These uncertainties

cannot be reduced by using more complex, sophisticated analytical models, but by integrated experimental and analytical research to generate experimental data and to improve analytical modeling schemes. This will be elaborated upon in Chaps. 6 and 7.

3.3 Generation of the Analytical Models

The topology of the analytical model generated for the structure in Fig. 1.1 is presented in Fig. 3.1. A planar idealization of one-half of the structure was made to arrive at this model. This and other idealizations that were required to generate the analytical model are discussed below.

3.3.1 Interactions

3.3.1.1 Planar vs. 3-D Response

Orthogonal interactions were neglected by analyzing a planar model of the structure subjected to only one lateral ground acceleration component of the actual 3-D ground shaking. Previous analytical and experimental research has shown that interactions between multi-directional flexural effects may result in significant differences in the planar response characteristics of R/C members, particularly when inelastic distortions in the order of twice the "yield" distortion are indicated by planar analysis [2, 6, 38]. These inelastic (as well as elastic) interactions are neglected by analyzing the planar model.

A further assumption is implicit in the planar analysis regarding the axial force histories of the vertical members. Even when the inelastic multi-directional interactions may be neglected at low distortion levels, the interactions between the three translational and three rotational ground motion components and the 3-D nature of the response lead to different axial force time-histories in the vertical members as compared with that obtained from planar analysis. The different axial force histories can significantly affect the stiffness, strength, and deformation capacity of these members.

Another phenomenon neglected in the planar analysis is torsion. Torsion arises due to (i) the rotational nature of the ground motion; and (ii) eccentricities between the centers of mass and rigidity due to the layout of the structural and nonstructural members, or, due to the difference in the responses of the vertical members under tension and compression, or, accidental torsion, even if none of these sources for eccentricities may be present. The accidental torsion is recognized in design (UBC) by specifying a minimum eccentricity (5 percent of the maximum building dimension) in plan at the level under consideration. It is not clear whether such a specification may be adequate in indirectly incorporating the torsional demands on the members of the structure arising due to the other sources outlined in (i) and (ii) which are not incorporated into the design process. In general, structural torsion increases the demands of all elements, but particularly the axial-flexural and shear demands of the vertical members as well as the diaphragms.

The interactions between the torsional, flexural, and axial distortions in the inelastic response of R/C members, particularly open or closed section core members, are complex phenomena which are not clearly understood at present. There are computer codes which incorporate some of the effects of multi-directional response on the axial-flexural demands of vertical members and the change in the axial force history of the corner columns [23]. The inelastic interactions between bi-axial moments as well as between axial-flexural-shear and torsional effects, however, are not considered. Consequently, the additional cost and complexity involved in the usage of a 3-D model in conjunction with such a computer code was not justified, considering that the idealizations and uncertainties involved in such analysis would still be extensive.

Another idealization concerning the planar analytical model in Fig. 3.1 is the neglect of the vertical component of the ground excitation. Incorporation of the vertical ground shaking may be important for certain types of long-span structures, but was not

considered significant for the building being analyzed.

3.3.1.2 Idealizations Regarding the Interactions in Planar Response

The actual three-dimensional nature of the ground shaking and of the response of the actual three-dimensional building structure was idealized into planar response through the considerations discussed above. To arrive at the model shown in Fig. 3.1, one-half of the building in Fig. 1.1 was considered. The four frames were lumped together into a single frame, the members of which had four times the strength and stiffness of the members of a typical frame in the structure. The analytical frame was then cut in half and folded into two, to reduce the degrees of freedom even further. The folding of these frames altered the axial force history of the frame columns. However, these members remained linear throughout the analysis, indicating that the altering of the axial force histories of the columns may not have been consequential in the overall response of the structure.

The diaphragm system was assumed axially infinitely rigid, resulting in equal horizontal displacements of both walls of the coupled wall systems as well as the frame joints that were on the same floor level. This assumption was not necessitated by limitations of the computer code which may incorporate finite axial rigidity of the diaphragm. The assumption was made due to the lack of information on the actual axial rigidity values of a beam-slab system and the correct distribution of this rigidity along the beam-slab system. Since any assumption on axial diaphragm rigidity is significantly consequential in the response, experimental information is urgently required to improve the state of the art in modeling diaphragm rigidity.

Another assumption that was made to arrive at the analytical model is regarding the out-of-plane flexural rigidity of the diaphragm system. Because of the differences in the deformation characteristics of the frame and the wall, the wall imposes vertical distortions to the frame members at the same floor level. The transverse beams and

the slab system were assumed to have negligible flexural rigidity in order to disregard these effects of vertical interaction. In order to study the effects of the horizontal interaction between the frames and the coupled wall system, analyses were also carried out on an isolated coupled wall model, shown in Fig. 3.2.

The analytical model of the frame-coupled wall structure in Fig. 3.1, was assigned one lateral degree of freedom for each of the 15 floors, as discussed above. A vertical and rotational degree of freedom were assigned to each wall and frame joints. The midspans of the beams of the middle bay of the frames around which the frames were folded into two were constrained against vertical displacement, as indicated in Fig. 3.1. The total degrees of freedom of this model were, therefore, 150, consisting of 15 lateral and 60 vertical displacement and 75 rotational degrees of freedom.

3.3.1.3 Interactions between the Structural and Nonstructural Components

Another kind of interaction which is significantly consequential in the response of structures is the interaction between the structural members and the nonstructural components, i.e., the exterior walls, partitions, and stairways. The effects of the nonstructural components on response become particularly important as the rigidities of these components increase [8]. These effects were neglected in the analytical model.

3.3.2 Deformation Characteristics of the Soil and the Foundation

The effects of soil and foundation deformations were neglected in modeling. Foundation rocking and differential settlement, in general, are the critical components of the soil and foundation deformations. If the foundation of each of the wall components can rock and settle independently, then these effects may increase the coupling girder demands substantially. The uncertainties involved in the proper modeling of soil, foundation, and their interaction, usually far exceed those encountered in the modeling of the

reinforced concrete super structure.

3.3.3 Modeling the Mass Characteristics

As the planar model in Fig. 3.1 represented one-half of the total lateral force resisting system of the building, only one-half of the total mass of each floor was lumped at that floor level of the analytical model. As all joints at floor level were assumed to have the same lateral displacement (and, therefore, lateral acceleration), the distribution of mass within a floor was not important in the model. Only the translational characteristics of the masses were considered, neglecting the rotary inertias. There are examples where mass was lumped at every other floor to reduce the degrees of freedom further [42], and it was shown that this may be admissible in certain cases. A detailed study of the consequences of different mass modeling schemes on dynamic response is required.

Forty percent of the floor live loads were also included in the mass computations, assuming these to be reactive. This assumption on the contribution of the live loads to the reactive mass may be critical for the cases when live load constitutes a considerable percentage of the dead loading, which was not the case in the present study (total live load considered was less than 10 percent of the dead load).

The gravity load corresponding to the mass of each floor was applied to the beam and column nodes as static loading and were retained during dynamic analyses. In computing the effect of gravity load on vertical members, tributary areas were used. A more refined gravity load analysis, considering relative axial and flexural rigidities of the structural members, was not undertaken to obtain a more precise distribution of gravity load to the vertical members. Such a relatively precise determination of the gravity load shares by the wall and column members may be critical for cases in which these

loads constitute a considerable percentage of the balanced load level of these members. (For the coupled wall elements in this study, the gravity loads constituted 25 percent of the balanced axial load.) A precise gravity load determination is important, not only for a correct representation of the element axial force-flexure yield states during response, but also for a more realistic determination of the elements' initial stiffnesses.

3.3.4 Damping Characteristics

A mass proportional viscous damping of 5 percent of the critical was assumed in the analyses. Assumptions regarding hysteretic damping will be discussed in subsequent sections. The assumptions on hysteretic damping, i.e., the energy dissipated due to the inelastic hysteretic response of the structural members, are usually more consequential on response than any assumptions on the viscous damping. In other words, the resisting force component of the structure due to the assumed viscous damping is usually considerably less critical than the component due to the restoring force characteristics (resistance) of the structure during inelastic earthquake response.

3.3.5 Topological Characteristics of the Elements

One-dimensional geometry was assumed for all structural elements. This is the simplest topological model that can be used for the wall members. Usage of 1-D members (line or stick members) for the walls may be a questionable idealization as it is equivalent to lumping the distribution of stress and strain over the cross section, thus expressing the extremely complex stress and strain distributions over the cross section in terms of force and distortion resultants at the centroid, and relating the nodal and interior displacements through the beam shape functions. Although this procedure is admissible for slender members, it is a questionable idealization when wall elements have depth and height dimensions close to each other. The shifting of the wall neutral axis and the considerably different demands from the

exterior and the interior edge members and the panel cannot be incorporated realistically in this model.

A more representative topological modeling of the walls may be possible if other computer codes which have nonlinear finite elements suitable for plane-stress states are utilized. On the other hand, the increased cost involved with such modeling may be prohibitive. Furthermore, there is no finite element to the authors' knowledge that incorporates a sliding mechanism (along cracks) in addition to cracking, yielding, and crushing, which are all required for a realistic micro-modeling of the wall panel.

Another possible approach in the topological modeling of walls is utilizing the "strut analogy," i.e., representing the edge members of the wall by vertical 1-D elements and the wall panel by diagonal 1-D elements. Such modeling is possible by using the existing library of DRAIN-2D [39] and is being contemplated for future studies. Extensive correlation of such a model to the existing test results is required for a successful representation of the characteristic deformation and failure modes of wall members observed in experimental studies.

3.3.6 Connections and Joints

All the joints were assumed to be rigid. The coupling girders were assumed to have rigid end eccentricities through the joint zones at the walls, as shown in Fig. 3.1.

Experiments indicate that R/C joints may undergo considerable deformation [14] and the assumption of "rigid joints and connections," (the joint retaining its original angle and all connecting elements undergoing the same end rotations at the joint) is not generally correct. Such sources of softening in the structure may be represented by using deformable connection elements which are available in the DRAIN-2D library. On the other hand, reliable quantitative information on the finite stiffness of joints

did not exist at the time of this study. As any realistic idealization regarding deformations at connections could not be supported by existing test data, this option in DRAIN-2D was not used. Recently some experimental data have been obtained and a promising analytical technique has been formulated to account for the deformation at the connection [19].

3.3.7 Nonlinear Response

3.3.7.1 Geometric Nonlinearities

Geometric nonlinearities are generally simplified in analysis of building structures into the "beam-column effect" and the "P- Δ effect." The beam-column effect which is the "effect of axial force on flexural stiffness" may be incorporated in DRAIN-2D analysis in an idealized manner, utilizing a truss bar geometric stiffness to modify the flexural stiffness of the column elements. The P- Δ effect, however, is not considered. Recent general purpose nonlinear analysis codes like ANSR II [29] incorporate both of these effects. For the frame-coupled wall structure, the inclusion of either of these effects was not observed to be important after checking the maximum displacements and drifts in conjunction with the axial forces of the members.

3.3.7.2 Material Nonlinearities

In nonlinear analysis, material nonlinearities and hysteresis may be introduced at the material [2], cross section [45, 48], or the element level [17, 22, 33]. Introducing material nonlinearities at the element level enables time-history analyses of complete structures at an affordable cost. The main limitation of this technique, however, is that the plasticity of the members are lumped at concentrated plastic hinges which are assumed to occur at the ends of the members. In the actual response of reinforced concrete elements, the propagation of yield and the distribution of plastic distortion over a length of the element are important

characteristics. Introducing nonlinearity and hysteresis at the cross section level may have the advantage of incorporating these characteristics in the analytical model [45].

The element library of DRAIN-2D contains a beam-column and a beam element which were used to represent the walls/columns and the coupling girders/frame beams of the structure, respectively. These elements are discussed in the following.

1. The Beam-Column Element

The beam-column element in DRAIN-2D was used to represent the walls and the frame columns of the structure. The element is two-component, i.e., analytically it is assumed to consist of two parallel elements, one of which is linearly elastic with a constant stiffness equal to the deformation hardening stiffness that is assigned to the element. The second component develops perfectly plastic hinges at either end,* when an axial-flexural yield interaction curve indicates a state of yield. The required input data for the element consists of the axial force-flexure yield interaction curve, the deformation hardening stiffness and the flexural, shear, and axial stiffnesses of the cross section. These input quantities for a typical wall and frame column element are indicated in Fig. 3.3. These quantities were determined through a synthesis of the cross sectional analysis results given in Chapt. 2. The element model incorporates constant linear elastic cross sectional stiffnesses (flexural, axial, and shear), in conjunction with a bi-linear, force-deformation elastic hardening plastic hysteresis. The flexural, axial, and shear stiffnesses as well

* The element actually develops mechanical hinges, i.e., hinges with zero flexural capacity, while the plastic moment capacity is assigned as end forces to the element.

as the strain hardening slope synthesized* from the moment-curvature response corresponding to a "representative" axial force level should be taken as a basis for these inputs. These quantities should then be modified to represent the member force-deformation characteristics which incorporate a number of effects not considered in moment-curvature computations, the most significant being the bond slip and discrete cracking.

The main idealizations that require consideration regarding the beam-column element may be listed as:

(1) Force-deformation is bi-linear. Incorporation of a tri-linear force-deformation relation may be consequential on response history.

(2) Hysteresis is elastic-hardening plastic without degradation. Reinforced concrete elements generally dissipate less energy than is defined by such hysteresis. If the energy dissipated through the wall plastic hinges consists of a significant percentage of the total energy dissipated by the structure, this idealization may lead to errors in the dynamic response quantities and history.

(3) The effect of axial force on flexural stiffness prior to yielding is not incorporated. This is a significantly consequential idealization, regarding the distribution of shears and moments of

* The axial, shear, and flexural stiffnesses that are determined from cross sectional analyses (moment-curvature responses), are used to derive element stiffness relations by the computer code, assuming that these stiffnesses are representative for all the cross sections of the element. As it is not possible to define unique cross sectional stiffnesses over the length of a reinforced concrete element under a distribution of axial, shear, and flexure, "equivalent" stiffnesses should be used to represent the stiffness of the elements. These elements were assumed to have been subjected to internal force levels inducing flexural cracking.

the two walls and, therefore, leads to errors in coupled wall response.

(4) The shear deformations were incorporated through a linear cross sectional shear stiffness. The relative contributions of shear and flexural deformations were then predetermined by virtue of the mechanics of the 1-D element, i.e., by the relative contributions of the "EI" and "GA" terms in the element elastic stiffness expressions.

After flexural yielding occurs, the relative contribution of shear deformations to overall deformations of the analytical element becomes even less, as the linear (elastic) shear deformation terms become considerably less significant with respect to inelastic flexural deformation terms. This is an important shortcoming of the analytical element in representing the response pattern of walls. When shear walls are used efficiently, usually the unit nominal shear stress is high, and the shear deformations are already important in the linear phase, and its significance increases in the post flexural yielding phase. If shear is high when flexural yielding starts, then a sliding shear deformation mechanism can develop before significant inelastic deformations due flexural yielding may occur [24, 52, 53]. The wall slides over horizontal planes with deformation characteristics completely different from the deformation pattern of a cantilever hinged at the base, which is falsely implied by the analytical model.

(5) Axial force-axial distortion terms remain elastic. As studies indicate [48], a strong coupling between axial and flexural, as well as shear responses, exists in the case of coupled walls, and this can affect the assumed axial force-axial deformations.

2. The Beam Element

The beam element in DRAIN-2D was utilized to represent the coupling girders and frame beams of the structure. This is a

single-component element consisting of a linear element with a point hinge at each end with elastic plastic moment-rotation responses. These hinges are assumed to have hysteresis characteristics based on those defined by the Takeda model [50]. The hysteresis that is modeled by the element is thus stiffness degrading.

The required input for the element consists of the stiffness and yield strengths of the hinges at each end, the deformation hardening stiffness for these hinges, and the flexural, shear, and axial rigidities of the linear elastic portion of the member. These quantities are shown in Fig. 3.4, and were derived from the cross sectional analysis results given in Chapt. 2. The axial stiffnesses were not used in the analyses as the axial distortions of the beams were neglected by virtue of the axially infinitely rigid diaphragm assumption.

In preparing the input data, assumptions regarding the effective slab width and slab steel were required, as well as a representative axial force level to determine the correct yield strength, as discussed in Chapt. 2.

Many of the discussions on the idealizations regarding the beam-column element are valid for the beam elements as well. Assumptions regarding the hysteretic response are particularly important for the beam elements as a major portion of the energy dissipated by the structure during response is usually through beam plasticity. The analytical model does not incorporate the effects of bond and shear on flexural hysteresis. Care is required to incorporate the effect of bond slip (or concentrated end notations due to bond slip) in the analytical element by either reducing the flexural stiffness of the linear portion or by assigning finite pre-yield stiffness to the end springs in the elastic range rather than assuming these to be rigid-plastic. In this manner, these springs would not be rigid-plastic but elastic-plastic. Some reinforced-concrete analysis codes incorporate additional end springs to incorporate

the effects of bond slip [33].

In conclusion, deriving the correct input for beam axial, flexural, and shear rigidities requires a careful assessment of the possible distributions of these stiffnesses along the member, i.e., changes in effective flange width, effective slab steel, height of neutral axis, amount of tension, and compression reinforcement at different cross sections should be considered. As the stiffnesses would also depend on the previous loading history of the cross sections, assumptions regarding the previous levels and distributions of internal force and distortion before the dynamic response takes place are also required. It, therefore, appears that the representation of the stiffness of the complete beam element with unique values of axial, flexural, and shear stiffnesses is an oversimplification of the actual case where these properties vary along the length of the beam. A realistic estimation of the previous maximum levels of internal force and distortion are especially critical to assess the possible contribution of bond slip to the end rotations. If the beams are assumed to have yielded, then the contribution of bond-slip to the total end rotation should be considerably more critical [19] than the contributions of the other factors and this should be incorporated into the input.

3.3.7.3 Effects of Strain Rate

An implicit idealization regarding the effects of strain rate on the material stress-strain characteristics is made in establishing the inputs for the beam-column and the beam elements by considering the static properties of the materials. It is thus being assumed that the velocity of deformations would not affect the assumed force-deformation properties for the structural elements. It has been shown that the strain rate may affect the stress-strain characteristics and strength of concrete considerably [13]. The effects of this parameter on the response of reinforcing steel, however, are not as significant [46].

3.3.8 Numerical Aspects of the Model

The general formulation and solution schemes for the nonlinear equations of motion are considered in this context. Differences in available computer codes are observed regarding:

(1) The state determination, i.e., determination of the changes in the restoring and damping forces of the structure, and the implementation of these changes during the integration of the equations of motion.

(2) The numerical integration scheme for the equations of motion.

(3) Corrective measures to minimize the accumulation of errors due to the state determination and numerical interpretation schemes that are utilized.

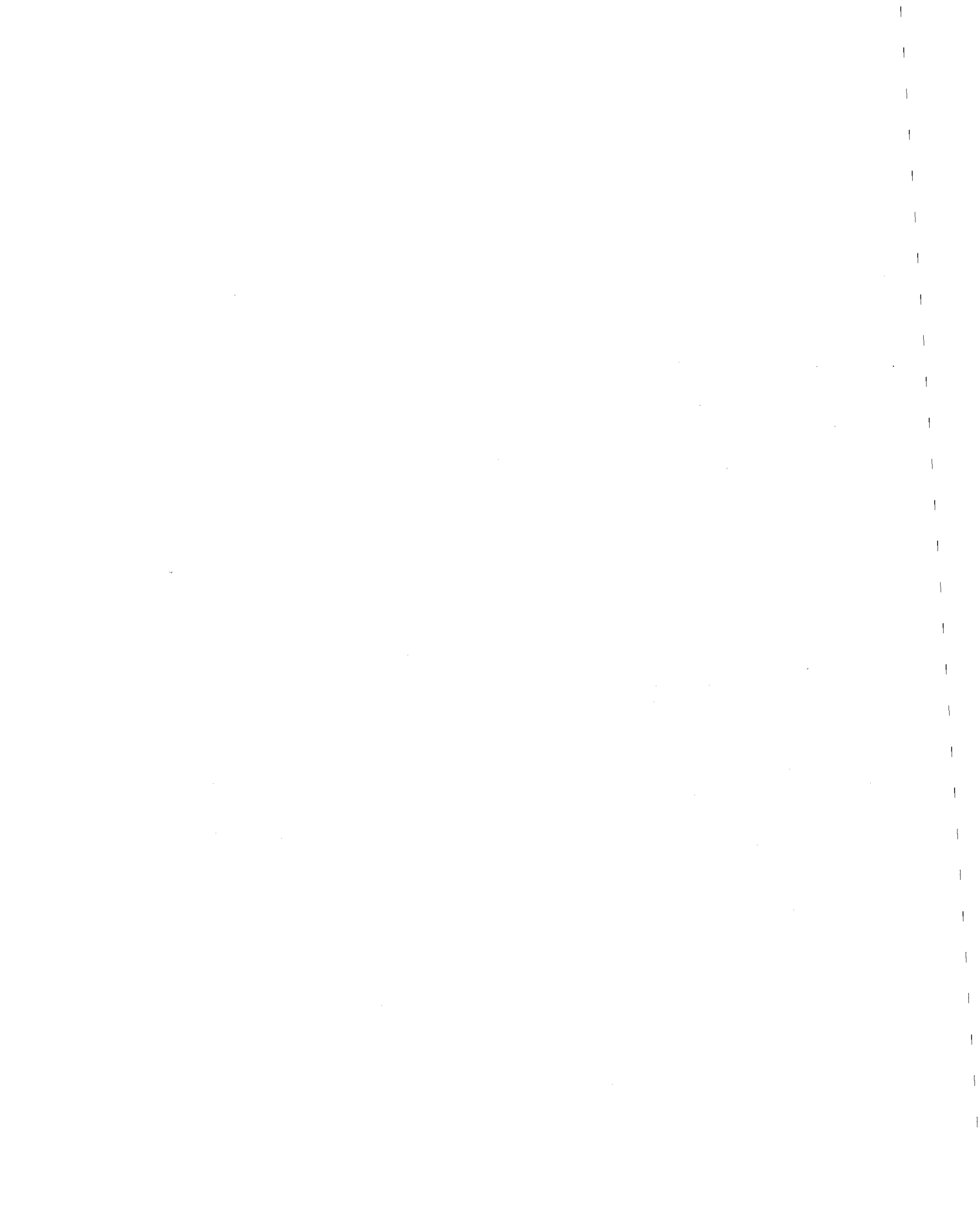
Available schemes for state determination and the corrective measures that are devised for different schemes are summarized by Zienkiewicz [56]. These schemes, mostly developed in conjunction with the general finite element theory, are adapted by computer code developers in general purpose nonlinear structural analysis codes.

The commonly used scheme for the numerical integration of the equations of motion is the one developed by Newmark [30]. Versions of this scheme, generally differing on the variation of acceleration within an integration step, are utilized in the structural analysis programs. In selecting DRAIN-2D as the code to be used in the analyses, the numerical aspects of the model that are built-in into this code are automatically accepted. The only parameter that the user may control in DRAIN-2D is the time step. No iterations are carried out on the element states during or subsequent to a time step, resulting in an equilibrium imbalance arising from nonlinearities in the structure. These imbalances are applied as residual forces to the structure during the next time step to eliminate the accumulation of the error. For the integration scheme, the acceleration was assumed to remain constant during the time step.

More recent codes such as ANSR II [29] enable a higher degree of user control on the numerical aspects of the model. In the case of ANSR II, the user may specify the parameters of the Newmarks' method [30], thus having a direct control over the assumed distribution of acceleration within the time step. Furthermore, the type of iteration, state determination, stiffness reformation and convergence criteria are specified by the user. These options give more freedom to the user at a certain cost. Cost was one of the important factors in the choice of DRAIN-2D as the analysis code, as, the simplicity in its solution processes is the main reason that DRAIN-2D is relatively affordable for extensive time-history analysis of complex structures.

Linear analyses were carried out to obtain the elastic response characteristics of the structure to form a basis for the selection of an appropriate time step for the analyses. These analyses are outlined in Chapt. 4. The first three periods of the linear frame-wall model were obtained as 0.99 sec., 0.28 sec., and 0.13 sec. respectively. For the analytical model of only the coupled wall in Fig. 3.2, these periods were 1.20 sec., 0.32 sec., and 0.15 sec., respectively. A time step of 0.02 sec. was then chosen based on: (1) the significant modal periods, (2) the possible interactions between the numerical idealizations and the response nonlinearities, and (3) the cost of analyses.

By choosing the time step of 0.02 sec., which is ~15 percent of the third period of the analytical model, it is acknowledged that some of the response characteristics which are influenced by the third and higher modes may not have been incorporated in the analyses. Also, the errors arising from equilibrium imbalances may have been significant enough to have affected the post-yield responses. Short trial analyses with a time step of 0.01 sec. indicated little change in the displacement and force responses as compared to those obtained with the 0.02 sec. time step. Hence, the 0.02 sec. time step was selected.



4. LINEAR DYNAMIC ANALYSES OF THE BUILDING

4.1 General

Linear spectral analyses of the structure were carried out using the computer code TABS [55]. The objectives of these analyses were:

(1) Study the linear dynamic characteristics of the analytical models of the building. (These models are shown in Figs. 3.1 and 3.2 and their development was discussed in the previous chapter.)

(2) Compare the code design (UBC-73) demands to the linear response demands arising from the ground motions that were considered (1940 El Centro, NS, and 1971 Pacoima Dam, S16E, Derived version).

(3) Investigate the effects of frame-wall interaction on the linear response characteristics of the structure.

4.2 Linear Dynamic Characteristics of the Structure

Lateral displacement profiles, mode shapes for the first three modes and the corresponding periods of the two models of the structure are given in Fig. 4.1. Cracked transformed cross sectional properties were defined for the member properties to obtain the displacements, mode shapes, and periods. In each model, one-half of the mass of each floor level was lumped at that floor level, as explained in Sec. 3.3.3. The same mass was thus assigned at the corresponding levels of the two models shown in Figs. 3.1 and 3.2. The 1973 UBC earthquake loads (Table 4.1) were applied to obtain the lateral displacement characteristics of the coupled wall-frame and the isolated coupled wall models.

The lateral displacement profiles of the two models shown in Fig. 4.1 indicate that the frames contribute to the average lateral stiffness of the structure in the order of 40 percent as the deflections of the isolated coupled wall model at the 8th and 15th floors are 1.44 and 1.47 times the deflections of the frame-coupled wall model at these floor levels, respectively. Furthermore, from the periods of the first mode corresponding to the two models, i.e., 1.20 vs. 0.99 sec., frame-wall

stiffness is 1.47 times the isolated wall stiffnesses. The effects of the frames on the mode shapes of the building are not significant, as indicated from Fig. 4.1. The periods, however, are altered in proportion to the square root of the ratio of the stiffnesses. The first three periods of the isolated coupled wall model are 21%, 14%, and 15% larger than the corresponding periods of the frame-coupled wall model. These periods are shown in Fig. 4.1.

4.3 Results of Analyses

The two models of the structure were analyzed by the modal spectral analysis option of TABS [55]. The linear acceleration spectra (with 5% damping) of the 1940 El Centro (NS) [47] and the 1971 Pacoima Dam (S16E, Derived) [41] ground acceleration records were used in the analyses. These acceleration spectra are shown in Fig. 4.2. Significant differences between the demands of the two ground motions are observed from these acceleration spectra for fundamental periods in the vicinity of 0.40 and 1.0 seconds.

The base shear and overturning moment demands from the coupled wall and frame are tabulated in Table 4.2, for the code (1973 UBC) specified "E" loading and the two ground motions. A significant increase (about 4 times for El Centro and approximately 12 times for the Derived Pacoima Dam motions) in the base flexural demands is observed in the case of spectral analysis as compared to the code demands, even after adjusting the "E" load demands by 1.4, thus incorporating the load factor of 1973 UBC for wall flexural design. Other observations made from this table are: The wall base shear and overturning moments were reduced when the frames were included for static (1973 UBC) analysis, and the DPD dynamic analysis, but they were increased for the El Centro analysis. The ground motion is, therefore, a significant variable in defining the effects of wall-frame interaction on the base shear and overturning moment demands. The frame base shears (for four frames, one-half of the building), were 18 percent of the base shear demands of one set of coupled walls

for all the static and dynamic analyses, as observed from Table 4.2 [i.e., $(4 \times 30)/656 = 0.18$].

The distribution of story shears along the height of the building, corresponding to one-half of the building, are shown in Figs. 4.3-4.5 for the static and dynamic (SRSS) analyses. The portion of the story shears resisted by the four frames of one-half of the building are also indicated in Figs. 4.3-4.5. It is observed that the contribution of the frames to the total story shear changes along the height of the structure as a result of the interaction. A SRSS analysis of only the first three modes of the structure was used to obtain these dynamic story shear distributions. These distributions, therefore, actually represent the envelope of the shear at each story, and the probability of occurrence of these envelope values at the same time is usually low. These distributions, however, were assumed to be probable in computing the moment to shear ratios at the base of the coupled wall when the frames were and were not included in the analyses. In each case of the static and dynamic analyses, the moment to shear ratio at the base of the coupled wall decreased (by ~15%) when the frames were included in the analysis. The distribution of frame shears for just one of the frames, during the static and dynamic responses of the coupled wall-frame model, are shown in Fig. 4.6.

The main observations from the linear analysis results may be listed as: (1) The inclusion of the frames in the analytical model of the building may increase the maximum dynamic base shear, depending on the ground motion; (2) The moment to shear ratio at the base of the coupled wall system decreases when the frames are considered in analysis. It is, therefore, concluded that static analysis of only the coupled wall system of the building for the purposes of design of the wall, as according to UBC, does not, in reality, result in a safer design of the wall system as compared to a design based on dynamic analysis where the wall-frame interaction is included in the analytical model. Although the UBC requires that a static analysis of walls and frames acting together should be considered as well, this situation leads to a lower base shear for the walls and does not govern the design of the lower floors of the walls.

The linear analyses were useful in showing that the structure, designed for the 1973 UBC code demands, would be subjected to base overturning moment demands approximately four and twelve times higher in the case of the El Centro and Pacoima ground motions. Depending on the overstrength provided to the structure, it may not require extensive inelastic energy dissipation to survive the El Centro ground motion. Extensive inelasticity should be anticipated, however, in the case of the Pacoima ground motion.

5. INELASTIC TIME-HISTORY ANALYSES OF THE BUILDING

5.1 General, Objectives and Scope

The general purpose nonlinear plane frame analysis code DRAIN-2D [39] was used to carry out time-history analyses of the building explained in Chapt. 2. The two analytical models of the building, developed in Chapt. 3 and shown in Figs. 3.1 and 3.2, were individually subjected to the El Centro [47] and Pacoima [41] ground acceleration records (Fig. 5.1). The analyses were conducted with the main objectives given in Sect. 1.2, some of which are now reviewed in greater detail:

(1) Assess the state of the art in analytical modeling of R/C buildings for the purpose of time-history analysis for response prediction. This was a major objective of the analyses. Inelastic time-history analyses of R/C buildings have been carried out both by researchers and professional engineers using general purpose inelastic analysis codes prepared for this reason [21, 27, 40, 44]. In certain cases the results of such analyses may have been interpreted and applied without adequate scrutiny and assessment of the uncertainties in modeling. It was, therefore, intended to carry out an especially critical review of the state of the art in analytical earthquake response simulation of reinforced concrete buildings with walls. This objective was considered in discussing and developing the analytical models in Chapt. 3. The results of the analyses will be interpreted with this same major objective.

(2) Investigate analytically the supply vs. demand relations for different limit states of response. This objective was selected as a means of assessing the soundness of code provisions that led to the present design of the building. The design philosophy of the code (UBC) specifies considerations of the serviceability, damageability and collapse limit states of response. Although the code demands corresponding to each of the different limit states

are not explicitly defined, the demand associated with the design lateral force, incorporating the appropriate load factors and the capacity reduction factors, as well as the applicable minimum requirements and reinforcement detailing provisions, is acknowledged to represent the beginning of the damageability demand at ultimate level. Quantitatively, this demand would be considerably higher than just the factored design lateral force, due to a large number of factors leading to different overstrengths of elements in axial-flexural, shear, and torsion responses, which will be discussed later.

The collapse limit state demand, according to the code, is implicitly characterized by flexural inelastic distortion levels four to six times that of the flexural distortions at yielding [43]. The design provisions, and particularly the detailing requirements, are assumed to safeguard against shear failure until these inelastic flexural distortions may be realized. To be able to quantify the ultimate limit state demand is considerably more complex than to establish the force levels for the beginning of the ultimate damageability limit state demand, as it is related to inelastic distortion rather than member force. Different types of ground motions, even if they may have similar peak acceleration magnitudes, may impose different levels of inelastic axial-flexural distortion demands and different ratios of axial flexural vs. shear force demands on the structural members.

The objective of analytically investigating the supply vs. demand relations of the building was undertaken together with an effort to define appropriate ground motions which may be considered as representative for the analyses of damageability and collapse limit state demands in regions of highest seismicity in North America.

(3) Investigate the effects of the frame-wall interaction at the damageability and ultimate limit state response levels.

5.2 Ground Motions

The ground motions selected for the analyses were the first

10 sec. of the S00E component of the 1940 El Centro ground acceleration record [47] and the first 10 sec. of the Derived Pacoima Dam Record [41]. The original S16E component of the Pacoima Dam record recorded during the 1971 San Fernando earthquake, was taken as a basis to obtain a derived version in order to represent the rock motion at the base of the dam. The ground acceleration records used in the analyses are shown in Fig. 5.1. The linear acceleration response spectra were shown in Fig. 4.2. The linear responses of the building to these ground motions were discussed in Chapt. 4.

The two ground acceleration records had peak accelerations only 17 percent different from each other (0.34 g for the El Centro and 0.4 g for the Pacoima records). The spectral acceleration demands, however, are observed to be considerably different from each other, observed from the spectra in Fig. 4.2, especially for the periods in the vicinity of 0.4 sec. and 1 sec. The acceleration (seismic force) demands of the Pacoima motion are observed to be more than twice the El Centro motion near these periods. These periods approximately correspond to the first and second periods of the two analytical models of the structure.

These ground acceleration records were selected for the time-history analyses due to: (1) their different characteristics, i.e., the El Centro motion is commonly accepted as a "white noise" type [31] while the Pacoima motion is representative of an "impulsive" type of earthquake, as observed from the accelerograms in Fig. 5.1. The responses of the structure, correspondingly, were expected to reflect the different characteristics of these motions; (2) Linear analyses carried out using the acceleration spectra of these records, presented in Chapt. 4, indicated that the response of the structure to the El Centro motion may lead to the beginning of the ultimate damageability level response, whereas the Pacoima motion should be expected to result in extensive inelasticity, which may characterize the near collapse limit state response. As explained in Sect. 5.1, one of the objectives of the analyses was to assess the responses at these limit states. Consequently,

these two ground motions were selected for the analyses without any scaling.

The duration of the ground acceleration records considered for the time-history analyses is an important parameter. In general, time-history analysis should be carried out through the total duration of the recorded ground excitation or until a collapse state for the structure may be realized. Limiting the duration of the analyses to 10 sec. was an idealization necessitated by the cost. In certain applications, the initial low-excitation duration of the ground acceleration record may be cut-off, starting the analysis with the high intensity portion of the record. This was not attempted as it alters the initial conditions of the response at the commencement of the high excitation duration of the ground acceleration record, which may be consequential in the computed maximum response quantities. Preliminary analyses carried out with the 15 sec. durations of the ground motions indicated that critical response maxima for the El Centro responses and all response maxima for the Pacoima responses were attained during the first 10 sec. of these excitations; hence, this duration was selected. It was thus assumed that accumulative inelastic deformations which may occur after the considered 10 sec. of response may be neglected in the assessments of the earthquake response of the structure.

5.3 Results of Analysis

5.3.1 General

The analysis code DRAIN-2D permits the retrieval of the following information: (1) The time-history of all nodal displacement quantities; (2) The time-history of all member end forces; (3) The time-history of all member plastic distortions, i.e., plastic hinge rotations; and (4) The envelopes of the response quantities in 1-3 at selected intervals. This data may be retrieved in the form of write-up on paper, magnetic tape, or both. The user may eliminate the generation of any part of this output, i.e., the analysis results may be obtained for only some of the members or, the time-history of any local or global response quantity may be obtained at less frequent intervals than the time step used in the analyses.

As the output phase of a time-history analysis involves considerable expenses, an optimization of the retrieved output is usually worthwhile. For the four analyses carried out in this study, only selected global displacements and member forces were specified. These were: (1) The horizontal displacement time-histories of each floor; (2) The flexure, shear, and axial force time-histories of all the wall elements; (3) The state of hinging and time-history of plastic rotation at the ends of all the elements. In addition, the envelopes of all the response quantities, i.e., all global displacements, all local forces and distortions, were obtained every 2 sec.

The time-history data was recorded on a magnetic tape which was subsequently processed to obtain computer plots. Additional data processing codes were prepared for reading the magnetic tape and plotting of the appropriate quantities.

5.3.2 Displacements-Distortions

5.3.2.1 Time-Histories of Lateral Displacements

The relative (to the base) displacement-time histories of the 4th, 10th, and 15th floors of the two models of the building when subjected to the El Centro and Pacoima ground motions are presented in Figs. 5.2 and 5.3. In each of these figures, the displacement responses of the coupled wall model and the coupled wall-frame model are compared.

The response histories in Fig. 5.2(a) and (b) indicate that for the El Centro excitation, higher mode effects are reflected on the displacement wave forms. This is not the case for the Pacoima responses in Fig. 5.3. A possible reason for this could be the different frequency contents of the two ground acceleration records. The El Centro record may activate the second and third modal responses of the models more so than the Pacoima record. Another reason for more apparent higher mode effects in the El Centro responses may be due to a lesser degree of inelasticity and softening experienced by the structure during the El Centro response as compared to the Pacoima response. An investigation of the level of inelasticity of the structure, which will be

discussed subsequently, revealed that the walls (and columns) remained linear during the El Centro responses of both models, while most of the coupling girders and frame beams developed plastic hinges at both ends. The walls of both models, as well as all coupling girder and frame beams, developed plastic hinges during the first large displacement excursion during the Pacoima excitation.

Comparison of the responses (to the El Centro record) in Fig. 5.2 indicates same maximum top displacements for the coupled wall, and coupled wall-frame models (4.98 in.). However, these maximum values occurred at different times (5.1 and 5.8 seconds) and in opposite directions. There are considerable differences in especially the top responses of the two models, indicating that the increased stiffness and, therefore, the frequency (due to the inclusion of the frames) of the coupled wall-frame model, in conjunction with the characteristics (frequency content and power, spectral coordinates and intensity) of the ground motion have led to different displacement response characteristics of the two models.

Comparison of the responses of the two models to the Pacoima record (Fig. 5.3) indicates that the response characteristics of the two models were more similar than in the case of the El Centro record. The maximum displacements have occurred in the same direction and at almost the same time. The number of zero crossings during the high excitation duration (2-10 sec.) are the same. The main difference between the responses of the two models appears to be a shifting of the center of vibration, i.e., a permanent offset displacement, observed in the case of the coupled-wall-frame model. As this model lacks the increased redundancy and energy dissipation capacity provided by the frames, its response exhibits a higher degree of unrecoverable deformation. Furthermore, the frames, when included in the model, resulted in a decrease of the maximum top displacement from 18.83 in. to 15.53 in., comparing to the coupled wall model, isolated from the frames. It appears that the energy demand of the earthquake was satisfied at a smaller lateral

displacement when the frames were included as this led to additional sources of energy dissipation, during the first inelastic excursion.

When the responses of the complete model (i.e., the coupled wall-frame model) to the two ground motions are compared, (Fig. 5.2(b) and 5.3(b)) noting the different displacement scales, significant differences in the displacement response characteristics caused by the two ground motions are observed. First yielding occurs at 1.94 sec. and 2.68 sec. for the El Centro and Pacoima responses, corresponding to top displacements of 2.46 in. and -1.78 in. for the two responses, respectively. The yielding locations and sequences will be discussed subsequently. The displacement direction is reversed soon after first yielding, after attaining 3.65 in. of top displacement during the El Centro response. The displacement at the top of the building had to increase to -15.53 in. before reversing, however, during the Pacoima response. The significantly higher inelastic displacement demands (energy demand) of the Pacoima motion is observed to arise from the main double large long duration pulse that exists between 2.4 - 3.7 sec. of the accelerationogram in Fig. 5.1

As discussed in Sect. 5.2, although the peak acceleration of the Pacoima record is only 18 percent higher than the El Centro record, the peak structural displacements caused by the Pacoima record is 3.12 times the corresponding displacement caused by the El Centro record. In conclusion, the structural response characteristics caused by the two ground motions are significantly different. This difference reinforces the requirement that different types of ground motions should be considered, rather than just one ground motion or only similar types of ground motion, before assessing a certain design or arriving at general conclusions regarding seismic response [12].

5.3.2.2 Effective Periods

It is possible to estimate "effective" structural periods from time-histories of displacements by counting the number of zero crossings during a certain duration. Periods, estimated in this manner, are compared to the fundamental periods computed for linear states of the

models (Chapt. 4) in Table 5.1.

It is observed from this Table that the linear fundamental period of the coupled wall model elongated from 1.20 sec. to 1.73 sec. (44%) during the El Centro excitation and to 1.89 sec. (58%) during the Pacoima excitation. The corresponding increases in the period of the coupled wall-frame model were 66% and 69%, for the El Centro and Pacoima excitations, respectively. The period elongations are observed to be larger for the coupled wall-frame model, i.e., during inelastic response the effective stiffness contributed by the frames is not as significant as it is during linear response. The period elongations in the Pacoima responses are considerably more than in the El Centro responses, as a consequence of the higher number of inelastic regions demanded by the Pacoima excitation which were in a state of yield simultaneously. Also, the effective periods during the earlier phases of the inelastic response are shorter than when the complete duration of inelastic response is considered, as shown in Table 5.1. This table demonstrates that, in general, substantial changes in the linear periods of a structure, depending on the level of inelasticity as well as the characteristics of the earthquake accelerogram, should be expected.

5.3.2.3 Displacement Profiles and Drifts

The profiles of lateral displacement at times corresponding to first yielding, maximum base shear, maximum base overturning moment, and maximum top displacement, are shown for the coupled wall-frame model, subjected to the El Centro and Pacoima ground motions, in Figs. 5.4 and 5.5. It is observed that the displacement profile associated with maximum base shear is influenced strongly with higher mode shapes. The displacement profiles associated with maximum overturning moment or maximum top displacement reflect the first mode shape.

A study of the envelopes of lateral floor displacements for the two models, caused by the two ground motions, may be carried out from

Fig. 5.6. The maximum lateral displacement demands of the El Centro excitation appear to be quite close for the two models along the height of the building. The top displacement demands of 4.98 in. are identical. The displacement demands of the Pacoima excitation along the height of the two models show a decrease of the top displacement from 18.83 in. to 15.53 in. when the frames are considered.

The displacement envelopes are not as useful as the drifts or drift indices (drift/story height) in assessing damage induced by a ground motion. It is possible to consider the drift of a certain floor relative to the base (total drift) or relative to the previous floor. The latter is commonly termed as the interstory drift. The best measure of damage, however, is considered to be the "tangential interstory drift" [28] obtained by eliminating, from the interstory drift, the rigid body component caused by the rotations of the structural system at the lower floors. A possible technique of computing tangential interstory drift is to subtract the interstory drift of the previous (lower) floor level from the computed interstory drift of the floor level under consideration. It follows, then, that it is usually the lower floors of a structure which experience the maximum tangential interstory drift and, therefore, the maximum level of damage.

The relation of the total, interstory, or tangential drifts to the actual damage realized by a structural system is not very explicit. The SEAOC recommendations [43] acknowledge a maximum interstory drift under the required lateral seismic forces, that for frame-wall structures is $(0.005)0.80=0.0040$, where 0.80 is the "K factor" used in computing the required seismic forces of the building. How this index is actually related to allowable distortions of different types of structural and nonstructural elements, as well as to the performances of the mechanical and electrical subsystems of the building, would depend upon the building and would require further investigations.

It is generally acknowledged that an interstory drift of 0.0025 would represent the allowable wind load distortion limit, and may be considered as the serviceability limit. The drift value given by the

SEAOC recommendations, 0.004 for buildings with dual bracing systems may be considered to reflect an initial damage-ability for nonstructural elements at ultimate state. It is important to realize, however, that different structural and nonstructural systems would have different drift limits at which damage and collapse are undergone. The bottom floor of a coupled shear wall structure may have brittle shear failure at a drift index of 0.01 while the corresponding floor of a ductile frame system may tolerate a drift index of 0.02 without extensive distress. The limitations of service and damage level drifts will, therefore, depend on the structural system and the mode of failure of the system (as affected by the levels of axial-flexural and shear forces).

The maximum interstory and tangential drifts and indices obtained for the two models of the building subjected to El Centro and Pacoima ground motions, are tabulated in Table 5.2. It is observed that in the El Centro responses of both models, although the maximum displacements are identical, the maximum interstory drifts of the two models are different. The coupled wall-frame model has about 10 percent less maximum drift than the coupled wall model.

The maximum interstory and tangential interstory drifts do not occur at the same levels of the building. The distributions of the maximum drifts along the elevation of the building obtained for the coupled wall-frame model subjected to the Pacoima excitation are shown in Fig. 5.7. The distribution of the drifts during the same analysis at the times of maximum base overturning moment and maximum top displacement (3.1 and 3.2 sec., respectively) are presented in Fig. 5.8. It appears that while the interstory drift is larger at the middle and upper floors of the building, the maximum tangential interstory drift is larger at the first story.

The maximum interstory drift indices obtained for the El Centro and Pacoima analyses of the coupled wall-frame model, 0.0028 and 0.009 respectively (Table 5.2), indicate that the Pacoima ground motion induced 3.2 times more drift than the El Centro. Relating these drifts to

actual damage, however, cannot be readily carried out, as explained before. In tests of isolated walls, similar in geometry and detailing to the walls of the coupled wall system [24, 52, 53], the tangential interstory drift indices corresponding to yielding and failure, under cyclic load histories, were 0.003 and 0.026, respectively.

5.3.2.4 Distribution of Plastic Hinging during Response

The study of the element states (state of plasticity at the ends of each element) is useful in assessing the damage experienced by the structure during the ground excitation. As discussed in Chapt. 3, the analytical model used in conjunction with DRAIN-2D prescribes locations of concentrated plastic hinging at the ends of each beam or column/wall element. In the experimental studies of deep girders, and especially the wall element responses, the cracking of concrete and yielding of reinforcement as caused by the axial-flexural and shear effects were observed to spread over the entire length of these elements. It is observed only for slender members ($a/d > 3.5$) that plasticity may be confined to a relatively short region that is nevertheless, at least as wide as the depth of the member. The plastic hinge distributions obtained from the analyses should, therefore, be interpreted with caution. Some of the plastic hinge occurrences or reversal of the direction of the plastic rotation, may be erroneous, depending on the time step, characteristics of the structure, and characteristics of the ground motion. A possible source of error in the numerical computation scheme should also be considered, as the correct element states are not implemented during the computations, as explained in Chapt. 3.

The distribution of plastic hinges of the coupled wall system at various time instances during the El Centro excitation of the coupled wall-frame model are shown in Fig. 5.9. The frame columns remained linear while only the shorter span frame beams between 6th and 14th floors developed plastic hinges during this excitation. It was observed, for the complete duration of the El Centro response, that

the maximum number of coupling girder plastic hinges and their locations were as indicated for 2.04 sec., Fig. 5.9. The maximum frame beam plastic rotation was 0.0006 radians as opposed to the maximum coupling girder plastic rotation of 0.0037 radians, which occurred at the 7th and 10th floors of the building at 5.8 and 2.04 sec. of response, respectively.

The distribution of plastic hinging during the first major displacement excursion of the Pacoima response is shown in Fig. 5.10. Following the spreading of plastic hinging over the coupled wall system from 2.68 sec. to 3.02 sec. of response, it is observed that the system is subjected to a monotonically increasing seismic force (and, therefore, distortion) demands during this time period. This pattern of response is caused by the first main long acceleration pulse of this earthquake. This long pulse, which starts at 2.37 sec., very rapidly reaches a large peak effective acceleration of 130 in./sec.² (0.34g) and then decreases to zero at about 3.02 sec., affected the structure similarly in manner to a continuously increasing monotonic lateral loading.

The distribution of plastic hinging over the complete coupled wall-frame system at 2.98 and 3.00 sec. of the Pacoima response is presented in Fig. 5.11. It is observed that the coupled wall system has developed a sufficient number of plastic hinges to form a mechanism at 2.98 sec. The stiffness provided by the deformation hardening of the plastic hinges and the frame columns provide the restoring force capacity of the structure. The wall under tension is observed to develop another hinge at the base of the second floor (where the axial tension is higher than at the first floor, at this time) at 3.00 sec., as indicated in Fig. 5.10. The moment gradient along the first floor wall member is decreased significantly due to the occurrence of this last plastic hinge. As a consequence, a major part of the shear force carried at the base of the wall under tension was released, as will be observed in the time histories of wall shear forces presented in next section. The sudden release of the shear force that is carried by a wall member may occur in reality if the

wall suddenly breaks and yields in tension throughout its cross section, or if the wall panel has a brittle compression-shear failure. It is not realistic, however, that a wall member having a height/width ratio smaller or equal to 1 and under tension would develop concentrated plastic hinges at each end and consequently, suddenly release its shear force while the seismic shear demands from the structure are still monotonously increasing, as indicated by the plastic hinge patterns at 2.98 sec., and 3.00 sec. in Fig. 5.11. This occurrence demonstrates an extremely critical limitation of the one-dimensional beam-column element modeling of a shear wall element. The actual axial-flexural and shear responses and the interactions between these responses are significantly more complex for a wall element than may be represented by the mechanics of a one-dimensional beam-column element when the height (length or span)/depth (width) ratio of the wall is smaller or equal to 1.

The maximum coupling girder rotation was observed to be 0.02 radians at 3.26 sec. at the 13th floor (5.4 times the maximum coupling girder rotation attained during the El Centro response). A maximum frame beam plastic rotation of 0.0056 radians (at 3.24 sec.) at the 12th floor was recorded. The walls under tension and compression developed base plastic rotations of 0.00175 radians and 0.00124 radians at 3.04 sec., respectively. These plastic distortions indicate that although the Pacoima ground motion resulted in substantial plastic rotation demands from coupling girders and walls, as well as frame beams, they are lower than what well-detailed girder and wall regions can develop.

5.3.3 Force Responses

5.3.3.1 General

The shear force, axial force, and bending moment responses of the coupled wall system, obtained from the time-history analyses of the two models of the building subjected to the El Centro and Pacoima ground motions, are presented in the following sections. The maximum force

responses and the moment/shear ratios at the base of the coupled wall system are summarized in Table 5.3.

5.3.3.2 Shear Force Time-Histories

The time-histories of the shear force at the bases and fourth floors of the walls of the coupled wall system are shown in Figs. 5.12-5.15. The fourth floor shears were obtained particularly to derive the force histories to be applied during the experimental investigations of a 4-1/2 story 1/3-scale model subassemblage of the coupled wall system [4].

The responses in Figs. 5.12 or Fig. 5.13 indicate that the shear forces of the two walls of the coupled wall system during the El Centro excitation were identical. As the walls remained linear during these responses, and since the analytical model recognizes the same elastic flexural stiffness for the wall members regardless of the level of axial force, the shear forces were computed to be identical.

Another observation from Fig. 5.12 and 5.13 regards the ratio of the fourth floor and the base shears during the response - this ratio is observed to change, indicating influence of higher modes on the distribution of shear force along the walls. The double peaks and high average frequency (higher than the fundamental frequencies) of the time histories of shear, support this observation. The maximum base shears of the coupled wall system during the El Centro excitation were 2414 kips at 4.9 sec. and 2675 kips at 4.8 sec. for the coupled wall and coupled wall-frame models, respectively, as shown in Table 5.3. The higher stiffness of the coupled wall-frame model is observed to have resulted in the attraction of a higher maximum base shear of the coupled wall system.

The time-history of wall shears during the Pacoima responses of the two models are presented in Figs. 5.14 and 5.15. It is observed that the fourth floor and base shears are different in both walls, this is unlike the El Centro responses. During the first response peak at 2.98 sec., as discussed in the previous section, the right wall which

is subjected to a tensile force does not resist as much shear at the base as the left wall. The base shears of the walls, during the first large displacement cycle shown in Figs. 5.2 and 5.3, have approximately the same period as the displacements, indicating that the seismic shears exhibited a similar pattern of increase and decrease as the lateral displacements, i.e., a first mode shear distribution during the critical large displacement cycle (between 2.3 and 4.3 sec.).

It was the existence of a severe long duration acceleration pulse in the Pacoima ground motion that led to the substantially higher demands than the El Centro motion. The maximum base shears of the coupled wall system was 3718 kips at 3.0 sec. and 4053 kips at 3.5 sec. for the coupled wall and coupled wall-frame models' responses, respectively. The stiffer coupled wall-frame model attracted considerably more shear than the coupled wall model, such that just the share of the coupled wall model was approximately 10 percent higher than when the frames were not included in the model. This increase was 11 percent for the El Centro excitation. The existence of the frame system, although it increases the redundancy and stabilizes the complete structural system, in return increases the dynamic demands from the coupled wall system. Another effect of the frames is to decrease the moment to shear ratio at the base of the coupled wall system, at the time of the maximum shear. This is observed from the last column in Table 5.3. The moment to shear ratio at the base of the coupled wall system at the time of maximum base shear decreased from 0.40H to 0.33H for the El Centro response and from 0.46H to 0.30H for the Pacoima response, when the frames were included in the analytical model. This effect of the frames will be discussed further in the next section.

5.3.3.3 Distribution of Seismic Shears throughout the Structure

The distribution of seismic shears along the elevation of the coupled wall system corresponding to the times of maximum base shear and maximum base overturning moment of the coupled wall system are presented in Figs. 5.16-5.19. The distributions obtained for the El Centro analyses are shown in Figs. 5.16 and 5.17, for the coupled wall

model and the coupled wall-frame model, respectively. Similarly, the corresponding results from the Pacoima analyses are shown in Figs. 5.18 and 5.19. From these figures, considerable differences between shear distributions at the time of the maximum base shear and base overturning moments are observed. These differences are best characterized by the ratio of the base shear to the base overturning moment (designated as α) of a certain seismic force distribution. These α values are significantly smaller at the times of the maximum base shear as compared to the times of the maximum overturning moment, regardless of the model or the ground motion considered. Furthermore, the α values at the time of maximum base shear decreased when the frames were included in the analysis, regardless of the ground motion considered in the analyses.

These observations are significant when the code shear design process of the wall system is considered [4]. First, the flexural and shear designs of a wall system are carried out using the same lateral force distribution. In the 1973 UBC, on which the design of the building was based, a load factor of 2.8 is used in shear design, as opposed to a load factor of 1.4 used in the flexural design. In 1979 UBC, the load factor to be used in shear was decreased to 2 from 2.8. In the ATC 3-06 [7] provisions, same load factor is used for both flexural and shear designs.

Another factor utilized by the codes in design is the strength reduction factor. A factor of 0.85 in the UBC codes and 0.6 in the ATC provisions are prescribed for this purpose for the shear design. The strength reduction factors used in the flexural design of the walls are not explicit as the edge members of the walls are designed to carry all axial-flexural demands assuming these to be pure axial load members. The strength reduction factors in UBC and ATC 3-06 for pure compression are 0.75 or 0.70, depending on whether hoops or spiral reinforcement is used, respectively. In pure tension, both UBCs and ATC 3-06 prescribe a factor of 0.85.

One of the basic criteria in the seismic design of reinforced concrete structures is to avoid premature shear failure before sufficient flexural yielding generates adequate energy dissipation. It should be guaranteed, therefore, that the shear strength of the structure under the combined state of stress induced by axial and flexural forces exceed the maximum shear that may be demanded during an earthquake, in conjunction with the axial-flexural capacity provided to the structure. As an idealization, assuming that the actual axial-flexural strength provided to a coupled wall system is actually equal to the nominal strength which is controlled by $1.4 E/\phi_f$ (where E is the total seismic shear, 1.4 , the load factor and ϕ_f the capacity reduction factor in axial-flexure), the design shear strength of the wall should be larger than the shear that can be developed, which corresponds to a load $(1.4E/\phi_f)(\alpha_f/\alpha_s)$, where α_f and α_s are the base overturning moment to shear ratios corresponding to the times of the maximum base overturning moment and maximum base shear. If this load condition is satisfied, in designing for shear, the structure will be able to reach its flexural yield capacity before its shear capacity, regardless of the distribution of seismic shears throughout the earthquake.

Assuming ϕ_f to be an average of 0.8 , the quantity $(1.4 E/\phi_f)(\alpha_f/\alpha_s)$ becomes $3.77E$ for the El Centro response of the coupled wall-frame system, i.e., the shear capacity of the coupled wall system should exceed $3.77E$ in order to guarantee flexural yielding occurring before shear failure, while the structure is subjected to the El Centro excitation. The 1973 UBC code required shear strength, as discussed previously is $3.29E$ ($=2.8E/\phi_s$, where ϕ_s is the capacity reduction factor in shear, 0.85). The 1973 UBC required load for estimating the required design shear strength is, therefore, close to but inadequate to guarantee against shear failure before flexural yield. The shear strengths required by 1979 UBC or ATC 3-06, normalized with respect to the same flexural design strength, are

even less than the shear strength required by the 1973 UBC code.

Considering the Pacoima response of the coupled wall-frame system, the quantity $(1.4E/\phi_f)(\alpha_f/\alpha_s)$ becomes 6.4E, significantly larger than 3.29E, the load for which shear strength design is required. Thus this indicates that shear failure at the base before flexural yielding is a strong possibility during the Pacoima response.

The discussion of whether the walls may undergo shear failure before flexural yielding and adequate flexural energy dissipation will be repeated again in a broader context in the next chapter. In reality, neither the supplied flexural strength nor the available shear strength of a coupled wall system may be estimated accurately by the code expressions, as there are a considerable number of sources of additional strength (overstrength) in both flexure and shear. Furthermore, the requirement to guarantee against shear failure before yielding may be satisfied with different moment to shear ratios, depending on whether the time of maximum shear is before or after the time of maximum overturning moment. All these will be discussed subsequently.

The envelopes of the seismic shear demands along the structure, obtained for the Pacoima and El Centro analyses are shown in Figs. 5.20 and 5.21. Fig. 5.20 presents the maximum shears attained at each floor of the walls during the analyses of the coupled wall system. The shear envelopes of the two walls are identical except for the base and the first floor (second story) envelopes obtained during the Pacoima responses. The change in the maximum shear responses of the base and the first floor (second story) is due to the yielding of the walls at the base and of the wall in tension just above the first floor.

The shear envelopes of the individual walls and the frame system of the coupled wall-frame model are presented in Fig. 5.21. The shear envelopes of the walls are identical for the El Centro responses. Also, the maximum shear attained by the frame is approximately constant

over the elevation of the building for the El Centro response. The shear envelope attained for the Pacoima response indicates different maxima at the base of the walls. The frame contributions are larger than the contributions of each wall at the two uppermost floors. The frame contributions from the second floor up are considerably uniform, similar to the El Centro response.

5.3.3.4 Axial Force Responses of the Walls

The time-histories of the axial force at the base and fourth floor of each wall (labeled in the figures as right and left wall), obtained during the El Centro and Pacoima analyses of the coupled wall and the coupled wall-frame models, are presented in Fig. 5.22-5.25. From these figures it can be seen that the change in axial forces at a given story of the two walls and at any time are equal in magnitude, but opposite in sense when the gravity load is considered as the line of reference for the changes in axial force. This is a consequence of the fact that changes in the wall axial forces with respect to the gravity loads arise from the changes in the shear forces at the ends of the coupling girders, which are equal in magnitude but opposite in sense at the ends of each girder. Unlike the shear force histories, higher mode effects do not appear significant in the axial force responses in Figs. 5.22-5.25.

The time of occurrence of the maxima of the tensile and compressive axial forces in the wall piers is indicated on the time histories. Computations showed that these times also corresponded to the time of the maximum base overturning moment at the base of the structure. The maximum bending moments at the base of individual walls did not occur at the same time. The coupling axial forces at the base contributed more than the wall bending moments to the total overturning moment resistance at the time of the maximum base overturning moment, for all the analyses. Consequently, the time of the maximum overturning moment coincided with the time of the maximum axial forces at the base.

The contributions of coupling forces and wall moments to the

base overturning moment resistances continuously changes, as expected, during response. At the time of maximum base overturning moment, these contributions were 64%, 18%, and 18% for the coupling action and bending moments of the walls under compression and tension, respectively, for the El Centro response of the coupled wall frame system. During the Pacoima response of the same system, these contributions were 51%, 30%, and 19%, respectively. As the walls yielded during the Pacoima excitation, the contributions of the walls under compression and tension were different. In reality, there should have been a difference even when the walls did not yield, due to the effect of axial force on flexural stiffness prior to yielding. This effect is not incorporated in the analytical model, as explained in Chapt. 3. It is of interest to note that the maximum wall axial forces for the coupled wall model is somewhat larger than for the frame-coupled wall model.

The envelopes of tensile and compressive axial forces in the walls at each floor level are shown in Figs. 5.26 and 5.27. It is observed that the wall axial forces at the base were decreased when the frames were included in the analyses. The maximum decrease was in the maximum wall tensile force, in the case of Pacoima responses, which was 10 percent (Fig. 5.27). The decrease caused by the contribution of the frames is a considerably advantage in utilizing the frames in addition to the wall system, as high magnitudes of axial force in the walls are indications of a number of critical problems, as explained in Chapt. 1 and elaborated in the following.

The maximum quantities of compressive and tensile forces observed at the base of the walls during the El Centro response of the coupled wall-frame system was 5646 kips and -1090 kips, respectively. These values were 6267 kips and -1671 kips, respectively, during the Pacoima response of the same system. The code (1973 UBC) axial force demands for the factored E loading ($1.4E + 1.4D + 1.4L$ and $1.4E + 0.9D$) were 4636 kips and -96 kips, at the base of the walls in compression and tension, respectively.

These figures indicate that the El Centro induced compressive force is 22 percent larger than the code demand while the tensile force obtained from analysis is 11.4 times larger than the code demand. The tensile force of -1090 kips, obtained for the El Centro response, results in a tensile stress of 244 psi, which does not appear to be sufficiently high to induce cracking for a design nominal concrete strength of 4000 psi.

The maximum axial forces obtained during the Pacoima response, 6267 kips of compression and -1671 kips of tension, are 1.35 and 16.88 times larger than the factored design loads defined by the 1973 UBC code. The compressive force is 74 percent of the balanced force of the cross section, which is significantly high and likely to result in an impairment of the inelastic (plastic) rotation capacity of the wall at the base. The inelastic rotation demand at the base of the compression wall at the time of occurrence of this maximum compressive force is 0.00124 radians.

It should be emphasized that this inelastic rotation is associated with a rigid-plastic point hinge, as explained in Chapt. 3, and should be interpreted with caution. It is an adequate indication, however, that the Pacoima excitation may require substantial inelastic end rotations from the wall. Whether the wall may provide this rotation capacity in conjunction with a compression of 6267 kips, 74 percent of its balanced force capacity is questionable and should be investigated experimentally. Most of the experimental studies on walls incorporated significantly smaller levels of axial force [4]. The moment-curvature responses in Fig. 2.8(a) indicate that a cross sectional curvature capacity of two to three times the approximate yield curvature are available at similar levels of axial force. Although it is not possible to relate curvature capacity to rotation capacity directly, this is sufficient indication that the wall may not possess the deformation capacity that is required due to the level of high axial compression.

The maximum tensile force of -1671 kips, obtained at the base of the wall under tension during the Pacoima response, is equivalent to 374 psi tensile stress at the cross section, which, when coupled with the flexure and shear, should be expected to cause significant cracking and loss of shear and flexural stiffness of this wall as compared to the compression wall.

These levels of axial force are a direct consequence of the flexural capacities of the coupling girders. The slab steel, which would cause an increase in the negative moment capacity, was not included in these analyses. The axial load levels may have been increased 10-30 percent, depending upon the amount of slab steel considered as effective.

5.3.3.5 Flexural Responses of the Walls

The wall bending moment time-histories, at the base and fourth floor level of each wall, obtained during the El Centro and Pacoima analyses of the coupled wall and coupled wall-frame models, are shown in Figs. 5.28-5.31. The maximum moments occurring at the base of the walls are indicated on these figures.

The bending moment responses of each wall during the El Centro excitation of the coupled wall or coupled wall-frame models are observed to be identical. In general, a difference in wall bending moments should have occurred if the effect of axial force on flexural stiffness was incorporated in the analyses. Even when this effect is neglected, different positive and negative moment yield capacities of the coupling girders would have been expected to cause a difference in the moment responses of individual walls. As the contribution of slab steel was neglected, and since the beam positive and negative moment reinforcements and, therefore, the corresponding flexural capacities of the coupling girders were very close to each other, this effect cannot be detected from the moment responses at the fourth floor level or at the base, in Figs. 5.28 and 5.29.

The bending moment responses at the base of the individual wall piers to the Pacoima excitation are observed to be different, as the walls yielded at different times and, therefore, flexural stiffnesses differed from each other. The fourth floor responses, however, remain similar, i.e., yielding of the wall at the first floor does not appear to influence the flexural stiffness of the fourth floor. This does not seem logical, and changes in the fourth floor moment responses of the two walls, due to different moment responses at the base, would have been expected in Figs. 5.30 and 5.31.

The bending moment envelopes of an individual wall pier obtained during the analyses are presented in Fig. 5.32. Although the presence of the frames has not affected the maximum moments at the base of the wall, their presence is observed to decrease the wall maximum moments between the third to eleventh floors of the structure. This decrease is considerable for the Pacoima excitation; the moment envelope of the eighth floor is reduced by approximately 25 percent when the frames were considered in the analyses.

The maximum moments observed at the base of the structure during the Pacoima responses are dependent on the defined flexural capacity, as the walls yielded during these responses. The maximum bending moment obtained during the El Centro responses is approximately a half of the maxima obtained for the Pacoima responses. The factored 1973 UBC code flexural demand (1.40E load demand) at the base of one of the walls was 268×10^3 kip-in., as opposed to the 490×10^3 kip in., maxima obtained during the El Centro responses of the coupled wall-frame model.

Hence, the El Centro moment demand is double the factored (1.40E) code demand. From the point of view of only the moment demand, this earthquake imposed approximately double the demand considered by the 1973 UBC code which, as discussed previously, could be considered as the initiation of the damageability at ultimate state demand. However, the actual provided flexural strength, especially corresponding to

axial force levels below the balanced force, is generally significantly higher than the design demand. This will be discussed in the next chapter, where results of code analysis, linear dynamic analyses, and time-history inelastic analyses, are compared.

To provide an assessment of both axial and flexural responses at the bases of the individual walls, the moment-axial force relations at the bases of walls obtained during the analyses of the coupled wall-frame model, are presented in Figs. 5.33 and 5.34. These figures indicate the axial force-moment domains in which the wall cross sections at the base remained during the excitations. The eccentricity is observed to be changing continuously. The axial flexural and shear stiffnesses during dynamic response should, therefore, be expected to be continuously changing and varying between significant limits, judging from these figures.

Another observation made from Fig. 5.34 regards the force-deformation relations utilized for the elements, i.e., yield is defined by imposing a mechanical hinge rather than a plastic hinge and by updating the member force vector to maintain the yield moment in this vector, for the elastic-plastic component of the two-component analytical element (DRAIN-2D manual). Consequently, the axial force-moment pair do not "travel" along the yield surface, as would be required by the plasticity theory, but are withdrawn back into the elastic domain by excitation, i.e., the unloading of the plastic hinge from the location where they first approached the yield surface. It appears then, that if the simulation of the plasticity of the analytical elements were more realistic, significantly different post-yield force histories may have been attained for these members. Analysis codes like ANSR [29] utilize elements for which force-displacement relations are defined by generalized flow rules. These codes, however, were not utilized due to their significantly

higher costs and because they cannot overcome other problems in analytical modeling of reinforced concrete which may be more consequential on the simulated response. These problems were investigated in detail in Chapt. 3.

5.3.4 Responses of Coupling Girders

The moment-plastic rotation responses of the plastic hinges at the left and right ends of the fourth floor coupling girder, obtained for the El Centro response of both the coupled wall and the coupled wall-frame models, are presented in Figs. 5.35 and 5.36, to illustrate the typical hysteretic responses of the coupling girders. Comparison of the responses of the left and right plastic hinges indicate [Fig. 5.35(a) vs. 5.35(b) or Fig. 5.36(a) vs. 5.36(b)] that these are close to being anti-symmetric, except for the difference (17 percent) in the negative and positive yield moments defined for this beam. The responses obtained for the coupled wall-frame model (Fig. 5.36) indicate moment-rotation histories different from the responses obtained for the coupled wall model (Fig. 5.35).

The moment-plastic rotation hysteresis relations are pre-defined in the computer code after the Takeda [50] hysteresis rules. The relations in Figs. 5.35 and 5.36 should, therefore, be in accordance with these hysteresis rules. The irregularities and deviations observed in these figures from the pre-defined hysteresis relations are caused by numerical errors arising from the magnitude of the time step used in the integration of the equations of motion. Consecutive points, defining the moment-rotation hystereses, are observed to be spaced too far apart during certain moment or rotation increments to have the computed hysteresis relations in perfect accordance with the pre-defined hysteresis rules.

The moment-plastic rotation relationships of the same beam, obtained

during the Pacoima response of the coupled wall-frame model, are presented in Fig. 5.37. Compared to the El Centro responses in Fig. 5.36, the irregularities due to the numerical errors arising from the integration time step are observed to be less. The magnitudes of the rotations attained during the Pacoima response are approximately 600 percent of the rotations attained during the El Centro response. This is demonstrated further in Fig. 5.38 in which the envelopes of maximum plastic rotations attained for the coupling girders are presented. It is observed that the presence of frames reduced the maximum rotation demands from the coupling girders, especially for the upper floors of the structure during the Pacoima response. This may be explained not only by the additional sources of energy dissipation provided by the frame beams, which would result in a decrease in the energy dissipation demands from the coupling girders, but also by the change in overall lateral deformation caused by the interaction. Consequently, the maximum plastic rotations of the girders should be expected to decrease when the frames are included in the analysis, which is observed to be the case, in Fig. 5.38. The results presented in Fig. 5.38 indicate that the addition of the frame is of great benefit in decreasing the large plastic rotation demands from the coupling girders of the upper stories of just isolated coupled wall systems which result from the lateral distortion pattern of this system.

Another observation from this figure is the substantial difference in the maximum plastic rotations attained during the El Centro and the Pacoima responses. For the coupled wall-frame model, maximum plastic rotations in the order of 0.02 radians and 0.003 radians are attained during the Pacoima and El Centro responses, at the twelfth and seventh floor levels, respectively. Whether the actual girders would possess plastic rotation capacities in the order of 0.02 radians would depend on the shear stress in conjunction with which this rotation would occur. The rotation history with which the maximum rotation is associated should also be considered in assessing

whether the analytically computed rotations may be supplied by the beam. The "cumulative rotation index" is, therefore, a useful measure as it is computed by adding all the post-yield rotations (in both bending directions) attained by the beam at a particular hinge throughout the response. Such indices obtained for the coupling girders are presented in Fig. 5.39. It is observed that the inclusion of the frames results in a decrease of the maximum cumulative rotation index of the coupling girders at the upper floor (12th-15th) girders during the Pacoima responses. For the coupled wall-frame model, CRI values in the order of 0.19 were attained at 12th-15th floors, during the Pacoima excitation. Comparing the maximum rotation of 0.02 radians and the cumulative rotation index of 0.19 with the experimental responses of reinforced concrete beams [10,25], these flexural distortion demands were observed to be available only when the nominal shear stress was less than $5 \sqrt{f'_c}$.

The distribution of the maximum positive and negative bending moments attained for the coupling girders during the analyses of the coupled wall-frame model are presented in Fig. 5.40. The coupling girders were designed in three groups, as explained in Chapt. 2, based on code demands obtained through linear analysis. The earthquake response demands are, therefore, regulated by the available yield capacity and deformation hardening characteristics, as defined for the analytical model in Chapt. 3. The contribution of the slab steel was neglected, as explained in Chapt. 3, in defining the coupling girder strength and stiffness characteristics.

The maximum shear stress attained by the coupling girders during the responses of the coupled wall-frame system are shown in Fig. 5.41. The maximum shear forces and moments obtained for the coupling girders are also tabulated in Tables 5.4 and 5.5. It is observed from Fig. 5.41 that the maximum shear stress is attained for the 9th floor beam during the Pacoima response as $5.14 \sqrt{f'_c}$, based on a concrete strength of 4000 psi. It follows, therefore, that the available coupling girder

flexural distortion capacities may be just adequate under these shear stresses in the order of $5 \sqrt{f'_c}$ or less, based on previous experimental studies on reinforced concrete beams of similar geometry as well as longitudinal and transverse steel quantity [10, 25].

An observation from Table 5.4 regards the effects of the frames on the girder demands. The frames appear to decrease the girder moment demands slightly (5%) for the Pacoima responses. A slight increase in the girder demands of 2% is observed in the El Centro responses when the frames were included in the analysis. Deformation hardening characteristics defined for these girders were 4% of the elastic stiffness, should be expected to cause considerable differences in the global response, as the strength and stiffness characteristics of the coupling girders were observed to be the critical parameters affecting response in previous studies, as explained in Chapt. 1. Further analytical studies which would incorporate different inputs for the coupling girders based on different modeling assumptions should be carried out to study the sensitivity of the response to these parameters.

6. EVALUATION OF STRUCTURAL RESPONSE

6.1 General

Evaluation of the structural response was the primary objective of the inelastic time-history analyses as this also leads to an assessment of the soundness of the design provisions used which resulted in the final proportioning, reinforcement detailing and the choices for the nominal material strengths of the structural members and their connections. The selection of the structural system and its preliminary proportions, as well as the final design process based on the Uniform Building Code provisions, as presented in Chapt. 2, constitute what can be considered the state of the practice in the design of reinforced concrete coupled wall-frame structures in regions of high seismic risk in the Western United States. A critical assessment of the analytically generated structural response is, therefore, also an analytical means of assessing this state of the practice, provided that the limitations of the analytical processes through which the structural responses are obtained are correctly realized and incorporated. The best means of assessing the state of the practice, of course, is through comprehensive post-earthquake investigations of actual structures and integrated analytical and large-scale experimental investigations of complete structures. Economic constraints do not generally enable experimental investigations of complete structures, in which case, tests of large-scale subassemblages incorporating critical regions (ex. lower floors) of the structure provide data regarding the state of the practice. The analytical studies presented in this report are part of such an integrated analytical and experimental investigation, and the following assessment is to be complemented by others [34] as more experimental and analytical data is generated.

6.2 Relations between the Demand vs. Supply Relations

An accepted manner of assessing analytical structural response is

to compare the force, distortion, and energy dissipation demands from the individual structural components to the corresponding supplies. The maximum values of forces and distortions, as well as the complete time-histories of these quantities should be considered in interpreting these demands. In inelastic earthquake responses of structures, the supplied strengths, deformations, and energy dissipation capacities of different structural components and their connections strongly influence the computed corresponding demands and their distributions through the structure. The supplies should be represented correctly in the analytical model for a realistic assessment of the demands. It follows, also, that the state of the art in the analytical response generation of R/C cannot be improved by just incorporating more sophisticated, finite element models or plasticity criteria unless the state of the art of estimating the actual axial-flexural and shear strength, stiffness, and hysteresis characteristics of reinforced concrete members and their connections for all the limit states, are also improved.

It should be repeated here that the analytical model used in the analyses was in essence an axial-flexural model, i.e., the axial and uniaxial flexural force-distortion relationships of the member cross sections were derived, based on hypothesized stress-strain properties for steel, confined, and unconfined concrete. These relationships formed the basis of the input for the force-displacement relations of the structure, as discussed in Chapt. 3. The correct shear force-shear distortion relations of the wall cross sections, as well as the influence of shear on the axial-flexural responses of these cross sections could not be represented realistically in the analytical model as discussed in Chapt. 3. This should be critically considered in assessing the demand vs. supply relations especially for the shear responses of these members.

6.3 Definition of Supplies

Several steps are involved in the design process of a structure

which influence its actual strength, stiffness, deformation, and energy dissipation capacity, i.e., the actual supplies of the structure. These are discussed in the following.

6.3.1 Service Level Demands

The unfactored gravity (D and L) and the larger of the wind or earthquake (E) loading defined by the building codes are acknowledged to constitute the service load level demands from the structure in the design process. The structure is analyzed under these loads to arrive at the service level displacements and stresses. Different building codes prescribe different service level earthquake forces to the same structure. For example, the service level earthquake base shear and overturning moment for one coupled wall system of the building in Fig. 1.1 were $4.5\%W$ and $3.06\%WH$, respectively, according to the 1973 UBC code, where W and H designate one-half of the total dead weight and the total height of the building. The corresponding quantities prescribed by the 1979 UBC code were $5.85\%W$ and $4.15\%WH$, respectively. UBC 1973 or 1979 codes require that the coupled walls should be capable of resisting all the lateral force regardless of the presence of the frame system, as well as a minimum torsional shear force, corresponding to an eccentricity of 5% of the building maximum plan dimension. These requirements were incorporated in the computed service level shear and overturning demands.

The ATC 3-06 provisions require $6\%W$ and $4.3\%WH$ as the base shear and base overturning moment for one-half of the complete building (modified for 5% minimum torsional eccentricity) at the first significant yielding of the structure. The ATC 3-06 provisions do not require all lateral load to be resisted by the wall systems, instead, the lateral load is required to be distributed to structural components with respect to their stiffnesses. In accordance with this requirement, an elastic analysis of the building in Fig. 1.1 was carried out and resulted in shear and overturning demands for one coupled wall system of $5\%W$ and $3\%WH$, respectively. Incorporating the frames has reduced the base shear to be resisted by the wall system by 20%, and the overturning moment by 43%. The base

overturning moment to shear ratio decreased from 0.72H to 0.60H.

6.3.2 Ultimate Limit State Demands

The member force and structural displacement and drift demands, obtained through nominal (elastic) analysis, based on the unfactored code demands (gravity and lateral loading) are magnified by load/displacement factors for ultimate limit state design. These demands are termed as the factored code demands and are assumed to represent the ultimate limit state force and displacement demands. In reality, due to the subsequent steps in design that will be discussed, the actual ultimate strength and the associated displacements of the structure are generally substantially different. At this design stage, where the factored code demands are established, the axial-flexural and shear demands are generally considered separately. The UBC and ATC 3-06 shear demands of ductile frame elements are based on the ultimate flexural capacities, rather than the shear forces obtained for each member as a result of elastic analysis. This is done in an attempt to ascertain that the frame members may develop their flexural capacities prior to shear failure. Both the axial-flexural and shear demands of the structural walls, however, are directly based on the results of elastic analyses carried out by the D, L and E loadings [4] which does not assure against shear failure before the flexural capacity is attained.

The UBC provisions prescribe different load factors for the flexural and shear ultimate limit state demands, in order to decrease the chances of premature shear failure of the walls prior to the attainment of their flexural capacities. ATC 3-06, however, does not distinguish between axial-flexural or shear effects in prescribing load factors, but modifies significantly the value of the reduction factor. The ultimate limit state flexural strength requirement of a cross section according to the 1973 or 1979 UBC is given by either $1.4D + 1.4L + 1.4E$ or $0.9D + 1.4E$, while ATC 3-06 prescribes either $1.2D + 1L + 1S + 1E$ or $0.8D + 1E$ for the flexural ultimate strength.

D, L, E and S stand for the dead, live, earthquake, and snow load effects, respectively. ATC 3-06 requires the incorporation of orthogonal effects while there is no such requirement of the 1973 or 1979 UBC. The ultimate level shear strength requirement of a wall cross section is given as either $1.4D + 1.4L + 2.8E$ or $0.9D + 2.8E$ by 1973 UBC. The same requirement of 1979 UBC is either $1.4D + 1.4L + 2E$ or $0.9D + 2E$. As discussed earlier, ATC 3-06 does not distinguish between the axial-flexural and shear ultimate limit state demands in specifying load factors.

6.3.3 Capacity Reduction Factors for Computed Ultimate State Demands

The strength of a certain cross section, evaluated with respect to the provisions of the code, is required by 1973 UBC, 1979 UBC and ATC 3-06, to be adjusted by a capacity reduction factor which is less than one. In effect, this is equivalent to amplifying the load factors further, although the adjustment is applied to the computed ultimate capacities rather than the demands. The capacity reduction factors prescribed by the 1973 UBC or 1979 UBC are 0.9 for flexure and tension, 0.75 for flexure and compression (for spirally reinforced members), and 0.85 for shear and torsion. The factors prescribed by ATC 3-06 are similar to the factors prescribed by the UBCs for axial-flexural effects. The capacity reduction factor for shear, however, is prescribed by 0.6 if the strength of the component is governed by shear.

Incorporating the capacity reduction factors together with the load factors, the required ultimate strengths of the coupled wall system become $(0.9D + 1.4E)/0.9$ for tensile-flexural, and, $(1.4D + 1.4L + 1.4E)/0.75$ for compressive-flexural effects, according to 1973 UBC or 1979 UBC. Corresponding strengths are $(0.8D + 1E)/0.9$ and $(1.2D + 1L + 1S + 1E)/0.75$, according to the ATC 3-06. For the shear design of the walls, the required ultimate shear strengths are (neglecting gravity effects), $2.8E/0.85$, $2E/0.85$, and $E/0.6$, for the 1973 UBC, 1979 UBC and ATC 3-06, respectively. Substituting

the values of E given in Section 6.3.1 for 1973 UBC, 1979 UBC, and ATC 3-06, the required wall ultimate shear strengths (for one set of coupled walls) become 14.82%W, 13.76%W, and 8.33%W, respectively. These shear strength demands, in conjunction with the base overturning moment to shear ratios,* indicate that the 1973 UBC requirements lead to a coupled wall system with the maximum shear strength demand per unit axial-flexural demand at the base.

This was the reason behind selecting the 1973 UBC designed version of the building as the objective of the analytical and experimental studies [4] as this version was expected to have the most favorable ultimate limit state response characteristics, i.e., maximum amount of flexural deformation and energy dissipation prior to a shear failure. Certain codes, such as the CEB code in Europe, specify material factors rather than the capacity reduction factors. The specified nominal yield strength of steel and the nominal concrete strength are reduced by different material factors in computing the supplied ultimate strength of members.

6.3.4 Code Assumptions Regarding Computation of Reinforcement

The assumptions that are made in order to evaluate the axial-flexural and shear strengths supplied by a certain element, in the process of its design are consequential in the actual capacities that the member may really attain. For example, supposing that the axial-flexural demands from a R/C frame member, adjusted by the capacity reduction factors, are given by the force-moment pair N and M, the design of member reinforcement will be determined based on the following assumptions regarding equilibrium and compatibility of strains (1973 UBC, Sect. 2610(c)): (1) Plane sections remain plane;

* Base overturning moment to shear ratios were 0.68H, 0.71H and 0.60H as a result of the 1973 UBC, 1979 UBC and ATC 3-06 prescribed "E" loadings, respectively. For the ATC 3-06 loading, 0.60H was obtained after considering frame wall interaction, as required by these provisions.

(2) Maximum usable strain at the extreme concrete compression fiber shall be assumed equal to 0.003; (3) Steel is elastic-perfectly plastic, maximum steel strength is f_y ; (4) Tensile strength of concrete shall be neglected in flexural computations; (5) Assumptions regarding concrete compressive stress block, as given in Sect. 2610(c).

The actual axial-flexural (N-M) ultimate limit state capacity of the member, (the reinforcement of which is computed based on the assumptions (1)-(5) above), will be higher than the flexural ultimate limit state N-M strength demands, as a consequence of the assumptions (1)-(5). As the maximum concrete strain may reach values significantly higher than 0.003, and as typical reinforcing steel possesses strain hardening characteristics that will increase the stress above the yield level in the order of approximately 20-60 percent, the actual flexural strength would be higher. Furthermore, the actual yield strength of the steel may be considerably higher than the nominal value for the yield strength. Also the actual concrete strength realized is generally considerably higher than the prescribed nominal design strength. This strength may further increase substantially in confined elements, which is a phenomenon not considered in code computations.

In addition to the assumptions (1)-(5), other provisions of the code regarding the minimum (or maximum) reinforcement percentages may be applicable in determining the member reinforcement. In such cases the supplied actual capacities would be higher than the N-M strength demands.

For axial-flexural design of wall cross sections, the discrepancy between the required supply and the actual strength based on the reinforcement computed by the code would be considerably larger than for beam or column cross sections. As the design provisions (1973 UBC, 1979 UBC, ATC 3-06) require the boundary elements of the walls to be capable of resisting all the axial-flexural effects on the cross section as axially loaded members, the computed capacities of the

cross section do not incorporate the vertical wall steel. Also, the actual compressive strength of the well-confined core concrete of the boundary member would be higher than the nominal concrete strength. Consequently, the actual axial-flexural capacities of a wall section would be considerably larger than the supplies computed by the code assumptions.

For the computed shear strength and the actual shear capacity of a wall (in conjunction with the axial-flexural demands), even greater discrepancies than axial-flexural supply computations may occur. The code approach in determining the supplied shear strength is based on experimental information on the shear response of beams; the total nominal shear stress v_u shall be computed by $v_u = \frac{V_u}{\phi h d}$ *

where d shall be taken equal to $0.8 \ell_w$ *. Part of the total shear stress is assumed to be carried by concrete v_c and the rest $v_u - v_c$ by the steel v_s . The shear stress v_c carried by concrete is usually assumed to be $2 \sqrt{f'_c}$ and the rest of the nominal shear stress is assumed to be resisted by the horizontal wall steel. In reality, the shear resisting mechanism of walls with confined edge members is significantly different than those of beams. While it is recognized that the capacity of the concrete panel to resist shear practically disappears when this panel is subjected to full reversal of deformation involving significant flexural/yielding, resistance offered by vertical steel, and particularly by well-confined edge members, can be very large, larger than the contribution of the panel concrete. As the code does not incorporate these contributions, the actual shear capacity of a wall would be substantially different from the code computed supply [4].

Another factor that may cause a discrepancy between computed strength and actual capacity is the usually larger amount of actual reinforcement provided at a cross section in order to provide the computed

* V_u = Shear force; ϕ = capacity reduction factor in shear,
 h =thickness of wall panel, d = effective depth, and ℓ_w = total depth of the wall.

required steel area. The constraints imposed by proper reinforcement detailing considerations may lead to specifying 10-20 percent larger flexural steel for a cross section than the computed amount. Transverse steel, similarly, may be specified as considerably more than required by the code [4].

The values of N considered in conjunction with the estimation of the flexural capacity and/or the shear capacity, when computed by code loads and procedures, can be in considerable error, particularly the N resulting from the shear of the coupling girders. An important source of discrepancy between the actual flexural strength as opposed to code computed supply, is the contribution of the slab steel. Investigations of the actual contribution of slab steel to the response of beam-column-slab subassemblages have been in progress in Berkeley [20]. As the code supply computations for the coupling beam flexural strength do not incorporate slab steel, the actual (negative) moment capacity of a beam may be considerably larger than the code based computations imply and, therefore, the beam shear and consequently the axial force N in the wall, can be miscalculated.

6.3.5 The Effect of Redistributions on the Actual Supplies of a Structure

In addition to the sources discussed in Sect. 6.3.4, another main reason that the actual supplies of a structure may be considerably different from the supplies based on the code computations, is the method of analysis generally followed in the design. All U.S. codes at present require only nominal elastic analysis as a basis for design. The slenderness effects in compression members may be incorporated by approximate procedures. Material nonlinearity, however, is not incorporated.

As the design of each member is based on the computed maximum cross sectional effects (modified with load and strength reduction factors as discussed in the previous sections) obtained from linear elastic analysis, the possible change in the actual capacity of the

structure due to nonlinear redistributions is not incorporated in the present code computed structural supply. The actual redistributions that occur within the cross section, member, and the whole structure (between members and joints) may lead to a significantly higher flexural strength of a structure provided that the axial and shear strengths of the members may withstand the accompanying increases in the flexural strength and their increases will not jeopardize the flexural ductility of the member. The stability constraints may also become critical when these strength increases are considered.

If the axial and shear capacities of the members or the stability considerations do not limit the increases in the strength of a structure, the nonlinear redistributions may result in an actual resistance capacity significantly higher than the strength supply computed by the code expressions and procedures.

Redistributions may, therefore, be an important source of over-strength, that is not incorporated in the code computations for the actual supplies of a R/C structure. Even redistributions at the cross sections level, i.e., transfer of stress from extreme fibers to relatively less-stressed fibers result in significant increases in both cross sectional moment and curvature capacities. Redistributions between different members, finally, lead to a utilization of the deformation hardening capacities of a large number of the structural members. Consequently, the larger the ductility of the members and the higher the structural redundancy, the higher would be the strength increase due to redistributions.

The state of the art in evaluating the realistic strength of cross sections, members, and structures requires further efforts to incorporate the actual extent of redistributions that may take place within a structure. For cross sectional analysis, besides the establishment of realistic multi-axial material stress-strain and hysteresis relations, it will also be necessary to utilize computational techniques that will enable the correct evaluation of section strength incorporating redistribution of stresses between different fibers [1, 3].

For member analysis, the redistributions that occur along cross

sections, i.e., the spread of yielding, should be incorporated in the analytical models in order to estimate the actual axial flexural capacity of a member [28, 45].

At the structural level, discrete models based on lumped plasticity (point hinges at each end of the member), require realistic inputs for these hinges in order to represent the actual extent of redistributions that may take place between the different components of the structure. As discussed in Chapt. 3, it is difficult to predict realistic and representative inputs for the member properties when the analytical model for the member does not incorporate the actual complex response characteristics observed for R/C members.

It follows that the state of the art needs considerable advancement to evaluate the actual capacity of R/C structures. The state of the practice, i.e., the code computational techniques, may result in substantial underestimates of actual structural capacity. These limitations should be realized in evaluating the analytically generated earthquake demands based on analytically generated supplies of the structure. This will be done in the next sections.

6.4 Evaluation of Axial-Flexural Supply vs. Demand Relations

6.4.1 Axial-Flexural Supply vs. Demand at the Base of the Walls

A comparison of the axial-flexural supply vs. demand relations at the base of the walls is given in Fig. 6.1. The supply N-M curves were computed and illustrated in Fig. 2.9. Obtaining the yield envelope, which is the axial-flexural supply defined as input for the nonlinear analyses, was explained in Chapt. 3 and was based on the material characteristics shown in Fig. 2.7. When a 1/3-scale model of the lower 4-1/2 floors of the coupled wall system was built and tested [34], the actual capacity at the base of the wall under compression was measured as indicated on the same figure, and the probable maximum capacity envelope was constructed, based on the measured actual material characteristics and incorporating an increase in concrete compressive

strength due to confinement [34].

During the tests of the model, the beams were also measured to have actual flexural capacities significantly exceeding the supplies that were defined for the analytical model, as will be discussed in Sect. 6.42, in the order of 100 percent. This was attributed to mostly the considerably higher yield and ultimate capacities of the reinforcement used, contribution of slab steel neglected in the analyses, a considerable underestimation of the deformation hardening, contribution of axial compression that was not considered in the analytical computations and other probable causes as discussed in Sect. 6.3.4 and 6.3.5 [34]. Thus, there were important discrepancies in the hypothetical, computed maximum axial-flexural supplies and the actually attained (measured) supplies for both, the coupling girders and the walls. Had these measured supplies been defined as the input for the analyses, the obtained demands shown in Fig. 6.1 for the Pacoima nonlinear analyses would have been considerably affected, since these demands were regulated by the supplies (as discussed in Sect. 6.2).

An important observation from Fig. 6.1 is the extreme differences observed between the factored 1973 UBC axial-flexural demands and the actual supplies that were realized after designing and constructing the walls with respect to these code demands.

The factored axial-flexural demands for 1979 UBC and ATC 3-06 are compared to 1973 UBC in Table 6.1. It is observed that the 1979 UBC demands are approximately 30 percent higher while the ATC 3-06 demands are approximately 25 percent lower than the 1973 UBC demands. The reflection of these differences on the actual, resulting capacities had the walls been designed and built based on the provisions of these codes, will be evaluated in future studies. As the resulting axial-flexural and shear demands specified for the design depend on a number of other minimum requirements in addition to the force demands, the relations between the actual axial-flexural capacities based on the provisions of different codes are not explicit.

Continuing with the interpretation of Fig. 6.1, the moment-axial force pair at the base of one wall is observed to occupy during the nonlinear analyses the shaded domain in Fig. 6.1. This phenomenon was discussed in Sect. 5.3.3.5 and Fig. 5.33 and 5.34. The demands from linear analyses are also indicated in both Fig. 6.1 and Table 6.1. For the El Centro responses, the coupling girder and frame beam inelasticity is observed to reduce the elastic wall axial-flexural demands approximately 65 percent, so that the walls remained linear during the excitation. During the Pacoima response, however, the wall is observed to have yielded, as discussed in Chapt. 5. The flexural strength attained in the analysis is approximately 57 percent less than the demand indicated by linear analysis under the Pacoima motion.

The profiles of the bending moment and axial force envelopes for the walls along the elevation of the building, obtained for the nonlinear responses, are compared with the corresponding 1973 UBC demands in Figs. 6.2 and 6.3. The distribution of maximum bending moments along the structure, shown in Fig. 6.2, indicates that the ratios of Pacoima or El Centro demands to the factored 1973 UBC demands change along the elevation of the walls. Although El Centro demand is only 56 percent larger than the code demand at the base, the difference is more than 200 percent between eighth and fourteenth floors.

The axial force envelopes for the walls are shown in Fig. 6.3. It is observed that the code demands for tension are underestimated considerably more than code demands for compression throughout the structure. It is of interest to note that while the code axial force demands for compression and tension utilize $1.4D+1.4L$ and $0.9D$ for the gravity load contribution, respectively, nonlinear analysis results incorporate $D+L$ for both compression and tension.

The observations from Table 6.1 and Figs. 6.1-6.3 lead to a number of assessments regarding the axial-flexural design of the wall cross section. The most significant observation regards the code design process which requires that the edge members provide all required axial-flexural capacity working as purely axially loaded members. The consequence mainly of this provision, when combined with the other factors contributing to the cross sectional overstrength, as discussed in Sect. 6.2, is an actual capacity which is, as observed from Fig. 6.1,

5.5 times larger than the code demand. When this overstrength is combined with the overstrength in the coupling girders, the result is a significant increase in the structural base overturning strength, as discussed previously in Sect. 2.2. This would result in an accompanying increase in demands from the foundation of the structure, which may not provide adequate supply for this increase. Depending upon the soil characteristics and design of the foundation system, the resulting displacements of the foundation would change the distribution of force and distortion over the complete structure. The effects of characteristics of soil and the foundation system on response will be investigated in future studies, as the implications of the observed flexural overstrength of the superstructure indicate a particular importance of this parameter.

A second consequence of the flexural overstrength of the coupled wall system would be an increase in the shear strength demands of the walls. If the supply to meet the increase in the shear strength demand is not available, a wall shear failure may occur prior to, or soon after, the flexural yielding at the base of the walls. This will be discussed further in the coming section 6.4.3.

It follows that the code design procedures for the axial-flexural design of the walls should either incorporate the actual flexural resistance of the complete wall cross section, or make allowances in the design of the footings and other structural components, and particularly, the shear design of the walls for the hidden flexural overstrength of the wall cross sections. There is no observed deficiency of axial-flexural capacity as even the hypothetical, underestimated axial-flexural strengths which were defined as input for the inelastic analysis were adequate to resist the El Centro excitation with the walls remaining linear. Although the walls yielded during the Pacoima response, the amount of inelastic deformation associated with this yielding was considered to be within acceptable limits, as discussed in Sect. 5.3.2. Since the Pacoima record represents the extreme earthquake and the combined strength and deformation capacity demands from the walls were supplied adequately, the axial-flexural strength may be concluded to be adequate.

The displacement and distortion demands from the structure will be discussed in Sect. 6.4.4, where the adequacy of axial-flexural strength, provided to the walls and the coupling girders,

as well as the adequacy of the stiffness provided to the structure will be verified. The problem, therefore, is in the too high axial-flexural overstrength, and to seek out measures to be able to reduce this axial-flexural overstrengths of the members without affecting the stiffness and shear capacities adversely.

6.4.2 Axial-Flexural and Shear Supply vs. Demand Relations for the Coupling Girders

The response of the coupling girders was discussed in Sect. 5.3.2.4 and 5.3.4. The factored design demands of the girders (which were also modified by the capacity reduction factors) are given in Table 6.2, together with the yield and ultimate capacities as determined from the detailed cross sectional analyses presented in Chapt. 2, and also given in Fig. 3.4, as the inputs to the analytical model. The yield capacities of the girders, as obtained from cross sectional analyses, are close to the code demands. The maximum difference between code demand and computed yield capacity is observed for the negative moment of type III beam, which is 24 percent. This is mainly due to providing more steel to the girder than the exactly required amount, as caused by the practical consideration of using only one type of reinforcement in the girder. As discussed previously, the slab steel was not considered in the cross sectional analyses, which is a significant parameter that will be included in future studies. The ultimate moments obtained from the cross sectional analyses are approximately 100 percent larger than the code demands. Also, the shear corresponding to the ultimate girder moments is 25-43 percent larger than the code demands for the different types of girders.

The main reason for the flexural overstrength of the girders is the strain hardening of the steel, which is neglected in the code flexural computations. The maximum increase in steel stress due to strain hardening is assumed to be 25 percent in the code for the computation of shear demands only, while an increase of 83 percent (from 60 ksi at yield to 110 ksi at ultimate) was assumed in the cross sectional analyses. Consequently

the maximum shear obtained from cross sectional analyses is larger than the code demand. It follows that the code computations considerably underestimate the computed flexural capacity and shear demand for the beams, arising mainly from the underestimation of the maximum strength of reinforcement. The increase assumed for the maximum strength of reinforcement over yield, 83 percent, in the cross sectional analyses, might not be considered as typical. However, stress-strain tests on commercially available reinforcement, purchased for the construction of the model of the coupled wall system [4] and from previous experiments conducted at Berkeley, have indicated that such increases are very frequent.

The maximum coupling girder moments and shears obtained during the time-history analyses are included in Table 6.2. The attained moment values are only 20-25 percent larger than the yield capacities defined in the analytical model. The Pacoima shear force demand from girder type III is observed to be 5 percent less than the code demand for this girder. The maximum force demands from the coupling girders are, therefore, substantially less than the ultimate capacities for these girders, which was also demonstrated in Fig. 5.40. Consequently, they were not subjected to shear stresses exceeding the code demand during the inelastic analyses. An assessment of the accuracy of the coupling girder properties obtained from cross sectional analyses and defined as input for the time-history analyses may be carried out by considering the moments and shears measured during the testing of the 1/3-scale model of the first 4-1/2 floors of the coupled wall system [34]. The measured positive and negative yield moment and shear values are included in Table 6.2. A substantial increase of 107 percent in the measured negative yield moment of the type III beam over the computed yield moment is observed. For the positive moment direction, the measured yield moment is 64 percent larger than the computed value. The measured shears at yield are approximately equal to the computed ultimate values. The main reason for the discrepancy in the negative

moment is the slab steel, which may have caused an increase in the beam negative moment reinforcement of 40 percent, if all the existing slab steel is assumed to have effectively participated with the beam reinforcement during the experimental response.

The beams were under increasing compressive forces during the test (due to redistribution of wall shears) which also caused an increase in the yield moments. The measured moment-rotation relations, from which the yield moment values were derived, are presented in Fig. 6.4. The experimental moment-rotation measurements were carried out over 4 in. gage lengths at the left and right ends of the beams, and include the rotation at the fixed-end caused by the slippage of reinforcement, and any further rotation that may have occurred over the first 4 in. at each end of the 56 in. long (1/3 scale) beam. The experimental responses shown in Fig. 6.4 were measured during the initial loading of the first large displacement cycle when the first yielding of the beams were observed. This loading was preceded by a number of full cycles of loading in the service load range.

The measured rotations, shown in Fig. 6.4, are precisely the physical counterparts of the rigid-hardening plastic point hinge responses of the analytical beam model used in the analyses. On the same figure, the primary loading paths for the point hinges of the type III beam are indicated together with the factored (including the ϕ factor) code demands for this beam. Figure 6.4 is thus more illustrative than Table 6.2 in demonstrating the extreme differences in: (1) code demand for cross sectional capacity; (2) analytically computed flexural capacity, neglecting slab steel and based on hypothetical material characteristics; and (3) the actual, measured responses when a model of the structure or an adequately large scaled subassembly of the structure is tested under representative load and displacement constraints. The differences in all the stiffness, strength and deformation hardening characteristics of the coupling girders were significantly influential in the analytically generated responses of the structure. As explained in Sect. 6.2, the

strength, stiffness, and hardening characteristics defined in the analytical model for these beams, affected the outcome of the force and distortion magnitudes, distributions, and time-histories of the complete structure.

The difference between the observed and computed characteristics at the right end of the beam (negative moment) in Fig. 6.4, is more difficult to anticipate than the left end of the beam (positive moment), as the slab steel accounts for a large portion of the strength discrepancy at the left end.

The axial force measured for beam III at the indicated yield point was in the order of 10 percent of its ultimate axial compression capacity and this was computed to possibly account for more than 30 percent of the observed discrepancy in strength in the positive moment direction [34]. Another contributor to the strength discrepancy is the 35 percent higher yield strength of the actual reinforcement. The computed vs. measured stiffness and hardening characteristics indicate that the rigid-plastic point hinge should not be considered rigid, but assigned a finite elastic stiffness to represent the actual response, incorporating the slip of reinforcement along its anchorage in the wall. The observed deformation hardening is approximately twice the analytically defined value, which should also be considered in future analytical modeling.

The implications of the beam flexural overstrengths, when coupled with the wall flexural overstrengths were discussed in Sect. 6.4.1. In addition to increasing the shear stress demands of the beams, the beam flexural overstrengths cause a direct increase in the wall coupling forces and thus the overturning capacity of the wall system at the base. This, in turn, results in an attraction of higher wall shears and increases the demands from the foundation-soil system. Also, the increased beam shear stress demands impair the deformation and energy dissipation capacity of the beams.

The beam flexural capacities require more realistic evaluation. The contribution of slab steel should definitely be incorporated in

establishing the beam flexural capacity. Attempts should be made to be able to design the beam with a flexural capacity closer to the demand. As discussed elsewhere, [4], proportioning the coupling girders for stiffness automatically leads to high flexural demands when elastic analysis is carried out. The code design procedure should be revised to permit the design of stiff beams without accompanying large flexural capacity, as may be attained by using a minimum reinforcement percentage and using grade 40 steel for the main flexural reinforcement of these coupling girders.

The shear design procedures, as defined by the code, require reassessment. The ϕ factor, and the 25 percent strain hardening incorporated in computing the shear demands, are observed to be inadequate to establish these demands realistically, as explained previously. As the computational techniques fall considerably short of estimating the actual shear demands from these beams, a remedy may be to decrease the maximum shear reinforcement spacing required by the code, or to use special inclined reinforcement, and to require each longitudinal bar to be restrained by a hoop corner. The inadequacy of the computational procedures used to establish the shear demand may only be overcome by indirect requirements that may insure the placing of adequate shear reinforcement in the beams so as to assure an actual shear capacity high enough to permit the necessary flexural yielding.

6.4.3 Shear Strength Supply vs. Demand for the Walls

6.4.3.1 General

A realistic assessment of the shear strength supply vs. demand relations of the walls become especially critical when the flexural overstrengths of the girders and the walls are considered. To satisfy a basic design criteria, that structural damage which may endanger lives should be avoided, the shear strength supply to the wall should be ascertained to be adequate for any demands that may arise at all the limit states, particularly at the collapse limit state. The three possible types of shear failure [37], (1) diagonal tension,

(2) sliding shear, and (3) shear compression (splitting and crushing of the wall panel concrete) modes of failure should be avoided.

The diagonal tension failure can be avoided by providing sufficient web (panel) reinforcement. The sliding shear failure is typical for walls in tension or for low levels of axial compression and high levels of shear. These conditions lead to large shear distortions without accompanying energy dissipation through flexure, and is, therefore, undesirable. The shear compression failure of the wall panel, typical of high compressive stress and high shear stress levels at regions of the wall panel, results in a sudden, brittle release of the panel shear force. This may lead to dangerous consequences, as the edge members, already subjected to high axial and shear force demands, may not be able to withstand the force released by the panel, and also fail in semi-brittle compression, punching or diagonal shear mode depending on how much area of wall panel, failed previously. It follows that a realistic and comprehensive assessment of the seismic shear demands and the actual existing shear strength supply of each wall (in fact the supply available in each component of the shear carrying mechanism of each wall, i.e., the edge members and panel, before and after crushing of the panel) is necessary to conclude the assessment of the structural supply vs. demand relations.

In carrying out an assessment of the shear design provisions of the code, the following possibilities should be considered:

(1) Is the shear strength demand, as defined by the code, realistic? This may be judged only after making a realistic estimate of the actual axial-flexural capacity, and by estimating the maximum possible shear demand from the wall during dynamic response in conjunction with this realistic axial-flexural capacity.

(2) Is the actual shear capacity of the wall system, (whose design is based on code provisions) governed by the actual mechanisms of shear resistance of the actually constructed complete structure and

in the presence of significant axial and flexural states of stress, adequate to supply the shear demands established as described in (1) above?

An estimation of the actual demands and supplies as outlined in (1) and (2) above, will be carried out in the following.

6.4.3.2 Shear Strength Demands Required by Different Provisions

The seismic shears to be considered for the axial-flexural and shear designs of the coupled wall system, with respect to the 1973 UBC, 1979 UBC, and ATC 3-06 provisions are shown in Fig. 6.5. Since each of these documents specify elastic analysis, the demands from each individual wall of the coupled wall system are identical. ATC 3-06 requires the design shears to be established by considering the interaction of walls and frames. Uniform Building Codes (1973 and 1979 editions) require that walls should also be capable of resisting the entire shear. These are the shears shown in Fig. 6.5 for UBC as this provision governs the design of the structure [4].

In comparing the design shear strength demands of different documents, the required shear strength should be judged in conjunction with the required flexural strength. Had the supplied flexural capacities been equal to the required flexural strengths, and had each of the walls contributed equally to the flexural and shear strength of the system, an assessment of the adequacy of shear strength demands of these documents would have been relatively simple from Fig. 6.5, as follows: The total overturning strength demand at the base of the coupled wall system may be obtained as 179×10^3 kip-ft, 90×10^3 kip-ft, and 133×10^3 kip-ft for the 1979 UBC, ATC 3-06, and 1973 UBC, respectively. The shear strength demands, corresponding to the same provisions, are observed to be 2351 kips, 1429 kips, and 2549 kips, respectively. In computing the overturning strength demands, the load factors, and in computing the shear strength demands, the load and capacity reduction factors specified by each document were incorporated. The ratios of the overturning strength to the shear

strength demanded by these provisions may be obtained as 76 ft (0.42H), 65 ft. (0.36H), and 52 ft. (0.28H), for the 1979 UBC, ATC 3-06, and 1973 UBC, respectively. The conceptual meaning of these ratios is as follows: the overturning moment capacity of the system at the base and the shear capacity of the system at the base would be attained simultaneously if an increasing resultant seismic force acting on the system is located at 0.42H, 0.36H, and 0.28H from the base of the system. It follows that the 1973 UBC provisions provide the highest safety against shear failure prior to the attainment of the overturning capacity, relative to the 1979 UBC and ATC 3-06 provisions. Since the resultant seismic force acting on the coupled wall system was located at 0.30H and 0.33H at the times of maximum base shear during the Pacoima and El Centro responses of the frame-coupled wall system, only the 1973 UBC provisions appear to provide an adequate margin against shear failure before the attainment of the flexural capacity.

In reality, none of the assumptions that were made to justify this assessment are true. (1) Actual axial flexural capacity of the wall system is many times larger than implied by the code demands, as discussed in Sects. 6.4.1 and 6.4.2. (2) While by virtue of the elastic analysis, or even inelastic analysis without incorporating the effect of axial force on stiffness, the demands from the coupled wall system would appear to be distributed equally to each wall, in reality there would be significant differences in the stiffnesses of the walls under compression and under tension, and this would result in an increase in the shear demands of the wall under compression due to redistribution of shear. (3) The base overturning moment to shear ratio at the time of maximum base shear, 0.30 H, was obtained through an analytical model containing many inadequacies. Values of α even lower than 0.30 H may be realized by a wall-frame system during dynamic response, especially for structural systems where frames have more significant contribution to the overall strength and stiffness. (4) Even if the assumptions were valid

and the system, designed in accordance with the 1973 UBC provisions, did have the considered margin against premature shear failure, this would not necessarily indicate that an adequate amount of energy dissipation would take place before shear failure. Depending on the dynamic characteristics of the structure and the ground motion, the overturning capacity of the structure may be attained with a shear smaller than the design shear. However, this would not outrule a sliding shear mode of failure under reversals of deformation. This mode of failure would lead to distortions without corresponding flexural energy dissipation, and may occur even when the shear demand may remain lower than the design shear capacity throughout the excitation.

To be able to predict whether a certain type of shear failure is imminent during a response, the complete history of the axial force and flexure should be evaluated together with the shear force at the critical regions of the wall. In reality, the sliding shear or the shear-compression (web crushing) types of shear failure are strongly influenced by the previous loading history, from the view of the damage, i.e., the deterioration of the resistance mechanisms to these types of shear failure. Therefore, the sense and magnitude of the axial force, flexure, and the state of damage of the wall, occurring in conjunction with a certain shear demand, should be considered altogether in assessing the probability of shear failure. During the Pacoima response, the maximum wall base shear demand occurred after the maximum flexural demand and extensive yielding of the walls have occurred and while the base of the compression wall was at a state of yield with a high level of compression. The probability of a shear failure would be substantial under such circumstances. There was no flexural yielding of the walls during the El Centro response; hence, the probability of a shear failure would be low.

It follows that the shear strength demands defined by the 1979 UBC or ATC 3-06 provisions do not provide as much margin against shear failure as the 1973 UBC provisions. The question of the safety of the structure designed with respect to the 1973 UBC provisions will be

discussed subsequently.

6.4.3.3 Establishing the Actual Shear Demands and Shear Capacity of the Walls

The shear strength supply vs. demand relations for one wall of the coupled wall system are summarized in Fig. 6.6 and Table 6.1. The shear strength demands specified by the Uniform Building Code are indicated in Fig. 6.6, together with the seismic shear demand envelopes of each story of the wall, obtained during the inelastic time-history analyses of the coupled wall-frame structure. From Table 6.1 and Fig. 6.6 it can be observed that: (1) The shear strength demands from the code and from the inelastic El Centro response are very close at the base of the wall; (2) The demands at the base obtained for the linear El Centro response and the inelastic Pacoima response are also close to each other and these are approximately twice the code and inelastic El Centro response demands; (3) The demands obtained for the linear Pacoima response are approximately twice the inelastic response demands of this motion.

The inelastic response demands for shear strength were obtained through an analytical model with three major sources of error which would affect these demands considerably.

(1) The wall and coupling girder axial-flexural capacities were underestimated significantly. If the analyses were carried out incorporating the actual observed axial-flexural capacities of the members, strength of the structure would have been more, attracting larger shear, and as the flexural yielding would have started under larger shear, it would have dissipated less energy.

(2) The shear mode of distortion of the individual wall components is not adequately incorporated in the analytical model, as discussed in Chapt. 3. The walls tend to have a predominant cantilever post-yield displacement mode, while in reality, flexural yielding should be expected to be accompanied by an increase in shear distortion and, therefore, a displacement mode closer to that of the frame with a soft story, in this case the first story.

Therefore, the effects of the wall-frame interaction after wall yielding would have been less, at particularly the lower floors of the building, if a more realistic post-yield deformation mode could have been incorporated in the analytical model. The shear strength demands of the walls may be in error due to this inadequacy, especially if the wall-frame interaction may affect the response considerably.

For the coupled wall-frame structure, as the frames did not affect the maximum response quantities (Chapt. 5) significantly, the contribution of the first source of error governs. The actual-inelastic response shear strength demands should, therefore, be expected to be more.

(3) The inadequacy of the analytical model to incorporate the actual flexural and shear stiffness of walls as affected by axial force, is the third, and perhaps the most, critical source of error in establishing realistic inelastic response demands. The flexure and shear attained by the wall under compression should be substantially larger than those attained by the wall under tension. This inadequacy in analytical modeling would underestimate the actual shear strength demand of the wall under compression at any time during response. In the case of impulsive ground motion, the shear envelopes could also be significantly affected from this inadequacy, especially if there is only one main loading excursion, similar to the one occurring during the Pacoima response.

The supply of shear capacity at the base of the wall, as defined by the code provisions, is indicated in Fig. 6.6. If the supply, based on the code computation, assuming a concrete shear stress of $2\sqrt{f'_c}$, and the horizontal panel steel contribution to shear stress of $(A_v f_y / b_w s)$ *, and an effective shear area of $(0.8hb_w)$ *, would have been the actual supply, none of the inelastic response demands could have been satisfied.

* A_v = area of shear reinforcement effective against shear, f_y = yield stress, b_w = web thickness, s = spacing of shear reinforcement, h = total depth of the wall cross section.

The actual shear strengths of each wall of the coupled wall system, measured during the testing of a 1/3-scale, 4-1/2 story subassemblage of the coupled wall system under a loading history derived from the inelastic Pacoima responses of the structure, are also indicated in Fig. 6.6 [34]. This information, obtained from the experimental research that is integrated with the analytical investigation reported here, enables a realistic assessment of the actual supply of each wall of the coupled wall system. The panel of the wall under compression failed in a shear-compression mode (after some flexural yielding) during a loading increment, under the indicated equivalent shear force, corresponding to a nominal shear force of $16.2 \sqrt{f'_c} A_v$, where A_v is the effective shear area defined by the code. The wall under tension was carrying only a nominal shear force of $1.6 \sqrt{f'_c} A_v$, which was 11 percent of the total base shear force in the tension wall. Although a direct comparison of the experimentally attained shear capacity with the demands obtained from the analytical model is not justified because of the inadequacies of the model, and the fact that the damage state at which the maximum shear demand is attained affects the capacity, an approximate assessment may be made by considering the average attained capacity. The average shear strength, $8.9 \sqrt{f'_c} A_v$, is adequate to resist the inelastic El Centro response shear strength demands. Pacoima response, however, is observed to lead to a highly probable shear failure. In fact, the wall may not have been able to supply even the El Centro shear strength demand if the actual axial-flexural strengths of the wall and coupling girders were incorporated in the analytical model. However, since the walls did not yield during the El Centro response, the shear resisting mechanisms would not have been weakened as in the experiment and the available supply of shear capacity may have been larger than the attained.

The only remedies against undesired mode of shear failure are to either reduce the shear demand or increase the shear strength supply. The most effective measure would be decreasing the axial-flexural strength of the coupling girders to the least acceptable level, as

would be required by service load demands. This would both decrease the demands (as the axial-flexural strength of the total structure will be reduced) and increase the available supplies as the shear capacity of the wall under tension may be utilized more, as its stiffnesses would increase if the level of tension could be decreased. The supply of the wall under compression may not decrease as much as the increase in the tension wall capacity.

6.4.4 Deformation Supply vs. Demand Relations

6.4.4.1 General

Even if the strength supply vs. demand relations of the structural components indicate an adequate supply of shear capacity, the structure should still be required to exhibit an adequate supply of stiffness and deformation capacity in order to be considered to have been adequately designed for all the limit state demands. The parameters (displacement and rotation quantities) that are usually used to judge such an adequacy are: (1) The maximum interstory drift at the service load level. (2) The maximum story drifts (interstory and tangential interstory drifts) as well as the largest inelastic curvatures or rotations of the critical regions at the damageability level, which for the structure under consideration, were characterized by the El Centro response of the structure. (3) The maximum lateral displacement and story drifts, or even more general, the maximum amount of hysteretic energy dissipation required from the structural components to be able to resist the extreme earthquake ground motion without collapse. The extreme earthquake ground motion was assumed to be characterized by the Pacoima accelerogram used in the analyses.

6.4.4.2 Experimental Force-Deformation Relations

Lateral force-displacement envelopes obtained during the testing of the 1/3-scale model of the 4-1/2 story coupled wall subassemblage [4, 34] are presented in Fig. 6.7 to aid the discussion on the deformation supply vs. demand relations. The envelopes of the lateral displacements of the first floor, measured at the exterior boundary of

each wall, are indicated in this figure. The test program had consisted of a number of full reversals of loading at the service level followed by a number of predominantly half cycles of displacement excursions at the post-yield level [34]. The envelopes of the displacements obtained during the excursions towards the indicated direction on Fig. 6.7 exhibit a significant growth of the diaphragm system during the loadings. It is observed that the lateral displacement of the wall in compression was consistently larger, and that the resulting growth of the diaphragm system increased with each of the following consecutive limit states that are indicated in Fig. 6.7: (1) flexural cracking of tension wall, (2) diagonal cracking of tension wall, (3) diagonal and vertical cracking of compression wall, (4) yielding of the coupling girders, (5) yielding of the tension wall, (6) yielding of the compression wall and crushing of the concrete cover of its exterior edge column, (7) crushing of the panel of the compression wall near the exterior edge column, and (8) shear failure of the edge column of the compression wall.

The implications of the diaphragm growth observed in Fig. 6.7 are of extreme importance indicating the invalidity of the internal force distributions obtained during inelastic response based on the axially infinitely stiff diaphragm assumption. The growth is observed to occur in varying amounts within the different portions of the diaphragm system along the wall under tension, the coupling girder which exhibited growth due to the accumulation of residual distortions, in spite of the compressive axial forces that were measured in them, and the wall under compression. It is, therefore, not possible to represent this growth just by assigning a uniform finite axial stiffness to the diaphragm system.

6.4.4.3 Service Level Drifts

This level is considered to correspond to the unfactored earthquake loading defined by the code. As discussed in Chapt. 4, this loading condition induced a maximum top displacement of 0.83 in. (0.038% H) in

the model simulating the complete structure. The maximum interstory drift index of 0.05% occurred at the seventh story. This is one-fifth of the 0.25% which is considered to be the allowable drift index under wind loading.

The lateral displacement and interstory drift index of the fourth floor of the model representing the coupled wall were obtained as 0.23 in. and 0.1%, from analysis using cracked transformed cross sectional properties of the members. The same quantities measured during the experiment under the corresponding load level, were 0.27 in. and 0.054%. The experimental displacement and drift index indicate that:

(1) The test specimen was more flexible than the analytical model based on cracked transformed cross sectional properties. During the test, at service load level, the specimen was not observed to exhibit cracking which would justify the cracked-transformed section assumption for all the members. However, especially due to the observed shear distortions of the walls which were not adequately represented in the analytical model, the measured displacements were larger.

(2) The deformation profile of the test specimen was considerably different from that given by the model, as the discrepancy in the analytical and measured interstory drifts is significantly larger than the discrepancy in the lateral displacement. This is attributed particularly to the one-dimensional analytical modeling of the wall members and the inadequacy of such modeling to incorporate the shear mode of deformation of the walls, which were observed to contribute a significant proportion of the total deformation even at the service load stage.

6.4.4.4 Damage Level Drifts and Rotations

The displacements and rotations obtained during inelastic responses were discussed in Sects. 5.3.2.3 and 5.3.2.4. The maximum displacement at the top of the coupled wall-frame system was 4.98 in. (0.23% H) during the El Centro response. The maximum interstory and the maximum tangential interstory drift indices were at the eighth floor and first

floor and were 0.28% and 0.064% respectively. The maximum plastic rotations attained for the coupling girders and frame beams were 0.0037 radians (sixth floor) and 0.0006 radians (tenth floor), respectively.

The type III coupling girder moment-rotation response, measured during the testing of the 1/3-scale model of the 4-1/2-story coupled wall subassembly, was presented in Fig. 6.4. The analytical maximum rotation of 0.0037 radians is observed to be still within the measured initial linear response range of the typical coupling girder. Also, the maximum interstory drift index of 0.28% is substantially smaller than the drift acknowledged in the 1979 UBC as indicating the initiation of the damage level response, which is 0.4% ($0.5\% \times K$, where K was 0.8 for the structure considered). The analytical drifts and rotations generated for the El Centro response thus indicate that the structure is able to survive the response with only minor structural yielding and slight nonstructural damage. It is important to consider, however, that the analytical model was observed to be stiffer than the test specimen. At the initiation of the yielding of the coupling girders, the test specimen had a fourth floor drift of 0.24% H, and an interstory drift index of 0.27% at the fourth floor. The maximum drift and interstory drift index at the fourth floor of the coupled wall model during the El Centro response, occurring after yielding of most of the coupling girders, were 0.17% H and 0.24%, respectively, less than the corresponding experimental quantities measured at just the initiation of girder yielding. The analytical model is, therefore, verified to be substantially stiffer than the test specimen at this limit state. The rotations at the fixed ends of the girders due to bond slip, the actual contributions of shear distortions of the walls and the rotations of walls at the foundation interface as well as rotations of the foundations themselves, are some of the mechanisms which are not incorporated in the analytical model and which increased the flexibility of the test specimen. Even the experimental interstory drift index of 0.27% at the fourth floor, however, is considerably less than 0.4%, the drift acknowledged by the code to correspond to the end

of service level and initiation of the damage level response. It may be concluded that the stiffness provided by the coupled wall system well exceed any existing requirement for the damage control considerations at the damageability level of response.

6.4.4.5 Collapse Limit State Deformations

The collapse limit state was characterized by the Pacoima response of the structure, as a collapse mechanism was reached for the coupled wall system. If it were not for the stiffness provided by the frame columns, which remained linear, and the deformation hardening of the plastic hinges, the structure would have attained a collapse mechanism. According to the commentary of the SEAOC provisions [43], the collapse state is implicitly defined as corresponding to four to six times the element deformations at the initiation of the damageability level. This would imply interstory drift indices in the order of four to six times 0.4%, which is the drift limit acknowledged by the SEAOC [43] and 1979 UBC provisions as corresponding to end of service load stage. As a result of this discussion, interstory drift indices in the order of 1.4% to 3.36% should have been expected at the collapse limit state, as implicitly considered in the design provisions. It is further expressed in the SEAOC commentary, that the structure, designed in conformance with its minimum requirements and provisions, should possess adequate energy dissipation capacity at interstory drift index levels of 1.4% to 3.36% which are assumed to be the distortions characterizing the collapse limit state.

The analytical responses of the building to the Pacoima ground motion indicated a maximum interstory drift index of 0.9%, occurring at the 10th, 11th, and 12th floors. This is considerably less than the distortion which was assumed to occur at the collapse state, and indicates that the structure possessed analytically substantially more stiffness at the collapse limit state than considered in the design provisions. This is favorable regarding the stability problems usually associated with large distortions at the collapse state, and

would have indicated a successful design, if it could have been verified that the analytical force, distortion, and energy dissipation demands from the structure at the collapse limit state were within the capacity of the structure. Although it was observed in Sect. 6.4.3, that there was a very high probability of a shear failure of the coupled wall system between 3.1 sec. and 3.5 sec. of the Pacoima response, the discussion of the distortion and energy dissipation demands at the collapse limit state are carried out in order to provide a complete example of the required assessments following a nonlinear time-history analysis.

The maximum analytically estimated demands for interstory drift index at the fourth floor, maximum tangential interstory drift index at the first floor and the maximum coupling girder rotation for type III girder at the fourth floor were, respectively, 0.67%, 0.40%, and 0.015 radians during the Pacoima responses of the structure. The corresponding average* quantities measured during the experiment prior to the failure of the wall panel were, respectively, 1.48%, 0.90%, and 0.025 radians. The experimentally measured quantities for the fourth floor and first floor interstory drift indices at failure substantially exceed the analytical demands, implying that the distortion capacity of the wall system is adequate for the analytical distortion demands.

It should be acknowledged, however, that the test specimen had a substantial loss of stiffness, observed from Fig. 6.7, at the collapse state, which was not adequately represented in the analytical model. Furthermore, the initial analytical stiffnesses were observed to be consistently substantially higher than the experimental counterparts, as discussed in Sect. 6.4.4. Consequently, the analytically generated distortions

* As explained earlier, since there was a substantial growth along the two walls and coupling girders at each floor level, only average quantities may be considered for lateral displacements and distortions of the system.

would not represent the actual demands and should be considered as lower bounds.

The coupling girders at even the third and fourth floors of the test specimen do not represent the girders subjected to the maximum rotation demands in the structure. Analysis indicated maximum plastic rotations of 0.015 radians and 0.019 radians at the fourth and ninth floor coupling girders (which were both type III) during the Pacoima response. These rotations occurred in conjunction with nominal shear stresses in the order of $5 \sqrt{f'_c}$. Previous experimental studies on girders of similar proportion and reinforcement percentages indicate [10, 25] that rotations in the order of 0.02 radians are within the capacity of such girders and the girder energy dissipation capacities may be considered to be adequate, as discussed in Sect. 5.3.4. During the experiment, the girders exhibited serious diagonal tension and shear cracking and separation from the slab along the slab-beam interface. They did retain, however, their flexural capacities.

The main conclusions of this section are: (1) Stiffness of the structure is adequate at all limit states compared with the code requirements; (2) The analytical model is substantially stiffer than the test specimen at all limit states; (3) The coupled wall system possessed adequate displacement, drift, and plastic rotation capacity and energy dissipation capacity required analytically at the collapse limit state, and would possibly have survived the Pacoima excitation if it had possessed adequate shear strength.

7. SUMMARY, CONCLUSIONS AND RECOMMENDATIONS

7.1 Summary

Analytical investigations of the seismic responses of R/C coupled wall-frame structural systems, carried out as part of an integrated analytical and experimental research program on the seismic responses of R/C wall-frame systems, are reported. The results from these analytical investigations are compared with some experimental results.

A 15-story R/C wall/coupled wall-frame prototype structure, shown in Fig. 1.1, was selected as the subject of the analytical investigations reported here. Preliminary design of this building was conducted in accordance with the 1973 and 1979 UBC. The 1973 UBC designed version was assessed to possess better behavior at ultimate limit states. This design was the basis for the two analytical models that have been formulated and analyzed in this report. It is also the basis for a large scale (1/3), 4-1/2 story subassemblage test specimen of one of the coupled walls being studied experimentally.

Progress reports on the experimental work are in preparation. Some of the observations and force and displacement measurements from the experimental investigations are used in this report to help assess the states of the art and practice in the design of R/C coupled wall-frame systems.

The two basic objectives of the analytical investigation were: (1) To carry out a comprehensive assessment of the state of the art of the inelastic response prediction of R/C coupled wall-frame structural systems; (2) To carry out an assessment of the state of the practice (code) regarding tall R/C coupled wall-frame structural system design, by the provisions of 1973 UBC, 1979 UBC, and ATC 3-06, utilizing the analytically generated seismic response demands and existing supplies of the structure, as well as some results obtained in the parallel and continuing experimental investigation on the 4-1/2 story subassemblage specimen.

Other objectives of the study included an investigation of the effects of coupled wall-frame interaction on response in order to assess the adequacy of the code (UBC and ATC 3-06) provisions. These provisions require the use of frames to complement the wall systems to resist lateral loading for buildings over 160 ft tall, and require that these frames be capable of resisting at least 25 percent of the total lateral force. The codes fail to provide guidelines for selecting optimum relative stiffness of the frames and walls.

7.2 Conclusions

Some specific conclusions regarding the state of the art in analytical modeling of structures were reported in Chapt. 3. Other conclusions were discussed regarding the linear and inelastic responses of the analytical models in Chapt. 4 and 5, and the comprehensive assessment of the generated and measured supply vs. demand relations of the structure in Chapt. 6. The specific conclusions will not be repeated here as these are best discussed within the context of the relevant data and subsequent deductions, as presented in earlier chapters. Only the general, relevant observations reached at this present stage of the continuing integrated experimental and analytical studies regarding the response of R/C wall/coupled wall-frame structural systems are formulated below.

(1) The present state of the art of analytical modeling of reinforced concrete for the generation of inelastic time-history response is inadequate to provide a realistic assessment of the force and distortion demands from a frame-coupled wall structural system imposed by a seismic ground motion. The main deficiency of the state of the art is not in the general theories of dynamics, finite element analysis, computational procedures, or theory of plasticity. There is no shortage of general purpose inelastic analysis codes, either, which incorporate varying degree of sophistication and various manners of modeling member force-deformation and hysteresis relationships, as well as step-by-step formulation of the equations of motion and the associated state

determination and solution processes.

The main problem lies in the difficulty and uncertainties regarding the realistic assessment of the axial, shear, torsional and flexural stiffness, strength and force-distortion hysteresis characteristics of reinforced concrete structures, particularly when the behavior of their members and/or critical regions are affected by the three-dimensional interactions between the different internal forces as well as by the distortions. In order to be able to formulate analytical models and to use the sophisticated computational methodologies and capabilities that are available, it is first necessary to eliminate the uncertainties in the state of the art in predicting realistic stiffness, strength, deformation, and hysteretic energy dissipation capacity of reinforced concrete structures.

Utilization of inelastic time-history analysis of reinforced concrete as a design tool, or to arrive at definite conclusions regarding the seismic response of a certain structural system should, therefore, be carried out with extreme precaution. The existing procedures of analytical modeling and computer codes for inelastic analysis may be used for parameter investigations or to establish certain bounds of response only if the significant uncertainties in the response of reinforced concrete are acknowledged and incorporated into the conclusions. The existence of a large number of general purpose inelastic analysis codes should not be accepted as justification of their usage without a clear recognition of: the actual response characteristics of reinforced concrete; the limitations of the analytical procedure to reflect these characteristics as discussed above; and the uncertainties involved in the quantitative assessment of input data regarding actual supplies of stiffness, strength, deformation capacity, and hysteretic energy dissipation of the structural components. The discussions in Chaps. 3, 4, 5, and 6 of this report should provide guidelines for the usage of general purpose inelastic analysis codes in such a context.

(2) The code provisions regarding seismic resistant design of R/C coupled wall-frame structures do not safeguard against a structure with undesirable ultimate limit state, and especially collapse state response characteristics. The 1973 UBC specifications were concluded to be more favorable than the 1979 UBC or ATC 3-06 specifications in this respect. Even the 1973 UBC designed structure, however, was assessed to be unable to escape an earlier shear-compression failure of the panel of the wall under compression during the Pacoima response. The Pacoima ground motion characterized the collapse limit state demands from the structure. A more significant observation was the probability of such a failure even during the El Centro response of the structure, which was considered to represent realistic damageability level of demands from the designed structure, although the demands from this earthquake significantly surpassed the factored design demands defined by the code.

The main reasons leading to an insufficient shear-compression capacity of the wall were assessed to be the code design process leading to excessive wall axial forces, and particularly wall overturning (axial-flexural) overstrength, and very large unfavorable redistribution of shear force. The wall overturning overstrength results mainly from the wall cross sections being overdesigned and from the overstrength of the already high flexural resistance capacity of the coupling girders. The coupling girders overstrength was a consequence of proportioning for maximum lateral stiffness and from determining flexural strength demands throughout a linear elastic analysis as required by the seismic code provisions. Main reasons for the observed overstrength of the coupling girders were the contributions of: the slab reinforcement; the higher value of the actual yielding of the main girder reinforcement when compared with the minimum yielding value specified by code; the increase in the strength resistance of the reinforcement beyond its actual yielding strength due to strain hardening; the development of axial compression in the girders arising due to redistribution of shear force between the walls; and other factors discussed in Chapt. 6.

The wall cross sections, (particularly when under compression), were observed to possess similarly high levels of axial-flexural overstrength since the code provisions require the edge members to be capable of resisting the complete axial-flexural demands from the cross section. The contribution of: the wall panel steel; the increase in the actual yield capacity of reinforcement over the nominal value and a further, more significant, increase due to strain hardening; and the increase in the actual compression concrete strength over the nominal value and a further, significant increase in this strength and, particularly its deformation capacity due to the effective confinement of the concrete at the edge members, were the main causes of the observed axial-flexural overstrength of the wall.

The axial-flexural overstrengths of the main components of the coupled wall system led to a substantial increase (200%) in the overall overturning strength of the structure, with respect to the factored code design demand, which was verified through experimental investigations.

(3) Combined Effects of Axial-Flexural Overstrength with Redistribution of Shear Resistance: the shear capacity of the wall cross sections was not capable of withstanding the increased shear force accompanying the increase in the overturning strength of the structure. This was mainly because the difference in the axial forces of the two walls led to an actual, measured redistribution of shear force such that the wall under compression was resisting nearly 90 percent of the total shear force even at low levels of lateral force (this occurrence was not incorporated into the analytical model). The increased shear demand from the wall under compression, when coupled with the high level of compressive stresses of the panel, arising due to the overstrengths discussed above, led to a shear-compression failure of the panel. The shear strength demands obtained from the inelastic response to the derived Pacoima ground motion indicate the high probability of the occurrence of such a failure, even at the considerably underestimated levels of these demands resulting from the analysis of the formulated analytical model (Chapt. 6).

(4) The contribution of the frames, even when these were designed to meet the minimum lateral strength demands required by the code, as in this study, were observed to be beneficial to the structural system. The stiffness of the overall structure is increased, leading to a better response at service level and better damage protection. Although due to this increase in stiffness the seismic shear force requirements increased, the advantages provided by the additional sources of energy dissipation and increased redundancy of the structural system were thought to justify the increase in shear force demands.

7.3 Recommendations to Improve the State of the Practice

(1) The R/C coupled wall-frame system design provisions of the UBC should be revised to incorporate a more realistic evaluation of the total shear force and of its distribution along the height of the structure to estimate the maximum possible story shear that can be developed. Furthermore, the establishment of the design story shear demands should be based on a more realistic estimation of the distribution of all the internal forces among the different lateral force resisting components (walls and frame columns and beams). This requires consideration of the actual axial-flexural strengths of the coupling girder and wall members, and the actual shear strength demands that may be required from the walls (in particular, the shear and compression stress state demands from the panels). To be able to carry out a realistic estimation of the shear strength supply present code provisions have to be improved incorporating more realistic shear resisting mechanisms of a R/C wall critical region when this region is subjected to seismic actions.

(2) For the time being it is suggested that to improve seismic hysteretic behavior of coupled wall systems, the design of its coupling girders should be done in such a way that they offer the minimum flexural strength compatible with the stiffness required at serviceability and damageability levels. Transverse reinforcement detailing of the girders should be carried out with proper recognition of the increased inelastic distortion and hysteretic energy dissipation demands from these girders.

(3) The proper frame stiffness and strength characteristics should be selected to balance the increases in seismic demands by the activation, at the proper level of demand, of the energy dissipation mechanisms that the frames possess. The frame-coupled wall interaction was observed to change the response characteristics of the structure considerably, even when the frames constituted only a minor portion of the structural stiffness and strength. The presence of the frames affected the distribution of wall shears such that the base overturning moment to shear ratio of the coupled wall system decreased as did the total dynamic base shear demand from the walls. These factors should be considered in the shear design of the walls. Furthermore, the conclusions reached by previous analytical studies on wall or coupled wall responses which did not incorporate the presence of frames, should be reassessed in view of these observed significant contributions of frames to the response of the complete structure.

REFERENCES

1. Aktan, A. E., and Pecknold, D. A., "Response of a Reinforced Concrete Section to Two-Dimensional Curvature Histories," ACI Journal, Proceedings, Vol. 71, May 1974.
2. Aktan, A. E., Pecknold, D. A., and Sozen, M. A., "R/C Column Earthquake Response in Two Dimensions," Journal of the Structural Division, ASCE, Vol. 100, No. ST10, October 1974.
3. Aktan, A. E., and Ersoy, U., "Analytical Study of R/C Material Hysteresis." Paper presented at the AICAP-CEB Symposium on "Structural Concrete under Seismic Actions," Rome, April 1979, and published in CEB Bulletin No. 132, 1979.
4. Aktan, A. E., and Bertero, V. V., "The Seismic Resistant Design of R/C Coupled Structural Walls," Report No. UCB/EERC-81/07, Earthquake Engineering Research Center, University of California, Berkeley, 1981.
5. Aktan, A. E., and Bertero, V. V., "Analytical and Physical Modeling of R/C Frame-Wall/Coupled Wall Structures." Paper presented at the Symposium on "Dynamic Modelling of Structures," Watford, England, November 1981 and to be published in the Proceedings.
6. Aoyama, H., and Yoshimura, M., "Tests of R/C Shear Walls Subjected to Bi-axial Loading," Proceedings, 7th World Conference on Earthquake Engineering, Istanbul, Turkey, September 1980.
7. ATC 3-06, "Tentative Provisions for the Development of Seismic Regulations for Buildings." Prepared by Applied Technology Council, National Bureau for Standards, 510, Washington, D.C., June 1978.
8. Axley, J. W., and Bertero, V. V., "Infill Panels: Their Influence on Seismic Response of Buildings," Report No. UCB/EERC 79/28, Earthquake Engineering Research Center, University of California, Berkeley, 1979.
9. Becker, J. M., and Mueller, P., "Seismic Response of Large Panel Precast Concrete Buildings," Advanced Design Concepts Seminar, PCI Convention, October 14-18, 1979, Dallas, Texas.
10. Bertero, V. V., Popov, E. P., and Wang, T. Y., "Hysteretic Behavior of Reinforced Concrete Flexural Members with Special Web Reinforcement," Report No. EERC 74-9, Earthquake Engineering Research Center, University of California, Berkeley, 1974.

11. Bertero, V. V., Popov, E. P., and Wang, T. Y., "Seismic Design Implications of Hysteretic Behavior of R/C Elements under High Shear," Proceedings of the Review Meeting U.S.-Japan Cooperative Research Program in Earthquake Engineering with Emphasis on the Safety of School Buildings. University of Hawaii, Honolulu, Hawaii, August 1975. Published by The Japan Earthquake Engineering Promotion Society, Tokyo, Japan, pp. 75-106.
12. Bertero, V. V., Herrera, R. A., and Mahin, S. A., "Establishment of Design Earthquakes: Evaluation of Present Methods," Proceedings, International Symposium on Earthquake Structural Engineering, St. Louis, August 1976.
13. Bertero, V. V., and Bresler, B., "Failure Criteria (Limit States)," Report No. UCB/EERC-77/06, Earthquake Engineering Research Center, University of California, Berkeley, 1977.
14. Bertero, V. V., "Seismic Behavior of Structural Concrete Linear Elements (Beams, Columns) and their Connections," Proceedings, AICAP-CEB Symposium on Structural Concrete under Seismic Actions, Rome, May 1979, pp. 123-212.
15. Bertero, V. V., "Seismic Behavior of R/C Structural Systems," Proceedings, 7th World Conference on Earthquake Engineering, Vol. 6, Istanbul, Turkey, September 1980, pp. 323-330.
16. Chávez, J. W., "Study of the Seismic Behavior of Two-Dimensional Frame Buildings, A Computer Program for the Dynamic Analysis: INDRA," Bulletin of IISEE, Vol. 18, 1980.
17. Clough, R. W., Benuska, K. L., and Wilson, E. L., "Inelastic Earthquake Response of Tall Buildings." Paper presented at the 3rd World Conference on Earthquake Engineering, New Zealand, January 1965.
18. Coull, A., and Choudbury, J. R., "Analysis of Coupled Shear Walls," Journal ACI, September 1967.
19. Ciampi, V., Eligehausen, R., Bertero, V., and Popov, E., "Analytical Model for Deformed Bar Bond under Generalized Excitations," Working Papers, IABSE Colloquium, Delft, Netherlands, June 1981, pp. 53-74.
20. Fiero, E., Popov, E., and Bertero, V., "Effect of Slab on the Earthquake Response of R/C Beam-Column Subassemblage," EERC Report in Preparation.
21. Gates, W. E., "The Art of Modelling Buildings for Dynamic Seismic Analysis," Proceedings, Workshop on Earthquake-Resistant Reinforced Concrete Building Construction (V. Bertero, Organizer), Vol. II, University of California, Berkeley, July 1977, pp. 887-937.

22. Giberson, M. F., "Two Nonlinear Beams with Definition of Ductility," Journal of the Structural Division, ASCE, Vol. 95, No. ST2, Proc. Paper 6377, February 1969, pp. 137-157.
23. Guendelman, I. R., and Powell, G. H., "DRAIN-TABS: A Computer Program for Inelastic Earthquake Response for Three-Dimensional Building Systems," Report No. UCB/EERC-77/08, Earthquake Engineering Research Center, University of California, Berkeley, 1977.
24. Iliya, R., and Bertero, V. V., "Effects of Amount and Arrangement of Wall-Panel Reinforcement on Hysteretic Behavior of Reinforced Concrete Walls," Report No. UCB/EERC-80/04, Earthquake Engineering Research Center, University of California, Berkeley, February 1980.
25. Ma, S. Y. M., Popov, E. P., and Bertero, V. V., "Experimental and Analytical Studies on the Hysteretic Behavior of Reinforced Concrete Rectangular and T-Beams," Report No. EERC-76/02, Earthquake Engineering Research Center, University of California, Berkeley, 1976.
26. Mahin, S. A., and Bertero, V. V., "An Evaluation of Some Methods for Predicting Seismic Behavior of Reinforced Concrete Buildings," Report No. EERC-75/5, Earthquake Engineering Research Center, University of California, Berkeley, 1975.
27. Mahin, S., "On the Use of Computers in the Seismic-Resistant Design of Reinforced Concrete Buildings," Proceedings, II, Workshop on Earthquake-Resistant Reinforced Concrete Building Construction (V. Bertero, Organizer), University of California, Berkeley, July 1977.
28. Mahin, S. A., and Bertero, V. V., "Prediction of Nonlinear Seismic Building Behavior," Journal of the Technical Councils of ASCE, Proceedings, ASCE, Vol. 104, No. TCI, November 1978.
29. Mondkar, D. P., and Powell, G. H., "ANSR-II: Analysis of Nonlinear Structural Response, User's Manual," Report No. UCB/EERC-79/17, Earthquake Engineering Research Center, University of California, Berkeley, 1979.
30. Newmark, N., "A Method of Computation for Structural Dynamics," Proceedings, ASCE, Engineering Mechanics Division, Vol. 85, No. EM3, July 1959.
31. Newmark, N., and Rosenblueth, E., Fundamentals of Earthquake Engineering, Englewood Cliffs, N.J.: Prentice-Hall, Inc., 1971.
32. Oesterle, R. G., et al., "Earthquake Resistant Structural Walls - Tests of Isolated Walls - Phase II," Report to NSF submitted by Construction Technology Laboratories, P.C.A., October 1979.

33. Otani, S., "SAKE - A Computer Program for Inelastic Response of Reinforced Concrete Frames to Earthquakes," Structural Research Series No. 413, Civil Engineering Studies, University of Illinois, Urbana-Champaign, November 1974.
34. Ozelcuk, A., Aktan, A. E., and Bertero, V. V., "Experimental Responses of R/C Coupled Structural Walls," EERC Report in progress.
35. Park, R., and Paulay, T., Reinforced Concrete Structures, John Wiley & Sons, Inc., 1975.
36. Paulay, T., "Earthquake Resistant Structural Walls," Proceedings, Workshop on Earthquake Resistant Reinforced Concrete Building Construction (V. Bertero, Organizer), University of California, Berkeley, July 1977.
37. Paulay, T., "The Design of Reinforced Concrete Ductile Shear Walls for Earthquake Resistance," Research Report, Department of Civil Engineering, University of Canterbury, Christchurch, New Zealand, February 1981.
38. Pecknold, D., and Shuarwardy, M., "Effects of Two-Dimensional Earthquake Motion on Response of R/C Columns," Proceedings, Workshop on Earthquake Resistant Reinforced Concrete Building Construction (V. Bertero, Organizer), University of California, Berkeley, July 1977.
39. Powell, G. H., "DRAIN-2D User's Guide," Report No. EERC-73/22, Earthquake Engineering Research Center, University of California, Berkeley, 1973.
40. Powell, G. H., "Computer Programs for Analysis of Seismic Response of Reinforced Concrete Buildings," Proceedings, II, Workshop on Earthquake-Resistant Reinforced Concrete Building Construction (V. Bertero, Organizer), University of California, Berkeley, July 1977, pp. 857-885.
41. Reimer, R. B., et al., "Evaluation of the Pacoima Dam Accelerogram," in "Earthquake Engineering at Berkeley - 1973," Report No. EERC-73/23, Earthquake Engineering Research Center, University of California, Berkeley 1973, pp. 27-36.
42. Saatcioglu, M., Derecho, A. T., and Corley, W. G., "Coupled Walls in Earthquake-Resistant Buildings," Report to NSF by Construction Technology Laboratories, Portland Cement Association, Skopie, Illinois, June 1980.
43. SEAOC, "Recommended Lateral Force Requirement Seismology Committee," Structural Engineers Association of California, San Francisco, 1959.
44. Selna, L. G., "Modelling of Reinforced Concrete Buildings," Proceedings, II, Workshop on Earthquake Resistant Reinforced Concrete Building Construction (V. Bertero, Organizer), University of California, Berkeley, July 1977, pp. 887-937.

45. Sucuoglu, H., and Aktan, A. E., "Hysteretic Response of R/C Frames," Reinforced Concrete Structures Subjected to Wind and Earthquake Forces, Publication SP-63, ACI Committee 442, 1980.
46. Staffier, S. R., and Sozen, M. A., "Effect of Strain Rate on Yield Stress of Model Reinforcement," Civil Engineering Studies, Structural Research Series No. 415, University of Illinois, Urbana, 1975.
47. Strong Motion Earthquake Accelerograms, Digitized and Plotted Data, Vol. II, part A., Corrected Accelerograms and Integrated Ground Velocity and Displacement Curves, Earthquake Engineering Research Laboratory, California Institute of Technology, Pasadena, California.
48. Takayanagi, T., and Schnobrich, W. C., "Computed Behavior of Reinforced Concrete Coupled Shear Walls," SRS Report No. 434, University of Illinois at Urbana-Champaign, December 1976.
49. Takayanagi, T., Derecho, A. T., and Corley, W. G., "Analysis of Inelastic Shear Deformation Effects in Reinforced Concrete Structural Wall Systems," CSCE-ASCE-ACI-CEB, International Symposium on "Nonlinear Design of Concrete Structures," University of Waterloo, Waterloo, Ontario, August 7-9, 1979.
50. Takeda, T., Sozen, M. A., and Nielsen, N. N., "Reinforced Concrete Response to Simulated Earthquakes," Journal of the Structural Division, ASCE, Vol. 96, No. ST12, December 1970.
51. Takizawa, H., "Notes on Some Basic Problems in Inelastic Analysis of Planar R/C Structures," Part I and Part II, Transactions of AIJ. No. 240, February 1976; and No. 241, March 1976, Japan.
52. Vallenias, J. M., Bertero, V. V., and Popov, E. P., "Hysteretic Behavior of Reinforced Concrete Structural Walls," Report No. UCB/EERC-79/20, Earthquake Engineering Research Center, University of California, Berkeley, 1979.
53. Wang, T. Y., Bertero, V. V., and Popov, E. P., "Hysteretic Behavior of Reinforced Concrete Framed Walls," Report No. EERC 75-23, Earthquake Engineering Research Center, University of California, Berkeley, 1975.
54. "Uniform Building Code," International Conference of Building Officials, Whittier, Ca., 1973, 1976, and 1979 editions.
55. Wilson, E. L., and Dovey, H. H., "Three Dimensional Analysis of Building Systems," Report No. EERC-72/8, Earthquake Engineering Research Center, University of California, Berkeley 1972.
56. Zienkiewicz, O. C., The Finite Element Method in Engineering Science, New York: McGraw-Hill, 1971.

T A B L E S



TABLE 2.1 BILINEAR MOMENT-CURVATURE RELATIONSHIPS: VALUES OF EFFECTIVE LINEAR ELASTIC FLEXURAL STIFFNESS AND YIELD MOMENT FOR THE WALL SECTION CORRESPONDING TO DIFFERENT AXIAL FORCE LEVELS

AXIAL LOAD (KIPS)	EFFECTIVE (EI) (KIP-IN ²)10 ⁹	YIELD MOMENT (KIP-IN)10 ⁵
15000	103.	10.6
10000	81.	13.
8750	78.	13.3
5000	74.	11.1
4000	72.	9.9
2000	70.	7.6
0	40.	5.6
-1500	32.	3.8
-3000	5.	2.0
-4200	2.	1.6

TABLE 2.2 BILINEAR MOMENT-CURVATURE RELATIONSHIPS: VALUES OF EFFECTIVE LINEAR ELASTIC FLEXURAL STIFFNESS AND YIELD MOMENT FOR THE COLUMN SECTION AT DIFFERENT AXIAL FORCE LEVELS

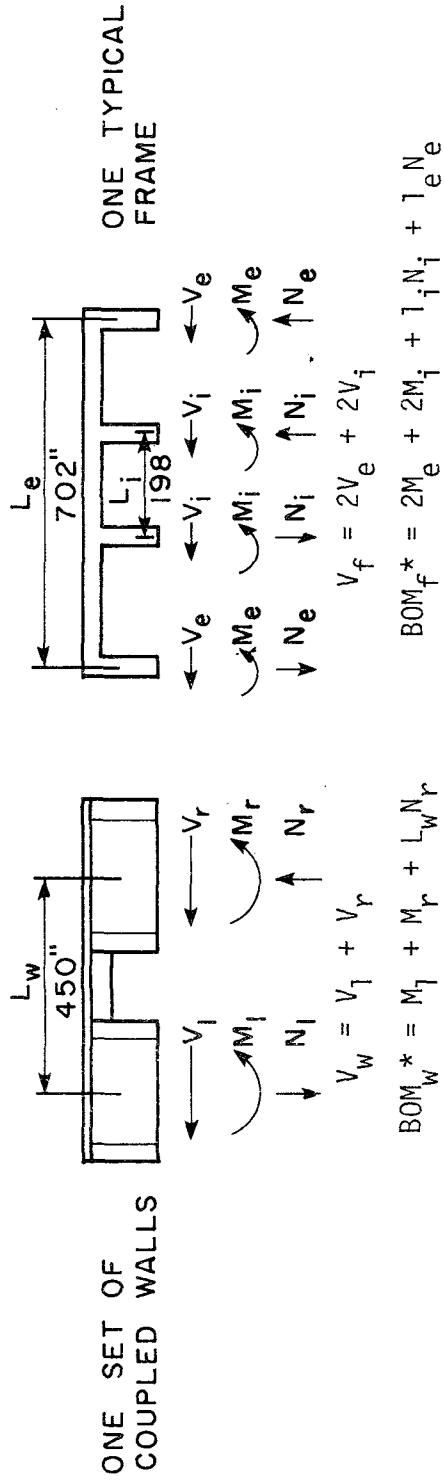
AXIAL LOAD (KIPS)	EFFECTIVE (EI) (KIP-IN ²)10 ⁷	YIELD MOMENT (KIP-IN)10 ³
4500	14.28	10
3400	19.44	17.5
1700	12.93	23.6
0	10.44	16.7
-900	5.94	9.5

TABLE 4.1 MAGNITUDE AND DISTRIBUTION OF THE EARTHQUAKE LOADING FOR THE PROTOTYPE COUPLED WALL SYSTEM (INCLUDING TORSION)

FLOOR	1973 UBC (ZONE 3)
	KIPS
15	86.76
14	91.63
13	85.09
12	78.54
11	72.00
10	65.45
9	58.91
8	52.36
7	45.82
6	39.27
5	32.73
4	26.18
3	19.64
2	13.09
1	6.55
<hr/>	
Total Base	774
Shear, Kips	

The point of application of the resultant "E" loading measured from the base of the wall, is: 1478 in. for the 1973 UBC loading, i.e., at 0.68 H where H = 180 ft.

TABLE 4.2 LINEAR DEMANDS FOR ONE SET OF COUPLED WALLS AND ONE TYPICAL FRAME AT THE BASE OF THE PROTOTYPE



ANALYSIS	WALLS RESIST ALL EQ EFFECTS INDIVIDUALLY		WALLS AND FRAMES RESIST ALL EQ EFFECTS TOGETHER	
	V_w kips	BOM_w 10 ³ kip-in	V_w kips	BOM_w 10 ³ kip-in
UBC 73 "E" LOADING	774	1144.18	656	807.35
EL CENTRO** S00 E, 0.33 g 5% DAMPING	4418	6188.34	5692	6963.61
DERIVED PACOIMA** S16E, 0.4 g 5% DAMPING	13012	19828.06	11554	14613.28
			V_f kips	BOM_f 10 ³ kip-in
			30	190.56
			257	727.73
			527	1533.08

* BOM: Base Overturning Moment, which is a measure of flexural demand.
 ** Modal Spectral Analysis, only the first three Modes of the structure were considered.

TABLE 5.1 COMPARISON OF PERIODS OF THE TWO MODELS IN SECONDS

STRUCTURAL MODEL:	LINEAR MODEL	TIME-HISTORY OF NONLINEAR RESPONSE		APPROXIMATE UBC EXPRESSION
		EL CENTRO	PACOIMA	
COUPLED WALL MODEL	1.20	1.73*	1.89*	1.15
COUPLED WALL-FRAME MODEL	0.99	1.64*(1.52)**	1.67*(1.60)**	1.15

* These are effective periods obtained by considering the number of zero crossings during the complete duration of inelastic response.

** These periods are obtained by considering only the first inelastic displacement wave form, idealized as a full sine wave.

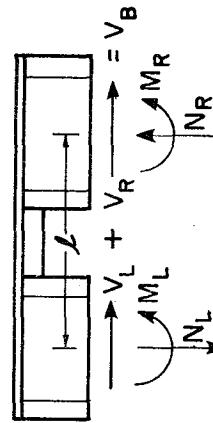
TABLE 5.2 MAXIMUM VALUES OF DISPLACEMENTS AND DRIFTS
OBTAINED FROM THE TIME-HISTORY ANALYSES

GROUND MOTION	ANALYTICAL MODEL	MAXIMUM DISPLACEMENT	MAXIMUM INTERSTORY DRIFT	MAXIMUM TANGENTIAL INTERSTORY DRIFT
EL CENTRO	Coupled Wall Model	4.98"	0.45"/.0031	0.089"/.00062
	Coupled Frame-Wall Model	4.98"	0.40"/.0028	0.092"/.00064
PACOIMA DAM	Coupled Wall Model	18.83"	1.70"/.012	0.461"/.0032
	Coupled Frame-Wall Model	15.53"	1.29"/.009	0.370"/.0026

All values for drift are given in inches and drift index, i.e., drift/story height.

TABLE 5.3 THE MAXIMUM SHEAR FORCES, AXIAL FORCES AND MOMENTS AT THE BASES OF THE WALLS OF THE COUPLED WALL SYSTEM

GROUND MOTION	ANALYTICAL MODEL	VALUE	t (sec)	V _B (Kips)	M _O (Kips-in)	M _L (Kips-in)	M _R (Kips-in)	N _L (Kips)	N _R (Kips)	α
EL CENTRO	CW	V _B (max)	4.9	2414	2,236,290	200,000	200,000	+4200	+293	0.40
	CW	M _O (max)	5.1	1626	3,849,638	382,669	382,669	+5692	-1162	0.62
	CWF	V _B (max)	4.8	2675	2,985,610	350,000	350,000	+4693	+170	0.33
	CWF	M _O (max)	5.8	1522	3,869,766	419,283	419,283	+5646	-1090	0.71
PACOIMA DAM	CW	V _B (max)	3.0	3718	3,244,712	937,112	568,600	+4100	+400	0.46
	CW	M _O (max)	3.1	1568	5,281,446	1,002,127	576,719	+6379	-1849	0.77
	CWF	V _B (max)	3.5	4053	3,719,617	830,806	428,831	+4883	+351	0.30
	CWF	M _O (max)	3.1	1506	5,322,165	1,072,991	677,074	+6267	-1671	1.10



$$M_O = M_L + M_R + \mathcal{L}N_L$$

t: time of occurrence

V_B: shear of both wall piers at the base of the wall

M_O: overturning moment at the base of the wall

M_L: moment at the base of the left wall pier

M_R: moment at the base of the right wall pier

N_L: axial force at the base of the left wall pier [(+) compression, (-) tension]

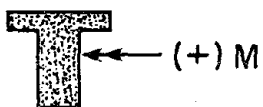
N_R: axial force at the base of the right wall pier [(+) compression, (-) tension]

α: moment to shear ratio

CW: coupled wall

CWF: coupled wall-frame

TABLE 5.4 MAXIMUM MOMENTS
ATTAINED BY THE COUPLING GIRDERS



FLOOR LEVEL	TYPE	MOMENTS IN 10 ² KIP-IN.			EL CENTRO RESPONSES		PACOIMA RESPONSES	
		M _C	M _Y	M _U	CW	CWF	CW	CWF
1	1	92	104	193	104	105	80	114
		115	127	239	124	123	137	136
2	2	159	180	337	181	183	177	202
		182	177	331	178	180	203	199
3	3	192	223	418	226	229	261	259
		214	261	476	263	264	297	295
4	3				226	231	267	265
					264	267	306	301
5	3				227	232	273	269
					263	268	310	305
6	3				227	233	279	272
					264	269	315	308
7	3				227	233	284	273
					263	269	320	310
8	3				227	233	287	275
					262	269	323	309
9	3				227	232	291	277
					263	269	328	313
10	2	159	180	337	183	187	237	224
		182	177	331	180	184	234	221
11	2				183	186	239	224
					179	183	236	221
12	2				183	186	241	225
					180	183	237	222
13	1	92	104	193	106	109	146	135
		115	127	239	128	131	168	156
14	1				106	109	146	134
					128	131	168	156
15	1				106	109	146	134
					129	131	168	155

CW: coupled wall model
 CWF: coupled wall frame model
 M_Y(+/-): yield moment capacity
 M_U(+/-): ultimate moment capacity
 M_C(+/-): 1973 UBC factored code demand for flexural design

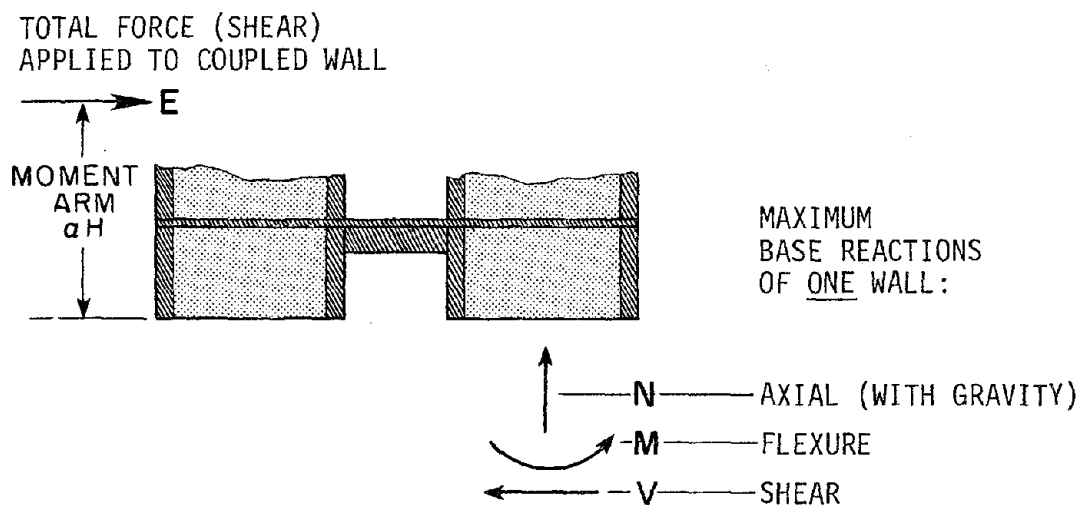
TABLE 5.5 MAXIMUM SHEARS ATTAINED
BY THE COUPLING GIRDERS

SHEAR FORCES IN KIPS

FLOOR LEVEL	TYPE	EL CENTRO CW	EL CENTRO CWF	PACOIMA CW	PACOIMA CWF	CODE DEMAND
1	1	136	136	151	149	243
2	2	214	216	240	239	301
3	3	291	295	332	330	377
4	3	292	297	340	337	
5	3	292	298	347	342	
6	3	293	299	354	345	
7	3	293	299	359	347	
8	3	292	299	363	349	
9	3	292	299	368	351	↓
10	2	216	221	280	264	301
11	2	216	220	283	265	↓
12	2	216	220	285	266	↓
13	1	140	143	187	173	243
14	1	140	143	187	172	↓
15	1	140	142	187	172	↓

CW: coupled wall model
 CWF: coupled wall-frame model
 Code Demand: 1973 UBC factored code demand for shear design

TABLE 6.1 COMPARISON OF FACTORED* CODE AND ANALYSIS
 MAXIMUM DEMANDS AT THE BASE OF COUPLED WALLS



CODE/ANALYSIS		FOR ONE WALL			TOTAL	MOMENT ARM	
		AXIAL FORCE* (KIPS)		FLEXURE* KIP-IN $\frac{3}{10}$	SHEAR* KIPS		(E) FORCE KIPS
		COMP.	TENS.				
1973 UBC		4802	323	269	1275	774	0.68H
1979 UBC		6374	1153	353	1175	999	0.71H
ATC 3-06		4364	176	189	722	865	0.60H
FRAMES ARE INCLUDED IN THE ANALYSES	EL CENTRO Linear	12386	7846	1206	2846	5692	0.60H
	EL CENTRO Nonlinear	5646 [†]	1090 [†]	419 [†]	1338**	2675**	0.33H**
	PACOIMA Linear	23626	19086	2501	5777	11554	0.60H
	PACOIMA Nonlinear	6267 [†]	1671 [†]	1073 [†]	2790**	4053**	0.30H**

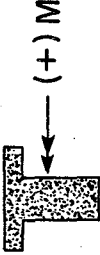
* Axial force and flexure are factored by (1.4) for 1973 UBC and 1979 UBC, by (1) for ATC 3-06. Shear is factored by 2.8/0.85 for 1973 UBC, 2/0.85 for 1979 UBC and 1/0.6 for ATC 3-06, i.e., capacity reduction factors were included in code shear demands.

** At time of maximum wall base shear.

† At time of maximum wall base overturning moment.

TABLE 6.2 COUPLING GIRDER SUPPLIES AND DEMANDS

GIRDER TYPE	DEMANDS				SUPPLIES			
	FACTORED (AND MODIFIED BY ϕ) 1973 UBC DEMANDS				RESULTS OF CROSS SECTIONAL ANALYSES: (INPUT FOR TIME-HISTORY ANALYSES)			
	M(+)	M(-)	V	$v(\sqrt{f'_c})$	M(+)(y/u)	M(-)(y/u)	V(u)	$v(u)(\sqrt{f'_c})$
I	9226	11502	226	3.31	10388/193000	12681/28900	287	4.20
II	14530	16807	301	4.41	17960/33100	17653/33700	397	5.81
III	19166	21442	372	5.45	22285/41800	26104/47600	532	7.79
GIRDER TYPE	MAXIMUM DEMANDS ATTAINED DURING ANALYTICAL (PACOIMA) RESPONSE				MEASURED VALUES AT YIELD, DURING EXPERIMENTAL RESPONSE			
	M(+)	M(-)	V	$v(\sqrt{f'_c})$	M(+)(y)	M(-)(y)	V(y)	$v(y)(\sqrt{f'_c})$
I	13500	15600	173	2.54	16200	27000	257	3.37
II	22200	22500	266	3.90	27000	36450	378	4.95
III	27700	31300	351	5.14	36450	54000	538	7.04

- Notes:
- 1) M in kip-inches, V in kips, v in $\sqrt{f'_c}$, psi units
 - 2) Experimental Response included only the first four floor girders
 - 3) y/u indicates yield/ultimate as computed
 - 4) Gravity loading of the beam was considered in code demands and analytical responses
 - 5) f'_c is 4000 psi nominal, 5000 psi measures, as used to compute $v(\sqrt{f'_c})$
 - 6) Sign convention is 

FIGURES

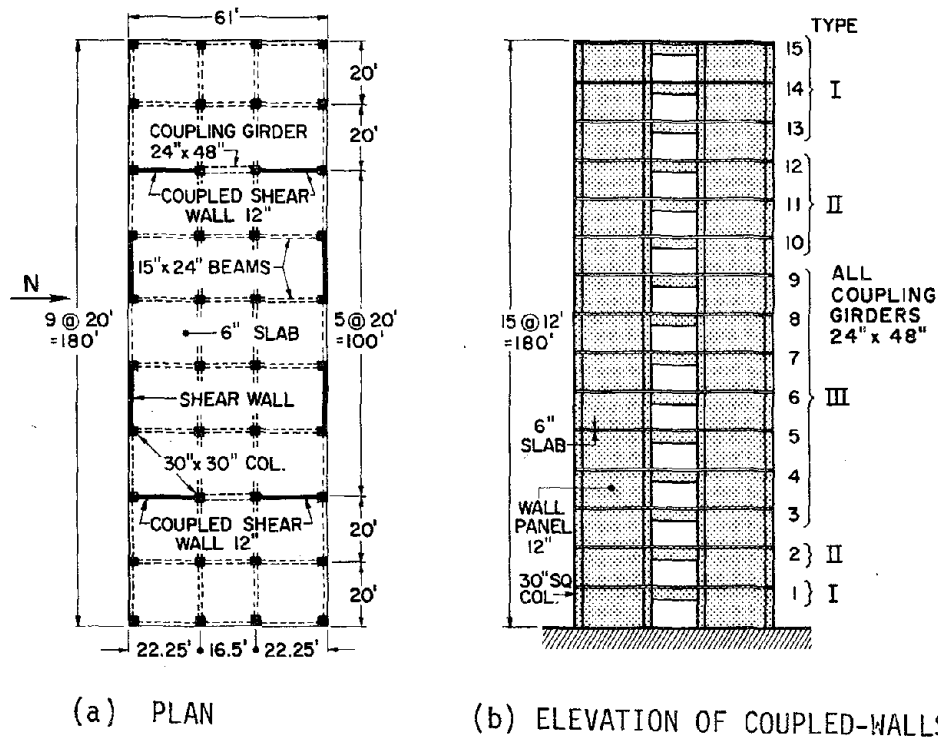


FIG. 1.1 STRUCTURAL LAYOUT OF THE 15-STORY R/C FRAME-COUPLED WALL BUILDING

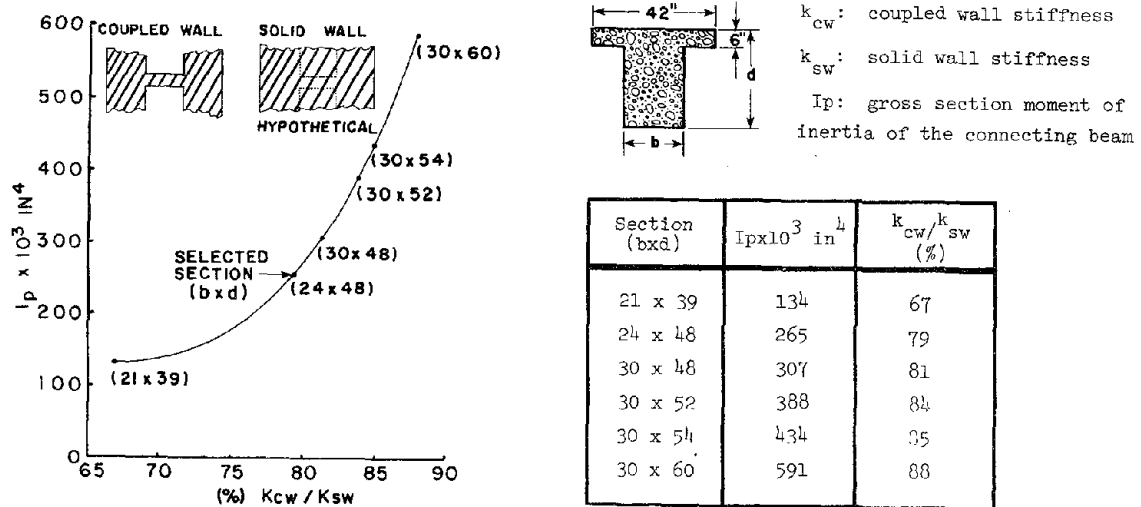


FIG. 2.1 CONTRIBUTION OF BEAM STIFFNESS TO THE STIFFNESS OF COUPLED WALLS

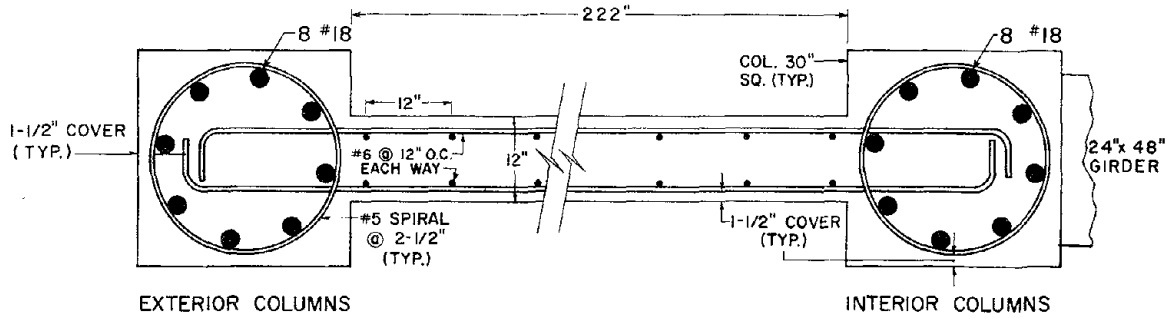


FIG. 2.2 WALL CROSS SECTION DESIGNED BY UBC-73 PROVISIONS

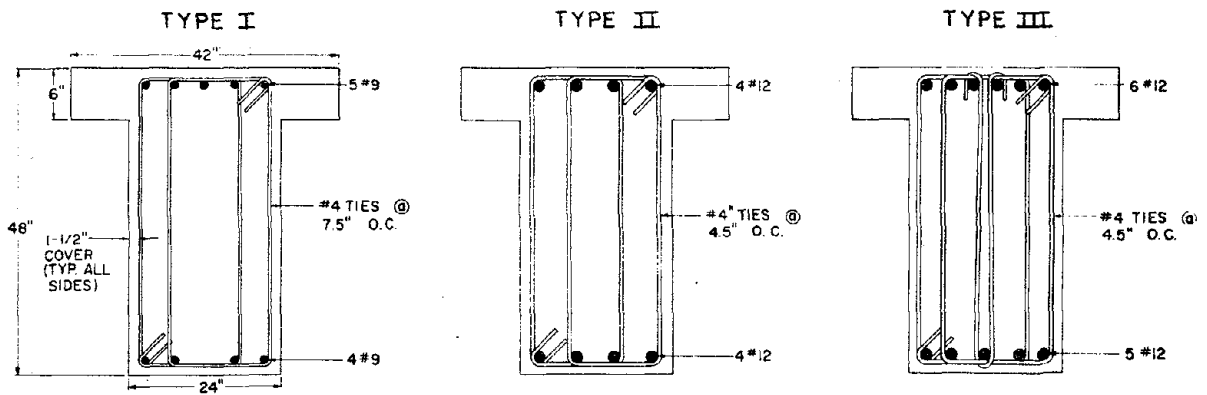


FIG. 2.3 COUPLING GIRDERS DESIGNED BY UBC-73 PROVISIONS

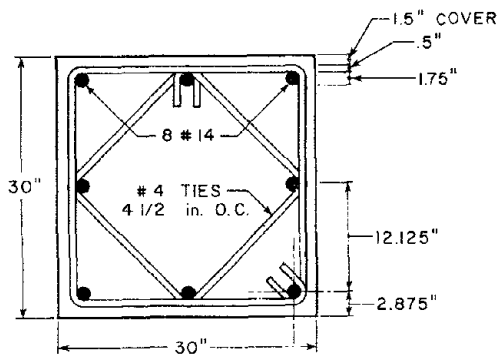


FIG. 2.4 FRAME COLUMNS DESIGNED BY UBC-73

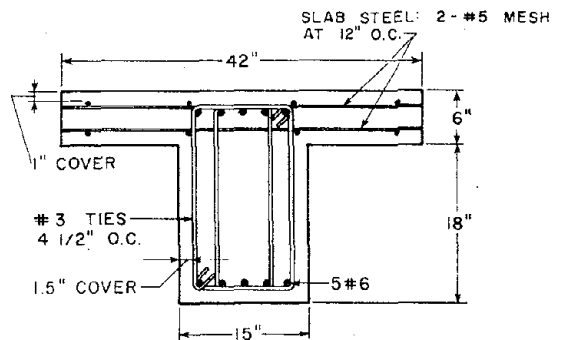
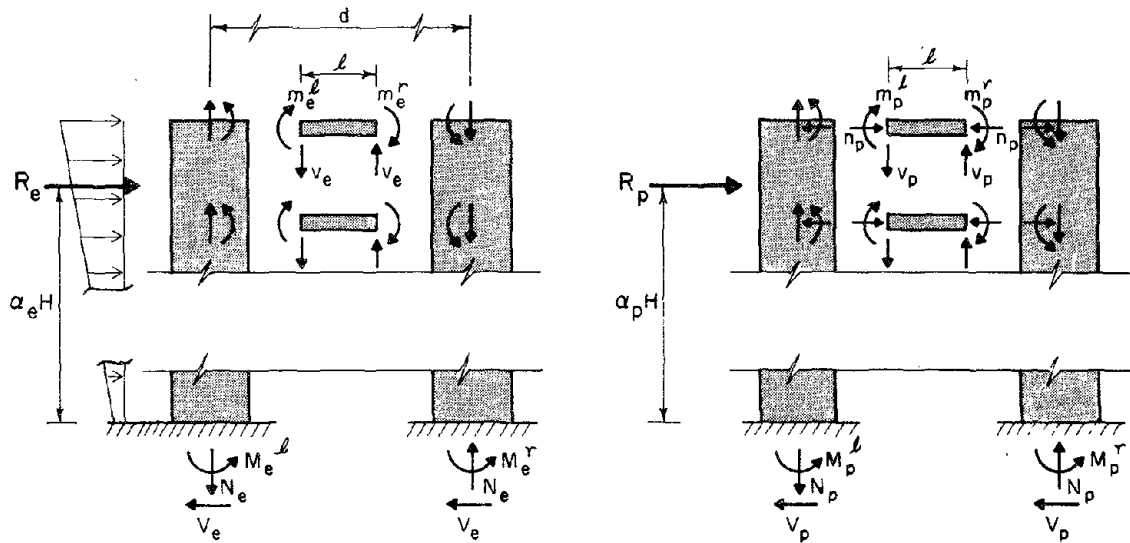


FIG. 2.5 FRAME BEAMS DESIGNED BY UBC-73



**FACTORED DESIGN DEMANDS
(LINEAR ANALYSIS)**

R_e : FACTORED EARTHQUAKE
LOAD - "1.4E" per UBC 73

EQUILIBRIUM:
 $(\alpha_e H) R_e = M_e^l + M_e^r + dN_e$

COLLAPSE STATE

R_p : COLLAPSE LOAD

EQUILIBRIUM:
 $(\alpha_p H) R_p = M_p^l + M_p^r + dN_p$

FIG. 2.6 OVERTURNING MOMENT RESISTANCES AT FACTORED EARTHQUAKE DESIGN LOAD AND COLLAPSE STATE

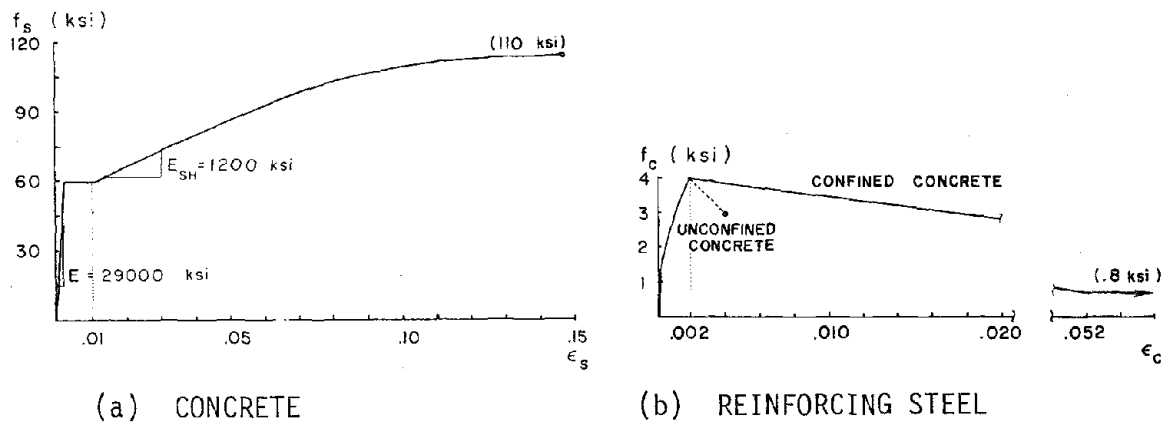


FIG. 2.7 ASSUMED MATERIAL STRESS-STRAIN CHARACTERISTICS IN GENERATING MOMENT-CURVATURE RESPONSES OF THE BEAMS AND THE WALL CROSS SECTIONS

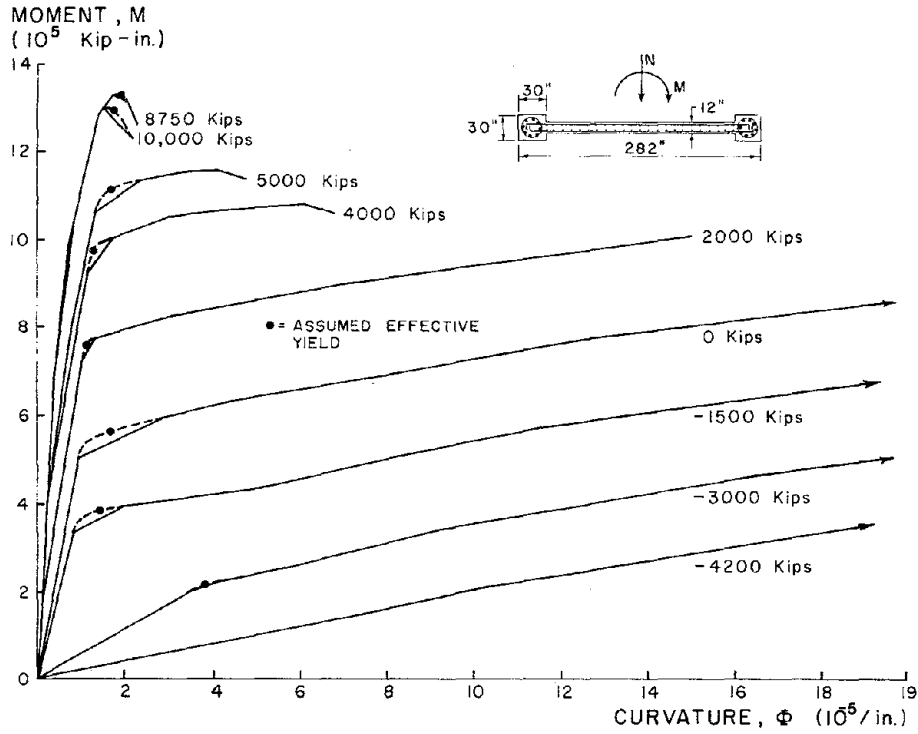


FIG. 2.8(a) MOMENT-CURVATURE RELATIONS FOR THE WALL CROSS SECTION FOR DIFFERENT LEVELS OF AXIAL FORCE, N

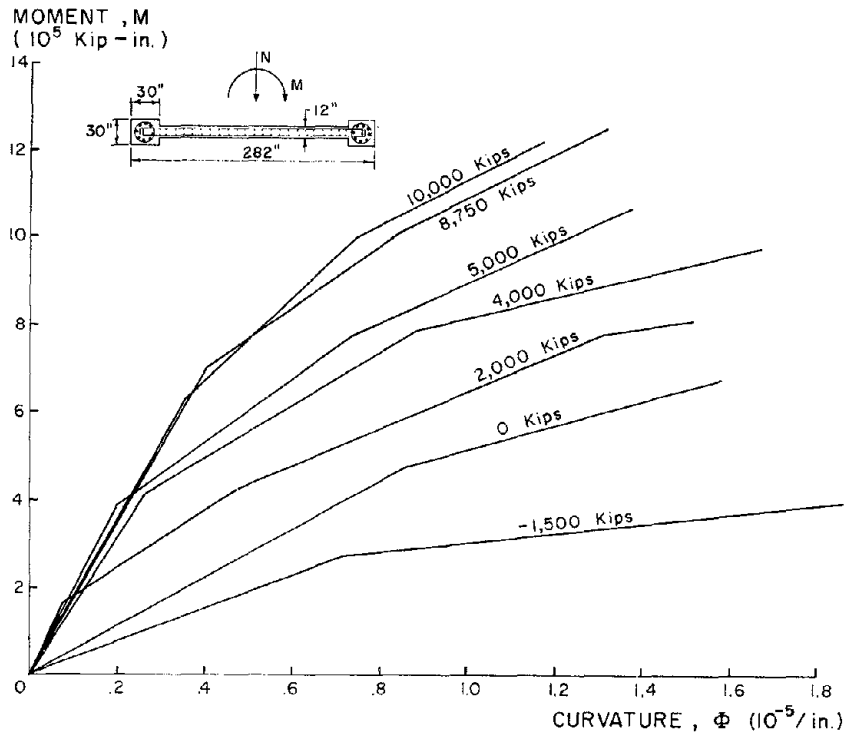


FIG. 2.8(b) PRE-YIELD MOMENT-CURVATURE RELATIONS FOR THE WALL CROSS SECTION FOR DIFFERENT LEVELS OF AXIAL FORCE, N

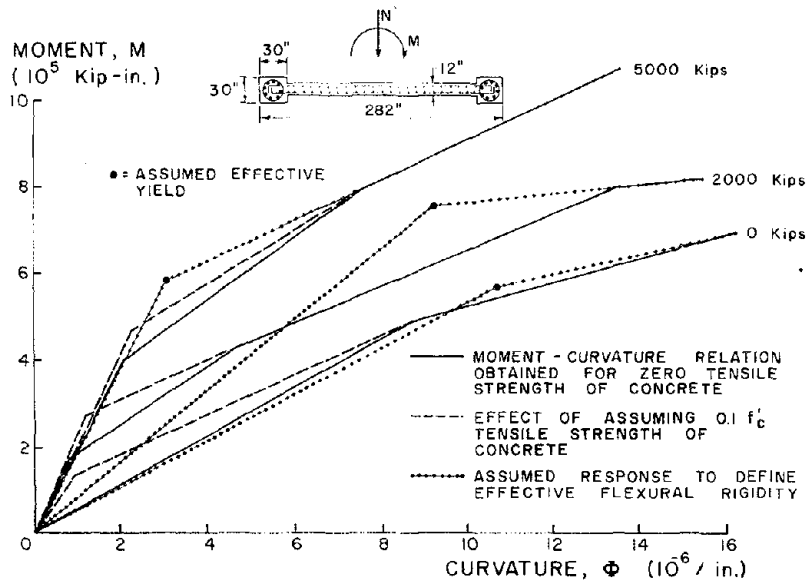


FIG. 2.8(c) THE EFFECT OF CONCRETE TENSILE STRENGTH ON THE SECTION MOMENT-CURVATURE RESPONSE

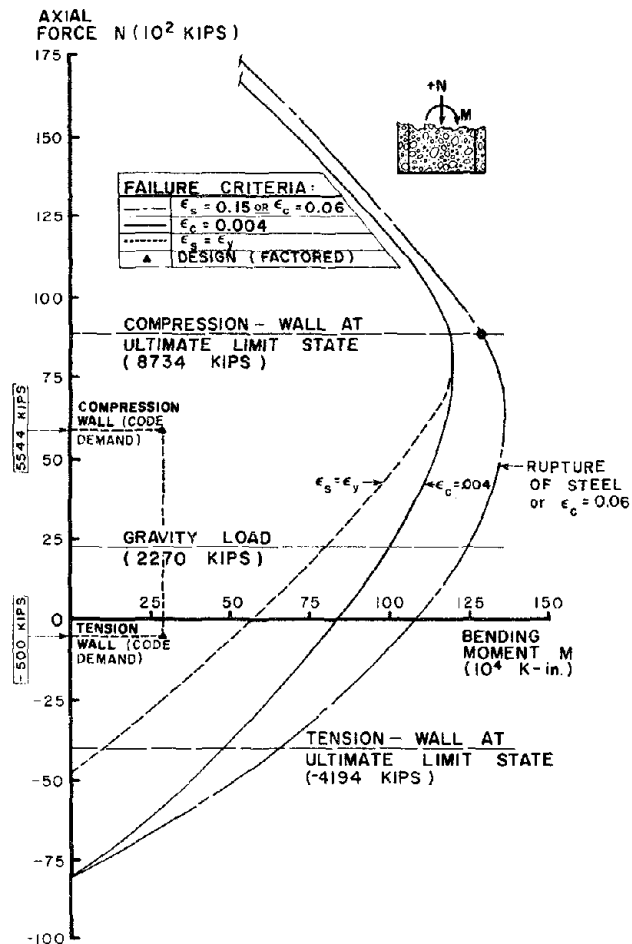
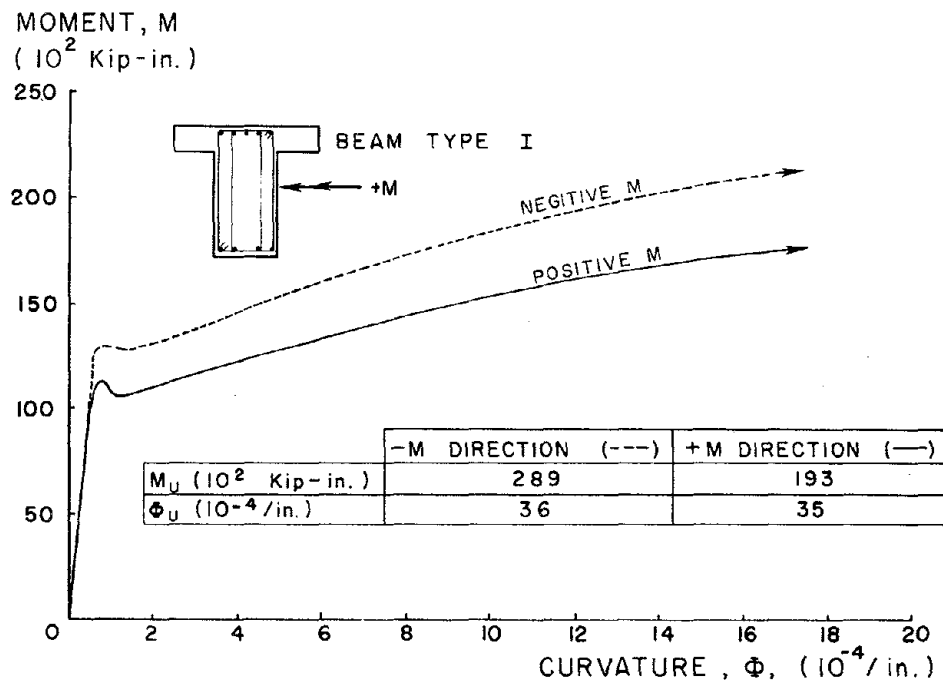
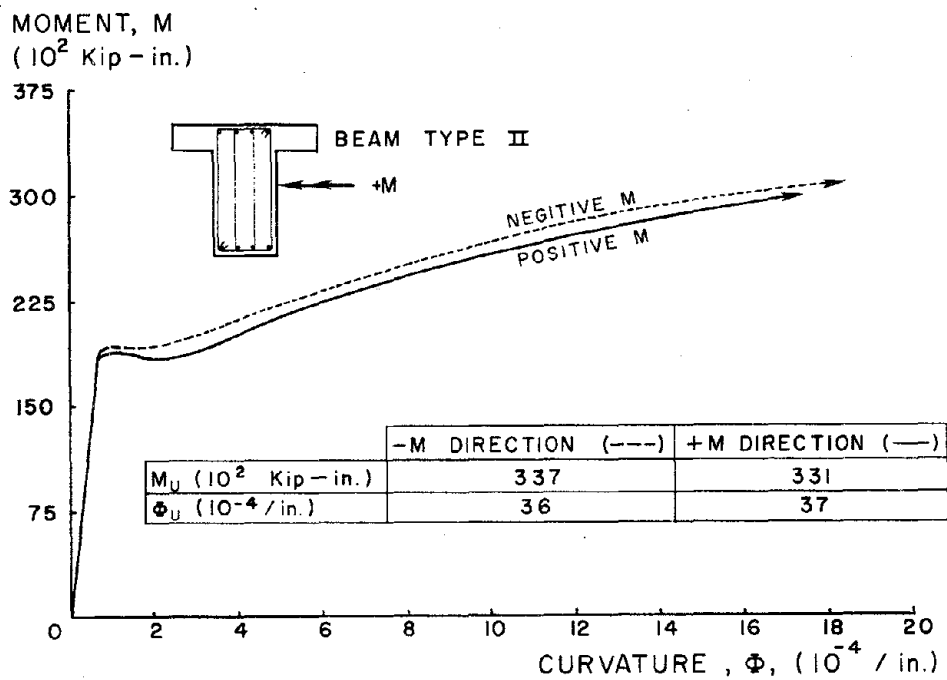


FIG. 2.9 AXIAL FORCE-BENDING MOMENT INTERACTION DIAGRAM FOR THE WALL SECTION DESIGNED BY UBC-73 PROVISIONS

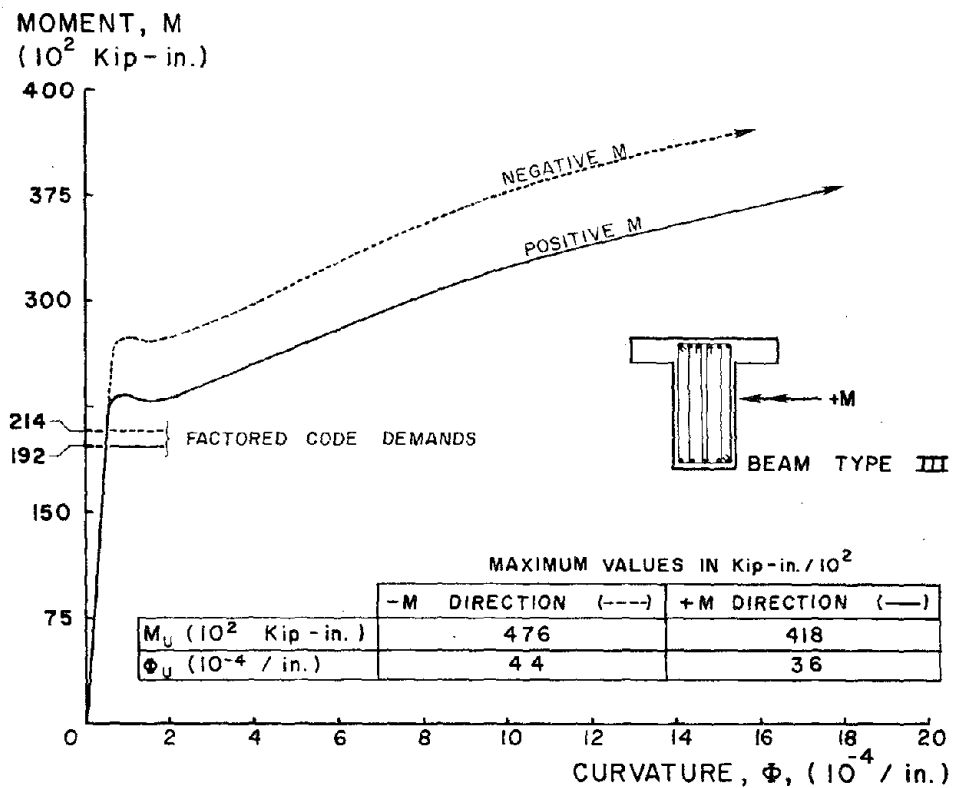


2.10(a) BEAM TYPE I



2.10(b) BEAM TYPE II

FIG. 2.10 MOMENT-CURVATURE RESPONSES IN BOTH BENDING DIRECTIONS, BEAMS TYPE I AND II



(c) BEAM TYPE III

FIG. 2.10 MOMENT-CURVATURE RESPONSES IN BOTH BENDING DIRECTIONS, BEAM TYPE III

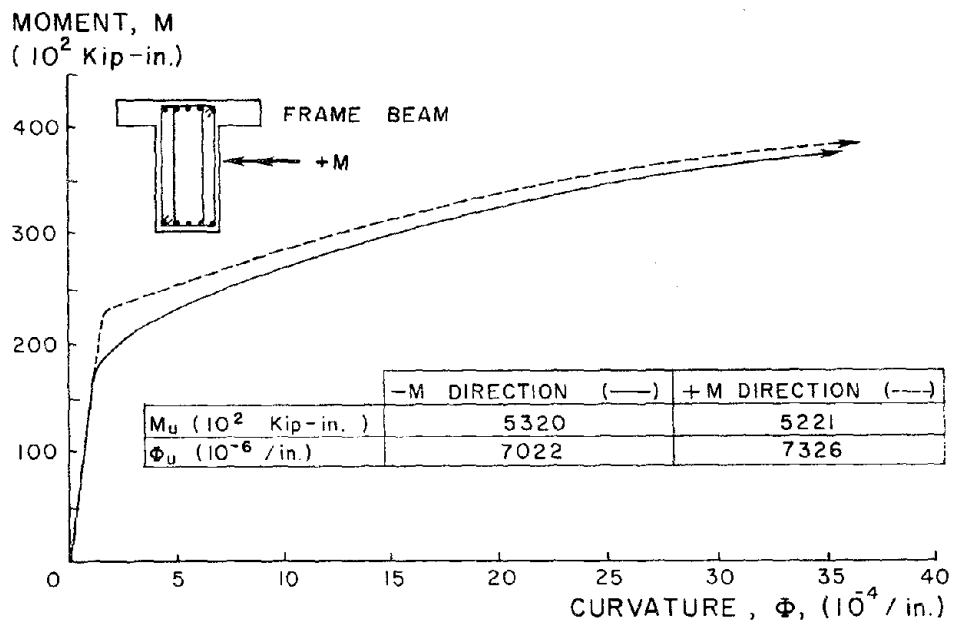


FIG. 2.11 MOMENT-CURVATURE RELATIONS FOR THE FRAME BEAM

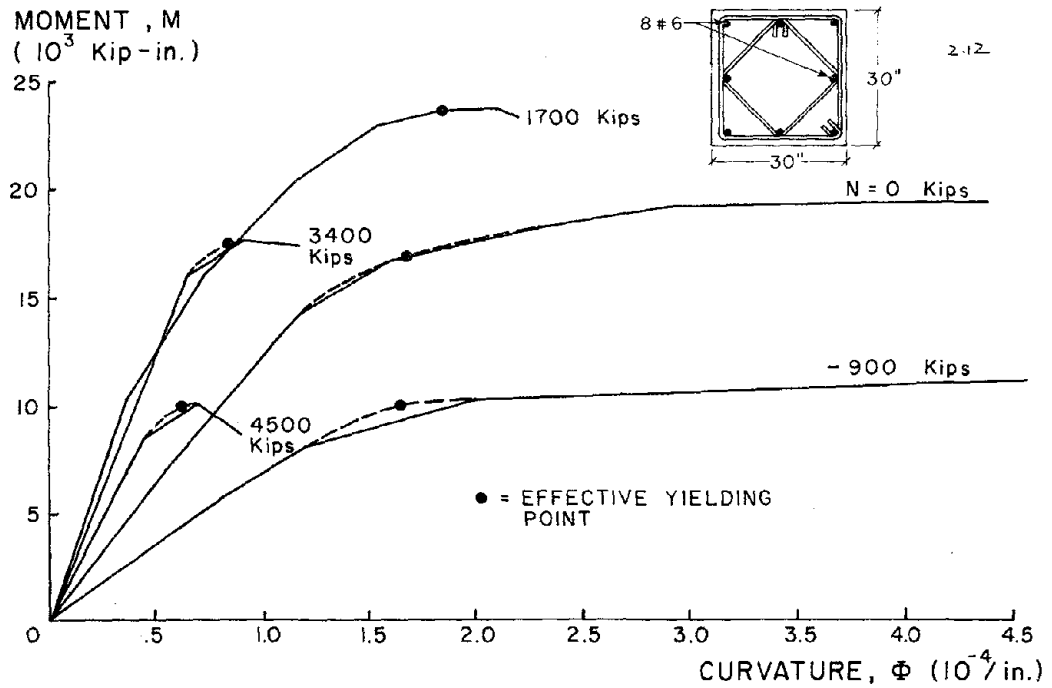


FIG. 2.12 MOMENT-CURVATURE RELATIONS FOR THE COLUMN SECTION AT DIFFERENT AXIAL FORCE LEVELS

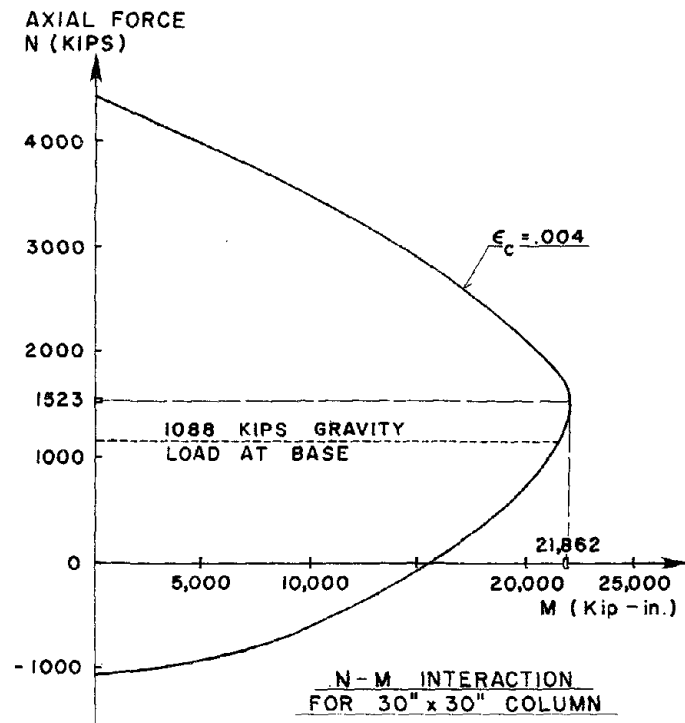


FIG. 2.13 AXIAL FORCE-BENDING MOMENT INTERACTION DIAGRAM FOR THE FRAME COLUMN

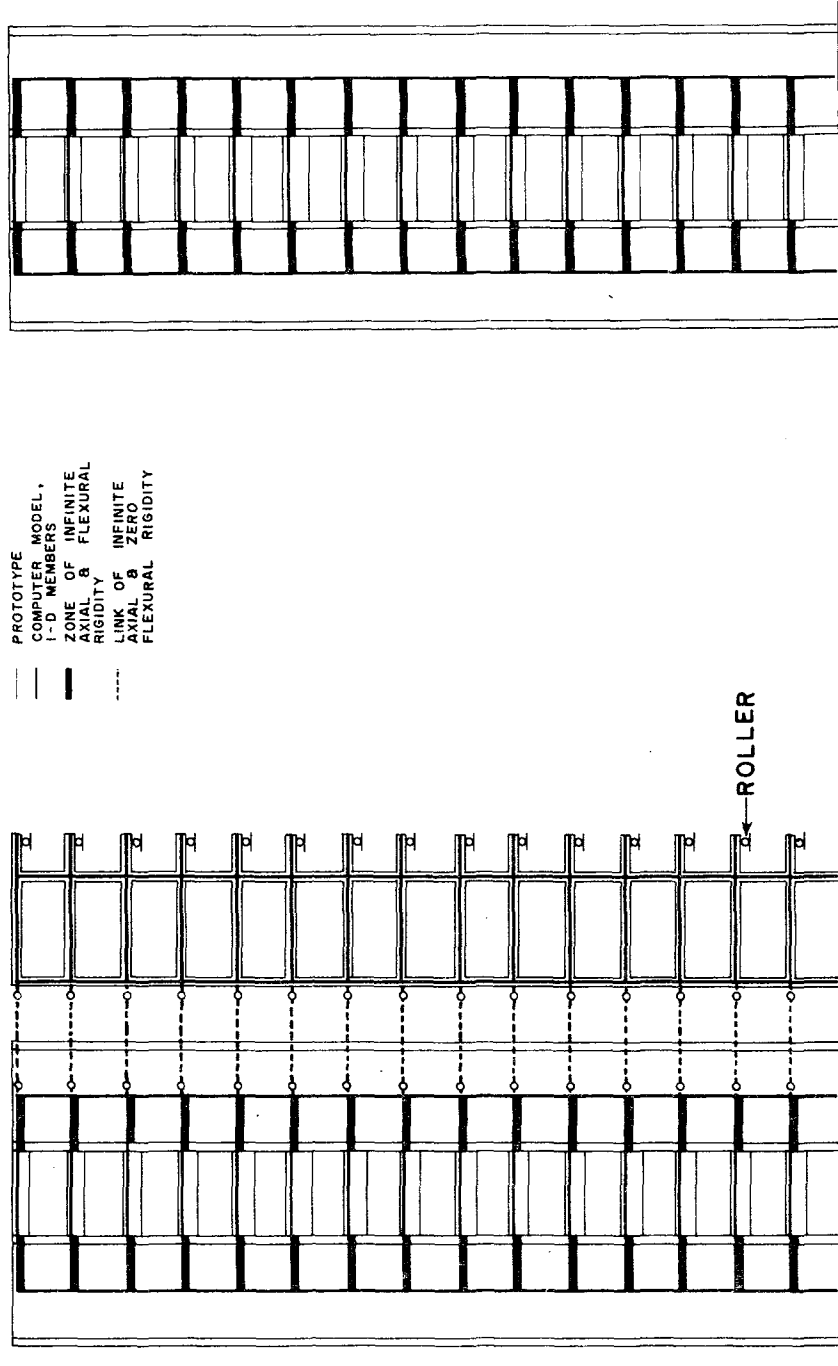


FIG. 3.1 COUPLED WALL-FRAME TOPOLOGICAL MODEL

FIG. 3.2 ISOLATED COUPLED WALL TOPOLOGICAL MODEL

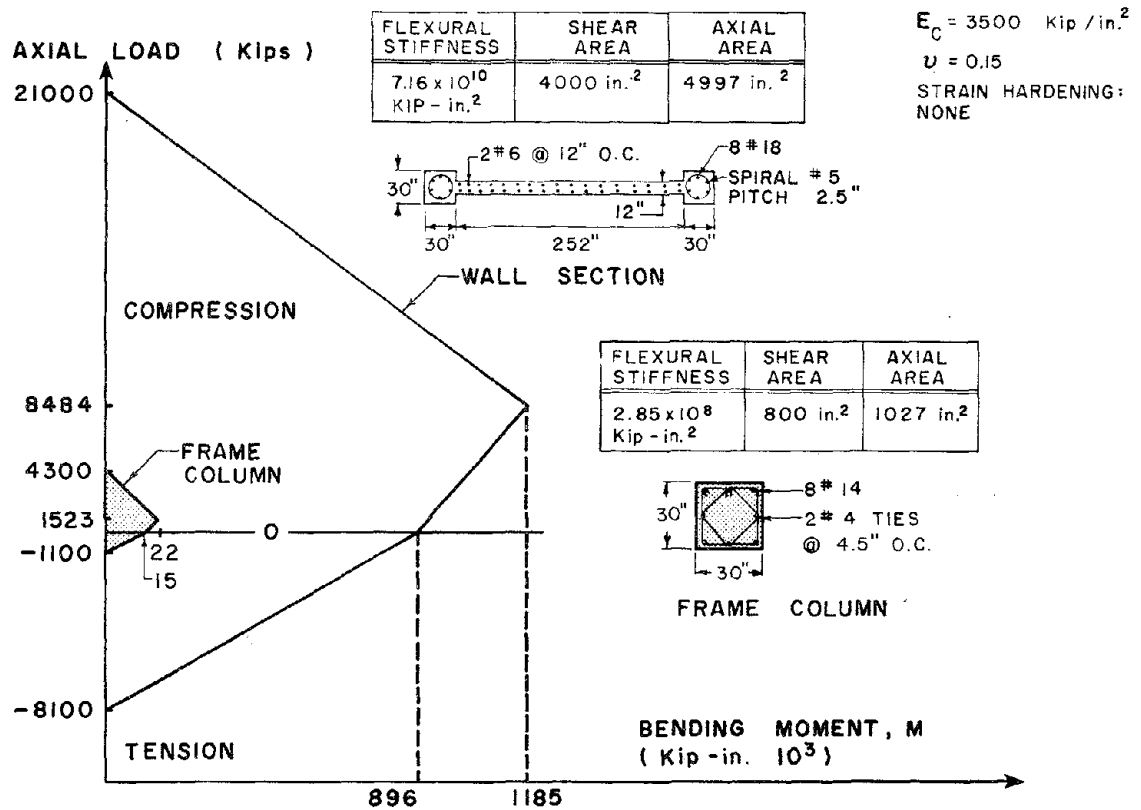
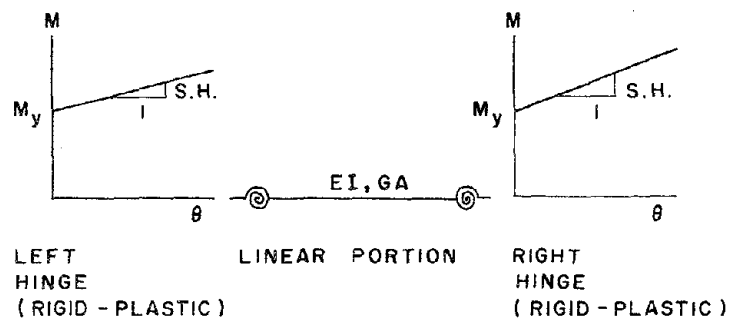


FIG. 3.3 PROPERTIES OF THE BEAM-COLUMN ELEMENTS



STIFFNESS DEGRADING BEAM ELEMENT

BEAM	YIELD MOMENT		EI(x10 ⁸)	SH(% of EI)	GA(x10 ⁶)	EA(x10 ⁶)
	POSITIVE	NEGATIVE				
GIRDER TY I	10388	12681	2.091	3.9	1.872	5.224
GIRDER TY II	17960	17653	3.069	4	1.872	5.173
GIRDER TY III	22285	26104	3.903	3.9	1.872	5.290
FRAME BEAM	25000	25000	0.246	2.7	1.521	3.500

All Units kips and inches

FIG. 3.4 PROPERTIES OF THE BEAM ELEMENTS

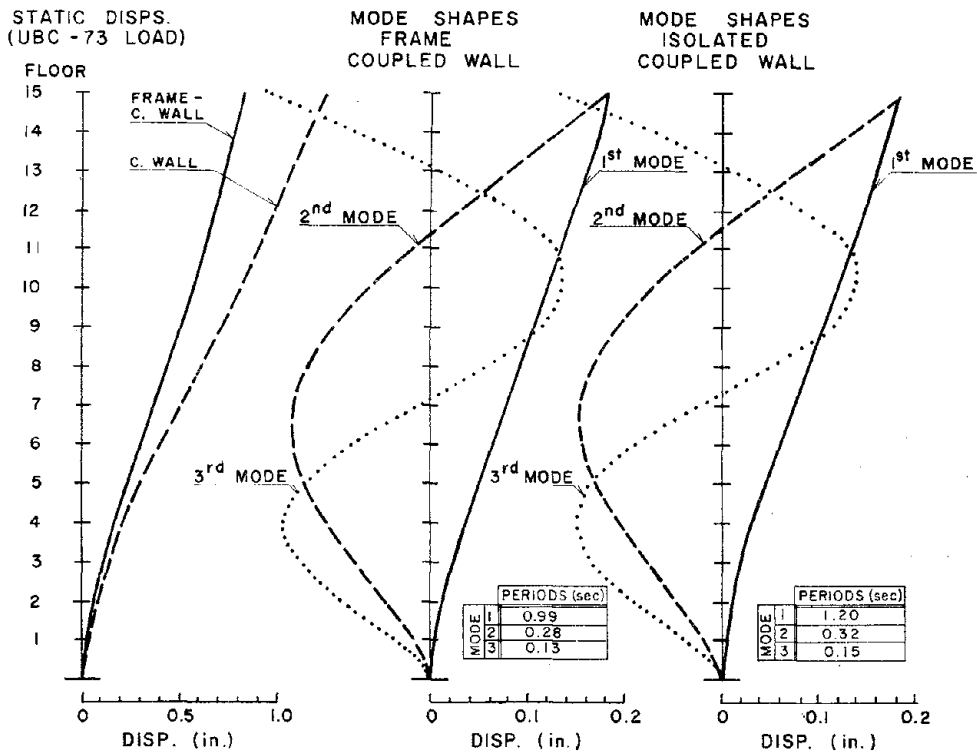


FIG. 4.1 STATIC DISPLACEMENTS, MODE SHAPES AND PERIODS

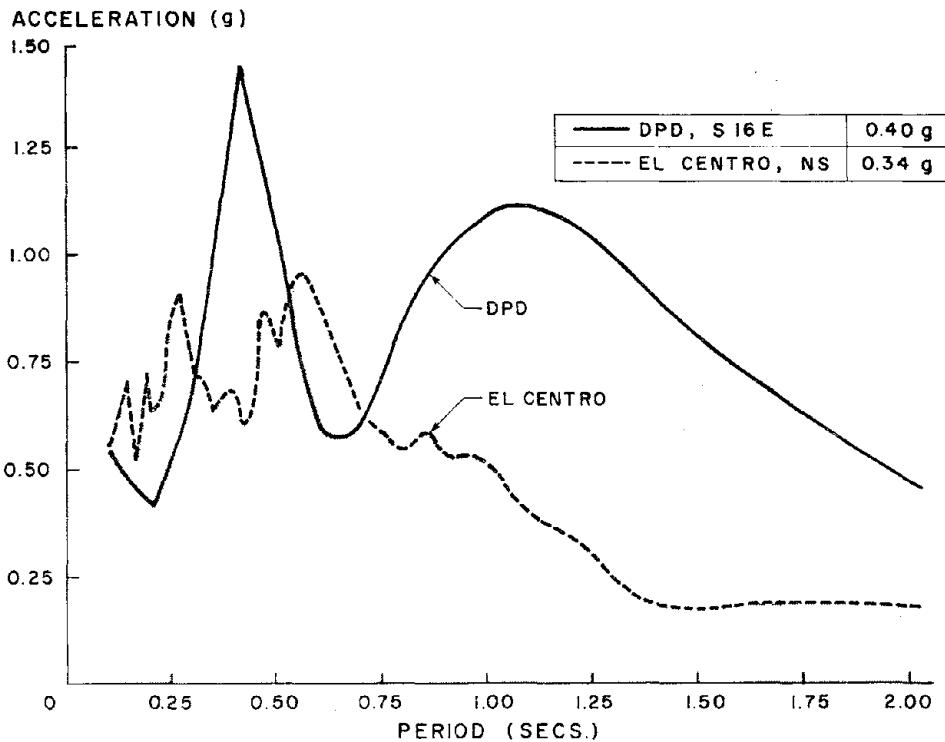


FIG. 4.2 LINEAR ACCELERATION SPECTRA FOR PACOIMA AND EL CENTRO RECORDS AND FOR 5% DAMPING COEFFICIENT

INTERACTION

NEGLECTED (---) CONSIDERED (—)

MOMENT TO SHEAR RATIO AT BASE OF THE COUPLED WALL 0.68H 0.57H

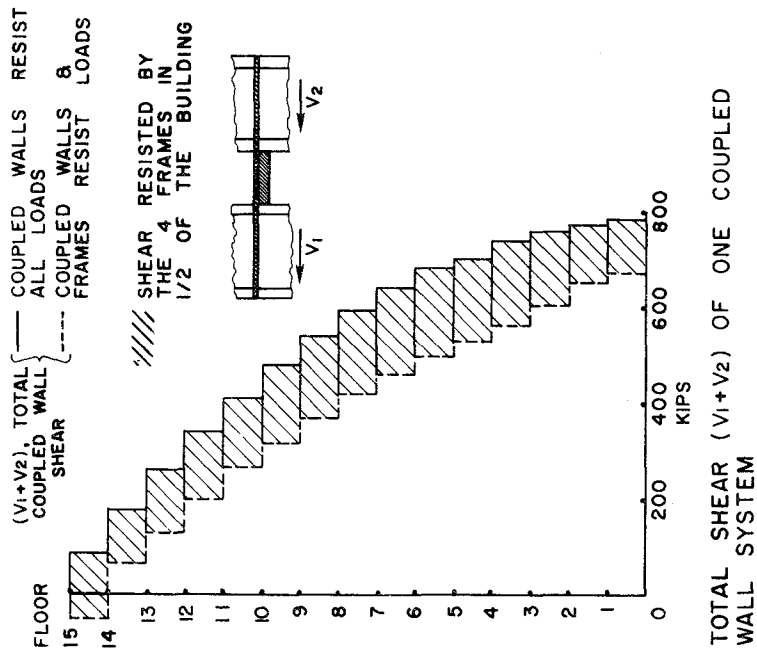


FIG. 4.3 TOTAL STORY SHEARS FROM STATIC UBC-73 "E" LOAD ANALYSIS, OF ONE-HALF THE SYMMETRIC BUILDING

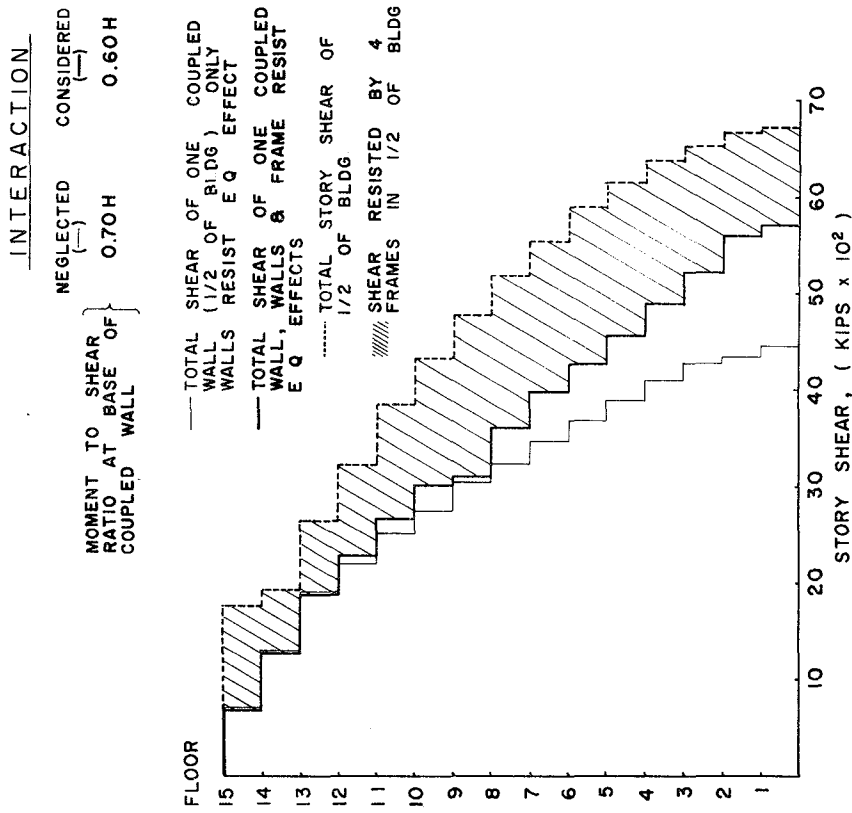


FIG. 4.4 TOTAL STORY SHEARS FROM MODAL SPECTRAL ANALYSIS CORRESPONDING TO EL CENTRO: WALLS CONSIDERED ACTING ALONE AND WITH FRAMES

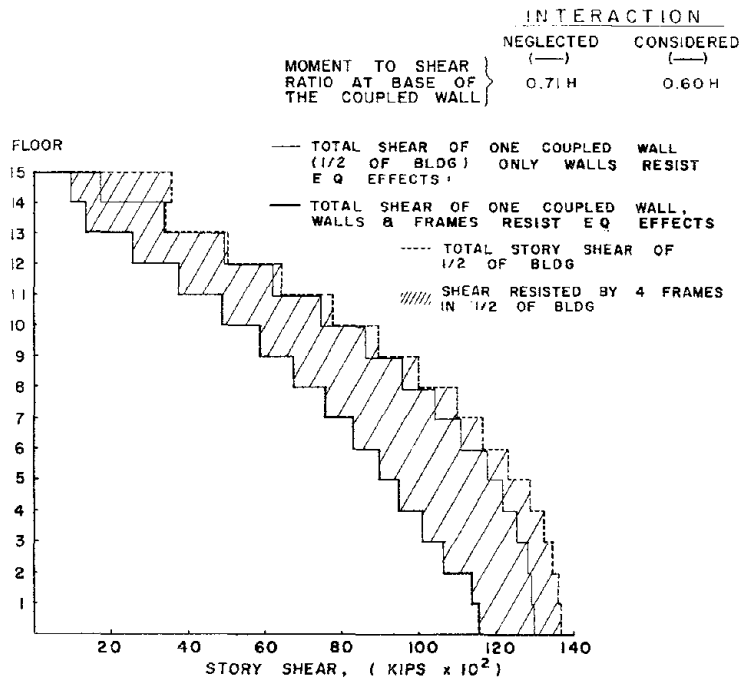


FIG. 4.5 STORY SHEARS FOR WALLS CONSIDERED ACTING ALONE AND WITH FRAMES RESULTING FROM SPECTRAL ANALYSIS CORRESPONDING TO PACOIMA RECORD

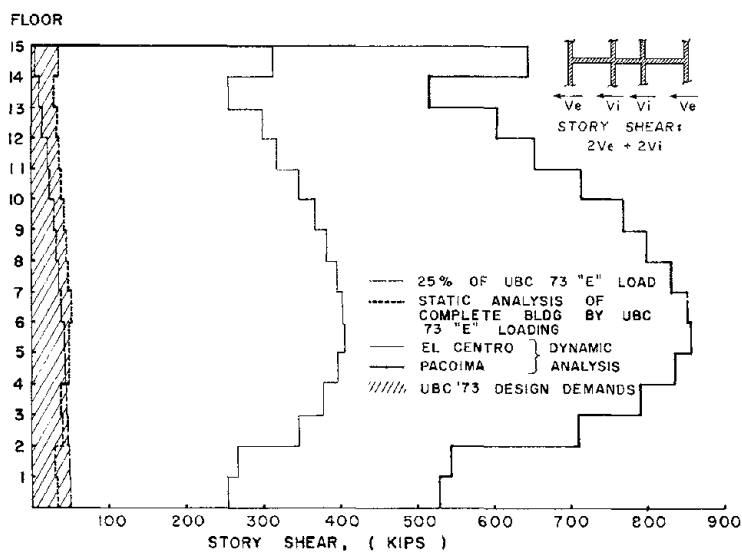
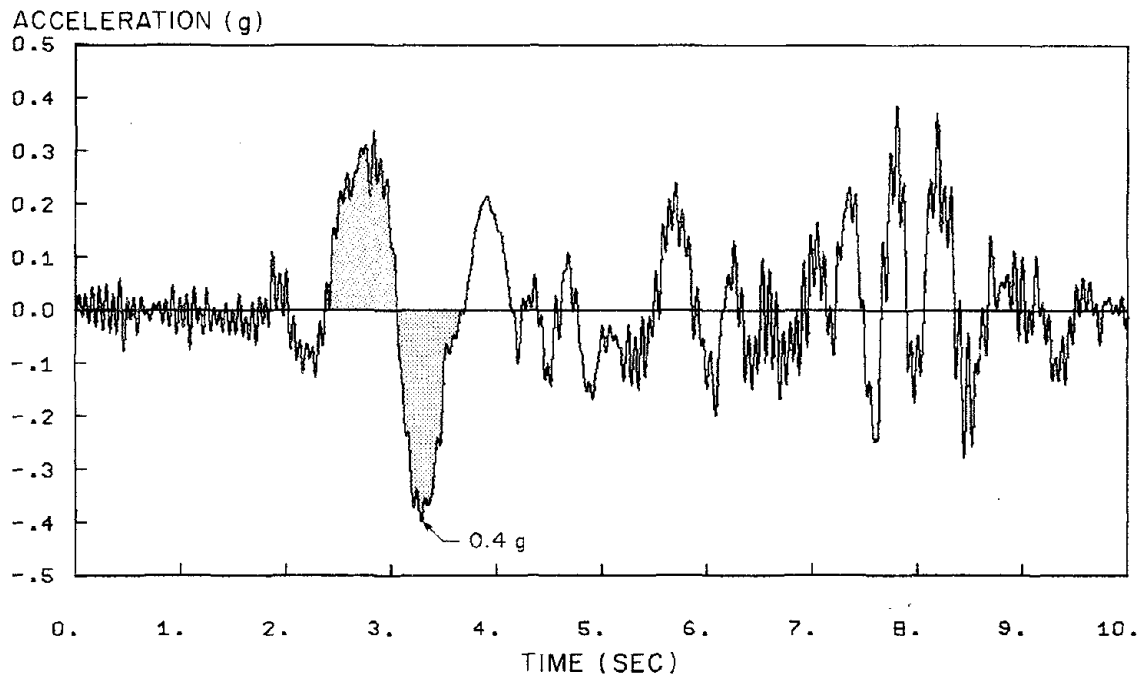
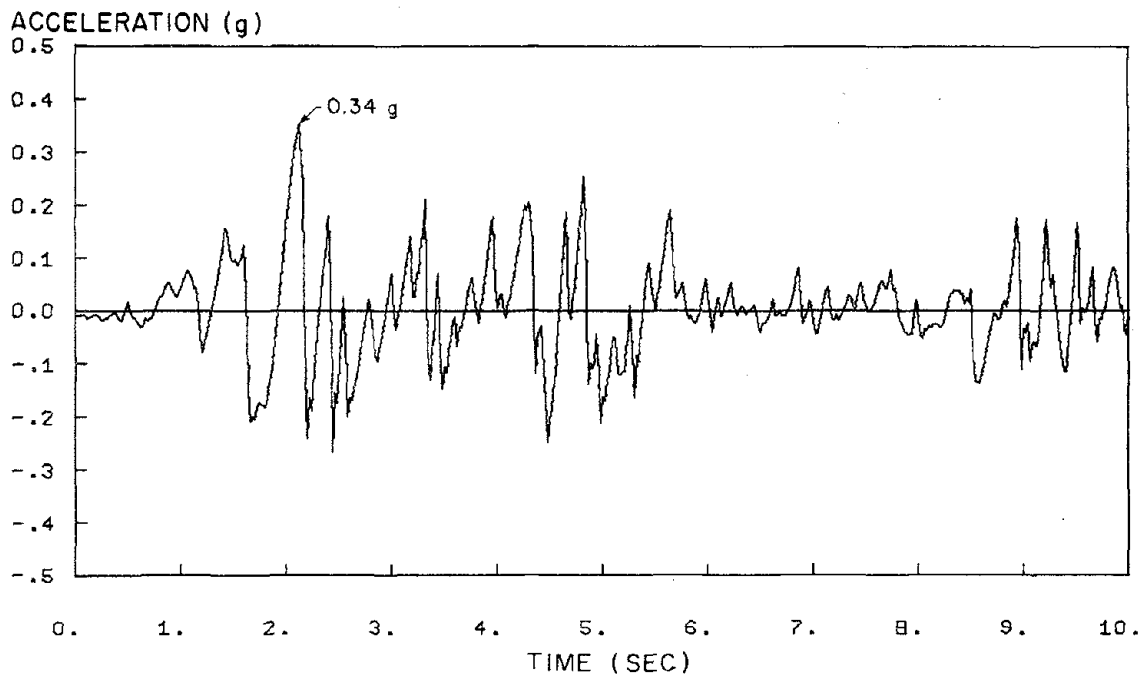


FIG. 4.6 FRAME STORY SHEAR DEMANDS BY CODE AND LINEAR DYNAMIC ANALYSIS FOR ONE TYPICAL FRAME OF THE PROTOTYPE

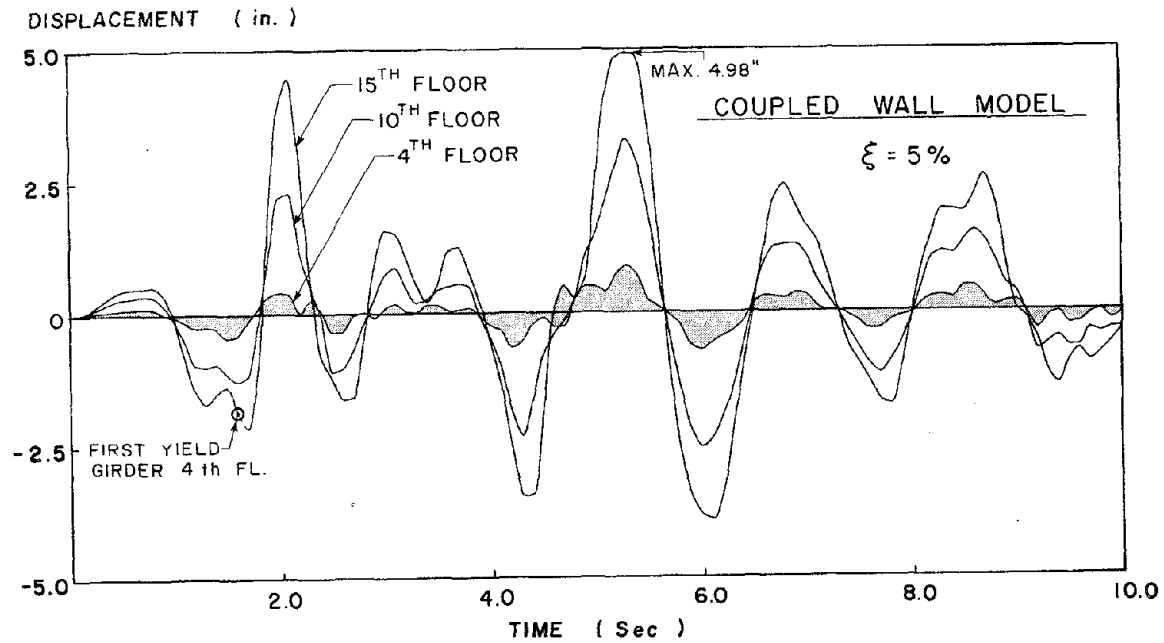


(a) EL CENTRO 1940 EARTHQUAKE N-S COMPONENT

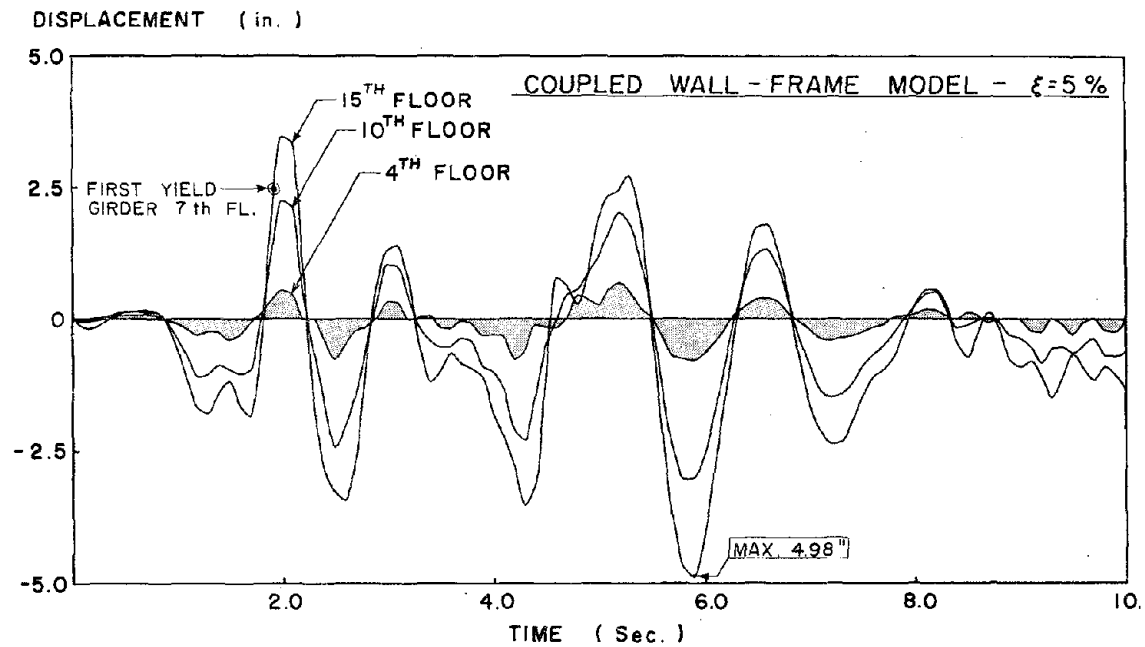


(b) DERIVED PACOIMA DAM RECORD

FIG. 5.1 THE ACCELEROGRAMS USED IN THE ANALYSES

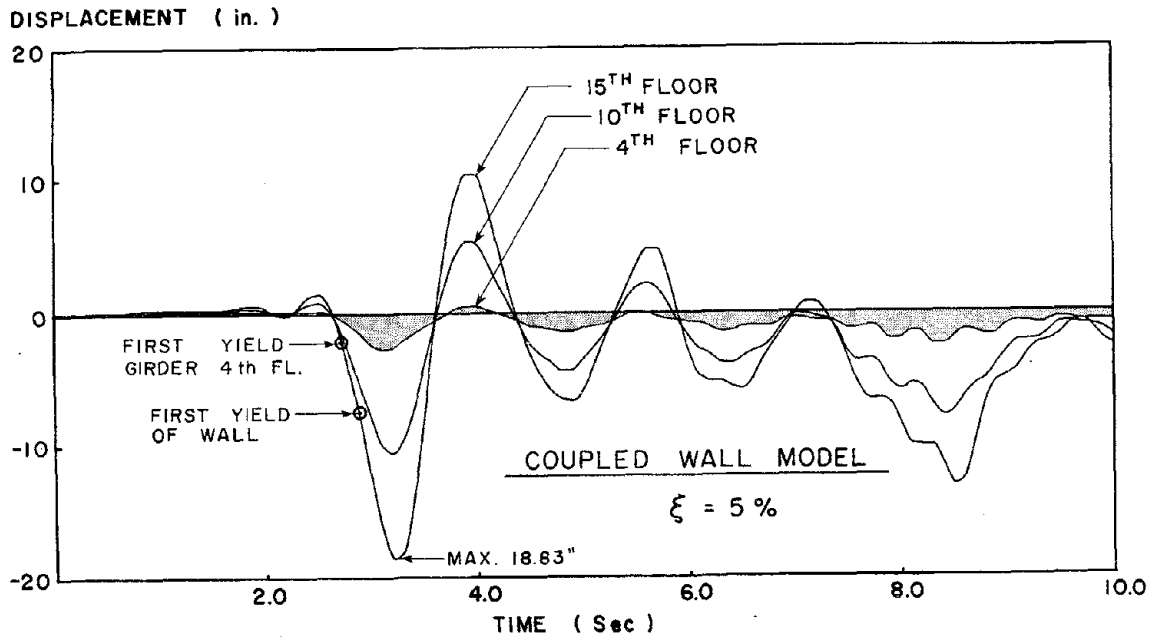


(a) LATERAL DISPLACEMENT, 4th, 10th, AND 15th STORIES, COUPLED WALL MODEL

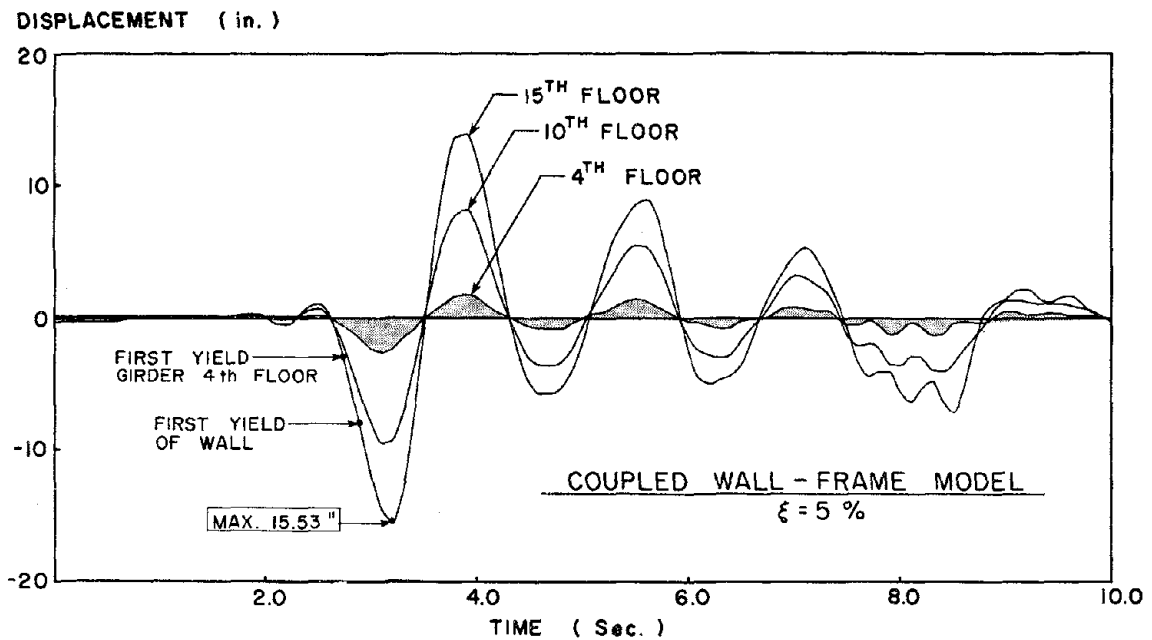


(b) LATERAL DISPLACEMENT, 4th, 10th, AND 15th STORIES, COUPLED WALL-FRAME MODEL

FIG. 5.2 TIME-HISTORY OF LATERAL DISPLACEMENTS OF THE COUPLED WALL AND THE COUPLED WALL-FRAME MODELS SUBJECTED TO THE EL CENTRO GROUND MOTION AND WITH $\xi = 5\%$



(a) LATERAL DISPLACEMENT, 4th, 10th, AND 15th STORIES, COUPLED WALL MODEL



(b) LATERAL DISPLACEMENT, 4th, 10th, AND 15th STORIES, COUPLED WALL-FRAME MODEL

FIG. 5.3 TIME-HISTORY OF LATERAL DISPLACEMENTS OF THE COUPLED WALL AND THE COUPLED WALL-FRAME MODELS SUBJECTED TO THE PACOIMA GROUND MOTION AND WITH $\xi=5\%$

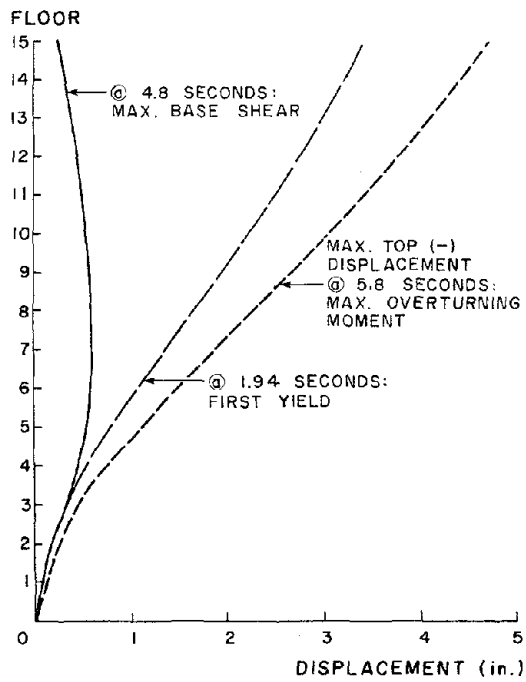


FIG. 5.4 DISPLACEMENT PROFILES OF THE COUPLED WALL-FRAME DURING EL CENTRO RESPONSE FOR $\xi=5\%$

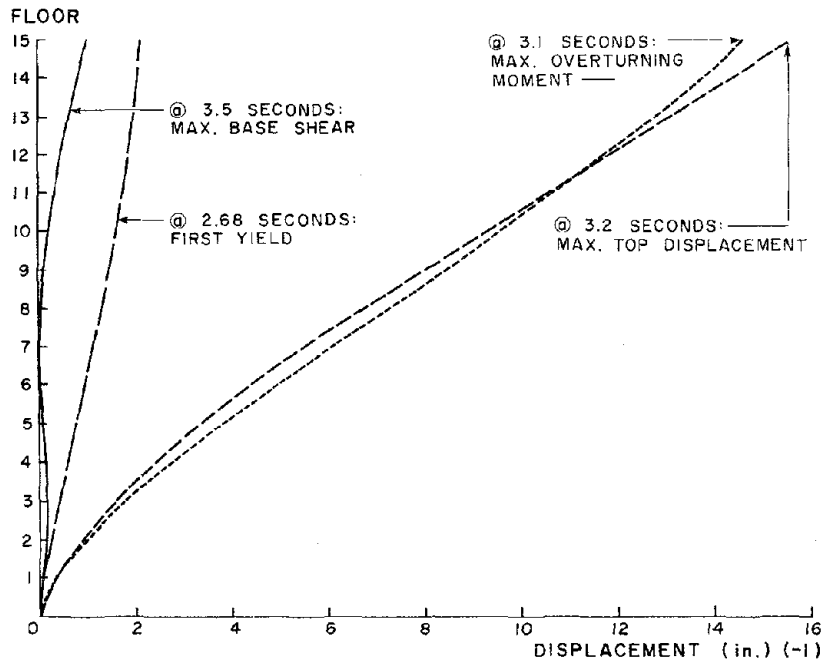
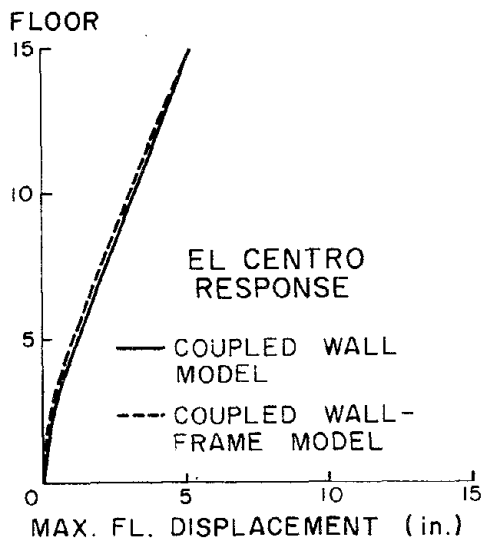
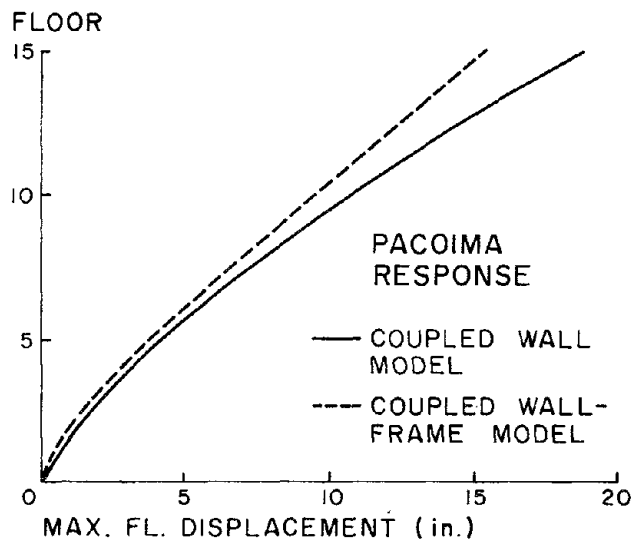


FIG. 5.5 DISPLACEMENT PROFILES OF THE COUPLED WALL-FRAME DURING THE PACOIMA RESPONSE FOR $\xi=5\%$



(a) EL CENTRO RESPONSE



(b) PACOIMA RESPONSE

FIG. 5.6 COMPARISON OF THE ENVELOPES OF MAXIMUM LATERAL FLOOR DISPLACEMENTS

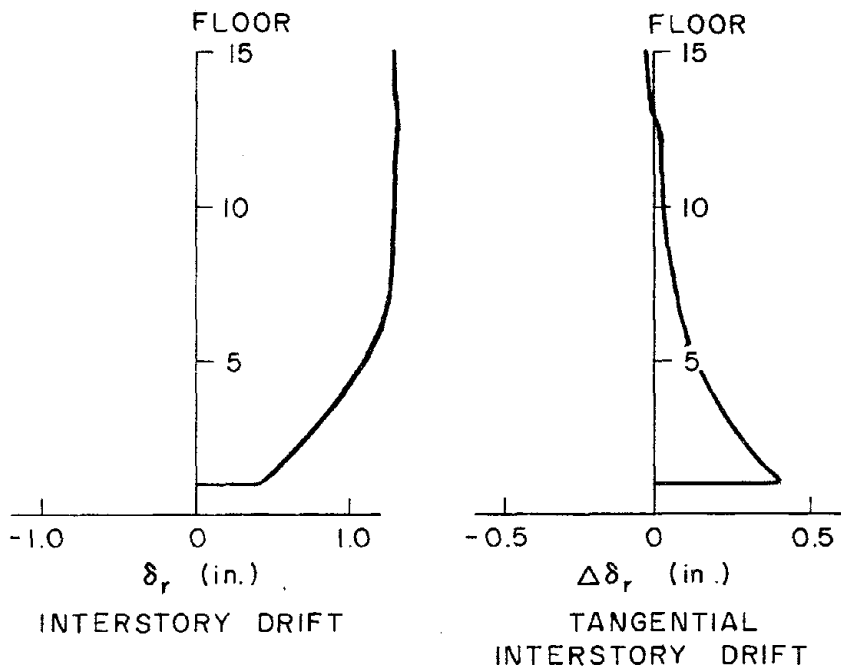
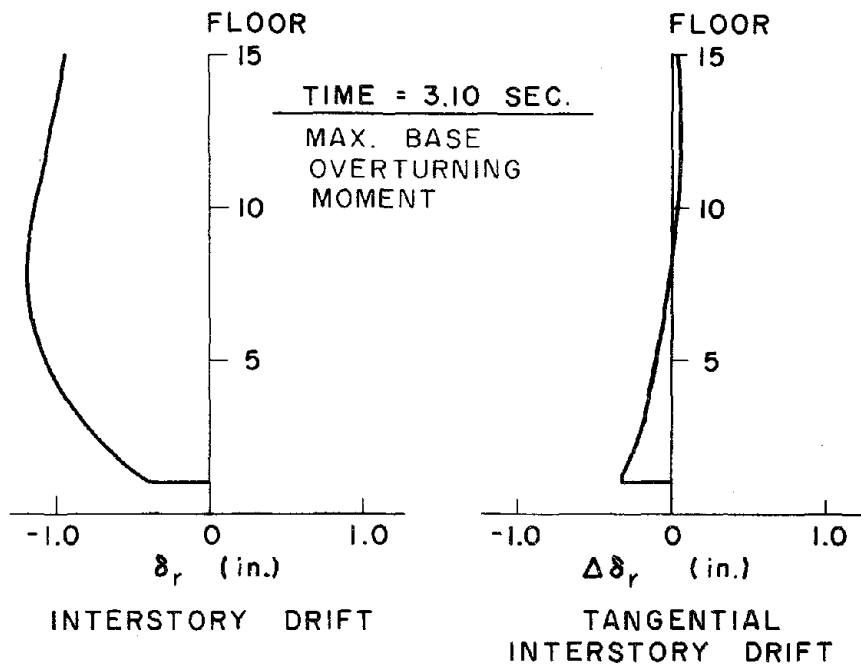
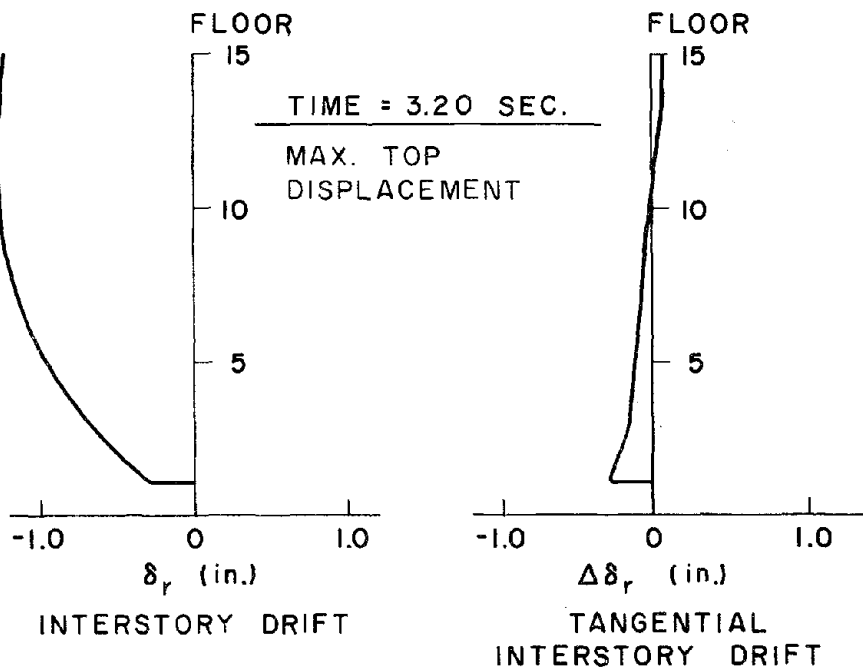


FIG. 5.7 ENVELOPES OF MAXIMUM INTERSTORY (δ_r) AND TANGENTIAL INTERSTORY DRIFT ($\Delta\delta_r$) FOR THE COUPLED WALL-FRAME MODEL SUBJECTED TO THE PACOIMA GROUND MOTION



(a) TIME OF MAXIMUM BASE OVERTURNING MOMENT, 3.10 SEC.



(b) TIME OF MAXIMUM TOP DISPLACEMENT, 3.20 SEC.

FIG. 5.8 PROFILES OF INTERSTORY DRIFT (δ_r) AND TANGENTIAL INTERSTORY DRIFT ($\Delta\delta_r$) AT 3.1 AND 3.2 SEC. OF THE PACOIMA RESPONSE: COUPLED WALL-FRAME MODEL

STATE OF THE PLASTIC HINGE

• = PLASTIC
 ○ = UNLOADING

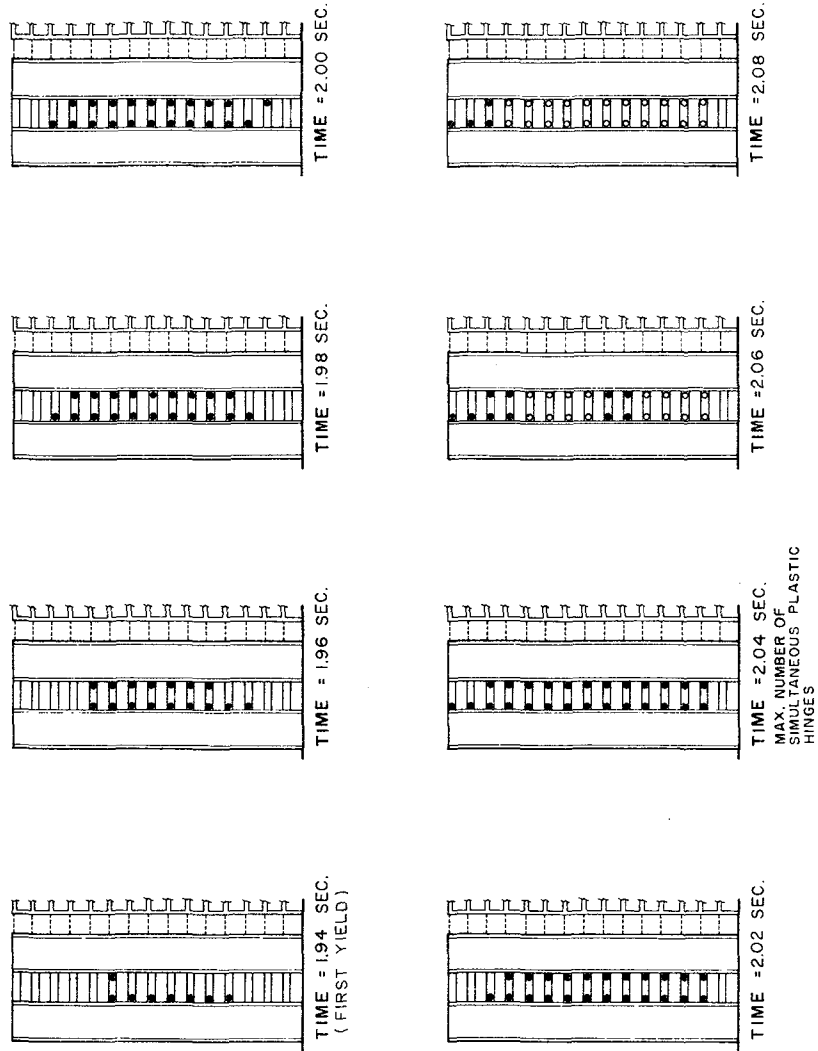


FIG. 5.9 THE DISTRIBUTION OF PLASTIC HINGES ON THE COUPLED WALL DURING THE RESPONSE OF THE COUPLED WALL-FRAME MODEL: EL CENTRO GROUND MOTION

STATE OF THE PLASTIC HINGE

- = PLASTIC
- = UNLOADING

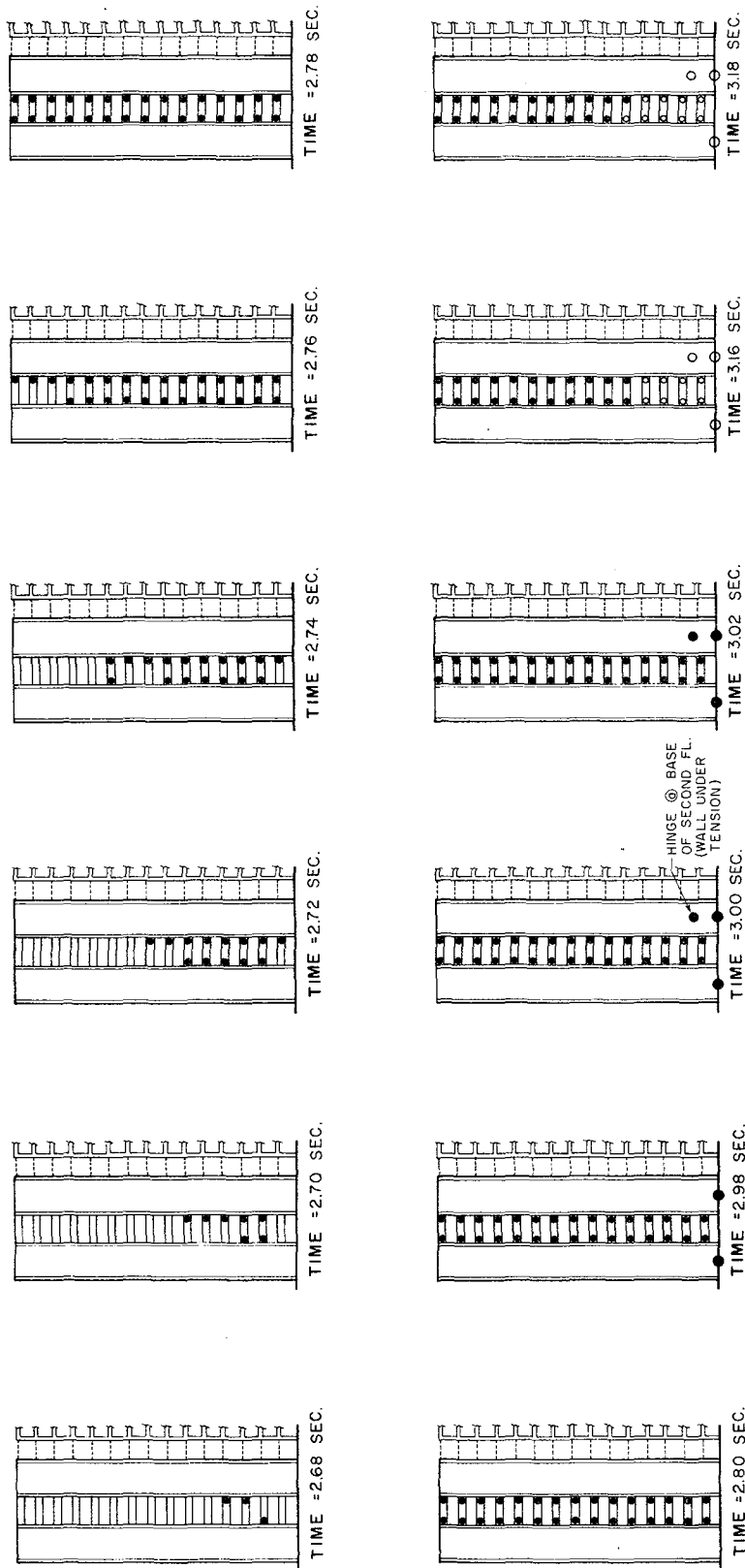


FIG. 5.10 THE DISTRIBUTION OF PLASTIC HINGES ON THE COUPLED WALL DURING THE RESPONSE OF THE COUPLED WALL-FRAME MODEL: PACOIMA GROUND MOTION

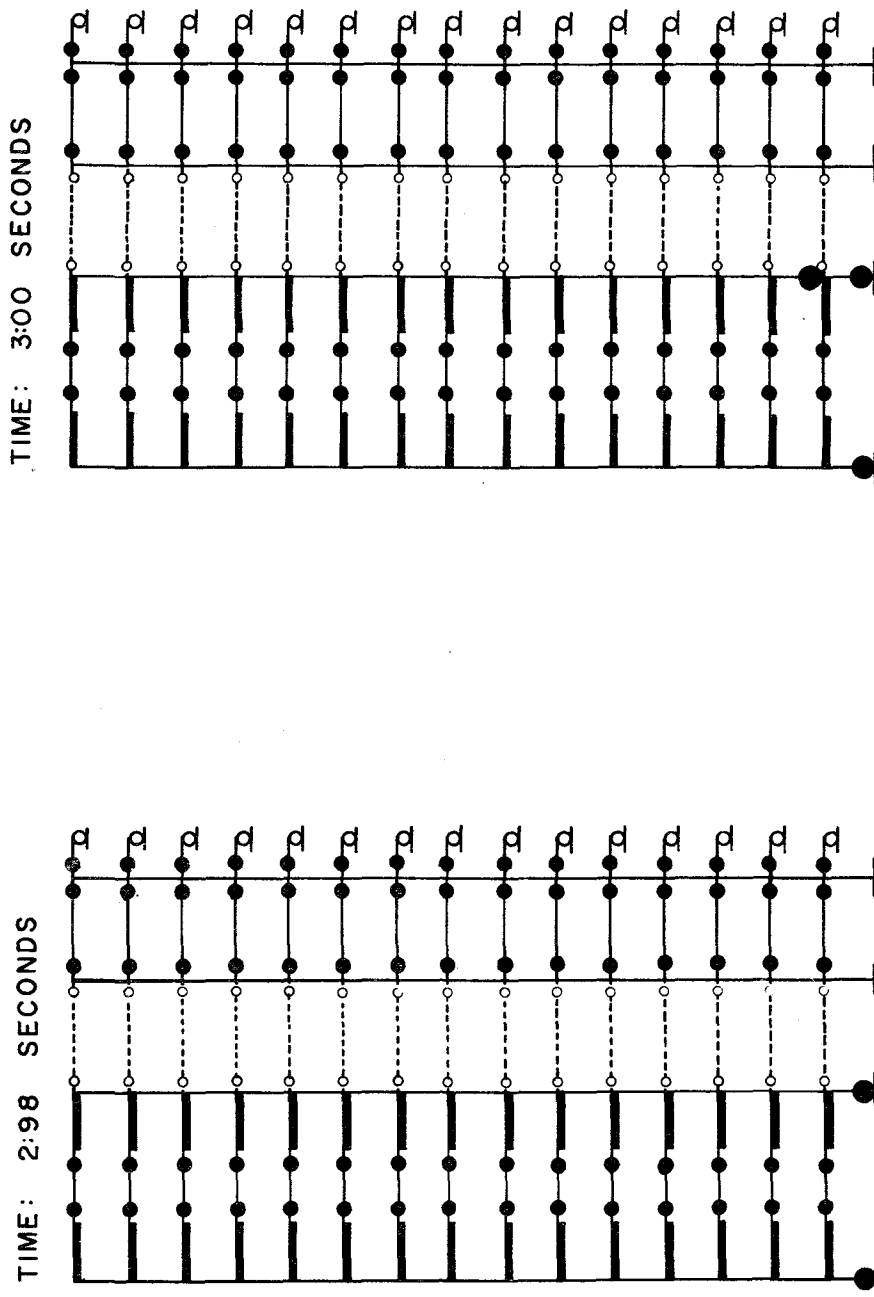
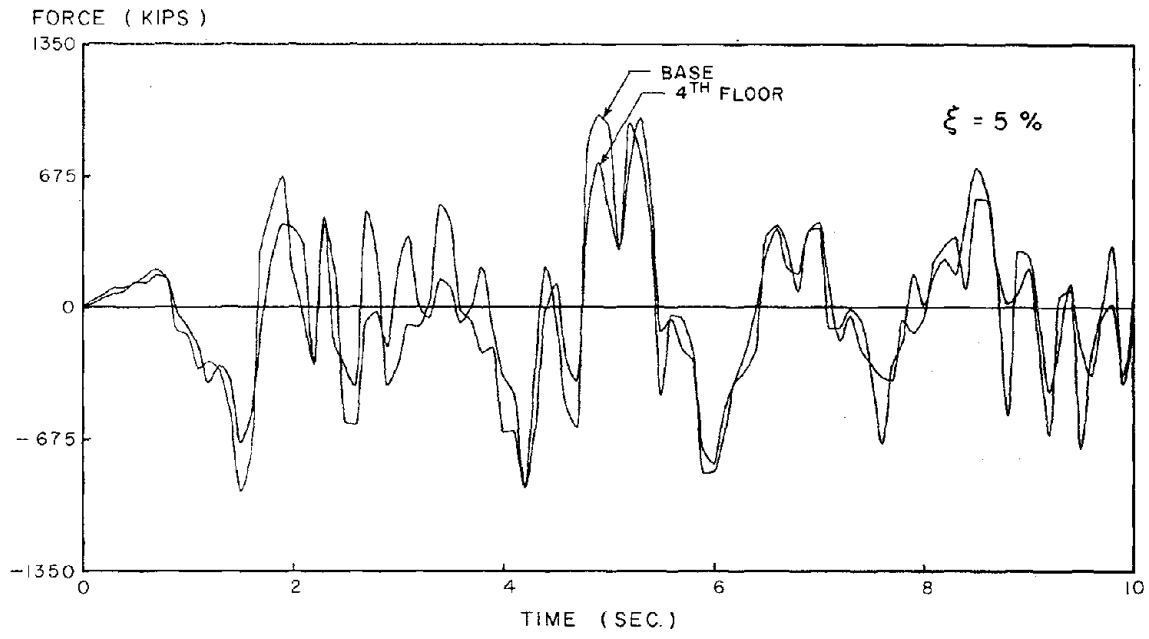
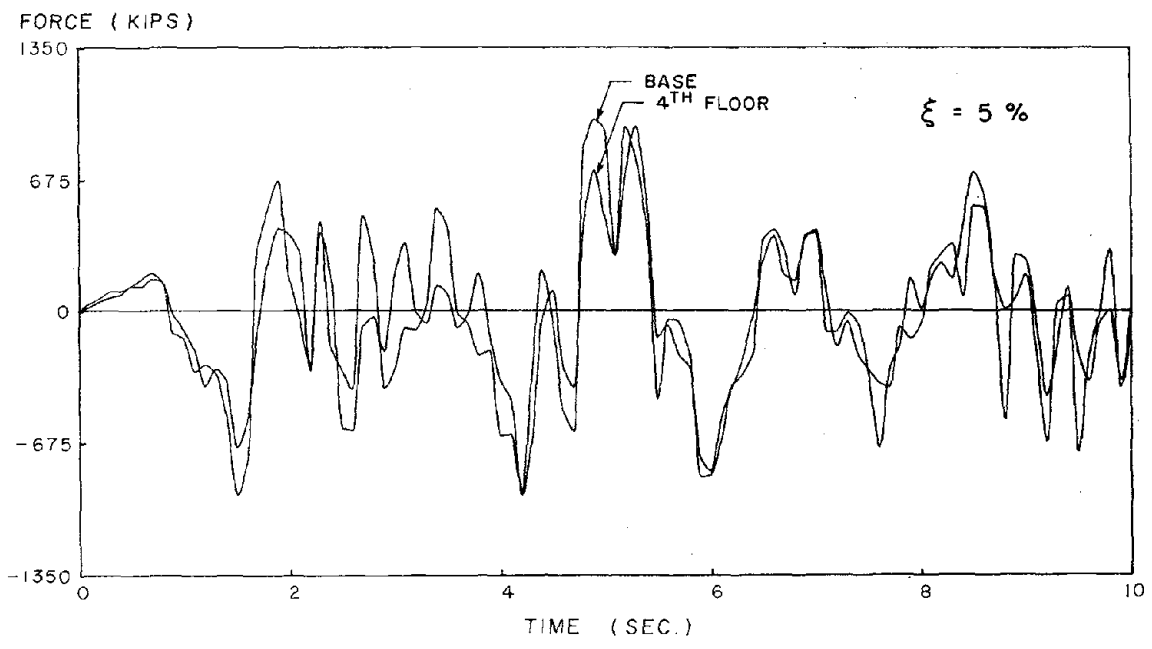


FIG. 5.11 THE PLASTIC HINGE PATTERNS OF THE COUPLED WALL-FRAME MODEL AT 2.98 AND 3.00 SEC. OF RESPONSE TO THE PACOIMA DAM RECORD

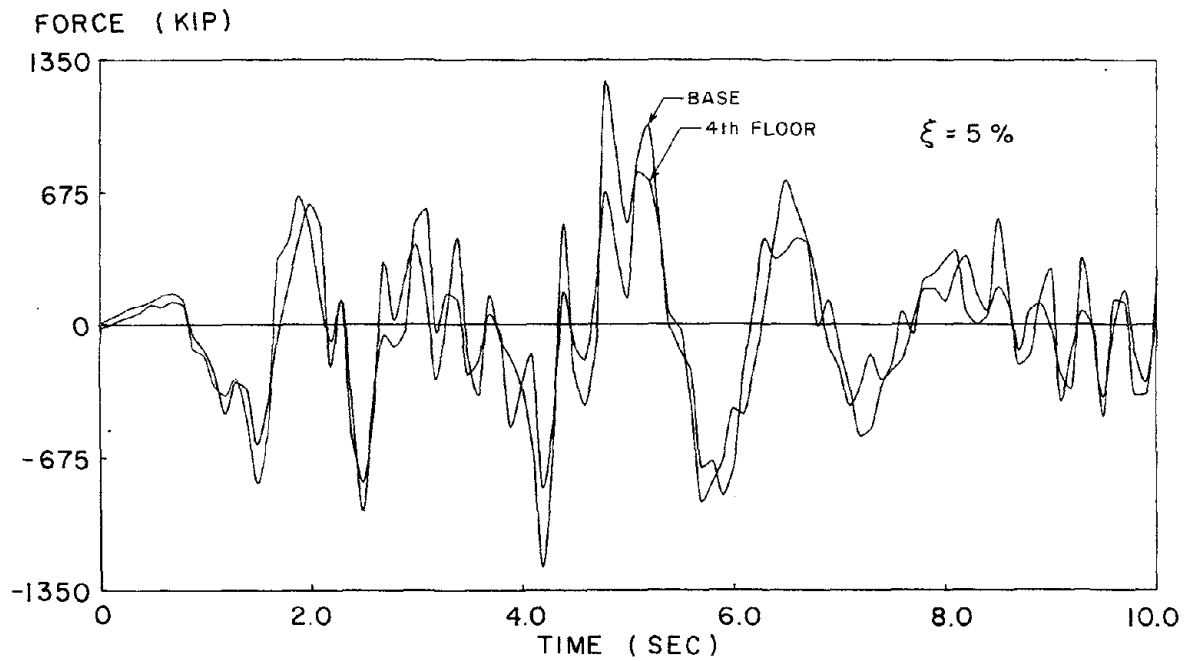


(a) WALL SHEAR FORCE, RIGHT WALL BASE AND 4th STORY

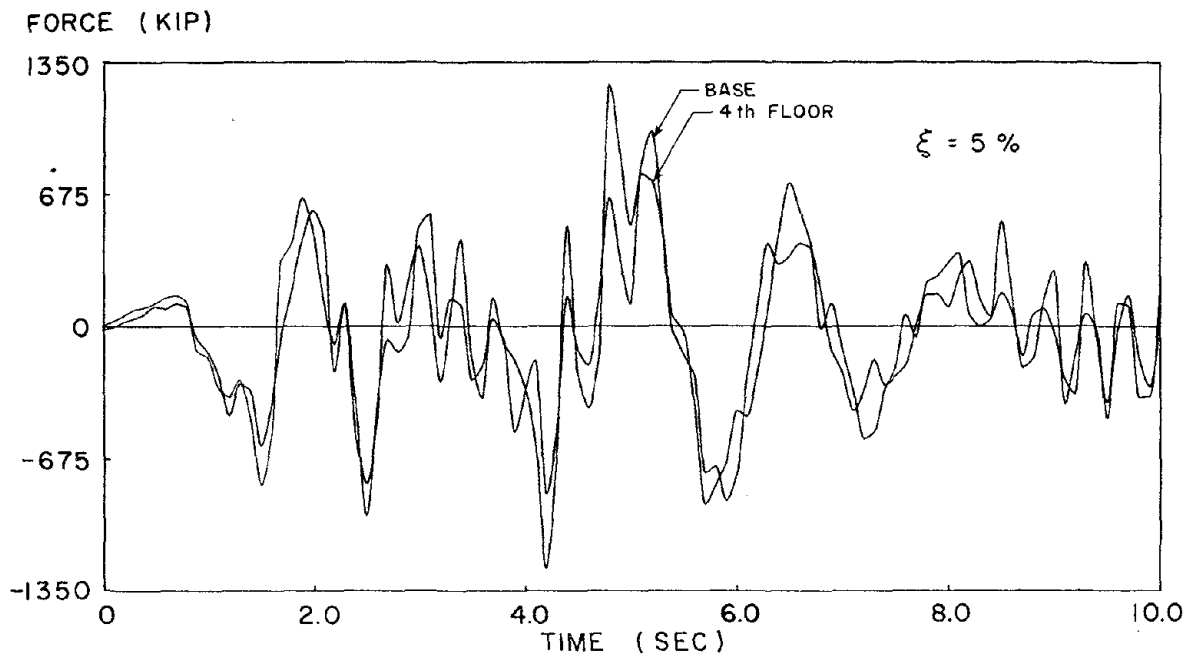


(b) WALL SHEAR FORCE, LEFT WALL BASE AND 4th STORY

FIG. 5.12 TIME-HISTORIES OF WALL SHEAR FORCES, EL CENTRO RESPONSE OF THE COUPLED WALL MODEL

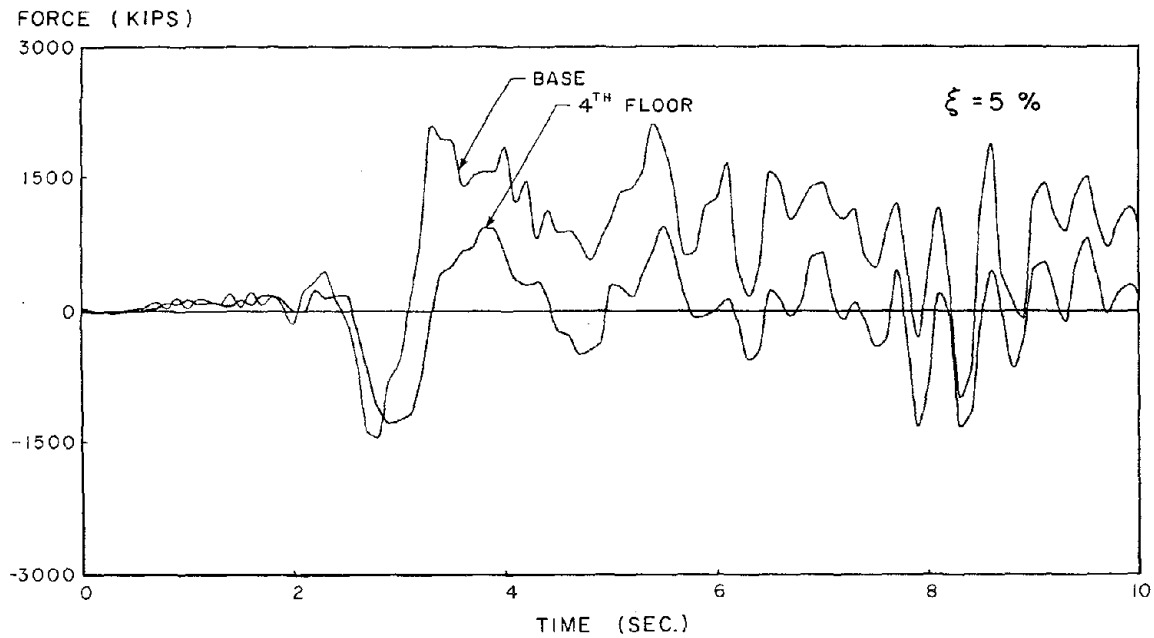


(a) WALL SHEAR FORCE, RIGHT WALL BASE AND 4th STORY

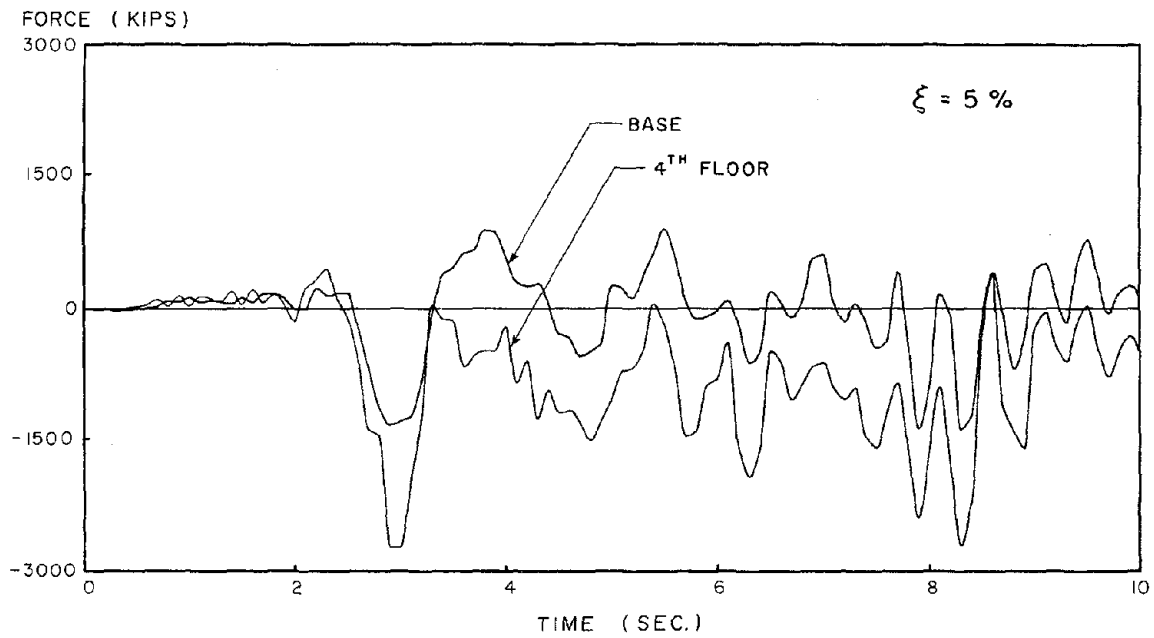


(b) WALL SHEAR FORCE, LEFT WALL BASE AND 4th STORY

FIG. 5.13 TIME-HISTORIES OF WALL SHEAR FORCES, EL CENTRO RESPONSE OF THE COUPLED WALL-FRAME MODEL

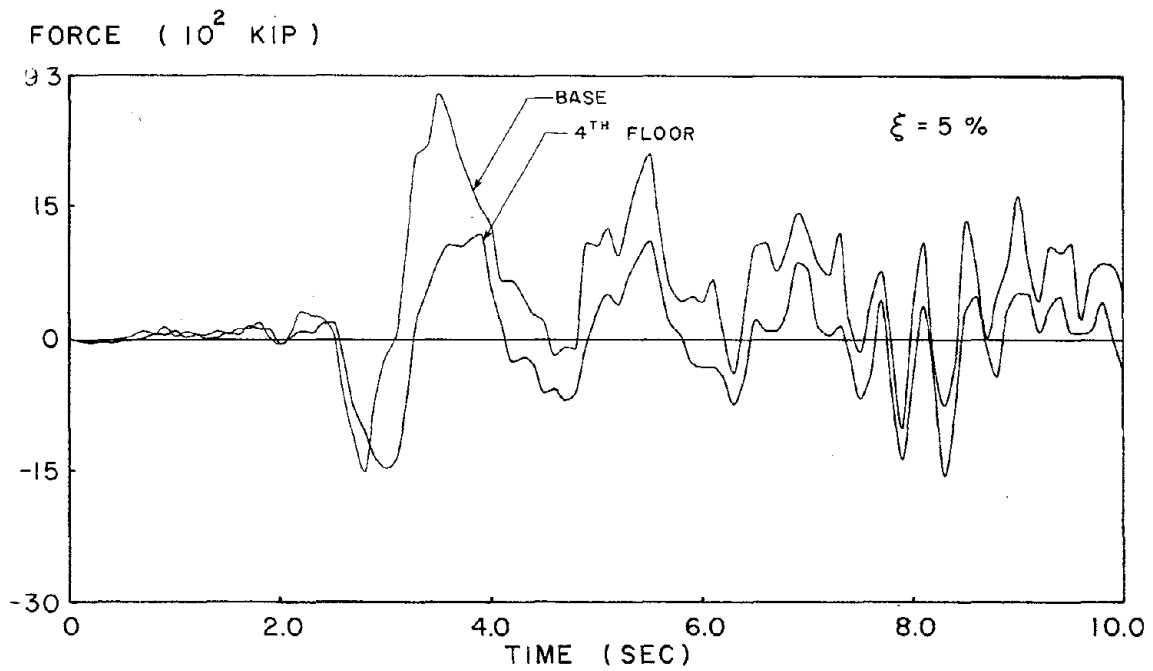


(a) WALL SHEAR FORCE, RIGHT WALL BASE AND 4th STORY

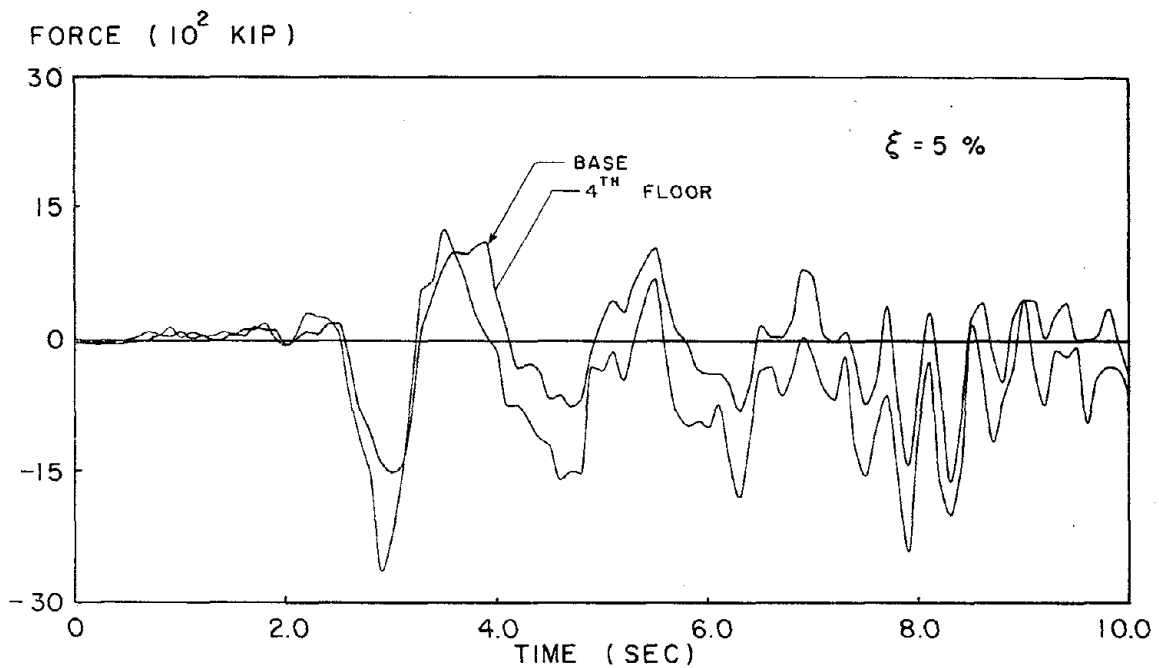


(b) WALL SHEAR FORCE, LEFT WALL BASE AND 4th STORY

FIG. 5.14 TIME-HISTORIES OF WALL SHEAR FORCES, PACOIMA RESPONSE OF THE COUPLED WALL MODEL



(a) WALL SHEAR FORCE, RIGHT WALL BASE AND 4th STORY



(b) WALL SHEAR FORCE, LEFT WALL BASE AND 4th STORY

FIG. 5.15 TIME-HISTORIES OF WALL SHEAR FORCES, PACOIMA RESPONSE OF THE COUPLED WALL-FRAME MODEL

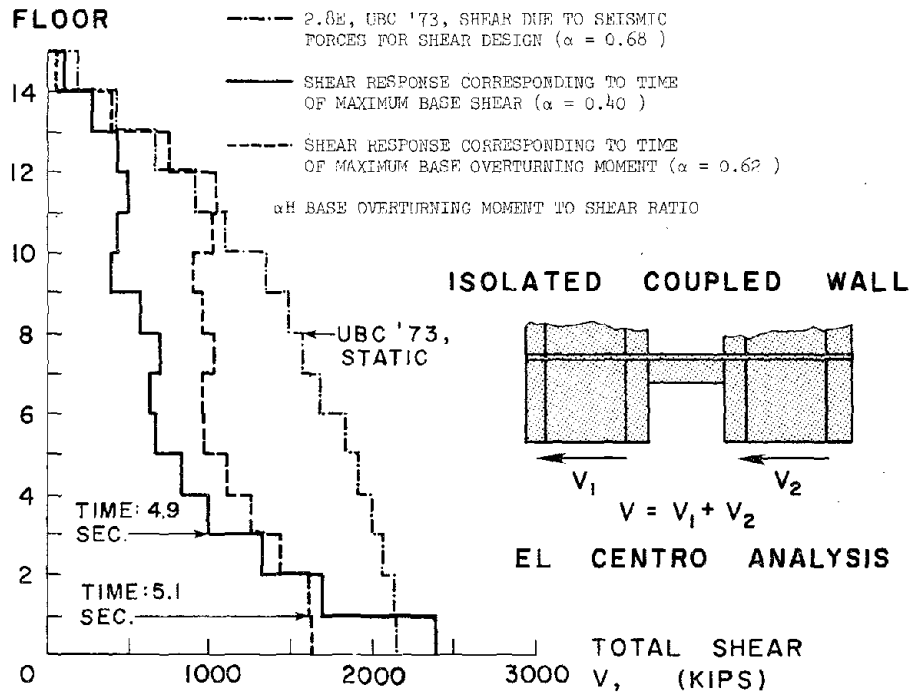


FIG. 5.16 THE DISTRIBUTION OF SEISMIC SHEARS ALONG THE HEIGHT OF THE COUPLED WALL MODEL, FOR THE COUPLED WALL MODEL SUBJECTED TO THE EL CENTRO GROUND MOTION

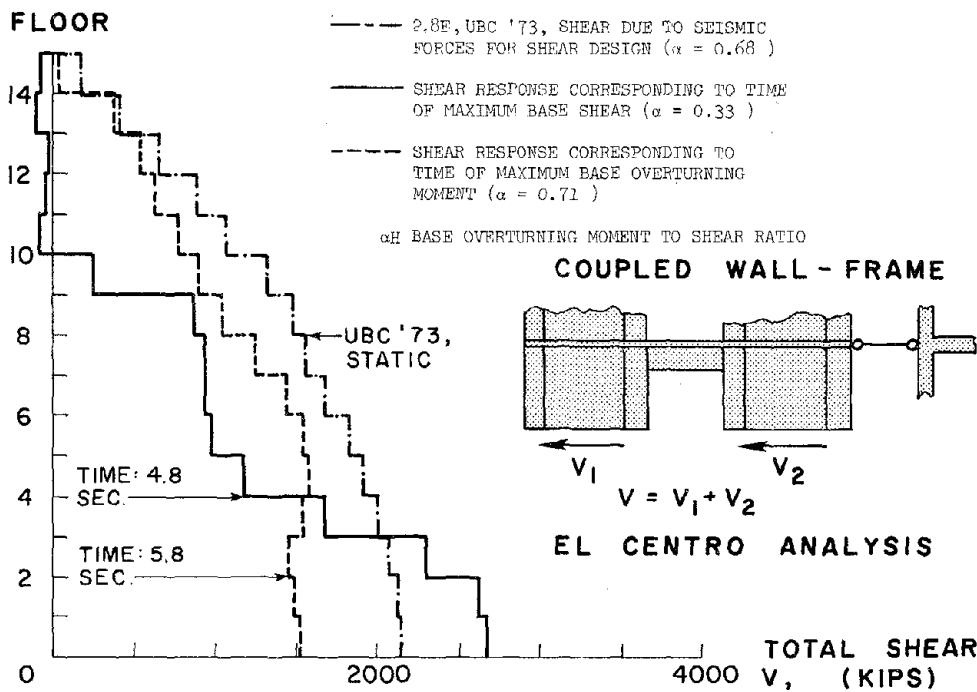


FIG. 5.17 THE DISTRIBUTION OF COUPLED WALL SEISMIC SHEARS ALONG THE HEIGHT OF THE COUPLED WALL, FOR THE COUPLED WALL-FRAME MODEL SUBJECTED TO THE EL CENTRO GROUND MOTION

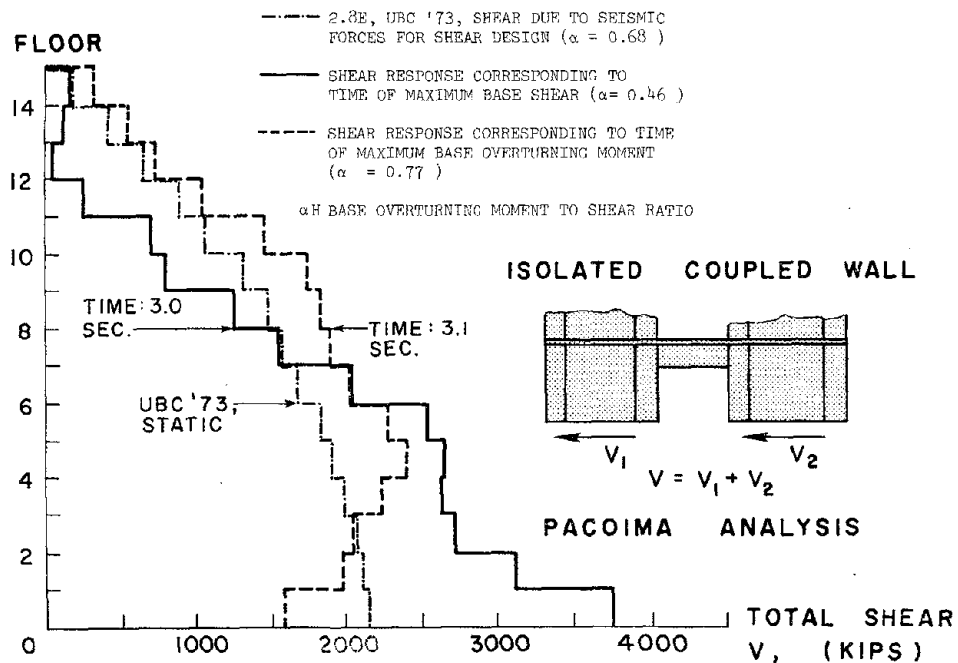


FIG. 5.18 THE DISTRIBUTION OF SEISMIC SHEARS ALONG THE HEIGHT OF THE COUPLED WALL, FOR THE COUPLED WALL MODEL SUBJECTED TO THE PACOIMA GROUND MOTION

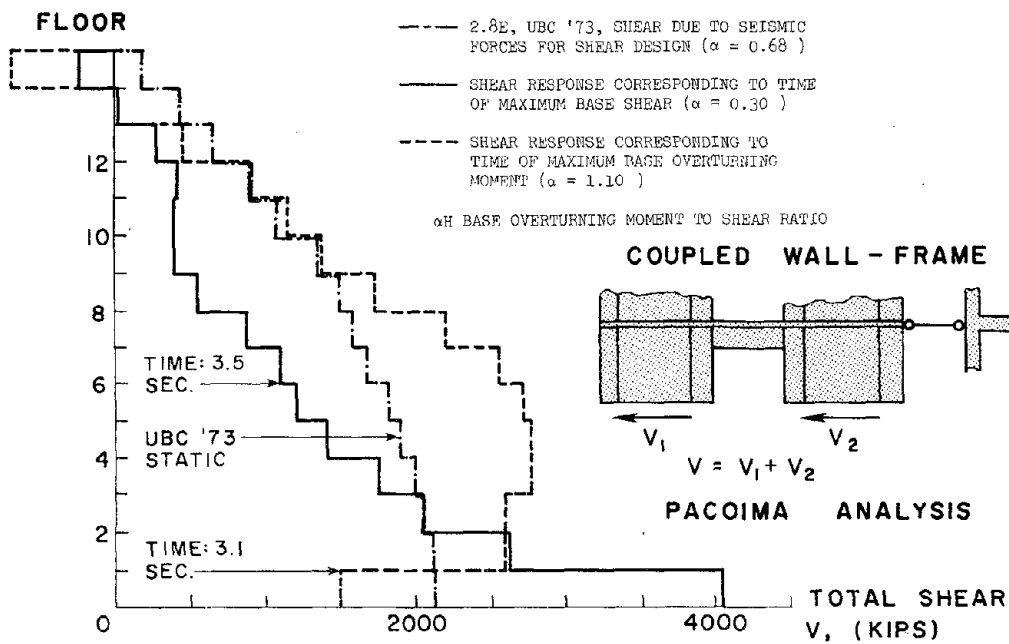


FIG. 5.19 THE DISTRIBUTION OF SEISMIC SHEARS ALONG THE HEIGHT OF THE COUPLED WALL FOR THE COUPLED WALL-FRAME MODEL SUBJECTED TO THE PACOIMA GROUND MOTION

COUPLED WALL MODEL

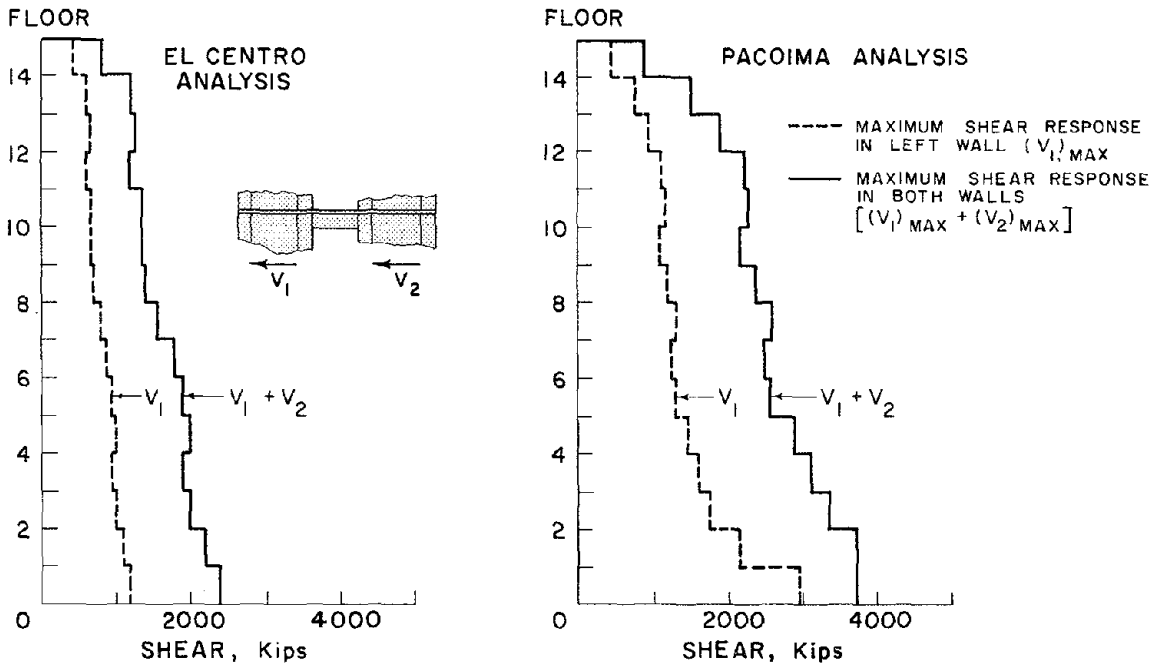


FIG. 5.20 ENVELOPES OF MAXIMUM SHEAR RESPONSE, COUPLED WALL MODEL

COUPLED WALL-FRAME MODEL

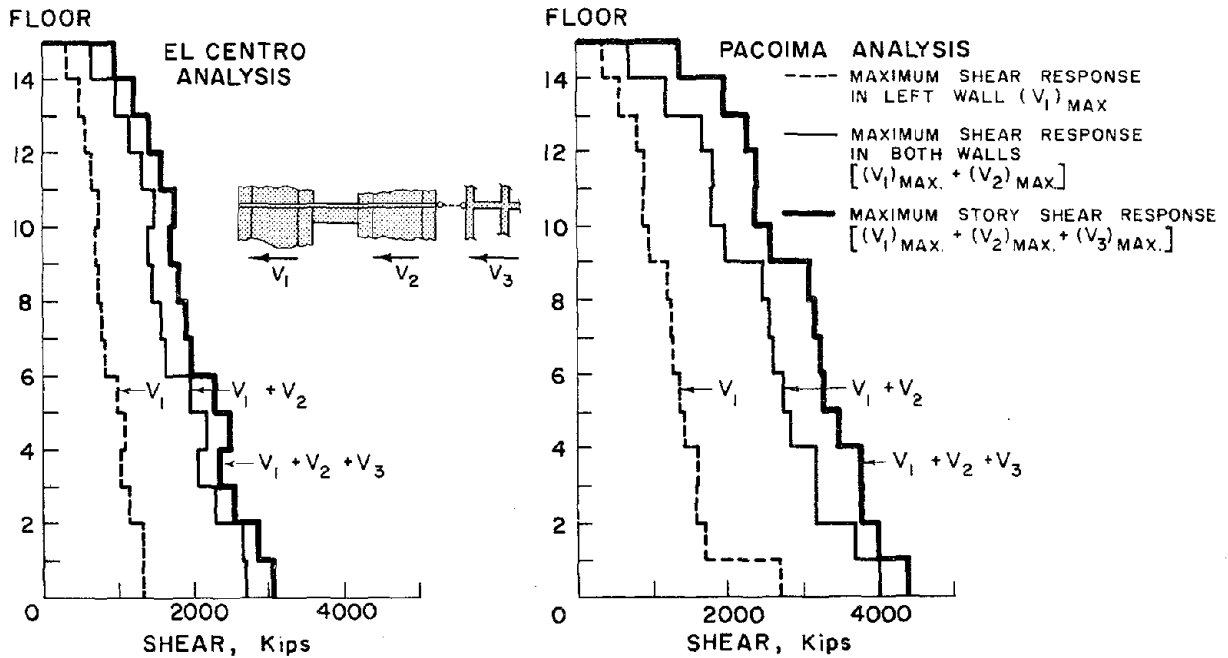
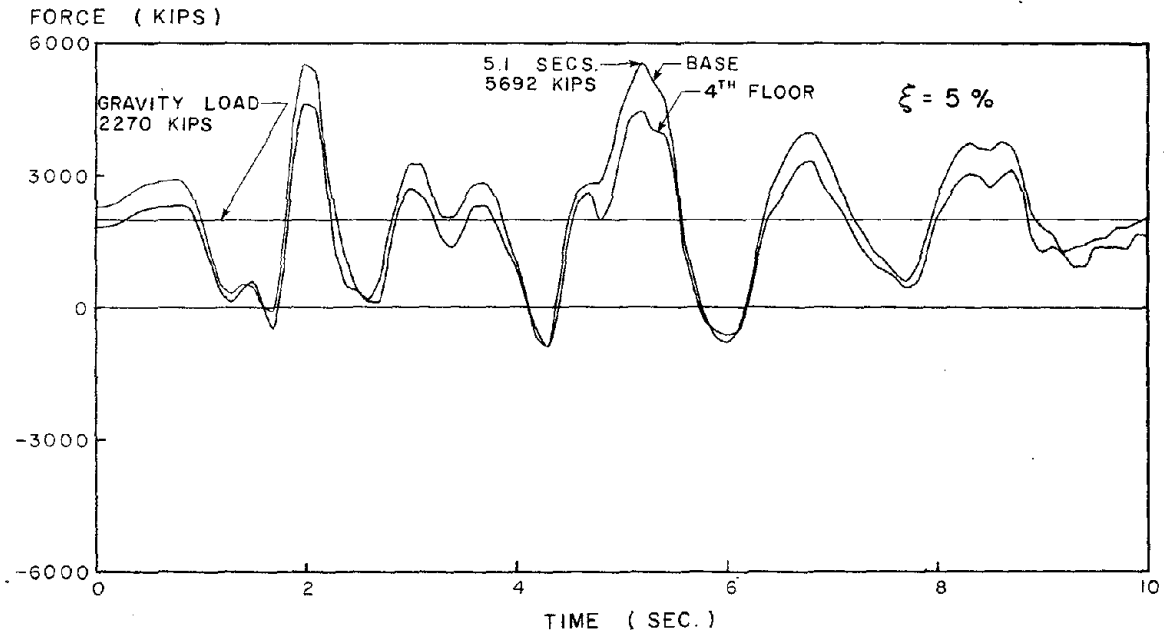
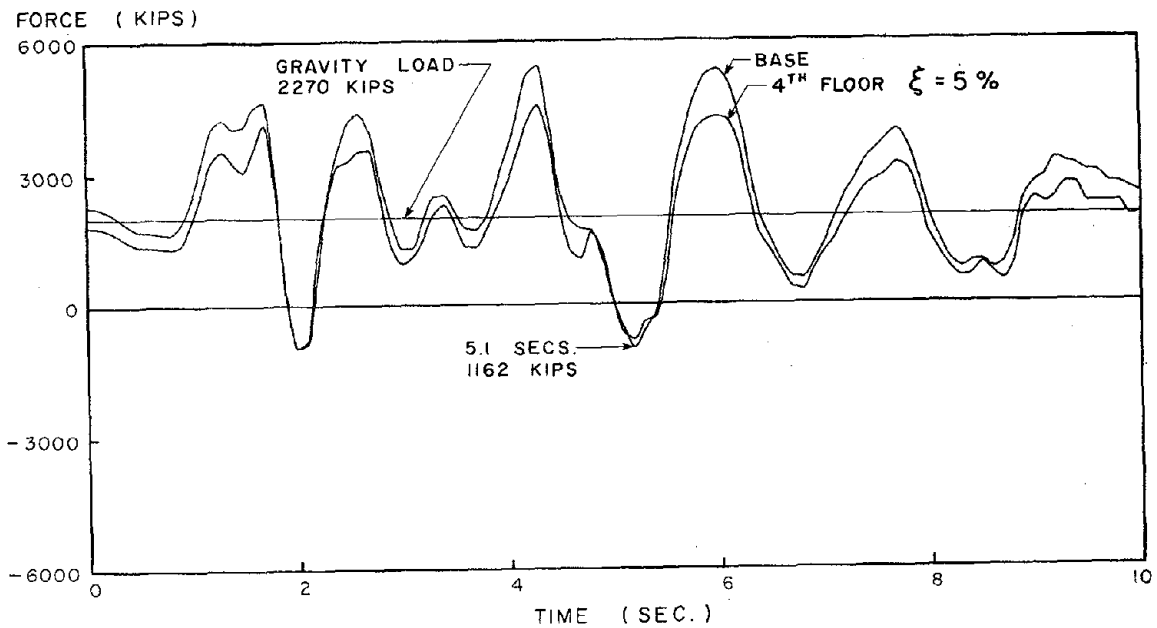


FIG. 5.21 ENVELOPES OF MAXIMUM SHEAR RESPONSE, COUPLED WALL-FRAME MODEL

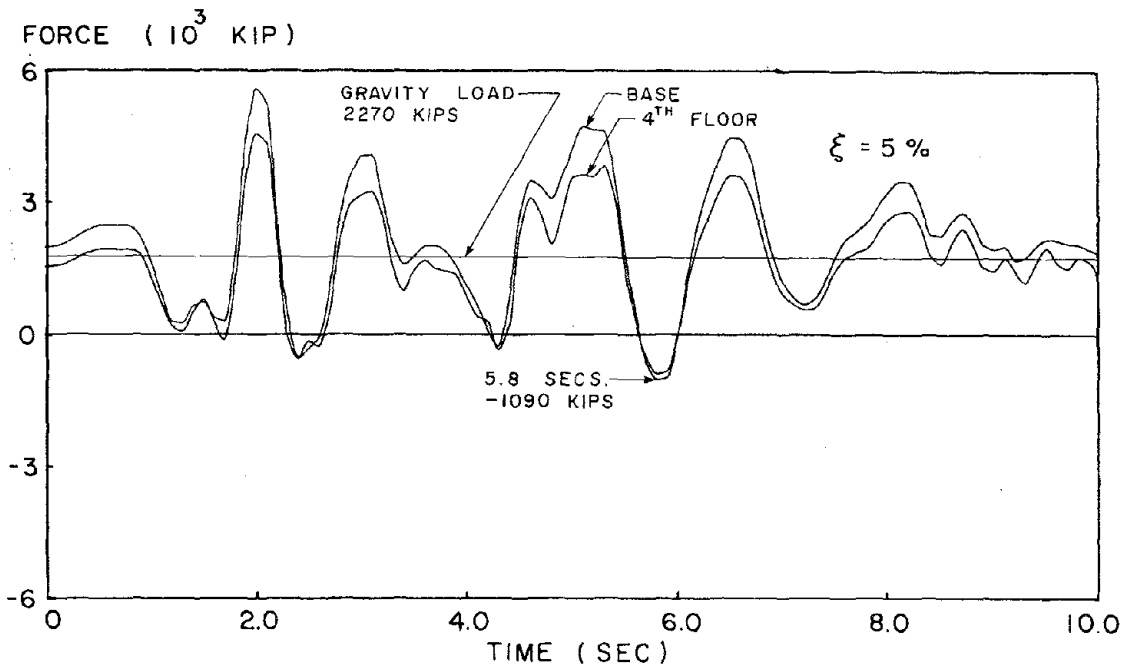


(a) WALL AXIAL FORCE, RIGHT WALL BASE AND 4th STORY

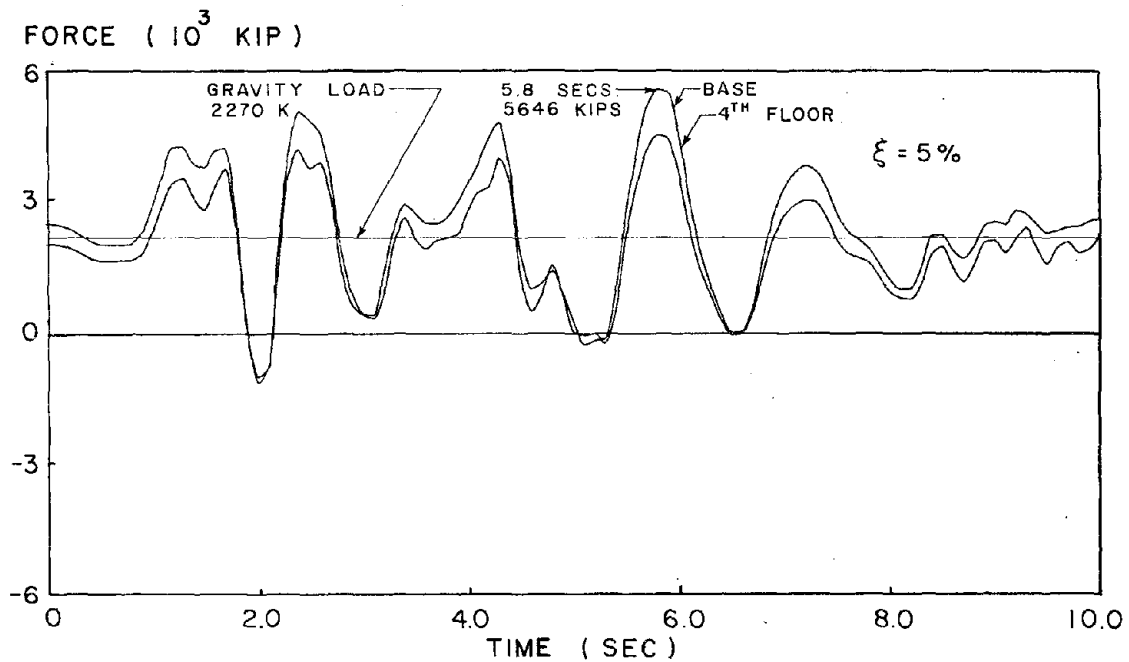


(b) WALL AXIAL FORCE, LEFT WALL BASE AND 4th STORY

FIG. 5.22 TIME-HISTORIES OF WALL AXIAL FORCES, EL CENTRO RESPONSES OF THE COUPLED WALL MODEL

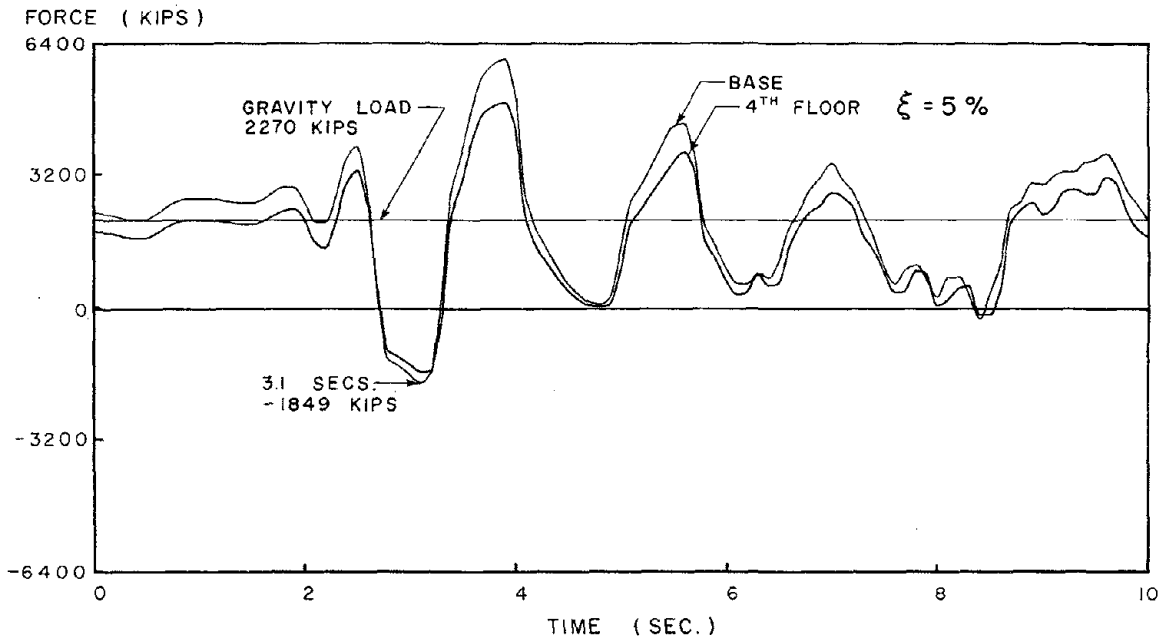


(a) WALL AXIAL FORCE, RIGHT WALL BASE AND 4th STORY

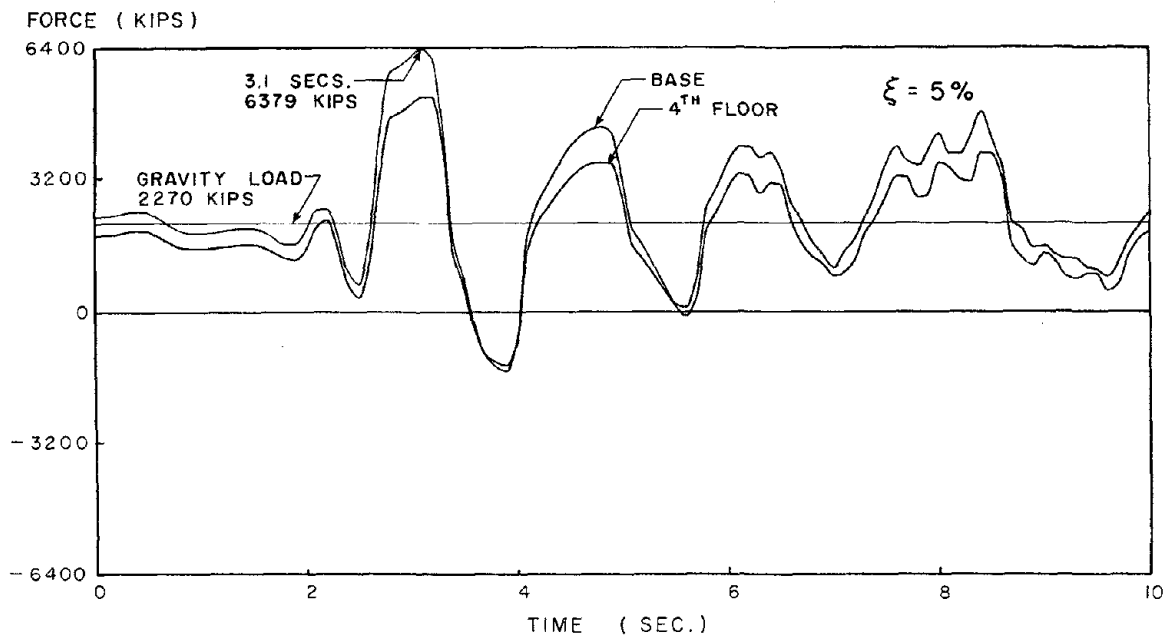


(b) WALL AXIAL FORCE, LEFT WALL BASE AND 4th STORY

FIG. 5.23 TIME-HISTORIES OF WALL AXIAL FORCES, EL CENTRO RESPONSES OF THE COUPLED WALL-FRAME MODEL

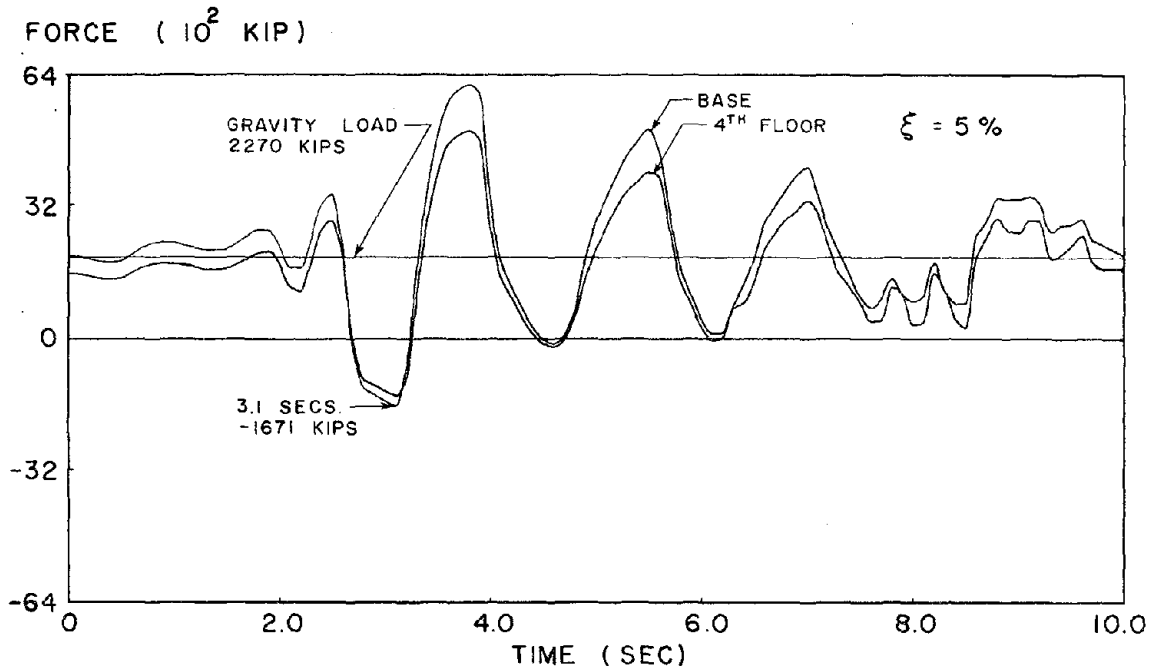


(a) WALL AXIAL FORCE, RIGHT WALL BASE AND 4th STORY

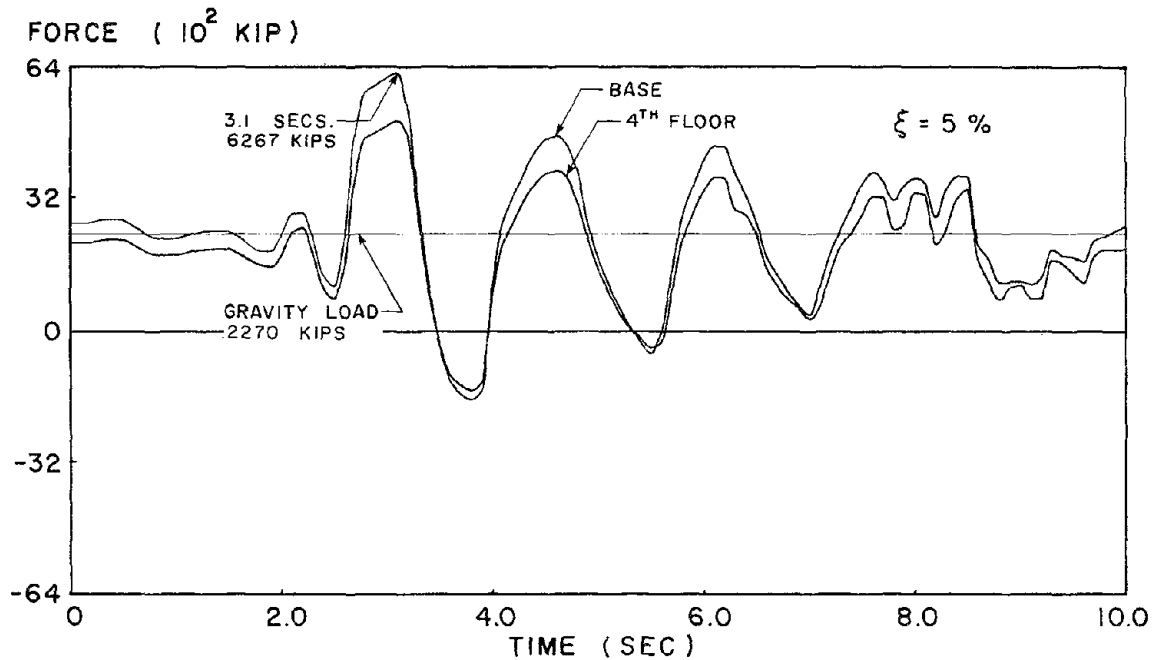


(b) WALL AXIAL FORCE, LEFT WALL BASE AND 4th STORY

FIG. 5.24 TIME-HISTORIES OF WALL AXIAL FORCES, PACOIMA RESPONSES OF THE COUPLED WALL MODEL



(a) WALL AXIAL FORCE, RIGHT WALL BASE AND 4th STORY



(b) WALL AXIAL FORCE, LEFT WALL BASE AND 4th STORY

FIG. 5.25 TIME-HISTORIES OF WALL AXIAL FORCES, PACOIMA RESPONSES OF THE COUPLED WALL-FRAME MODEL

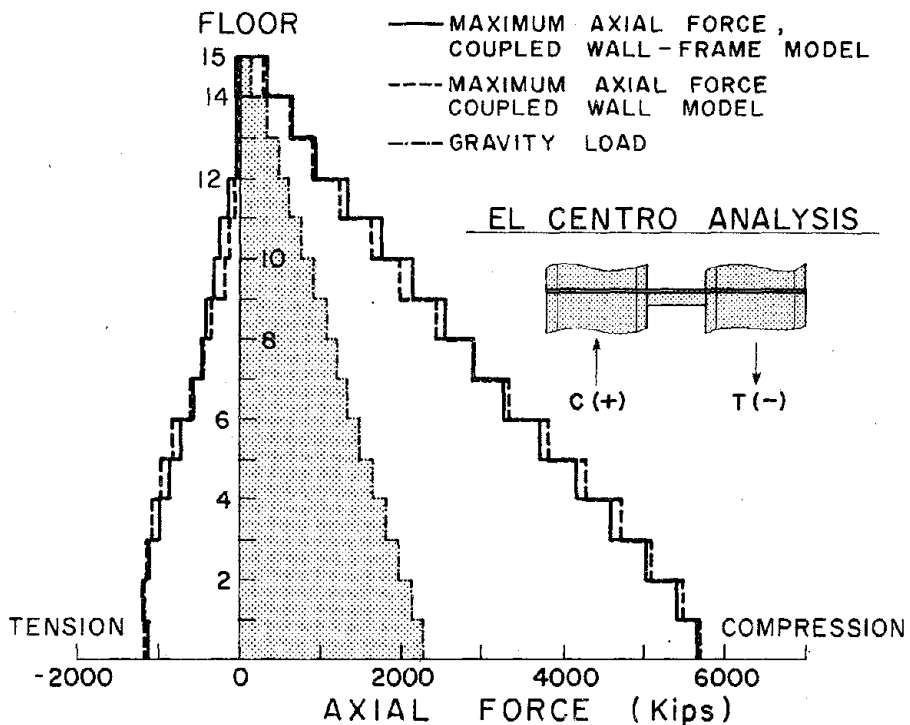


FIG. 5.26 ENVELOPES OF WALL AXIAL FORCES, EL CENTRO ANALYSES

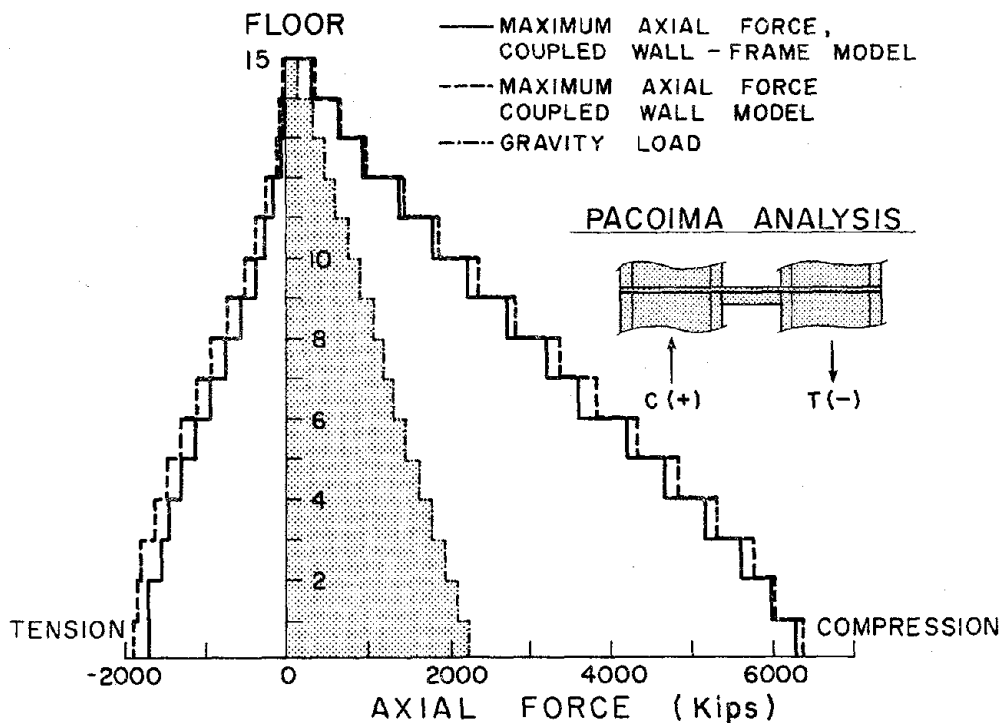
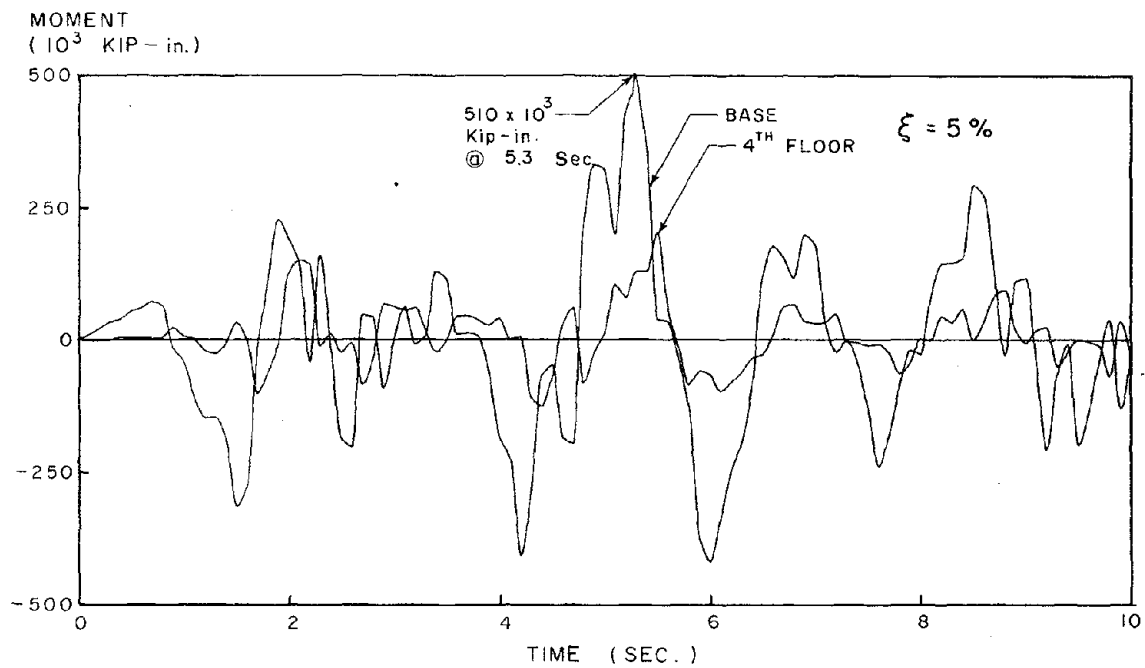
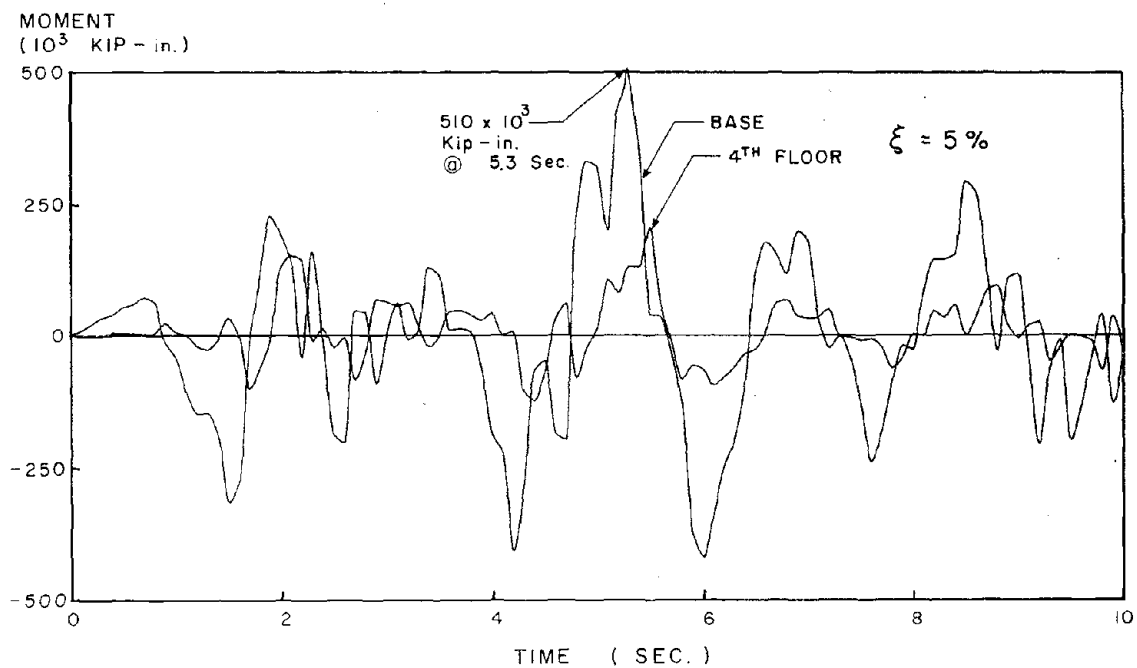


FIG. 5.27 ENVELOPES OF WALL AXIAL FORCES, PACOIMA ANALYSES

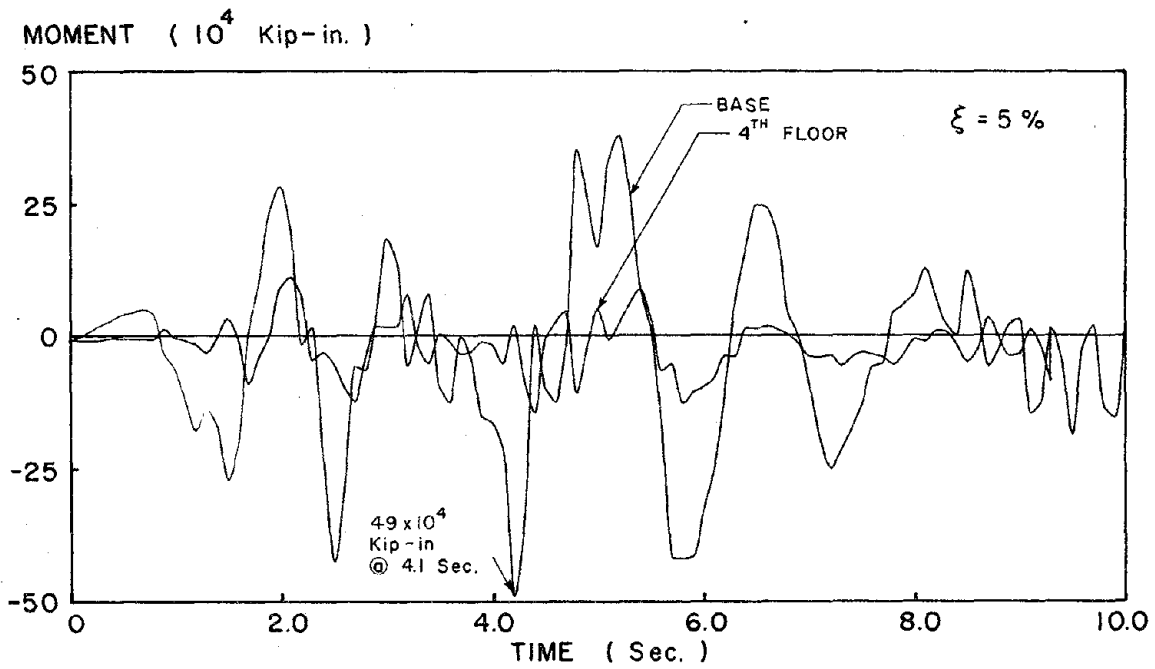


(a) WALL BENDING MOMENT, RIGHT WALL BASE AND 4th STORY

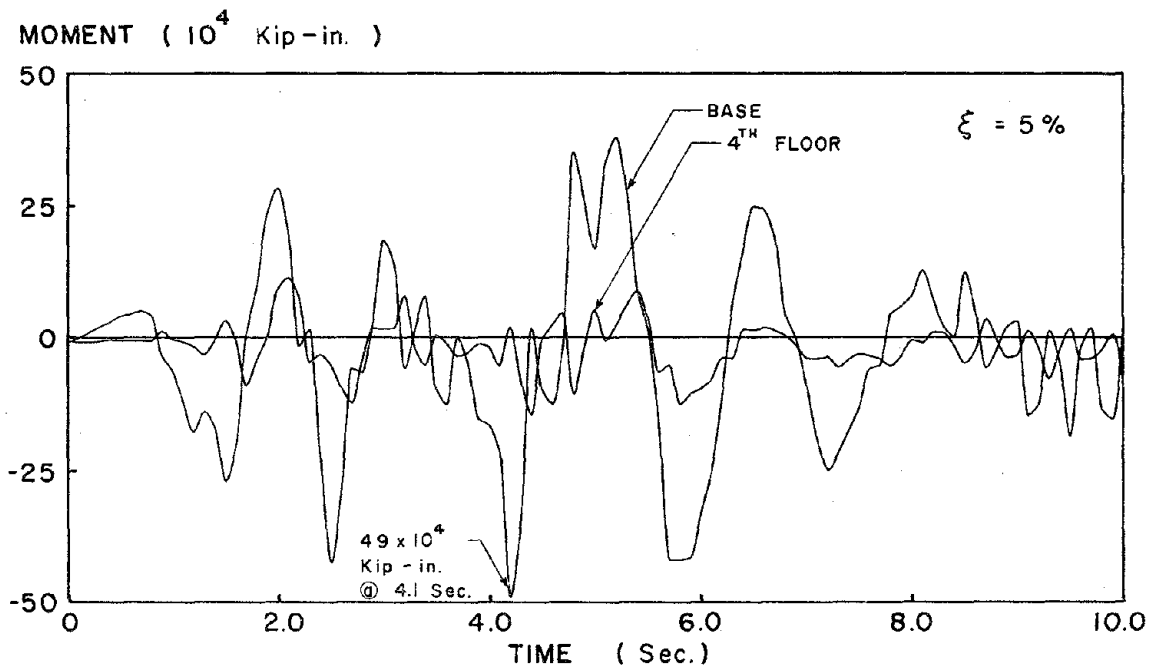


(b) WALL BENDING MOMENT, LEFT WALL BASE AND 4th STORY

FIG. 5.28 TIME-HISTORIES OF WALL BENDING MOMENTS, EL CENTRO RESPONSES OF THE COUPLED WALL MODEL

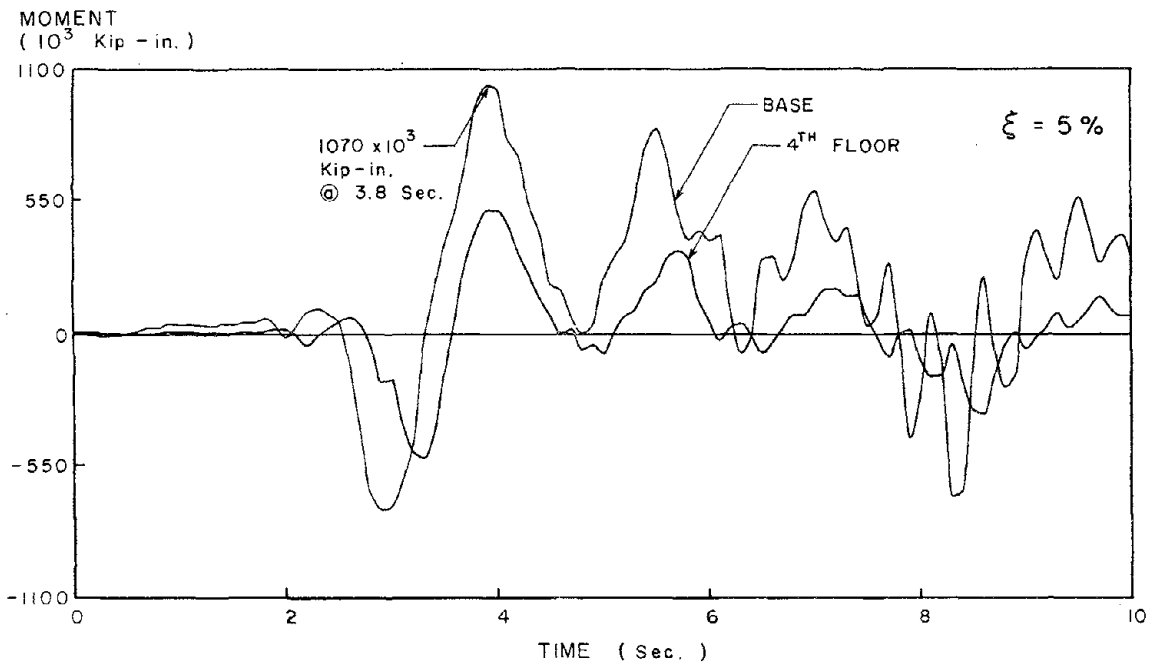


(a) WALL BENDING MOMENT, RIGHT WALL BASE AND 4th STORY

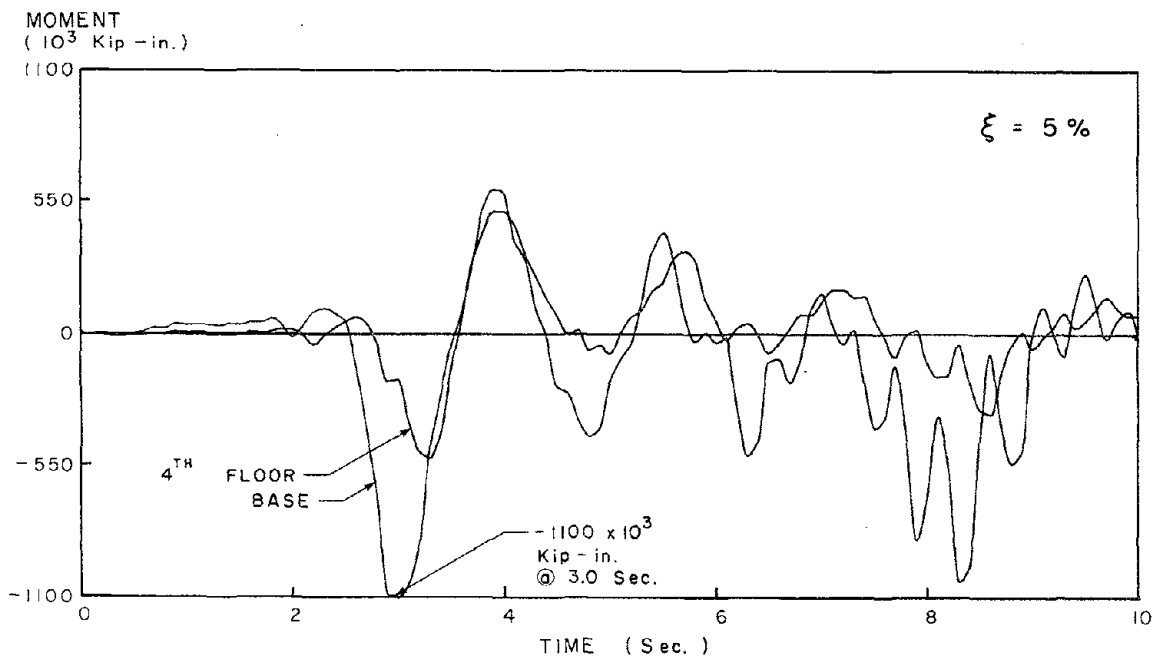


(b) WALL BENDING MOMENT, LEFT WALL BASE AND 4th STORY

FIG. 5.29 TIME-HISTORIES OF WALL BENDING MOMENTS, EL CENTRO RESPONSES OF THE COUPLED WALL-FRAME MODEL

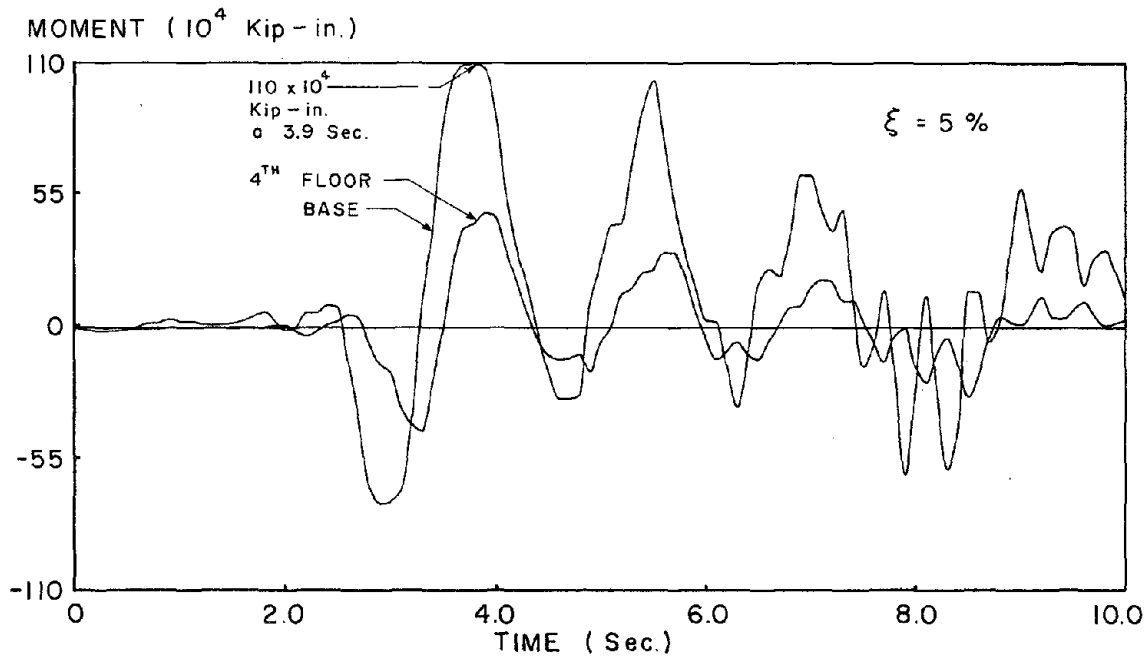


(a) WALL BENDING MOMENT, RIGHT WALL BASE AND 4th STORY

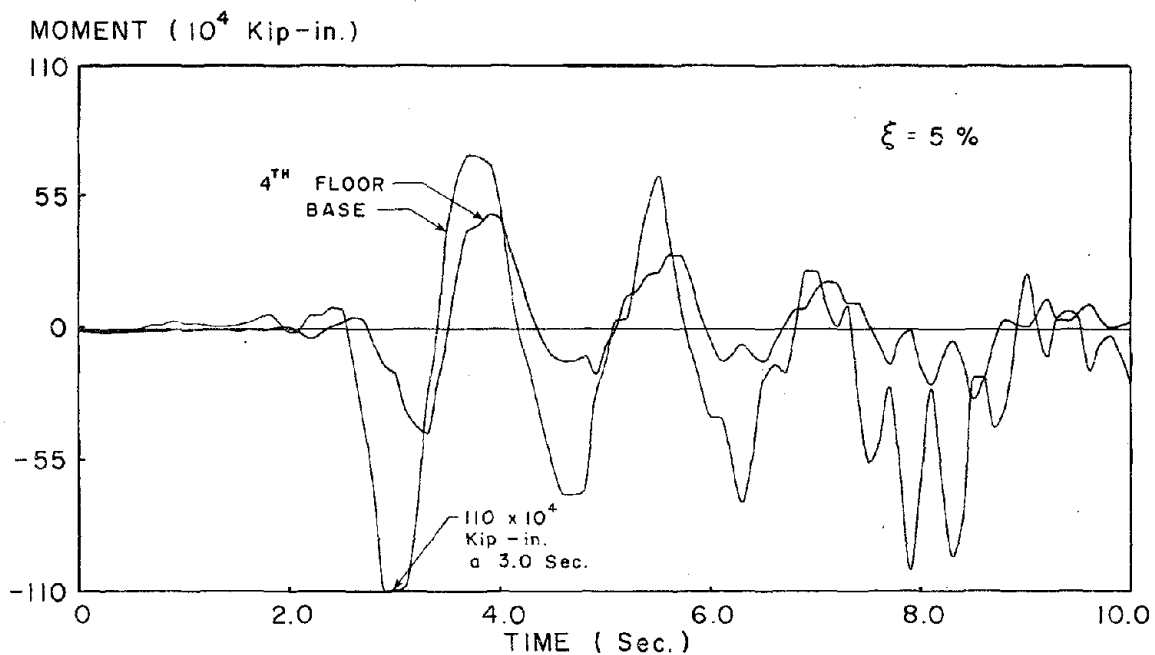


(b) WALL BENDING MOMENT, LEFT WALL BASE AND 4th STORY

FIG. 5.30 TIME-HISTORIES OF WALL BENDING MOMENTS, PACOIMA RESPONSES OF THE COUPLED WALL MODEL



(a) WALL BENDING MOMENT, RIGHT WALL BASE AND 4th STORY



(b) WALL BENDING MOMENT, LEFT WALL BASE AND 4th STORY

FIG. 5.31 TIME-HISTORIES OF WALL BENDING MOMENTS, PACOIMA RESPONSES OF THE COUPLED WALL-FRAME MODEL

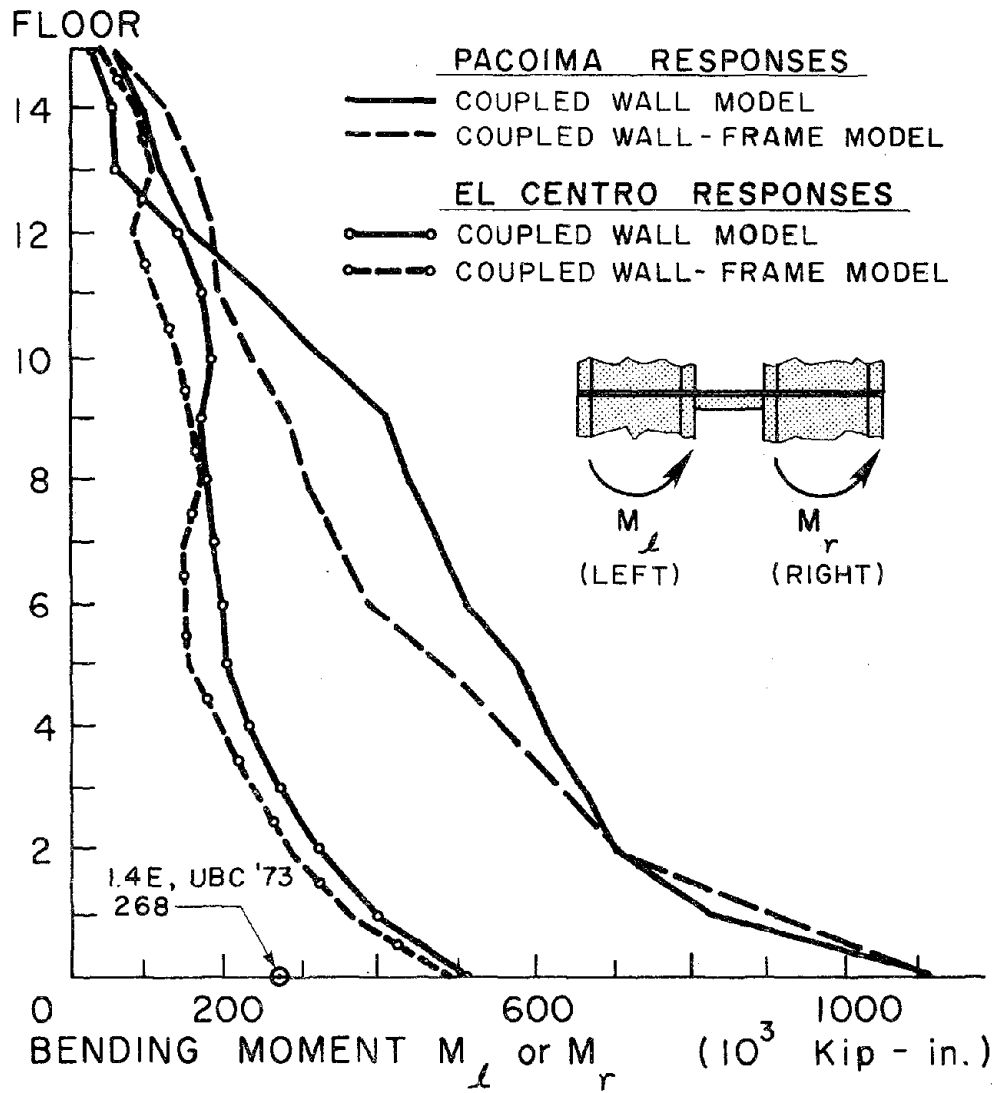
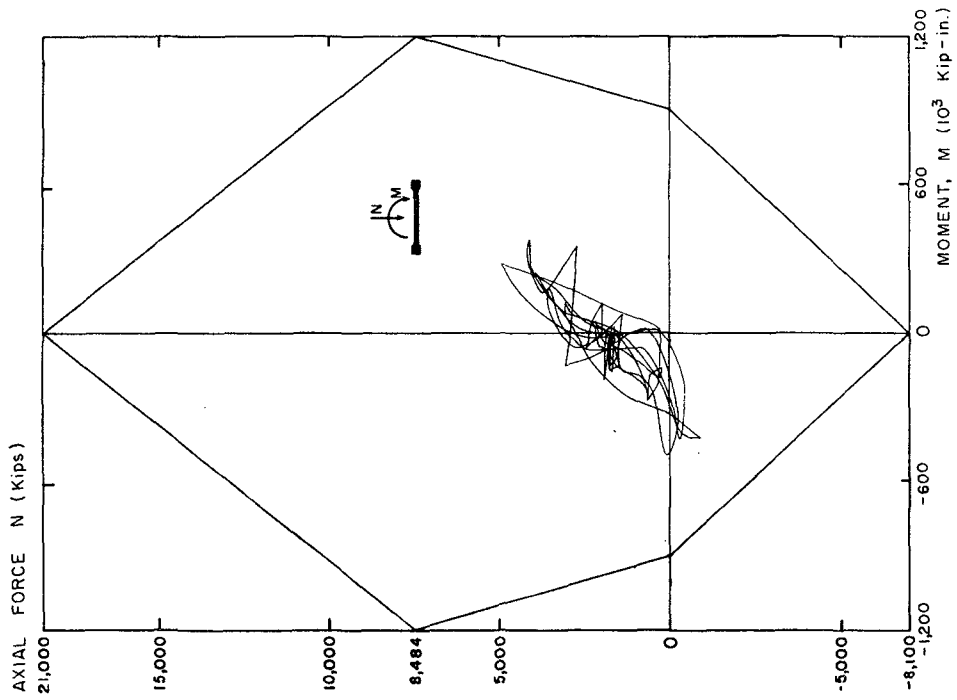
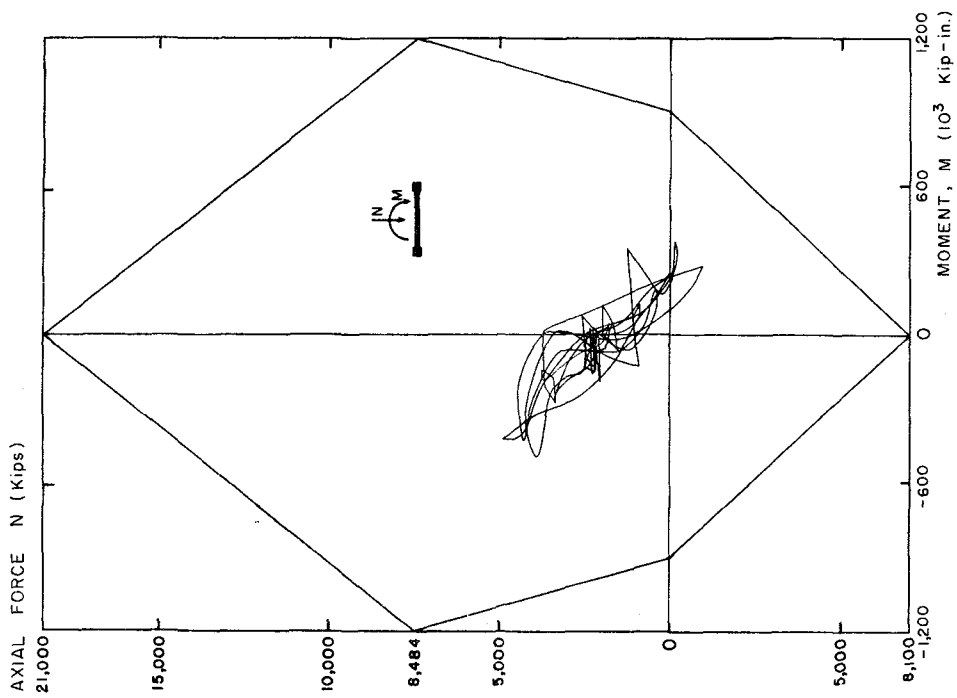


FIG. 5.32 BENDING MOMENT ENVELOPES OF ONE WALL PIER OBTAINED DURING THE TIME-HISTORY ANALYSES

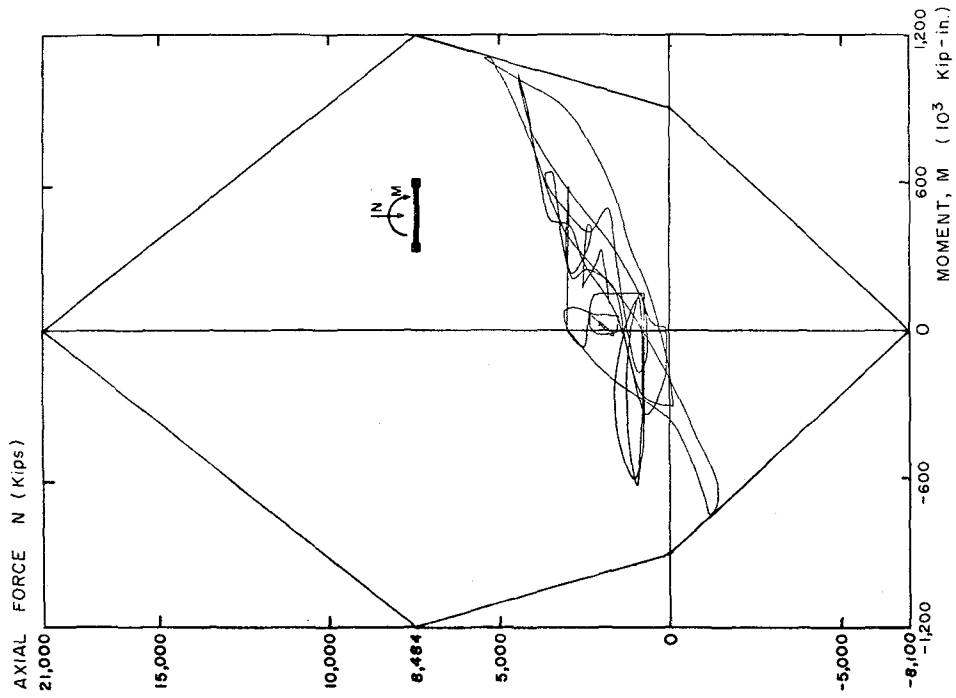


(a) MOMENT VS. AXIAL FORCE, LEFT WALL BASE

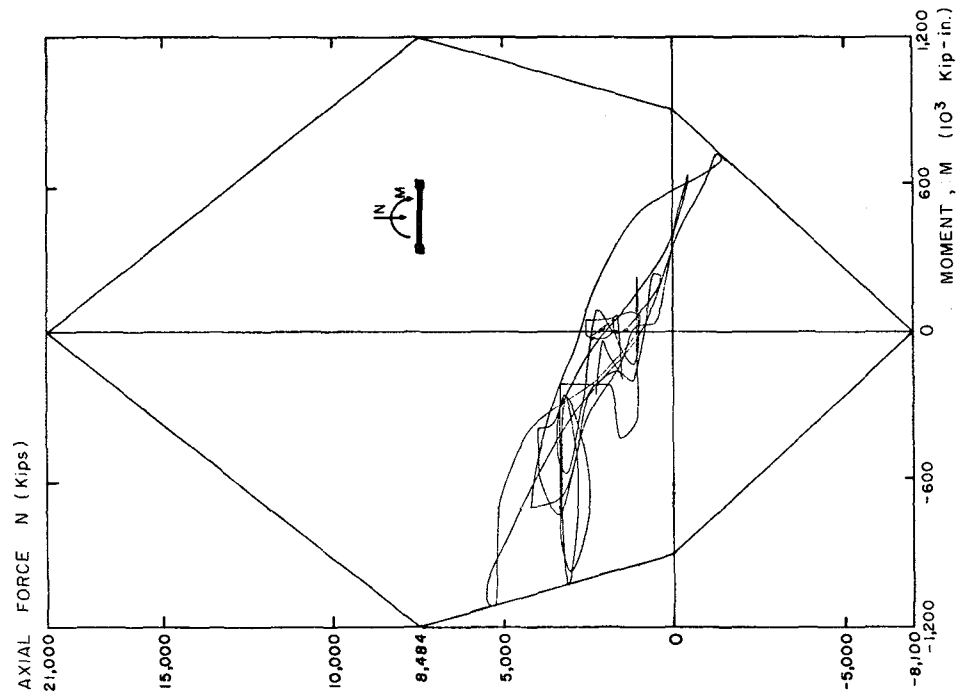


(b) MOMENT VS. AXIAL FORCE, RIGHT WALL BASE

FIG. 5.33 MOMENT-AXIAL FORCE RELATIONS AT THE BASES OF THE INDIVIDUAL WALLS, EL CENTRO RESPONSES OF THE COUPLED WALL-FRAME MODEL

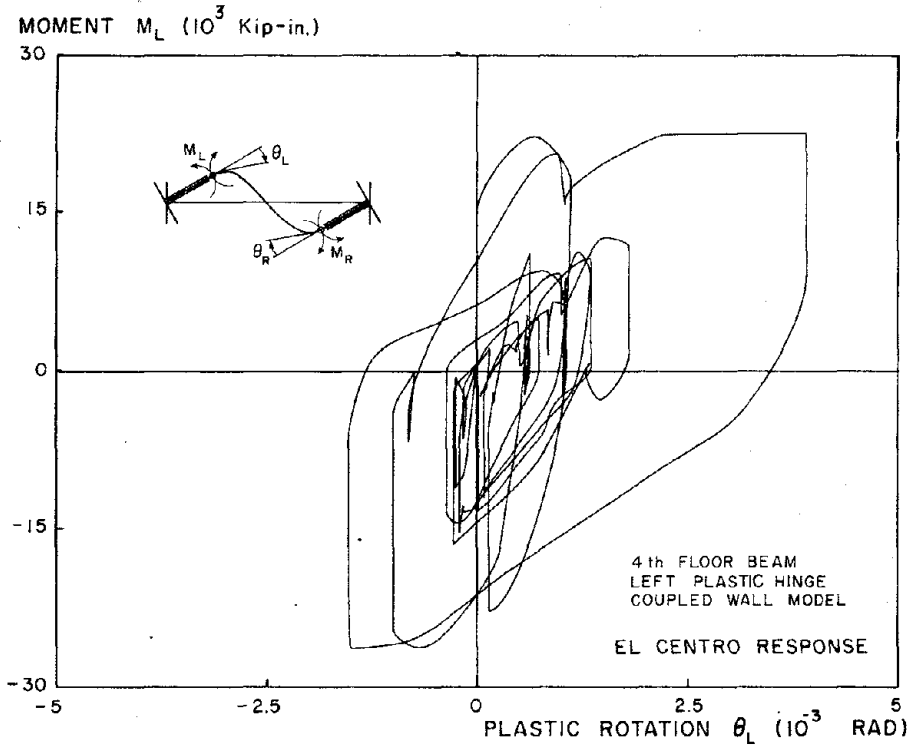


(a) MOMENT VS. AXIAL FORCE, LEFT WALL BASE

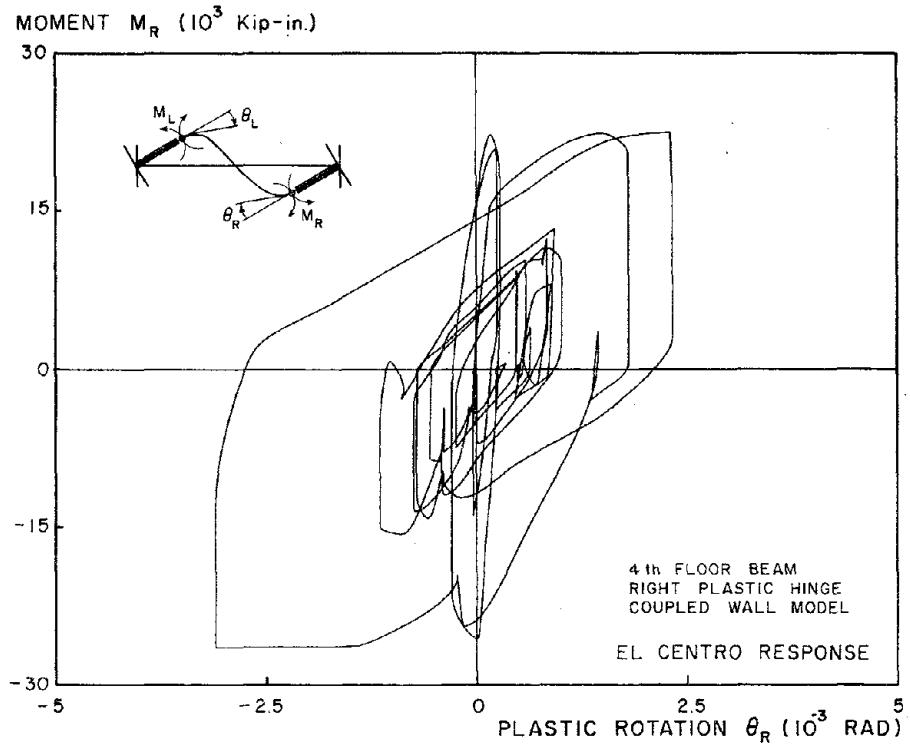


(b) MOMENT VS. AXIAL FORCE, RIGHT WALL BASE

FIG. 5.34 MOMENT-AXIAL FORCE RELATIONS AT THE BASES OF THE INDIVIDUAL WALLS, PACOIMA RESPONSES OF THE COUPLED WALL-FRAME MODEL

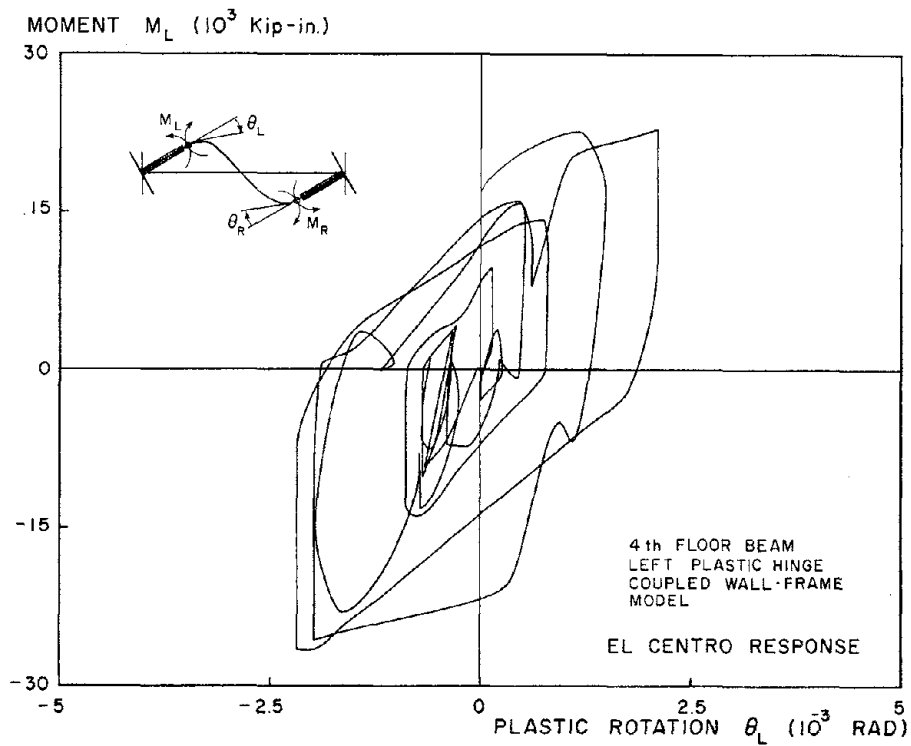


(a) MOMENT VS. PLASTIC ROTATION, LEFT HINGE, 4th STORY

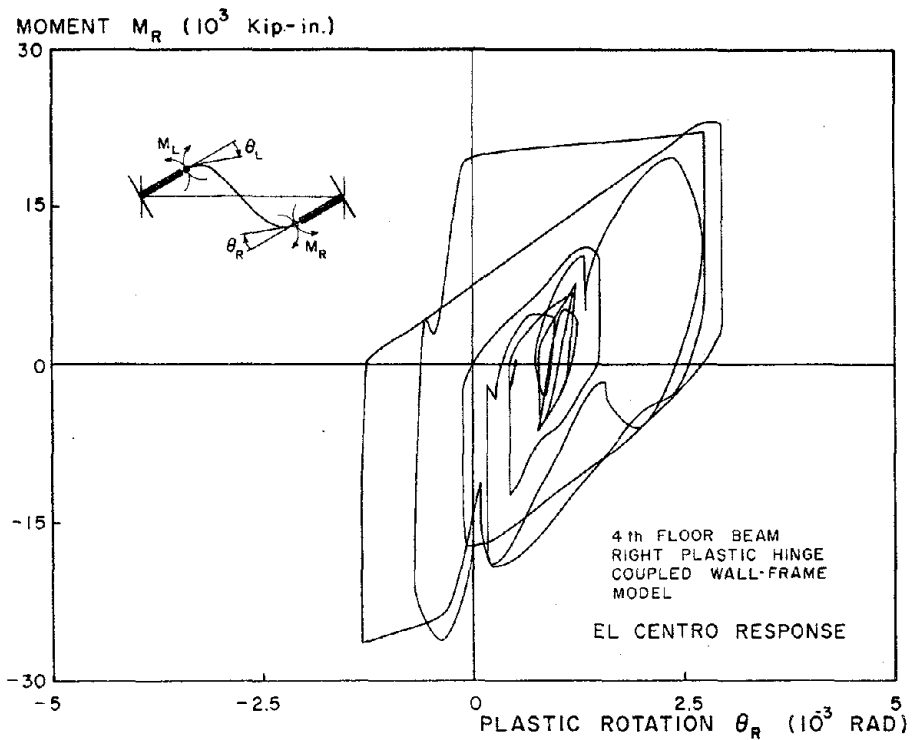


(b) MOMENT VS. PLASTIC ROTATION, RIGHT HINGE, 4th STORY

FIG. 5.35 MOMENT-PLASTIC ROTATION RELATIONSHIPS FOR THE FOURTH FLOOR BEAM, EL CENTRO RESPONSES OF THE COUPLED WALL MODEL

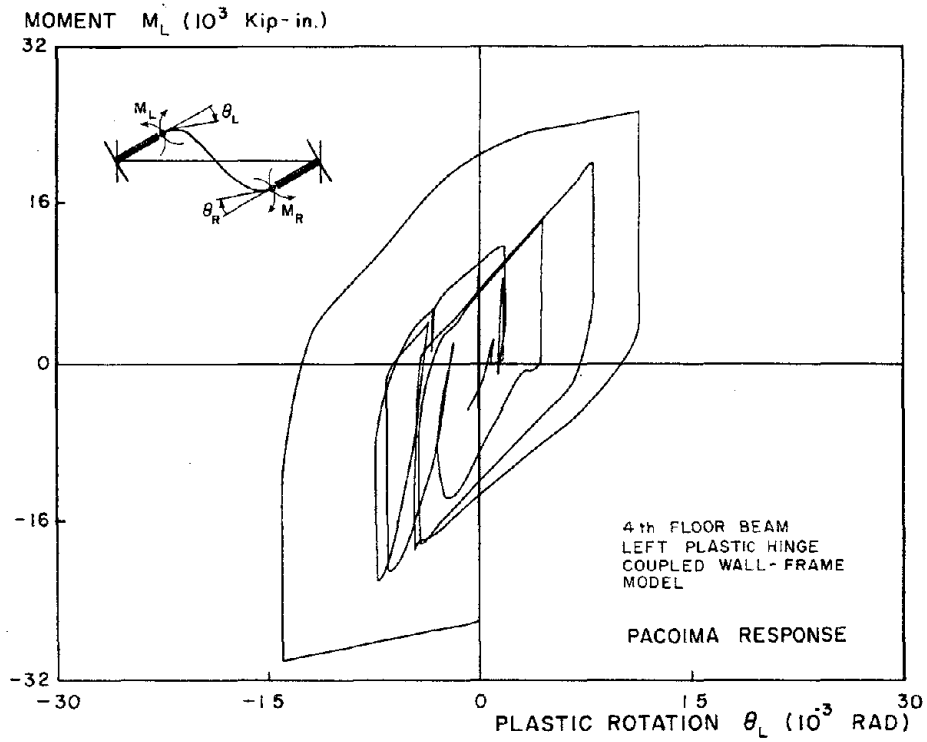


(a) MOMENT VS. PLASTIC ROTATION, LEFT HINGE, 4th STORY

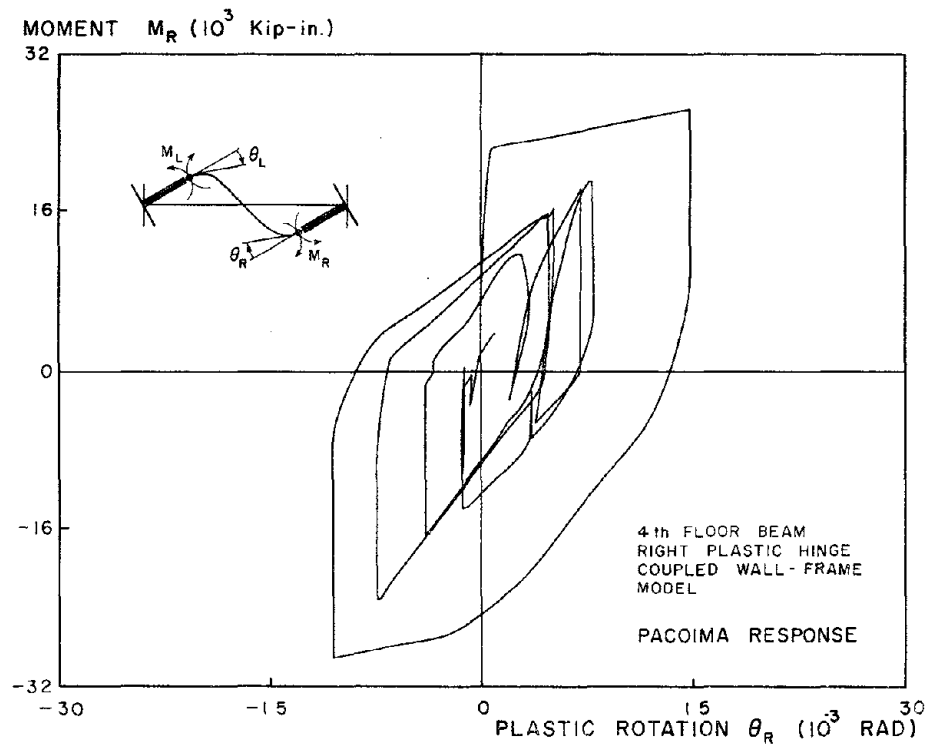


(b) MOMENT VS. PLASTIC ROTATION, RIGHT HINGE, 4th STORY

FIG. 5.36 MOMENT-PLASTIC ROTATION RELATIONSHIPS FOR THE FOURTH FLOOR BEAM, EL CENTRO RESPONSES OF THE COUPLED WALL-FRAME MODEL



(a) MOMENT VS. PLASTIC ROTATION, LEFT HINGE, 4th STORY



(b) MOMENT VS. PLASTIC ROTATION, RIGHT HINGE, 4th STORY

FIG. 5.37 MOMENT-PLASTIC ROTATION RELATIONSHIPS FOR THE FOURTH FLOOR BEAM, PACOIMA RESPONSES OF THE COUPLED WALL-FRAME MODEL

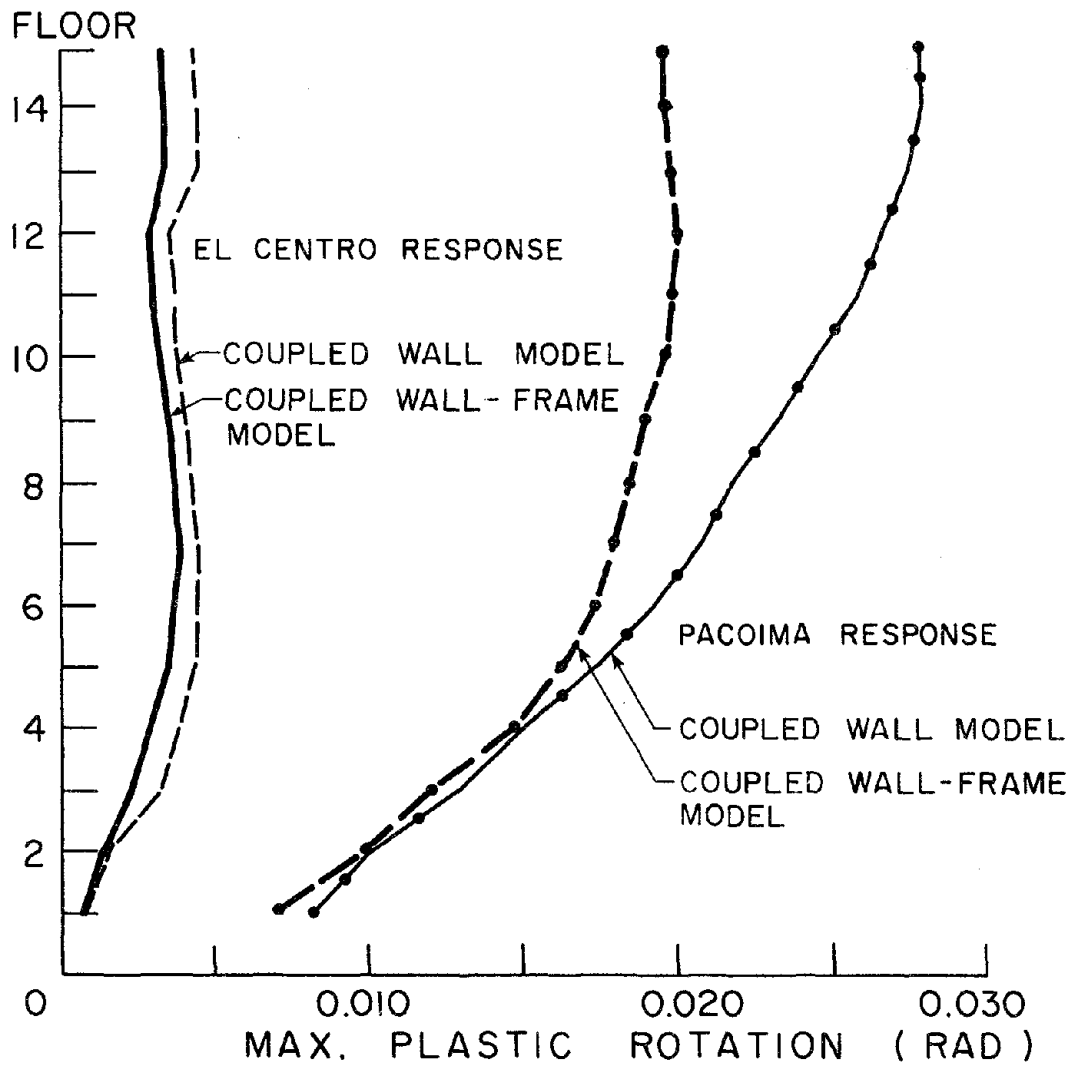
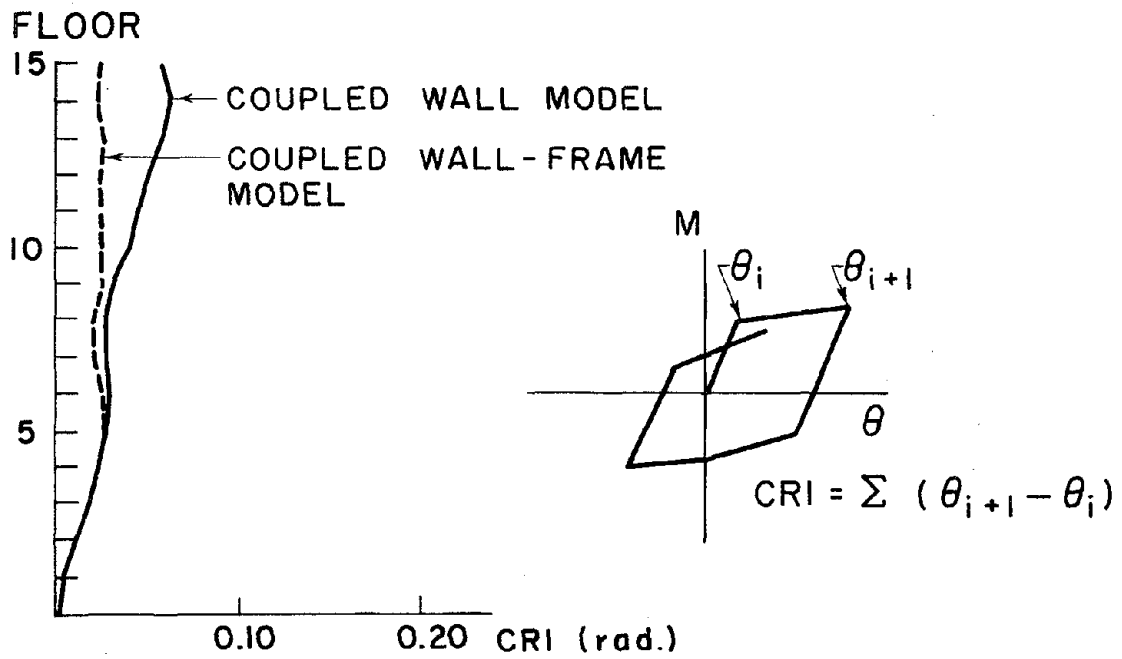
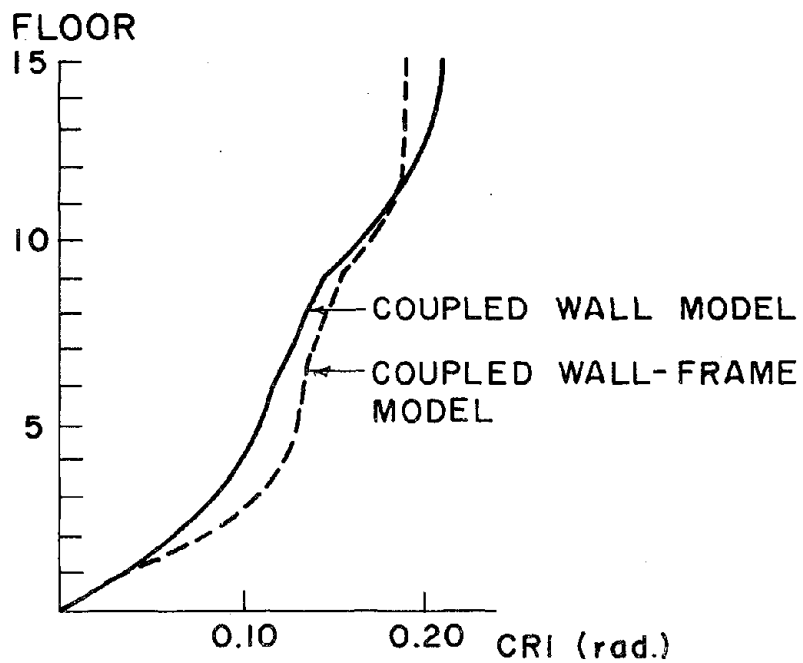


FIG. 5.38 ENVELOPES OF MAXIMUM PLASTIC ROTATION ATTAINED FOR THE COUPLING GIRDERS ALONG THE ELEVATION OF THE STRUCTURE

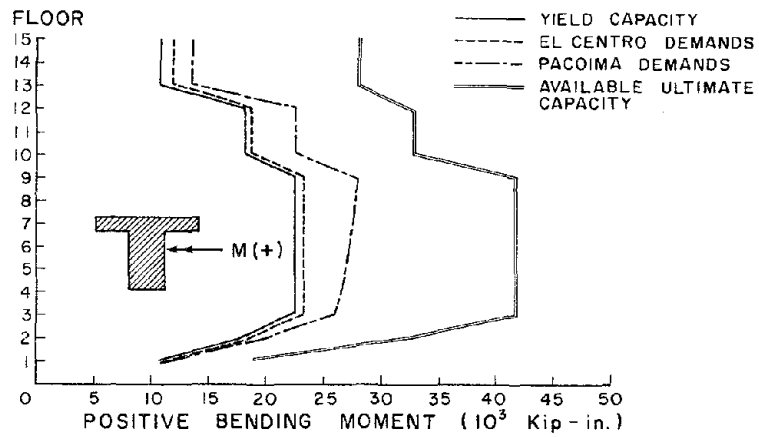


(a) EL CENTRO RESPONSES

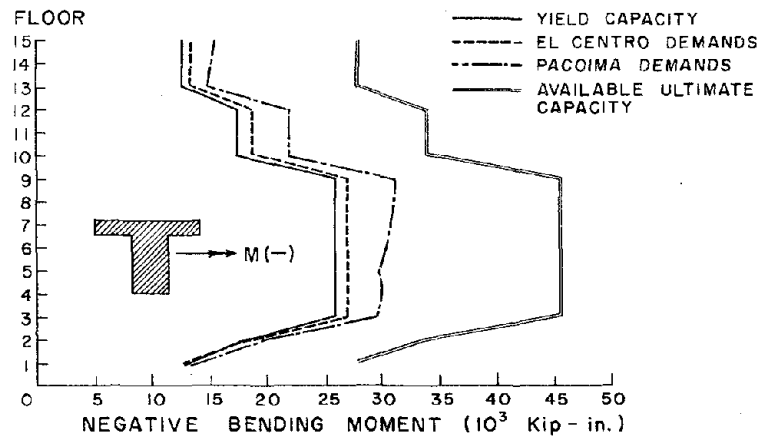


(b) PACOIMA RESPONSES

FIG. 5.39 THE MAXIMUM CUMULATIVE ROTATION INDEX (CRI) ATTAINED FOR THE COUPLING GIRDERS ALONG THE ELEVATION OF THE STRUCTURE (AT EITHER END)



(a) POSITIVE BENDING MOMENT



(b) NEGATIVE BENDING MOMENT

FIG. 5.40 MAXIMUM POSITIVE AND NEGATIVE BENDING MOMENT DEMANDS FROM THE COUPLING GIRDERS, COUPLED WALL-FRAME MODEL

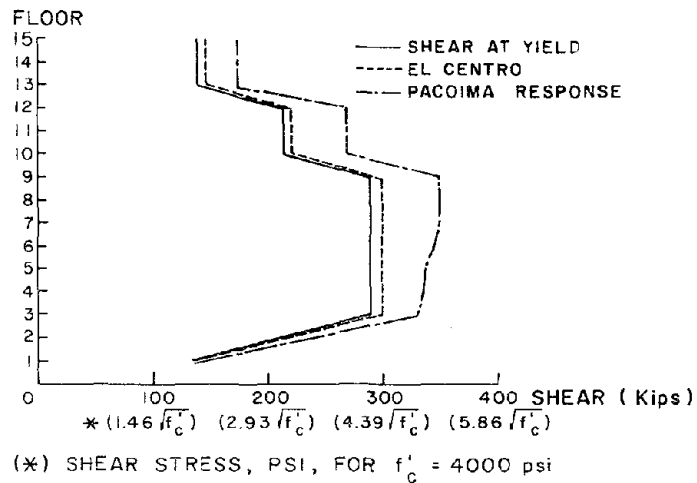


FIG. 5.41 DISTRIBUTION OF MAXIMUM COUPLING GIRDER SHEAR FORCES AND STRESSES, FOR THE COUPLED WALL-FRAME MODEL

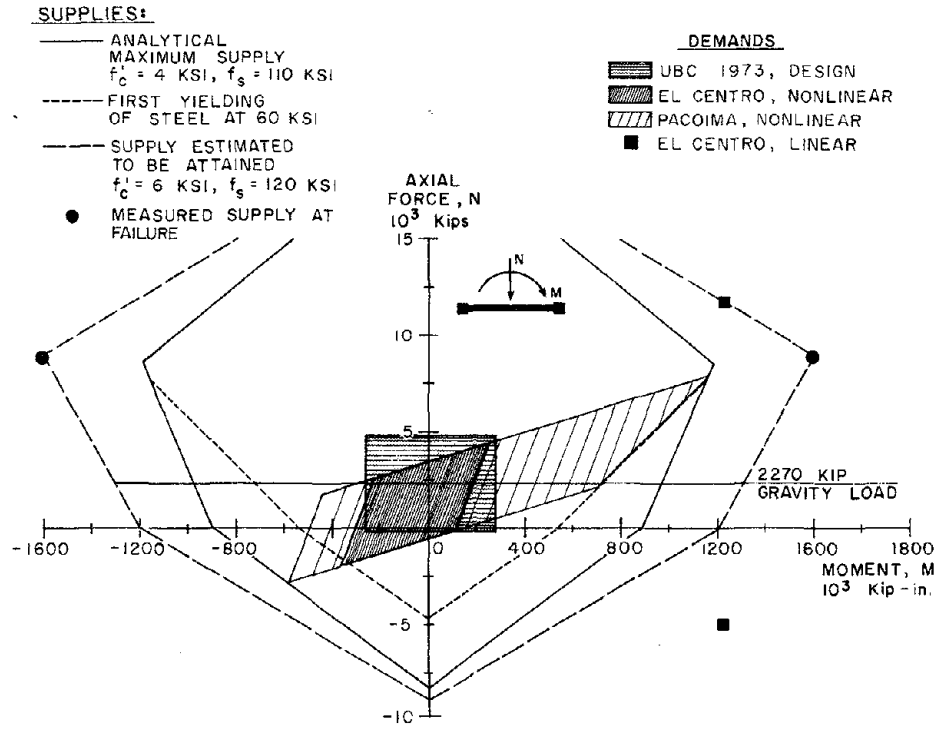


FIG. 6.1 AXIAL-FLEXURAL SUPPLIES AND DEMANDS AT THE BASE OF ONE WALL SECTION

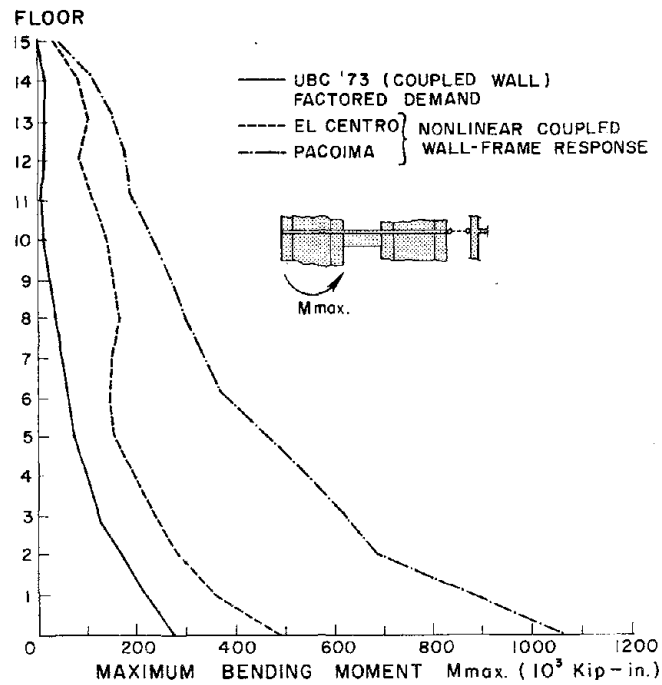


FIG. 6.2 ENVELOPES OF BENDING MOMENT ATTAINED ALONG THE ELEVATION OF ONE WALL

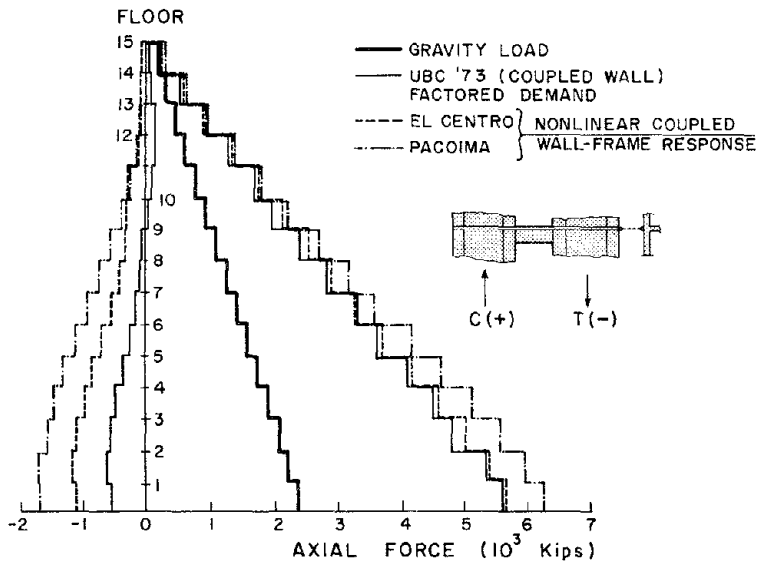


FIG. 6.3 ENVELOPES OF AXIAL FORCE IN WALLS, COUPLED WALL-FRAME RESPONSE

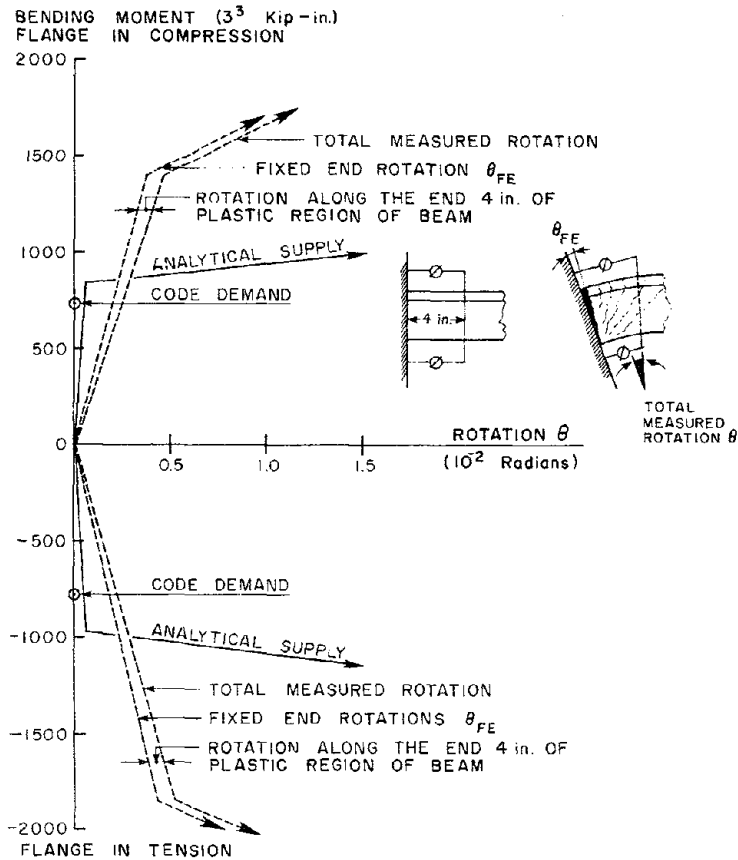


FIG. 6.4 MOMENT-ROTATION RELATIONS OF THE COUPLING GIRDER TYPE III AT GIRDER-WALL INTERFACE

PROVISION:	AXIAL - FLEXURAL DEMANDS @ BASE	SHEAR DEMANDS @ BASE
----- ATC 3-06	$E = 5.02 \% W^*$	$E / 0.6 = 8.37 \% W^*$
----- UBC 1979	$1.4 E = 8.19 \% W$	$2E / 0.85 = 13.76 \% W$
----- UBC 1973	$1.4 E = 6.34 \% W$	$2.8E / 0.85 = 14.92 \% W$

* W IS ONE HALF OF THE BUILDING WEIGHT

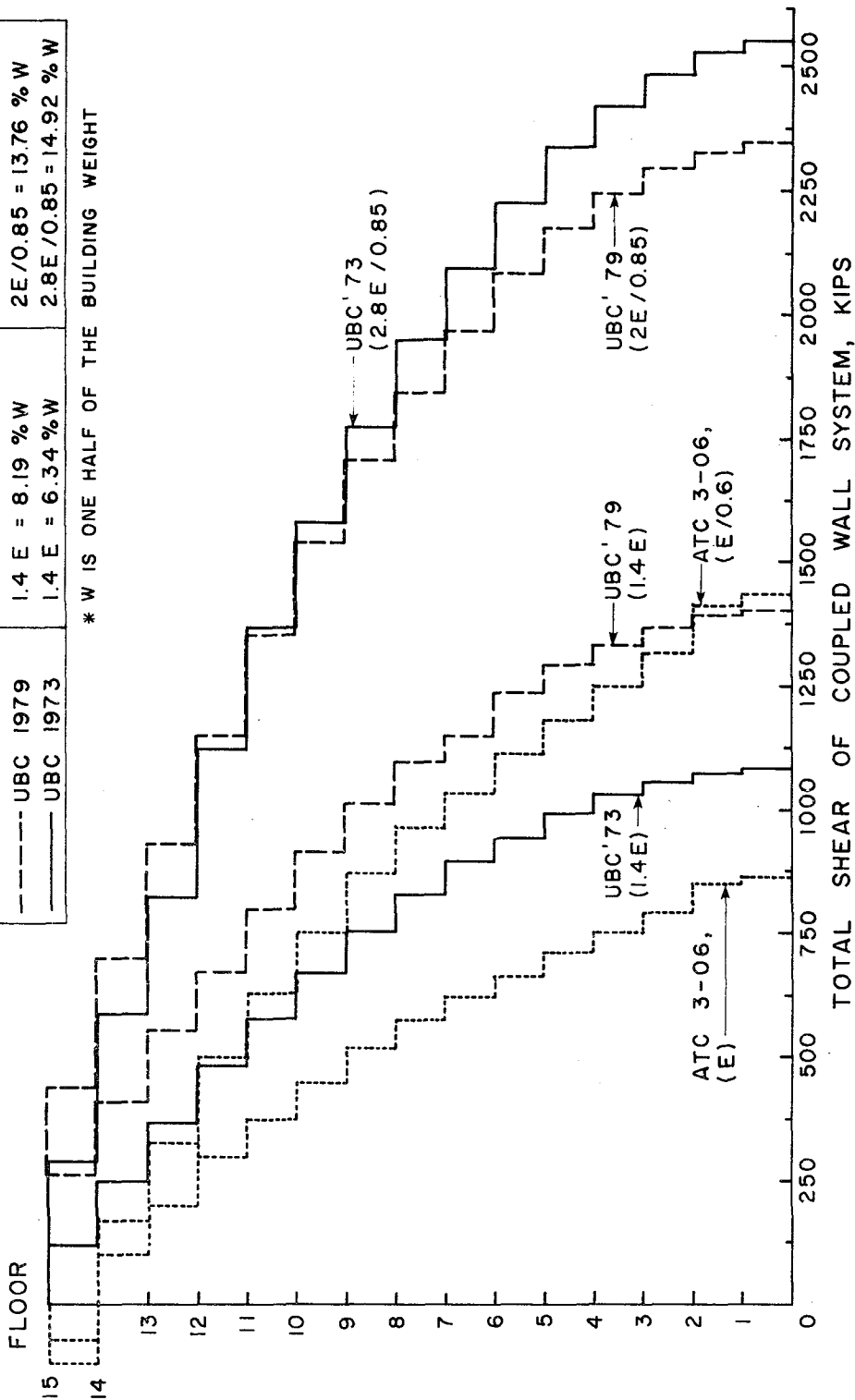


FIG. 6.5 SEISMIC STORY SHEAR DEMANDS FOR AXIAL-FLEXURAL AND SHEAR DESIGN OF COUPLED WALL BASED ON DIFFERENT CODE PROVISIONS

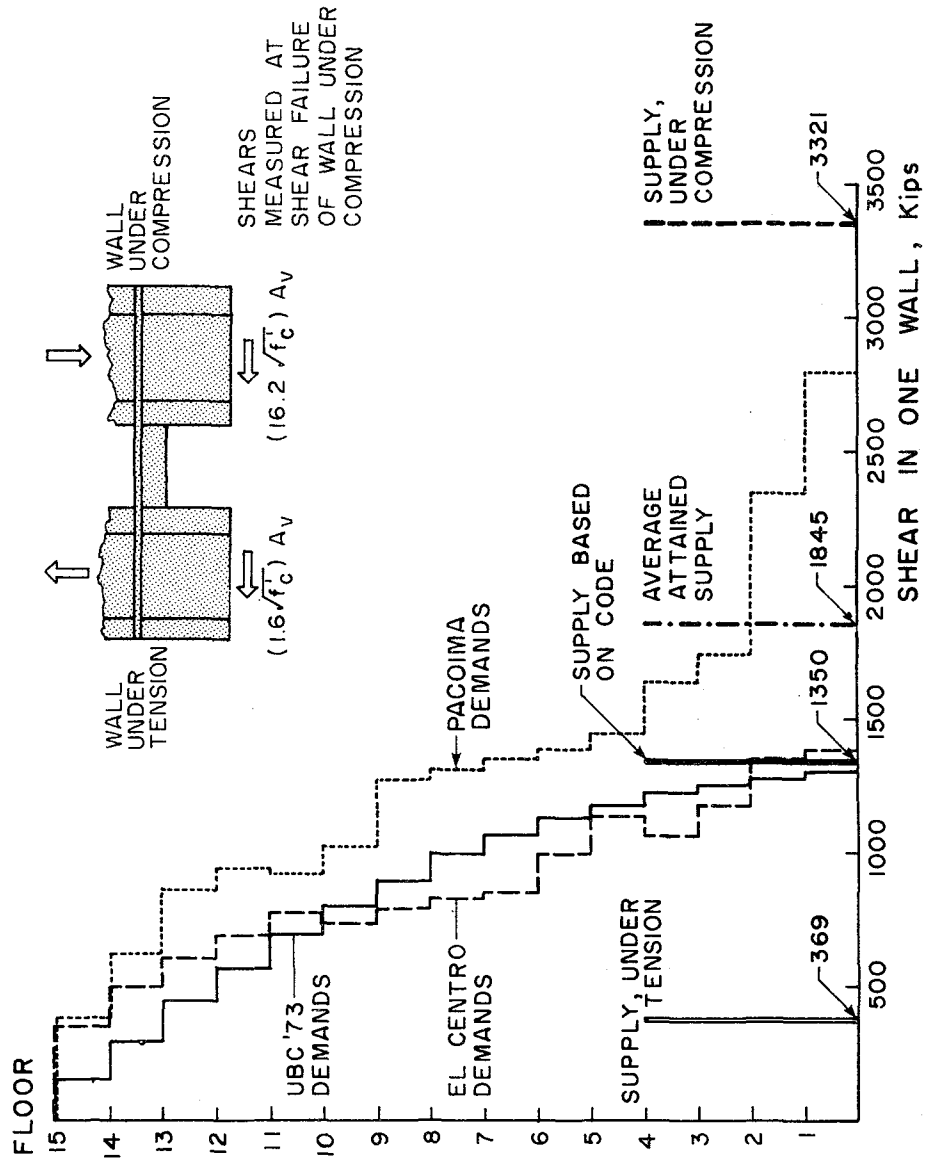


FIG. 6.6 SHEAR STRENGTH SUPPLIES AND DEMANDS FOR ONE WALL

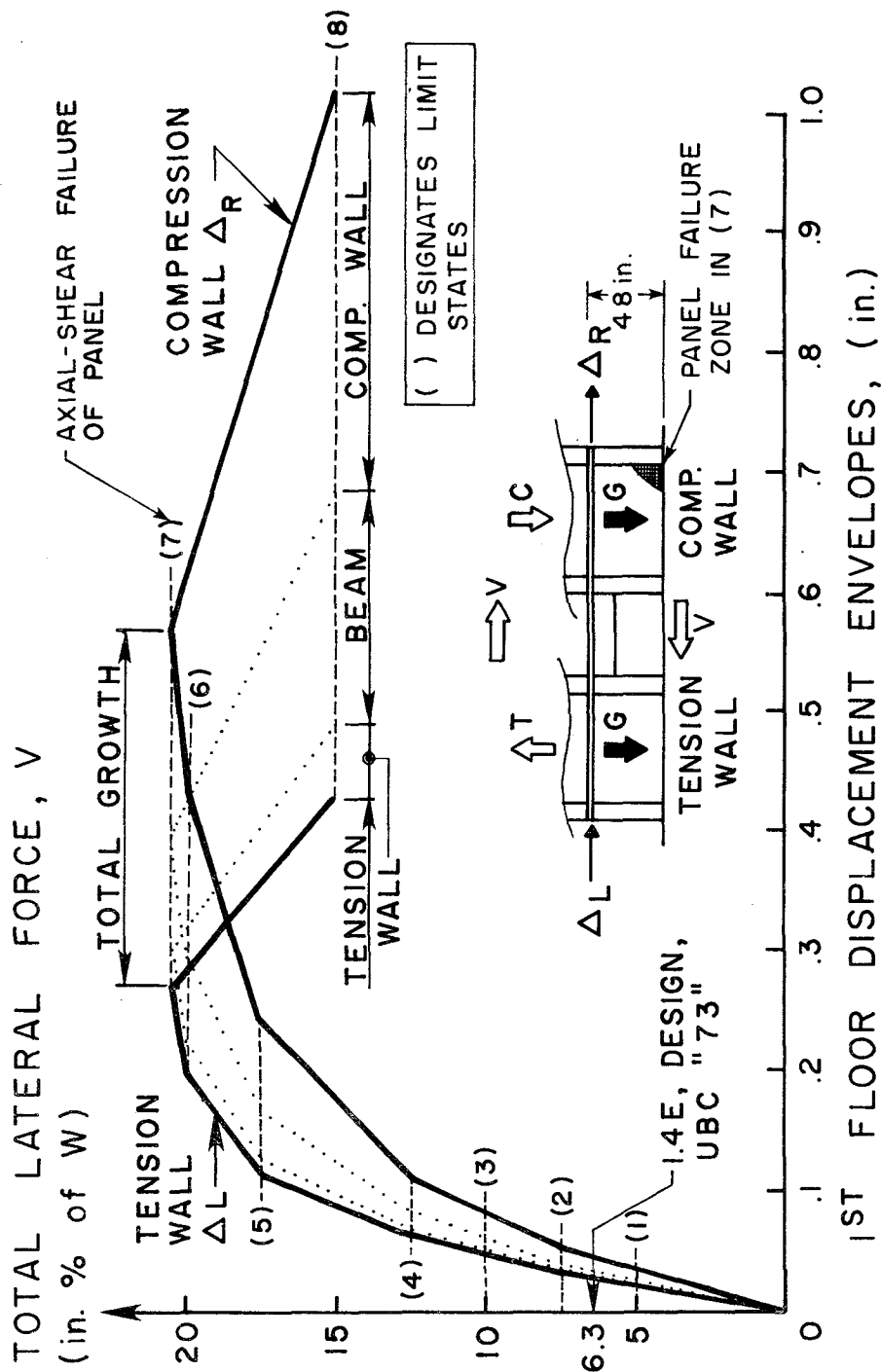


FIG. 6.7 FIRST FLOOR LATERAL FORCE-DISPLACEMENT EXPERIMENTAL RESPONSE ENVELOPES FOR THE TWO WALLS OF THE COUPLED WALL SPECIMEN

EARTHQUAKE ENGINEERING RESEARCH CENTER REPORTS

NOTE: Numbers in parentheses are Accession Numbers assigned by the National Technical Information Service; these are followed by a price code. Copies of the reports may be ordered from the National Technical Information Service, 5285 Port Royal Road, Springfield, Virginia, 22161. Accession Numbers should be quoted on orders for reports (PB --- ---) and remittance must accompany each order. Reports without this information were not available at time of printing. The complete list of EERC reports (from EERC 67-1) is available upon request from the Earthquake Engineering Research Center, University of California, Berkeley, 47th Street and Hoffman Boulevard, Richmond, California 94804.

- UCB/EERC-77/01 "PLUSH - A Computer Program for Probabilistic Finite Element Analysis of Seismic Soil-Structure Interaction," by M.P. Romo Organista, J. Lysmer and H.B. Seed - 1977 (PB81 177 651)A05
- UCB/EERC-77/02 "Soil-Structure Interaction Effects at the Humboldt Bay Power Plant in the Ferndale Earthquake of June 7, 1975," by J.E. Valera, H.B. Seed, C.F. Tsai and J. Lysmer - 1977 (PB 265 795)A04
- UCB/EERC-77/03 "Influence of Sample Disturbance on Sand Response to Cyclic Loading," by K. Mori, H.B. Seed and C.K. Chan - 1977 (PB 267 352)A04
- UCB/EERC-77/04 "Seismological Studies of Strong Motion Records," by J. Shoja-Taheri - 1977 (PB 269 655)A10
- UCB/EERC-77/05 Unassigned
- UCB/EERC-77/06 "Developing Methodologies for Evaluating the Earthquake Safety of Existing Buildings," by No. 1 - B. Bresler; No. 2 - B. Bresler, T. Okada and D. Zisling; No. 3 - T. Okada and B. Bresler; No. 4 - V.V. Bertero and B. Bresler - 1977 (PB 267 354)A08
- UCB/EERC-77/07 "A Literature Survey - Transverse Strength of Masonry Walls," by Y. Omote, R.L. Mayes, S.W. Chen and R.W. Clough - 1977 (PB 277 933)A07
- UCB/EERC-77/08 "DRAIN-TABS: A Computer Program for Inelastic Earthquake Response of Three Dimensional Buildings," by R. Guendelman-Israel and G.H. Powell - 1977 (PB 270 693)A07
- UCB/EERC-77/09 "SUBWALL: A Special Purpose Finite Element Computer Program for Practical Elastic Analysis and Design of Structural Walls with Substructure Option," by D.Q. Le, H. Peterson and E.P. Popov - 1977 (PB 270 567)A05
- UCB/EERC-77/10 "Experimental Evaluation of Seismic Design Methods for Broad Cylindrical Tanks," by D.P. Clough (PB 272 280)A13
- UCB/EERC-77/11 "Earthquake Engineering Research at Berkeley - 1976," - 1977 (PB 273 507)A09
- UCB/EERC-77/12 "Automated Design of Earthquake Resistant Multistory Steel Building Frames," by N.D. Walker, Jr. - 1977 (PB 276 526)A09
- UCB/EERC-77/13 "Concrete Confined by Rectangular Hoops Subjected to Axial Loads," by J. Vallenias, V.V. Bertero and E.P. Popov - 1977 (PB 275 165)A06
- UCB/EERC-77/14 "Seismic Strain Induced in the Ground During Earthquakes," by Y. Sugimura - 1977 (PB 284 201)A04
- UCB/EERC-77/15 Unassigned
- UCB/EERC-77/16 "Computer Aided Optimum Design of Ductile Reinforced Concrete Moment Resisting Frames," by S.W. Zagajeski and V.V. Bertero - 1977 (PB 280 137)A07
- UCB/EERC-77/17 "Earthquake Simulation Testing of a Stepping Frame with Energy-Absorbing Devices," by J.M. Kelly and D.F. Tsztoo - 1977 (PB 273 506)A04
- UCB/EERC-77/18 "Inelastic Behavior of Eccentrically Braced Steel Frames under Cyclic Loadings," by C.W. Roeder and E.P. Popov - 1977 (PB 275 526)A15
- UCB/EERC-77/19 "A Simplified Procedure for Estimating Earthquake-Induced Deformations in Dams and Embankments," by F.I. Makdisi and H.B. Seed - 1977 (PB 276 820)A04
- UCB/EERC-77/20 "The Performance of Earth Dams during Earthquakes," by H.B. Seed, F.I. Makdisi and P. de Alba - 1977 (PB 276 821)A04
- UCB/EERC-77/21 "Dynamic Plastic Analysis Using Stress Resultant Finite Element Formulation," by P. Lukkunapvasit and J.M. Kelly - 1977 (PB 275 453)A04
- UCB/EERC-77/22 "Preliminary Experimental Study of Seismic Uplift of a Steel Frame," by R.W. Clough and A.A. Huckelbridge 1977 (PB 278 769)A08
- UCB/EERC-77/23 "Earthquake Simulator Tests of a Nine-Story Steel Frame with Columns Allowed to Uplift," by A.A. Huckelbridge - 1977 (PB 277 944)A09
- UCB/EERC-77/24 "Nonlinear Soil-Structure Interaction of Skew Highway Bridges," by M.-C. Chen and J. Penzien - 1977 (PB 276 176)A07
- UCB/EERC-77/25 "Seismic Analysis of an Offshore Structure Supported on Pile Foundations," by D.D.-N. Liou and J. Penzien 1977 (PB 283 180)A06
- UCB/EERC-77/26 "Dynamic Stiffness Matrices for Homogeneous Viscoelastic Half-Planes," by G. Dasgupta and A.K. Chopra - 1977 (PB 279 654)A06

UCB/EERC-77/27 "A Practical Soft Story Earthquake Isolation System," by J.M. Kelly, J.M. Eidingen and C.J. Derham - 1977 (PB 276 814)A07

UCB/EERC-77/28 "Seismic Safety of Existing Buildings and Incentives for Hazard Mitigation in San Francisco: An Exploratory Study," by A.J. Meltner - 1977 (PB 281 970)A05

UCB/EERC-77/29 "Dynamic Analysis of Electrohydraulic Shaking Tables," by D. Rea, S. Abedi-Hayati and Y. Takahashi 1977 (PB 282 569)A04

UCB/EERC-77/30 "An Approach for Improving Seismic - Resistant Behavior of Reinforced Concrete Interior Joints," by B. Galunic, V.V. Bertero and E.P. Popov - 1977 (PB 290 870)A06

UCB/EERC-78/01 "The Development of Energy-Absorbing Devices for Aseismic Base Isolation Systems," by J.M. Kelly and D.F. Tsztsoo - 1978 (PB 284 978)A04

UCB/EERC-78/02 "Effect of Tensile Prestrain on the Cyclic Response of Structural Steel Connections," by J.G. Bouwkamp and A. Mukhopadhyay - 1978

UCB/EERC-78/03 "Experimental Results of an Earthquake Isolation System using Natural Rubber Bearings," by J.M. Eidingen and J.M. Kelly - 1978 (PB 281 686)A04

UCB/EERC-78/04 "Seismic Behavior of Tall Liquid Storage Tanks," by A. Niwa - 1978 (PB 284 017)A14

UCB/EERC-78/05 "Hysteretic Behavior of Reinforced Concrete Columns Subjected to High Axial and Cyclic Shear Forces," by S.W. Zagajski, V.V. Bertero and J.G. Bouwkamp - 1978 (PB 283 858)A13

UCB/EERC-78/06 "Three Dimensional Inelastic Frame Elements for the ANSR-I Program," by A. Riahi, D.G. Row and G.H. Powell - 1978 (PB 295 755)A04

UCB/EERC-78/07 "Studies of Structural Response to Earthquake Ground Motion," by O.A. Lopez and A.K. Chopra - 1978 (PB 282 790)A05

UCB/EERC-78/08 "A Laboratory Study of the Fluid-Structure Interaction of Submerged Tanks and Caissons in Earthquakes," by R.C. Byrd - 1978 (PB 284 957)A08

UCB/EERC-78/09 Unassigned

UCB/EERC-78/10 "Seismic Performance of Nonstructural and Secondary Structural Elements," by I. Sakamoto - 1978 (PB 281 154 593)A05

UCB/EERC-78/11 "Mathematical Modelling of Hysteresis Loops for Reinforced Concrete Columns," by S. Nakata, T. Sproul and J. Penzien - 1978 (PB 298 274)A05

UCB/EERC-78/12 "Damageability in Existing Buildings," by T. Blejwas and B. Bresler - 1978 (PB 80 166 978)A05

UCB/EERC-78/13 "Dynamic Behavior of a Pedestal Base Multistory Building," by R.M. Stephen, E.L. Wilson, J.G. Bouwkamp and M. Button - 1978 (PB 286 650)A08

UCB/EERC-78/14 "Seismic Response of Bridges - Case Studies," by R.A. Imbsen, V. Nutt and J. Penzien - 1978 (PB 286 503)A10

UCB/EERC-78/15 "A Substructure Technique for Nonlinear Static and Dynamic Analysis," by D.G. Row and G.H. Powell - 1978 (PB 288 077)A10

UCB/EERC-78/16 "Seismic Risk Studies for San Francisco and for the Greater San Francisco Bay Area," by C.S. Oliveira - 1978 (PB 81 120 115)A07

UCB/EERC-78/17 "Strength of Timber Roof Connections Subjected to Cyclic Loads," by P. Gülkan, R.L. Mayes and R.W. Clough - 1978 (HUD-000 1491)A07

UCB/EERC-78/18 "Response of K-Braced Steel Frame Models to Lateral Loads," by J.G. Bouwkamp, R.M. Stephen and E.P. Popov - 1978

UCB/EERC-78/19 "Rational Design Methods for Light Equipment in Structures Subjected to Ground Motion," by J.L. Sackman and J.M. Kelly - 1978 (PB 292 357)A04

UCB/EERC-78/20 "Testing of a Wind Restraint for Aseismic Base Isolation," by J.M. Kelly and D.E. Chitty - 1978 (PB 292 833)A03

UCB/EERC-78/21 "APOLLO - A Computer Program for the Analysis of Pore Pressure Generation and Dissipation in Horizontal Sand Layers During Cyclic or Earthquake Loading," by P.P. Martin and H.B. Seed - 1978 (PB 292 835)A04

UCB/EERC-78/22 "Optimal Design of an Earthquake Isolation System," by M.A. Bhatti, K.S. Pister and E. Polak - 1978 (PB 294 735)A06

UCB/EERC-78/23 "MASH - A Computer Program for the Non-Linear Analysis of Vertically Propagating Shear Waves in Horizontally Layered Deposits," by P.P. Martin and H.B. Seed - 1978 (PB 293 101)A05

UCB/EERC-78/24 "Investigation of the Elastic Characteristics of a Three Story Steel Frame Using System Identification," by I. Kaya and H.D. McNiven - 1978 (PB 296 225)A06

UCB/EERC-78/25 "Investigation of the Nonlinear Characteristics of a Three-Story Steel Frame Using System Identification," by I. Kaya and H.D. McNiven - 1978 (PB 301 363)A05

- UCB/EERC-78/26 "Studies of Strong Ground Motion in Taiwan," by Y.M. Hsiung, B.A. Bolt and J. Penzien - 1978 (PB 298 436)A06
- UCB/EERC-78/27 "Cyclic Loading Tests of Masonry Single Piers: Volume 1 - Height to Width Ratio of 2," by P.A. Hidalgo, R.L. Mayes, H.D. McNiven and R.W. Clough - 1978 (PB 296 211)A07
- UCB/EERC-78/28 "Cyclic Loading Tests of Masonry Single Piers: Volume 2 - Height to Width Ratio of 1," by S.-W.J. Chen, P.A. Hidalgo, R.L. Mayes, R.W. Clough and H.D. McNiven - 1978 (PB 296 212)A09
- UCB/EERC-78/29 "Analytical Procedures in Soil Dynamics," by J. Lysmer - 1978 (PB 298 445)A06
- UCB/EERC-79/01 "Hysteretic Behavior of Lightweight Reinforced Concrete Beam-Column Subassemblages," by B. Forzani, E.P. Popov and V.V. Bertero - April 1979(PB 298 267)A06
- UCB/EERC-79/02 "The Development of a Mathematical Model to Predict the Flexural Response of Reinforced Concrete Beams to Cyclic Loads, Using System Identification," by J. Stanton & H. McNiven - Jan. 1979(PB 295 875)A10
- UCB/EERC-79/03 "Linear and Nonlinear Earthquake Response of Simple Torsionally Coupled Systems," by C.L. Kan and A.K. Chopra - Feb. 1979(PB 298 262)A06
- UCB/EERC-79/04 "A Mathematical Model of Masonry for Predicting its Linear Seismic Response Characteristics," by Y. Mengi and H.D. McNiven - Feb. 1979(PB 298 266)A06
- UCB/EERC-79/05 "Mechanical Behavior of Lightweight Concrete Confined by Different Types of Lateral Reinforcement," by M.A. Manrique, V.V. Bertero and E.P. Popov - May 1979(PB 301 114)A06
- UCB/EERC-79/06 "Static Tilt Tests of a Tall Cylindrical Liquid Storage Tank," by R.W. Clough and A. Niwa - Feb. 1979 (PB 301 167)A06
- UCB/EERC-79/07 "The Design of Steel Energy Absorbing Restrainers and Their Incorporation into Nuclear Power Plants for Enhanced Safety: Volume 1 - Summary Report," by P.N. Spencer, V.F. Zackay, and E.R. Parker - Feb. 1979(UCB/EERC-79/07)A09
- UCB/EERC-79/08 "The Design of Steel Energy Absorbing Restrainers and Their Incorporation into Nuclear Power Plants for Enhanced Safety: Volume 2 - The Development of Analyses for Reactor System Piping," "Simple Systems" by M.C. Lee, J. Penzien, A.K. Chopra and K. Suzuki "Complex Systems" by G.H. Powell, E.L. Wilson, R.W. Clough and D.G. Row - Feb. 1979(UCB/EERC-79/08)A10
- UCB/EERC-79/09 "The Design of Steel Energy Absorbing Restrainers and Their Incorporation into Nuclear Power Plants for Enhanced Safety: Volume 3 - Evaluation of Commercial Steels," by W.S. Owen, R.M.N. Pelloux, R.O. Ritchie, M. Faral, T. Ohhashi, J. Toplosky, S.J. Hartman, V.F. Zackay and E.R. Parker - Feb. 1979(UCB/EERC-79/09)A04
- UCB/EERC-79/10 "The Design of Steel Energy Absorbing Restrainers and Their Incorporation into Nuclear Power Plants for Enhanced Safety: Volume 4 - A Review of Energy-Absorbing Devices," by J.M. Kelly and M.S. Skinner - Feb. 1979(UCB/EERC-79/10)A04
- UCB/EERC-79/11 "Conservatism in Summation Rules for Closely Spaced Modes," by J.M. Kelly and J.L. Sackman - May 1979(PB 301 328)A03
- UCB/EERC-79/12 "Cyclic Loading Tests of Masonry Single Piers; Volume 3 - Height to Width Ratio of 0.5," by P.A. Hidalgo, R.L. Mayes, H.D. McNiven and R.W. Clough - May 1979(PB 301 321)A08
- UCB/EERC-79/13 "Cyclic Behavior of Dense Course-Grained Materials in Relation to the Seismic Stability of Dams," by N.G. Banerjee, H.B. Seed and C.K. Chan - June 1979(PB 301 373)A13
- UCB/EERC-79/14 "Seismic Behavior of Reinforced Concrete Interior Beam-Column Subassemblages," by S. Viathanatepa, E.P. Popov and V.V. Bertero - June 1979(PB 301 326)A10
- UCB/EERC-79/15 "Optimal Design of Localized Nonlinear Systems with Dual Performance Criteria Under Earthquake Excitations," by M.A. Bhatti - July 1979(PB 80 167 109)A06
- UCB/EERC-79/16 "OPTDYN - A General Purpose Optimization Program for Problems with or without Dynamic Constraints," by M.A. Bhatti, E. Polak and K.S. Pister - July 1979(PB 80 167 091)A05
- UCB/EERC-79/17 "ANSR-II, Analysis of Nonlinear Structural Response, Users Manual," by D.P. Mondkar and G.H. Powell July 1979(PB 80 113 301)A05
- UCB/EERC-79/18 "Soil Structure Interaction in Different Seismic Environments," A. Gomez-Masso, J. Lysmer, J.-C. Chen and H.B. Seed - August 1979(PB 80 101 520)A04
- UCB/EERC-79/19 "ARMA Models for Earthquake Ground Motions," by M.K. Chang, J.W. Kwiatkowski, R.F. Nau, R.M. Oliver and K.S. Pister - July 1979(PB 301 166)A05
- UCB/EERC-79/20 "Hysteretic Behavior of Reinforced Concrete Structural Walls," by J.M. Vallenias, V.V. Bertero and E.P. Popov - August 1979(PB 80 165 905)A12
- UCB/EERC-79/21 "Studies on High-Frequency Vibrations of Buildings - 1: The Column Effect," by J. Lubliner - August 1979 (PB 80 158 553)A03
- UCB/EERC-79/22 "Effects of Generalized Loadings on Bond Reinforcing Bars Embedded in Confined Concrete Blocks," by S. Viathanatepa, E.P. Popov and V.V. Bertero - August 1979(PB 81 124 018)A14
- UCB/EERC-79/23 "Shaking Table Study of Single-Story Masonry Houses, Volume 1: Test Structures 1 and 2," by P. Gülkan, R.L. Mayes and R.W. Clough - Sept. 1979 (HUD-000 1763)A12
- UCB/EERC-79/24 "Shaking Table Study of Single-Story Masonry Houses, Volume 2: Test Structures 3 and 4," by P. Gülkan, R.L. Mayes and R.W. Clough - Sept. 1979 (HUD-000 1836)A12
- UCB/EERC-79/25 "Shaking Table Study of Single-Story Masonry Houses, Volume 3: Summary, Conclusions and Recommendations," by R.W. Clough, R.L. Mayes and P. Gülkan - Sept. 1979 (HUD-000 1837)A06

UCB/EERC-79/26 "Recommendations for a U.S.-Japan Cooperative Research Program Utilizing Large-Scale Testing Facilities," by U.S.-Japan Planning Group - Sept. 1979(PB 301 407)A06

UCB/EERC-79/27 "Earthquake-Induced Liquefaction Near Lake Amatitlan, Guatemala," by H.B. Seed, I. Arango, C.K. Chan, A. Gomez-Masso and R. Grant de Ascoli - Sept. 1979(NUREG-CRL341)A03

UCB/EERC-79/28 "Infill Panels: Their Influence on Seismic Response of Buildings," by J.W. Axley and V.V. Bertero Sept. 1979(PB 80 163 371)A10

UCB/EERC-79/29 "3D Truss Bar Element (Type 1) for the ANSR-II Program," by D.P. Mondkar and G.H. Powell - Nov. 1979 (PB 80 169 709)A02

UCB/EERC-79/30 "2D Beam-Column Element (Type 5 - Parallel Element Theory) for the ANSR-II Program," by D.G. Row, G.H. Powell and D.P. Mondkar - Dec. 1979(PB 80 167 224)A03

UCB/EERC-79/31 "3D Beam-Column Element (Type 2 - Parallel Element Theory) for the ANSR-II Program," by A. Riahi, G.H. Powell and D.P. Mondkar - Dec. 1979(PB 80 167 216)A03

UCB/EERC-79/32 "On Response of Structures to Stationary Excitation," by A. Der Kiureghian - Dec. 1979(PB 80166 929)A03

UCB/EERC-79/33 "Undisturbed Sampling and Cyclic Load Testing of Sands," by S. Singh, H.B. Seed and C.K. Chan Dec. 1979(ADA 087 298)A07

UCB/EERC-79/34 "Interaction Effects of Simultaneous Torsional and Compressional Cyclic Loading of Sand," by P.M. Griffin and W.N. Houston - Dec. 1979(ADA 092 352)A15

UCB/EERC-80/01 "Earthquake Response of Concrete Gravity Dams Including Hydrodynamic and Foundation Interaction Effects," by A.K. Chopra, P. Chakrabarti and S. Gupta - Jan. 1980(AD-A087297)A10

UCB/EERC-80/02 "Rocking Response of Rigid Blocks to Earthquakes," by C.S. Yim, A.K. Chopra and J. Penzien - Jan. 1980 (PB80 166 002)A04

UCB/EERC-80/03 "Optimum Inelastic Design of Seismic-Resistant Reinforced Concrete Frame Structures," by S.W. Zagajeski and V.V. Bertero - Jan. 1980(PB80 164 635)A06

UCB/EERC-80/04 "Effects of Amount and Arrangement of Wall-Panel Reinforcement on Hysteretic Behavior of Reinforced Concrete Walls," by R. Iliya and V.V. Bertero - Feb. 1980(PB81 122 525)A09

UCB/EERC-80/05 "Shaking Table Research on Concrete Dam Models," by A. Niwa and R.W. Clough - Sept. 1980(PB81 122 368)A06

UCB/EERC-80/06 "The Design of Steel Energy-Absorbing Restrainers and their Incorporation into Nuclear Power Plants for Enhanced Safety (Vol 1A): Piping with Energy Absorbing Restrainers: Parameter Study on Small Systems," by G.H. Powell, C. Oughourlian and J. Simons - June 1980

UCB/EERC-80/07 "Inelastic Torsional Response of Structures Subjected to Earthquake Ground Motions," by Y. Yamazaki April 1980(PB81 122 327)A08

UCB/EERC-80/08 "Study of X-Braced Steel Frame Structures Under Earthquake Simulation," by Y. Ghanaat - April 1980 (PB81 122 335)A11

UCB/EERC-80/09 "Hybrid Modelling of Soil-Structure Interaction," by S. Gupta, T.W. Lin, J. Penzien and C.S. Yeh May 1980(PB81 122 319)A07

UCB/EERC-80/10 "General Applicability of a Nonlinear Model of a One Story Steel Frame," by B.I. Sveinsson and H.D. McNiven - May 1980(PB81 124 877)A06

UCB/EERC-80/11 "A Green-Function Method for Wave Interaction with a Submerged Body," by W. Kioka - April 1980 (PB81 122 269)A07

UCB/EERC-80/12 "Hydrodynamic Pressure and Added Mass for Axisymmetric Bodies," by F. Nilrat - May 1980(PB81 122 343)A08

UCB/EERC-80/13 "Treatment of Non-Linear Drag Forces Acting on Offshore Platforms," by B.V. Dao and J. Penzien May 1980(PB81 153 413)A07

UCB/EERC-80/14 "2D Plane/Axisymmetric Solid Element (Type 3 - Elastic or Elastic-Perfectly Plastic) for the ANSR-II Program," by D.P. Mondkar and G.H. Powell - July 1980(PB81 122 350)A03

UCB/EERC-80/15 "A Response Spectrum Method for Random Vibrations," by A. Der Kiureghian - June 1980(PB81 122 301)A03

UCB/EERC-80/16 "Cyclic Inelastic Buckling of Tubular Steel Braces," by V.A. Zayas, E.P. Popov and S.A. Mahin June 1980(PB81 124 885)A10

UCB/EERC-80/17 "Dynamic Response of Simple Arch Dams Including Hydrodynamic Interaction," by C.S. Porter and A.K. Chopra - July 1980(PB81 124 000)A13

UCB/EERC-80/18 "Experimental Testing of a Friction Damped Aseismic Base Isolation System with Fail-Safe Characteristics," by J.M. Kelly, K.E. Beucke and M.S. Skinner - July 1980(PB81 148 595)A04

UCB/EERC-80/19 "The Design of Steel Energy-Absorbing Restrainers and their Incorporation into Nuclear Power Plants for Enhanced Safety (Vol 1B): Stochastic Seismic Analyses of Nuclear Power Plant Structures and Piping Systems Subjected to Multiple Support Excitations," by M.C. Lee and J. Penzien - June 1980

UCB/EERC-80/20 "The Design of Steel Energy-Absorbing Restrainers and their Incorporation into Nuclear Power Plants for Enhanced Safety (Vol 1C): Numerical Method for Dynamic Substructure Analysis," by J.M. Dickens and E.L. Wilson - June 1980

UCB/EERC-80/21 "The Design of Steel Energy-Absorbing Restrainers and their Incorporation into Nuclear Power Plants for Enhanced Safety (Vol 2): Development and Testing of Restraints for Nuclear Piping Systems," by J.M. Kelly and M.S. Skinner - June 1980

UCB/EERC-80/22 "3D Solid Element (Type 4-Elastic or Elastic-Perfectly-Plastic) for the ANSR-II Program," by D.P. Mondkar and G.H. Powell - July 1980(PB81 123 242)A03

UCB/EERC-80/23 "Gap-Friction Element (Type 5) for the ANSR-II Program," by D.P. Mondkar and G.H. Powell - July 1980 (PB81 122 285)A03

UCB/EERC-80/24 "U-Bar Restraint Element (Type 11) for the ANSR-II Program," by C. Oughourlian and G.H. Powell July 1980(PB81 122 293)A03

UCB/EERC-80/25 "Testing of a Natural Rubber Base Isolation System by an Explosively Simulated Earthquake," by J.M. Kelly - August 1980(PB81 201 360)A04

UCB/EERC-80/26 "Input Identification from Structural Vibrational Response," by Y. Hu - August 1980(PB81 152 308)A05

UCB/EERC-80/27 "Cyclic Inelastic Behavior of Steel Offshore Structures," by V.A. Zayas, S.A. Mahin and E.P. Popov August 1980(PB81 196 180)A15

UCB/EERC-80/28 "Shaking Table Testing of a Reinforced Concrete Frame with Biaxial Response," by M.G. Oliva October 1980(PB81 154 304)A10

UCB/EERC-80/29 "Dynamic Properties of a Twelve-Story Prefabricated Panel Building," by J.G. Bouwkamp, J.P. Kollegger and R.M. Stephen - October 1980(PB82 117 128)A06

UCB/EERC-80/30 "Dynamic Properties of an Eight-Story Prefabricated Panel Building," by J.G. Bouwkamp, J.P. Kollegger and R.M. Stephen - October 1980(PB81 200 313)A05

UCB/EERC-80/31 "Predictive Dynamic Response of Panel Type Structures Under Earthquakes," by J.P. Kollegger and J.G. Bouwkamp - October 1980(PB81 152 316)A04

UCB/EERC-80/32 "The Design of Steel Energy-Absorbing Restrainers and their Incorporation into Nuclear Power Plants for Enhanced Safety (Vol 3): Testing of Commercial Steels in Low-Cycle Torsional Fatigue," by P. Spencer, E.R. Parker, E. Jongewaard and M. Drory

UCB/EERC-80/33 "The Design of Steel Energy-Absorbing Restrainers and their Incorporation into Nuclear Power Plants for Enhanced Safety (Vol 4): Shaking Table Tests of Piping Systems with Energy-Absorbing Restrainers," by S.F. Stiemer and W.G. Godden - Sept. 1980

UCB/EERC-80/34 "The Design of Steel Energy-Absorbing Restrainers and their Incorporation into Nuclear Power Plants for Enhanced Safety (Vol 5): Summary Report," by P. Spencer

UCB/EERC-80/35 "Experimental Testing of an Energy-Absorbing Base Isolation System," by J.M. Kelly, M.S. Skinner and K.E. Beucke - October 1980(PB81 154 072)A04

UCB/EERC-80/36 "Simulating and Analyzing Artificial Non-Stationary Earthquake Ground Motions," by R.F. Nau, R.M. Oliver and K.S. Pister - October 1980(PB81 153 397)A04

UCB/EERC-80/37 "Earthquake Engineering at Berkeley - 1980," - Sept. 1980(PB81 205 374)A09

UCB/EERC-80/38 "Inelastic Seismic Analysis of Large Panel Buildings," by V. Schricker and G.H. Powell - Sept. 1980 (PB81 154 338)A13

UCB/EERC-80/39 "Dynamic Response of Embankment, Concrete-Gravity and Arch Dams Including Hydrodynamic Interaction," by J.F. Hall and A.K. Chopra - October 1980(PB81 152 324)A11

UCB/EERC-80/40 "Inelastic Buckling of Steel Struts Under Cyclic Load Reversal," by R.G. Black, W.A. Wenger and E.P. Popov - October 1980(PB81 154 312)A08

UCB/EERC-80/41 "Influence of Site Characteristics on Building Damage During the October 3, 1974 Lima Earthquake," by P. Repetto, I. Arango and H.B. Seed - Sept. 1980(PB81 161 739)A05

UCB/EERC-80/42 "Evaluation of a Shaking Table Test Program on Response Behavior of a Two Story Reinforced Concrete Frame," by J.M. Blondet, R.W. Clough and S.A. Mahin

UCB/EERC-80/43 "Modelling of Soil-Structure Interaction by Finite and Infinite Elements," by F. Medina - December 1980(PB81 229 270)A04

UCB/EERC-81/01 "Control of Seismic Response of Piping Systems and Other Structures by Base Isolation," edited by J.M. Kelly - January 1981 (PB81 200 735)A05

UCB/EERC-81/02 "OPTNSR - An Interactive Software System for Optimal Design of Statically and Dynamically Loaded Structures with Nonlinear Response," by M.A. Bhatti, V. Ciampi and K.S. Pister - January 1981 (PB81 218 851)A09

UCB/EERC-81/03 "Analysis of Local Variations in Free Field Seismic Ground Motions," by J.-C. Chen, J. Lysmer and H.B. Seed - January 1981 (AD-A099508)A13

UCB/EERC-81/04 "Inelastic Structural Modeling of Braced Offshore Platforms for Seismic Loading," by V.A. Zayas, P.-S.B. Shing, S.A. Mahin and E.P. Popov - January 1981(PB82 138 777)A07

UCB/EERC-81/05 "Dynamic Response of Light Equipment in Structures," by A. Der Kiureghian, J.L. Sackman and B. Nour-Omid - April 1981 (PB81 218 497)A04

UCB/EERC-81/06 "Preliminary Experimental Investigation of a Broad Base Liquid Storage Tank," by J.G. Bouwkamp, J.P. Kollegger and R.M. Stephen - May 1981(PB82 140 385)A03

UCB/EERC-81/07 "The Seismic Resistant Design of Reinforced Concrete Coupled Structural Walls," by A.E. Aktan and V.V. Bertero - June 1981(PB82 113 358)A11

UCB/EERC-81/08 "The Undrained Shearing Resistance of Cohesive Soils at Large Deformations," by M.R. Pyles and H.B. Seed - August 1981

UCB/EERC-81/09 "Experimental Behavior of a Spatial Piping System with Steel Energy Absorbers Subjected to a Simulated Differential Seismic Input," by S.F. Stiemer, W.G. Godden and J.M. Kelly - July 1981

- UCB/EERC-81/10 "Evaluation of Seismic Design Provisions for Masonry in the United States," by B.I. Sveinsson, R.L. Mayes and H.D. McNiven - August 1981
- UCB/EERC-81/11 "Two-Dimensional Hybrid Modelling of Soil-Structure Interaction," by T.-J. Tzong, S. Gupta and J. Penzien - August 1981(PB82 142 118)A04
- UCB/EERC-81/12 "Studies on Effects of Infills in Seismic Resistant R/C Construction," by S. Brokken and V.V. Bertero - September 1981
- UCB/EERC-81/13 "Linear Models to Predict the Nonlinear Seismic Behavior of a One-Story Steel Frame," by H. Valdimarsson, A.H. Shah and H.D. McNiven - September 1981(PB82 138 793)A07
- UCB/EERC-81/14 "TLUSH: A Computer Program for the Three-Dimensional Dynamic Analysis of Earth Dams," by T. Kagawa, L.H. Mejia, H.B. Seed and J. Lysmer - September 1981(PB82 139 940)A06
- UCB/EERC-81/15 "Three Dimensional Dynamic Response Analysis of Earth Dams," by L.H. Mejia and H.B. Seed - September 1981 (PB82 137 274)A12
- UCB/EERC-81/16 "Experimental Study of Lead and Elastomeric Dampers for Base Isolation Systems," by J.M. Kelly and S.B. Hodder - October 1981
- UCB/EERC-81/17 "The Influence of Base Isolation on the Seismic Response of Light Secondary Equipment," by J.M. Kelly - April 1981
- UCB/EERC-81/18 "Studies on Evaluation of Shaking Table Response Analysis Procedures," by J. Marcial Blondet - November 1981
- UCB/EERC-81/19 "DELIGHT.STRUCT: A Computer-Aided Design Environment for Structural Engineering," by R.J. Balling, K.S. Pister and E. Polak - December 1981
- UCB/EERC-81/20 "Optimal Design of Seismic-Resistant Planar Steel Frames," by R.J. Balling, V. Ciampi, K.S. Pister and E. Polak - December 1981
- UCB/EERC-82/01 "Dynamic Behavior of Ground for Seismic Analysis of Lifeline Systems," by T. Sato and A. Der Kiureghian - January 1982 (PB82 218 926) A05
- UCB/EERC-82/02 "Shaking Table Tests of a Tubular Steel Frame Model," by Y. Ghanaat and R. W. Clough - January 1982 (PB82 220 161) A07
- UCB/EERC-82/03 "Experimental Behavior of a Spatial Piping System with Shock Arrestors and Energy Absorbers under Seismic Excitation," by S. Schneider, H.-M. Lee and G. W. Godden - May 1982
- UCB/EERC-82/04 "New Approaches for the Dynamic Analysis of Large Structural Systems," by E. L. Wilson - June 1982
- UCB/EERC-82/05 "Model Study of Effects on the Vibration Properties of Steel Offshore Platforms," by F. Shahrivar and J. G. Bouwkamp - June 1982
- UCB/EERC-82/06 "States of the Art and Practice in the Optimum Seismic Design and Analytical Response Prediction of R/C Frame-Wall Structures," by A. E. Aktan and V. V. Bertero - July 1982.
- UCB/EERC-82/07 "Further Study of the Earthquake Response of a Broad Cylindrical Liquid-Storage Tank Model," by G. C. Manos and R. W. Clough - July 1982
- UCB/EERC-82/08 "An Evaluation of the Design and Analytical Seismic Response of a Seven Story Reinforced Concrete Frame - Wall Structure," by A. C. Finley and V. V. Bertero - July 1982
- UCB/EERC-82/09 "Fluid-structure Interactions: Added Mass Computations for Incompressible Fluid," by J. S.-H. Kuo - August 1982

- UCB/EERC-82/10 "Joint-Opening Nonlinear Mechanism: Interface Smeared Crack Model,"
by J. S.-H. Kuo - August 1982
- UCB/EERC-82/11 "Dynamic Response Analysis of Techii Dam," by R. W. Clough, R. M.
Stephen and J. S.-H. Kuo - August 1982
- UCB/EERC-82/12 "Prediction of the Seismic Responses of R/C Frame-Coupled Wall
Structures," by A. E. Aktan, V. V. Bertero and M. Piazza - August
1982

